Stepping stones in CO2 utilization

Synthesis and evaluation of oxalic- and glycolic acid (co)polyesters

Murcia Valderrama, M.A.

Maria Alejandra Murcia

Stepping Stones in CO₂ Utilization.

Synthesis and evaluation of oxalic- and glycolic acid (co)polyesters

Stepping stones in CO$_2$ utilization: Synthesis and evaluation of oxalic- and glycolic acid (co)polyesters

Maria Alejandra Murcia Valderrama

Stepping stones in CO_2 utilization: Synthesis and evaluation of oxalic- and glycolic acid (co)polyesters

Van 't Hoff Institute for Molecular Sciences, University of Amsterdam

Stepping Stones in CO_2 Utilization

Synthesis and Evaluation of Oxalic and Glycolic acid (co) Polyesters

ACADEMISCH PROEFSCHRIFT

ter verkrijging van de graad van doctor
aan de Universiteit van Amsterdam
op gezag van de Rector Magnificus
prof. dr. ir. P.P.C.C. Verbeek
ten overstaan van een door het College voor Promoties ingestelde commissie,
in het openbaar te verdedigen in de Agnietenkapel
op donderdag 20 oktober 2022, te 13.00 uur

door Maria Alejandra Murcia Valderrama
geboren te Duitama

Promotiecommissie

Promotor:	prof. dr. G.J.M. Gruter	Universiteit van Amsterdam
Copromotor:	dr. R.J. van Putten	Avantium
Overige leden:	prof. dr. B. de Bruin	Universiteit van Amsterdam
	dr. A. Astefanei	Universiteit van Amsterdam
	dr. S. Grecea	Universiteit van Amsterdam
	prof. dr. M. Honing	Universiteit Maastricht
	prof. dr. C.E. Koning	Rijksuniversiteit Groningen
	dr. ir. J.J. Kolstad	Avantium

Faculteit der Natuurwetenschappen, Wiskunde en Informatica

Contents

CHAPTER I
Introduction

The potential of oxalic - and glycolic acid based polyesters (review). Towards CO$_2$ as a feedstock (Carbon Capture and Utilization - CCU)
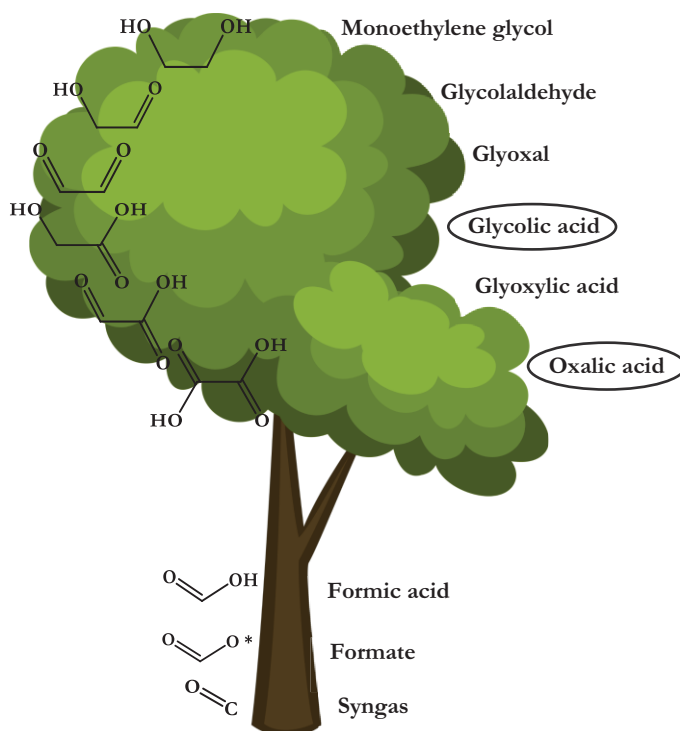
Abstract

Plastic materials are indispensable in everyday life because of their versatility, high durability, lightness and cost-effectiveness. As a consequence, worldwide plastic consumption will continue to grow from around 350 million metric tons per annum today to an estimated 1 billion metric tons per annum in 2050. For applications where polymers are applied in the environment or for applications where polymers have a bigger chance of ending up in the environment, (bio) degradable polymers need to be developed to stop endless accumulation of non-degradable polymers irreversibly littering our planet. As monomers and polymers represent more than 80% of the chemical industry's total production volume, a transition from fossil feedstock today (99% of the current feedstock for polymers is fossil-based) to a significantly larger percentage of renewable feedstock in the future (carbon that is already "above the ground") will be required to meet the greenhouse gas reduction targets of the Paris Agreement (>80% CO_2 reduction target for the European Chemical Industry sector in 2050).

The combination of the predicted polymer market growth and the emergence of new feedstocks creates a fantastic opportunity for novel sustainable polymers. To replace fossil based feedstock, there are only three sustainable alternative sources: biomass, CO_2 and existing plastics (via recycling). The ultimate circular feedstock would be CO_2: it can be electrochemically reduced to formic acid derivatives that can subsequently be converted into useful monomers such as glycolic acid and oxalic acid. In order to assess the future potential for these polyester building blocks, we will review the current field of polyesters based on these two monomers. Representative synthesis methods, general properties, general degradation mechanisms, and recent applications will be discussed in this review. The application potential of these polyesters for a wide range of purposes, as a function of production cost, will also be assessed. It is important to note that polymers derived from CO_2 do not necessarily always lead to lower net overall CO_2 emissions (during production or after use, e.g. degradation in landfills). This needs to be evaluated using robust LCA's and this information is currently not available for the materials discussed in this review.

1.1   Introduction

In December 2015, a global climate agreement was adopted at the Paris climate conference. The long-term goal (by 2050) is to ensure that the increase in global average temperature stays well below 2 °C above pre-industrial levels.[1] This initiative arose from the growing concern over worldwide CO_2 emissions, which have been proven to contribute significantly not only to global warming but also to ocean acidification.[2]

While for energy many alternatives are available, for plastic materials the only alternative carbon sources for (virgin) materials are biomass and in the long-term CO_2. As can be seen in **Fig. 1.1**, worldwide plastic consumption is increasing significantly. In 2016 production

reached 355 million tons per year with China and Europe leading the market.[3] Future plastic production is projected to double by 2035[4] and almost quadruple by 2050.
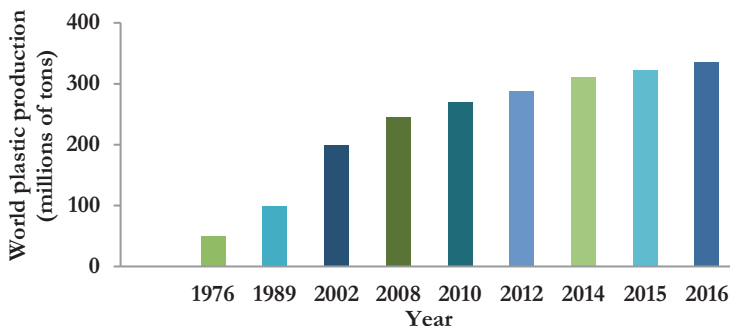
Fig. 1.1 World plastic production between 1976 and 2016.

By 2016, packaging represented 26% of the total volume of plastics used. However, in the same year, 95% of the plastic packaging material value was lost to the economy after short single-use application.[6] At the same time, these single-use products show low recycling rates, which is typically caused by lower value applications, complex logistics for collection and low quality recycling inputs. Traditional plastic recycling can be energy intensive and not economically viable. Feedstock (chemical) recycling for example, offers the advantage of recovering the petrochemical constituents of the polymer. However, today the price of the petrochemical feedstock is very low compared with the cost of producing monomers from plastic waste.[7] Another example is closed-loop mechanical recycling (2% of all plastic) which keeps the quality of the materials at a similar level by cycling materials into the same application (e.g. from PET bottle to PET bottle).[6] The approach of open loop mechanical recycling has been more broadly adopted for large-scale treatment of plastic waste, but there are still limitations with the technology. Each type of plastic responds differently to the process according to its chemical makeup (inherent immiscibility), mechanical behavior, and thermal properties, which makes the production of recycled resins more challenging.[8,9] Furthermore, it is not possible to process mechanically certain plastics such as temperature-sensitive plastics, composites and plastics that do not flow at elevated temperatures (as in the case of thermosets).[8] Also, the technologies used currently cannot be applied to many polymeric materials (poly(ethylene terephthalate) (PET) and polyethylenes are the focus).

Implementing strategies to decouple plastics from fossil feedstocks, to reduce leakage into ecosystems and ultimately to make plastics re-enter the economy by reuse, repurposing or recycling remain a major challenge. In Europe, a complete ban on Single-Use plastics has been proposed and implementation is expected in phases in the next 5-10 years.[10] This ban is suggested, because 70% of the plastic in our oceans is single-use plastic. Although Asia is a major source for ocean plastic, the EU initiative will influence consumer mind-set by encouraging more responsible material use initially in Europe. This will hopefully also have an effect around the globe.

With this in mind, strategies first and foremost for recycling of existing and novel plastic materials, either by mechanical means or via chemical pathways, need to be further developed. When recycling is not feasible, sustainable waste disposal options need to be developed and materials used in these products need to be selected with "end-of-life" as an important design parameter. In addition, reuse and repurposing should be very high on the agenda. This may require better materials to allow cheap and efficient cleaning. For applications where materials inevitably end up in nature (e.g. seed- and fertilizer coatings), (bio) degradability of polymers becomes ever more important.

Biodegradable polymers have received increasing attention since the 1970's. Whether a polymer can be considered biodegradable or not, is defined in guidelines and definitions established by national and international standardization organizations.[11] According to the ASTM (American Society for Testing and Materials) definition, a polymer is considered biodegradable if it can be decomposed or degraded into simple molecules from the action of naturally occurring micro-organisms such as bacteria, fungi and algae.[12] Degradation is a process of polymer chain breakage by the cleavage of bonds in the polymer backbone. This is characterized by a reduction in molecular weight and mechanical properties.[13] Depending on the environment (e.g. soil, aquatic sediments, sealed vessels), different standarized tests can be applied to evaluate the biodegradability of a polymer (e.g. ISO and OECD norms).

Biodegradability is a valuable property regarding environmental and economic sustainability for agricultural applications where plastic material leads to high leakage in the environment. Currently, the agricultural sector is increasingly oriented towards the replacement of traditional plastics for biodegradable materials[14] with the formulation of novel films[15-18], compost bags, plant pots, etc. Therefore, disposal also represents a challenge for agricultural applications when there is interest in crop production growth. Collection and recycling of the agricultural plastic films becomes more demanding considering the world's increasing population; films for greenhouses, silage and mulching are among those in higher demand, with Asia as the fastest growing market. The latter accounted for over 40% of the total plastic films used in agriculture in 2012.[19] Some of the advantages offered by mulch films include insect and weed control, increase in air and soil temperature, minimization of soil erosion and reduced evaporation.[20] These plastics, however, are contaminated with soil after use and therefore not collected by many recycling facilities.[21] Consequently, higher costs for landfilling are involved in the production process. With this in mind, the need for replacement with biodegradable plastics becomes more apparent.

Another agrochemical application with promising prospects for biodegradable polymers is the controlled release fertilizer (CRF) technology. The factors determining the rate, pattern, and duration of release are well known and can be tuned during the preparation of the product.[22] By encapsulating the fertilizer in polymeric membranes, nutrients are continuously provided to a crop in a controlled manner.[23] In fact, about half of the applied

fertilizers, depending on the application and soil conditions, are lost to the environment, resulting in water contamination.[24] Hence, the release of nutrients from CRF should ideally be linked to the nutrient uptake of the crop[17], thereby minimizing environmental pollution. The use of polymers for seed coatings also benefits agricultural systems: by covering the seeds, improvements in size, weight, and shape of crops can be achieved. This is important for an improved precision of planting. Furthermore, this technology helps to protect the seeds from pests and diseases, thus contributing to germination enhancement and a decrease of the need for fungicides.[25]

Before continuing, it is good to emphasize the distinction between "biopolymers" and "bio-based polymers". Biopolymers are polymers that occur in nature and are produced in biological systems: cellulose, chitin, starch, DNA, proteins, polyesters made by bacteria (polyhydroxyalkanoates or PHA's), etc. Biopolymers (under this definition) are therefore always biodegradable. Bio-based polymers are polymers (partly) derived from biomass feedstock. The bio-based content is defined by the fraction of bio-based carbon and ranges from approximately 20% (Coca-Cola's 'plant-bottle' PET) to 100% (Natureworks PLA).[26] The fact that a material is bio-based is unrelated to its biodegradability. Biodegradability is linked to the chemical structure and not to the origin of the feedstock. Poly(lactic acid) (PLA), for instance, is both bio-based and compostable, while some fossil-based polymers can also be completely biodegradable, exemplified by polycaprolactone.[27] Bio-based polyethylene (PE) or partly bio-based "plant-bottle' PET are neither biodegradable nor compostable; they are identical to fossil-based PE and PET. For a material to be considered compostable it has to fulfill a set of harmonized guidelines established under the main standards ASTM, ISO or EN. According to the European standard norm UNI EN 13432 (2002) for instance, a product can be defined as compostable if under defined conditions (58 °C for 12 weeks) it is for at least 90% converted under influence of microorganisms into water, carbon dioxide and biomass.[28]

The combination of the predicted polymer market growth and the emergence of new feedstocks is creating a great opportunity to develop and commercialize novel (sustainable) polymers. Polyesters derived from the renewable monomers glycolic acid and oxalic acid have been previously studied for applications where biodegradability is a relevant characteristic. However, their use has been limited to high-end industries (the biomedical field and the oil and gas sector). This is related to the significant effort that is still required to optimize upscaling of the production processes in order to reduce the manufacturing costs. In the last decade, CO_2 as a feedstock (CCU or Carbon Capture and Use) has seen increasing interest due to electrification and the accompanying need for energy storage. CO_2 is a valuable feedstock since it is naturally abundant, nontoxic, inexpensive, a non-oxidant and renewable. CO_2 can be used directly for applications such as enhanced oil recovery by CO_2 flooding[29] or as solvent[30] (especially in the supercritical state).

Another direct form of CO_2 utilization is the production of polyesters (polyhydroxyalkanotes (PHA)) through a biological process. Cyanobacteria and anoxygenic photosynthetic bacteria (e.g. purple sulfur bacteria) have been reported to produce PHA as an intracellular energy and carbon storage compound.[31] Purple sulfur bacteria for example, operates under anaerobic conditions.[32] With CO_2 being the only carbon source and sunlight being the sole energy source, this process is carbon efficient and much more sustainable than other processes for direct use of CO_2.[33] Although CO_2 possesses a low free energy (it is thermodynamically stable), there are reactions where no external energy input is needed because the co-reactant can supply enough energy to achieve sufficient conversion. Some examples of co-reactants are hydroxides, amines or olefins.[34] In other cases, a moderate energy supply is required and the reaction occurs by attaching the entire CO_2 moiety to the other reactant to make polycarbonates from epoxides and CO_2.[35-38]

Carboxylates, ureas, lactones, isocyanates and polycarbonates can be produced in this way. Muthuraj et al.[39] recently reviewed the progress on polymer blends of CO_2-based polymers and copolymers, with a focus on materials containing aliphatic polycarbonates. Finally, some reactions require high external energy supply in the form of heat, electrons or irradiation to produce reduced forms of CO_2 such as formate, formaldehyde and methanol. Amongst the strategies to reduce CO_2, the electrochemical route has received significant attention recently. Ganesh et al.[40] reviewed the developments in the electrochemical conversion of carbon dioxide into renewable fuel and chemicals. In this publication, the authors highlight some of the companies that are currently using this strategy to develop technologies to produce value-added chemicals or fuels. Liquid Light Inc., which was acquired by Avantium in 2016, is an example of a company that develops CO_2-based polymer building blocks. Their focus is on the 2 electron reduction of CO_2 to formate and the product tree therefrom (**Fig. 1.2**).

Fig. 1.2 The Liquid Light/Avantium CO_2 product tree.

Avantium is looking into existing and new polyester materials that can be produced from these CO_2-based building blocks. In fact, the production of CO_2-derived polymers as a Carbon Capture and Utilization (CCU) option is still in its infancy.[41]

Monomers and polymers represent more than 80% of the chemical industry's total product volume and 99% of the current feedstock for polymeric materials is fossil-based. A transition to renewable feedstocks is required to achieve a significant effect in reducing CO_2 accumulation. One can of course debate if the chemical use of CO_2 as a polymer building block will actually have an impact on the climate or not, even if these polymers would be deployed in bulk applications. It is, however, our firm belief that in order to reach the extremely ambitious CO_2 reduction targets defined in the Paris agreement (90% CO_2 emission reduction (versus 1991) by 2050) reduction of CO_2 emission is required in all sectors, therefore also in the chemical industry. This is also reflected in the European reduction targets as published by the European Committee (**Fig. 1.3**).
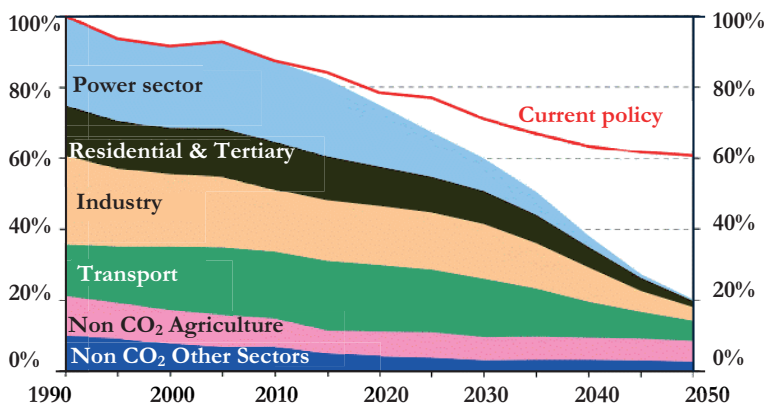
Fig. 1.3 EU GHG emissions towards an 80% domestic reduction (100% =1990). Reprinted from [42].

Taking all of this into account, this review intends to assess the state of the art and potential future potential of oxalic acid - and glycolic acid based polyesters and their copolymers. Synthesis methods, general properties, general degradation mechanisms, and recent and potential applications will be discussed. The application volume potential of these polyesters will also be assessed as a function of production cost for a wide range of applications.

It is important to note that polymers derived from CO_2 do not necessarily always lead to lower net overall CO_2 emissions (during production of after use, e.g. degradation in landfills). This needs to be evaluated using robust LCA's and this information is currently not available for the materials discussed in this review.

1.2 Polyesters as a promising CO_2 outlet

Polyesters are polymers built from repeating units linked together by ester groups. They have been proven suitable for numerous applications, in particular packaging, by providing ease of fabrication into structural materials such as films with excellent clarity, dielectric strength, tear resistance, dimensional stability, chemical inertness and good barrier properties. Polyesters can be synthesized with step-growth and chain-growth polymerization. In the first process, condensation products are formed by the reaction between bifunctional molecules, with each new bond created in an individual step. During initiation, monomers react to generate first dimers, trimers and longer oligomers. This trend continues until most monomer units are used. For polyesters, a straightforward approach for step-growth polymerization involves esterification reactions between dicarboxylic acids and diols.

High molecular weight polymers tend to appear only towards the end of the reaction, which implies that long reaction times and/ or high degrees of polymerization are necessary when this characteristic is required. Chain-growth polymerization involves chains with active endgroups that react with unreacted monomer. Unlike the step-growth polymerization, chain-growth polymers increase only from the chain-ends. Thus the chains expand linearly throughout the process. Radicals, carbanions and organometallic complexes are among the reactive endgroups for this type of polymerization. Common monomers for chain-growth include cyclic compounds such as lactones.[43] For certain polyesters, such as poly(lactic acid) (PLA) or poly(glycolic acid) (PGA), ring opening polymerization (ROP), via a chain-growth mechanism, is preferred over step-growth polymerization. With that approach polymers with high molecular weight, better processability and more accurate property control are obtained.[44]

1.3 Glycolic acid and its polyesters

1.3.1 Glycolic acid

DuPont has been one of the pioneers in developing and optimizing technologies to produce glycolic acid (GA). In 1939 they proposed a continuous process to form glycolic acid by a reaction of formaldehyde with water and excess carbon monoxide using sulfuric acid as catalyst.[45] The reaction was carried out at a pressure above 5 atm and at a temperature between 140 and 225 °C. As part of the continuous process, a solvent mixture containing GA, water and sulfuric acid was used to absorb formaldehyde and water in a gas scrubber. The obtained solution, containing approximately equal amounts of formaldehyde and water, was passed through a conversion chamber filled with glass beads, where it was contacted with carbon monoxide. The formaldehyde was then converted to give a product containing GA, water and sulfuric acid. Subsequently, a part of the GA was removed by distillation or

crystallization and the residue, still containing a high amount of GA, was returned to the scrubber to absorb more formaldehyde and water. In 2004, DuPont patented a technology using enzymatic synthesis to produce highly pure GA.[46] A flow of formaldehyde and hydrogen cyanide is reacted at 90-150 °C to produce highly pure glycolonitrile. The glycolonitrile is subsequently contacted with a biocatalyst with nitrilase activity, derived from the gender *Acidovorax facilis,* resulting in an aqueous solution containing ammonium glycolate. The GA, with a claimed purity of 99.9 %, is recovered from the aqueous ammonium glycolate solution using ion exchange. The energy requirements are lowered by implementing this enzymatic biochemical process, which is reflected in economic advantages for the overall production.

Glycolic acid is currently produced by ethylene glycol oxidizing microorganisms[47], or by hydrolysis of glycolonitrile.[48] Chemolithotrophic iron- and sulfur-oxidizing bacteria have also been used for producing glycolate.[49] The two leaders covering the glycolic acid market are DuPont and the Chinese company Zhonglan Industry Co. Between 1965 and 1966 the production capacity of Dupont was already estimated at 60,000 tons per year.[50] Furthermore, glycolic acid can be produced from formate, obtained from the electrocatalytic reduction of CO_2 in an electrochemical cell, as described in **Fig. 1.2** and paragraph 1.4.1.

1.3.2 Poly(glycolic acid)

The fact that glycolic acid is a monomer that can be obtained from CO_2 makes poly(glycolic acid) (PGA) a very appealing polymer from a durability standpoint. PGA is the simplest aliphatic polyester, since it possesses a linear molecular structure without any side chains (**Fig. 1.4 (a)**).
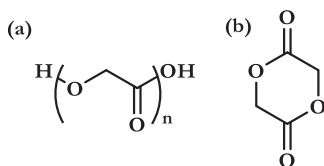
Fig. 1.4 (a) Poly(glycolic acid) chemical structure; **(b)** Cyclic diester of glycolic acid.

The first synthesis attempts by Carothers in 1932[51] did not succeed in the production of high molecular weight polymer. An improved strategy achieving this goal was reported in 1954, with a process to prepare PGA directly from glycolide (GL), the cyclic diester of glycolic acid (**Fig. 1.4 (b)**). GL was polymerized to PGA using ring opening polymerization (ROP).[52] One of the interesting properties of PGA is its relatively facile degradability (2-4 weeks in vivo[53]). This property has resulted in medical applications such as sutures.
PGA is hydrophilic and has a melting temperature (T_m) of about 225 °C, a glass transition temperature (T_g) between 35 °C and 40 °C, and a crystallization temperature (T_c) between 190 and 200 °C.[54] It is thermally stable until approximately 280°C. A weight loss of 3% has

been reported to occur at about 300 °C, according to the TGA thermogram (no heating rate or duration was stated).[55] The Melt Flow Index (MFI) reported for the commercial PGA resin is 22 ~6 g·10min^{-1} (at 2.16 kg of load and 250 °C).[56] It has been observed that the use of additives during processing, such as nucleating agents, plasticizers, antioxidants and catalyst deactivators, can deteriorate the melt stability of PGA.[57]

PGA has a density of 1.5 g·cm^{-3} and very high mechanical strength and toughness with an elastic modulus *(E)* of around 6.5 GPa and tensile strength (*σ*) of 220 MPa (commercial resin).[56] Bio-absorbable sutures was the first application that made use of these favorable mechanical properties.[58] Good barrier properties have been reported for PGA in several patents by the Kureha company. These properties have been compared to other important high barrier polymers for food packaging applications.[59-64] Interestingly, polyvinylidene chloride (PVDC), polyethylene vinyl alcohol (EVOH) and the polyamide containing meta-xylene groups (PA MXD6) show higher oxygen permeability (OP) under high relative humidity (RH) conditions compared to PGA[64] (**Table 1.1**). Furthermore, PGA has comparable water vapor permeability (WVP) (0.165 g·mL·m^{-2}·day^{-1} at 40 °C and 90% RH) to Nylon 12, the least water absorbable polyamide available on the market.[64] PGA is highly crystalline (46-60 %) compared to other biodegradable polymers such as polycaprolactone (PCL) and poly(*L*-lactic acid) (PLLA). It exhibits a very unique molecular and crystalline structure.

Table 1.1 Oxygen permeability of polyesters of interest.

Polymer	Temperature (°C)	RH (%)	OP (mL.mm.m^{-2}·day^{-1}·bar^{-1})	Reference
PGA	20	80	0.0135	[59,60]
PLA Biophan 121	23	50	20.25	[61]
PET	23	50	5	[62]
Polyethylene (PE)	23	50	200	[62]
EVOH 70% crystalline	20	100	0.15	[63]
PA MXD6	30	80	0.2	[64]

Montes de Oca et al.[65] have investigated the structure of PGA fibers using solid-state NMR spectroscopy; they proposed that the dipolar intermolecular interactions exist between adjacent chains packed in the crystal unit cell. This can explain the unusually high density of PGA and the slower degradation rate of PGA crystals than its amorphous counterpart.[66] In a different study, Yu et al.[66] investigated the crystallization and structural evolution of PGA via temperature-variable WAXD and FTIR analysis. The authors found that the intermolecular dipolar interactions and C–H···OC H-bonds were formed in the crystalline phase of PGA; this might explain the unusual physical performances of PGA compared to the other aliphatic polyesters. Furthermore, it was observed through polarized optical microscopy that PGA does not form normal spherulites but unique hedrites during crystallization. This differs from the typical morphology of other aliphatic polyesters with similar chemical structure (e.g. PLLA).

The high degree of crystallinity limits the solubility of PGA in most organic solvents with the exception of highly fluorinated organic solvents such as hexafluoroisopropanol (HFIP).[67] Although typical processing techniques, such as extrusion, injection molding and compression molding can be utilized to manufacture PGA products in the melt, rigorous control of operational conditions is required, given the polymer's high sensitivity to hydrolytic degradation.[68]

The Japanese corporation Kureha started commercial production of PGA in 2011 at the DuPont Belle plant in the USA with an annual production capacity of 4000 tons.[64] This established them as the world's first industrial-scale manufacturing facility for high molecular weight PGA with the trademark Kuredux®.[56,64] Kureha obtains its primary feedstock, glycolic acid, from the DuPont Belle site located in the same area.[50]

1.3.2.1 Polymerization techniques

Currently, the two most studied routes to polymerize PGA are polycondensation of glycolic acid (GA) and Ring Opening Polymerization (ROP) of glycolide (GL). In the direct polycondensation, water is formed as a condensation product. Complete removal of water is difficult, which is avoided when polymerizing GL.

1.3.2.1.1 Direct polycondensation of glycolic acid

One of the first reported PGA syntheses[69] was a polycondensation of GA (step growth polymerization) at 215-245 °C using antimony trioxide as catalyst, starting at atmospheric pressure and subsequently reducing this to 7 mbar. This (**Scheme 1.1**) did not become the preferred method for PGA production since the formation of water triggers the reverse reaction of the equilibrium, resulting in low molecular weight products.
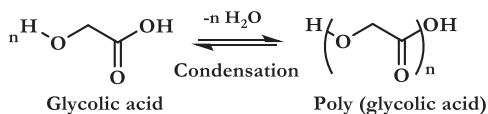
Scheme 1.1 Polycondensation of glycolic acid.

Two equilibrium reactions are involved in the polymer polycondensation: 1) the dehydration equilibrium for esterification and 2) the ring-chain equilibrium involving depolymerization to glycolide (**Scheme 1.2**). As explained by Takahashi et al.[70], the polycondensation reaction tends to generate an oligomer with low molecular weight. This oligomer decomposes into glycolide under high temperature and high vacuum conditions required for water removal, hindering chain-growth to high molecular weight polyester. This polymer degradation by formation of glycolide is in equilibrium with PGA formation.

(a)

(b)
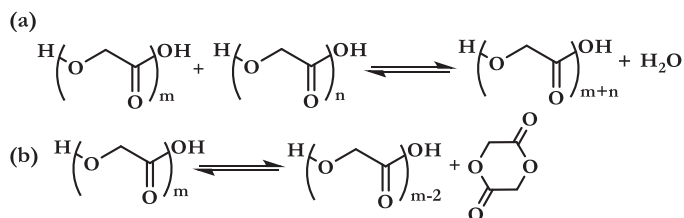
Scheme 1.2 Principal equilibrium reactions involved in PGA polycondensation.

In 2013, the VTT Technical Research Centre of Finland patented a simplified production method for producing high molecular weight PGA directly from GA.[71] The process is based on subjecting GA to condensation polymerization in the presence of a hydroxy-terminated monomer (e.g. hexanediol, butanediol) and stannous octoate ($Sn(Oct)_2$) as catalyst. The reaction is first carried out in the molten state under a nitrogen atmosphere; subsequently, the pressure is reduced in the course of four hours from 500 to 30 mbar and the temperature is gradually increased to 190 °C. Both the pressure and the temperature are maintained for 24 hours; the water formed during the condensation polymerization is continuously removed. The products formed have a number average molecular weight (M_n) of about 10.8 kg·mol⁻¹. This is too low for applications that require the other characteristics of this material, like crystallinity and good barrier properties. For this reason, the obtained products are considered "prepolymers" and are subsequently introduced in melt mixing equipment with a chain extender (e.g. diepoxides and diisocyanates) to provide a linear polymer having a M_n between 45.5 kg·mol⁻¹ and 52.3 kg·mol⁻¹. With the described procedure, the VTT technology provides telechelic polymers of glycolic acid. The term "telechelic" indicates that the polymers/prepolymers are capable of being subjected to polymerization through their reactive endgroups. In other words, the obtained prepolymer can be copolymerized with for instance a diisocyanate through reactive extrusion in a twin screw extruder. In this way, molded objects can be directly prepared once the high molecular weight has been produced.

1.3.2.1.2   Ring opening polymerization of glycolide

ROP of glycolide (GL) can proceed through anionic, cationic, or coordination mechanisms using antimony, zinc, lead or tin catalysts[52] (**Scheme 1.3**). GL is usually formed in a depolymerization process of PGA.[72] Initially, low molecular weight PGA oligomers are generated from the glycolic acid by esterification (step-growth polymerization). Subsequently, these oligomers are thermally degraded through intramolecular transesterification to cyclic dimers in a backbiting mechanism. The GL formed is isolated using overhead removal by operating under reduced pressure.
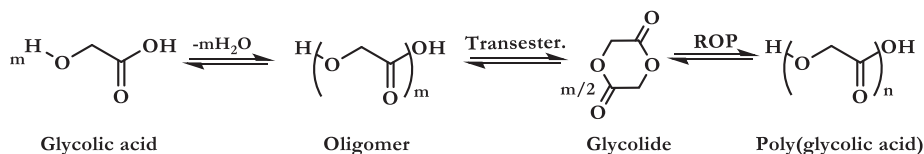
Scheme 1.3 Glycolide formation and ROP reaction of glycolic acid.

1.3.2.1.2.1 Glycolide formation

Bathia et al.[73] obtained GL with a continuous method by heating glycolic acid at 180-200 °C and gradually decreasing the pressure from 1000 to 200 mbar. The reaction occurred in the presence of an antimony catalyst (0.5-0.8 wt%) with depolymerization. However, the process generated polymers with strong viscosity, which complicated the material's flow. Because of this, further treatment was required to lower the molecular weight before it could be used for the glycolide preparation step. In 1993 DuPont patented an improved process[74] to obtain GL from glycolic acid oligomers using yttrium, rare earth metals, tin or antimony compounds as catalysts at relatively high amounts (2-6 wt%). The process was carried out at 180-280 °C starting at atmospheric pressure and reducing this gradually to 10 mbar with continuous distillation of the cyclic dimer. By increasing the catalyst concentration, the glycolide synthesis reactions can be accelerated relative to the dehydration reactions. In this way, the molecular weight and viscosity can be maintained at low, manageable level.

An improved methodology for synthesizing high purity glycolide for subsequent ROP polymerization was patented by the Kureha Corporation in 2014.[75] According to Yamane et al.[64], upscaling of the conventional method used until then to prepare GL had significant issues. One of them is the high viscosity and instability of GA oligomer, which makes effective heat transfer difficult. This can promote undesired side reactions like tar formation. Another issue occurs with the evaporated GL, since it tends to deposit and polymerize, resulting in obstructed distillation lines. The process proposed by the Japanese company involves initial solubilization of the oligomer using tetraethylene glycol dimethyl ether (TEGDME); a high boiling (280-420 °C) polar organic solvent. The mixture is heated to 240-290 °C at reduced pressure under inert atmosphere. Under these conditions, depolymerization reactions occur. The resulting glycolide and solvent are co-distilled out of the system and the GL is subsequently recovered. Because the obtained product is co-distilled with the organic solvent, the accumulation on the walls of the reaction vessel and distillation lines can be avoided. The mother liquor from which glycolide was isolated is then recycled to the process. In order to carry out the continuous depolymerization reaction in the same vessel, fresh amounts of the GA oligomer and organic solvent must be constantly supplied. By using this method, the production efficiency was improved and adverse reactions were suppressed.

Another issue in this process is the formation of organic acids, such as diglycolic acid (the ether formed from two glycolic acid molecules) and methoxyacetic acid, in the process, contaminating the GA oligomer. The acids were observed when using an industrial grade aqueous solution of glycolic acid for the GL production. The presence of dicarboxylic acids has a negative impact on the GL production process since dicarboxylic acids "seal" the hydroxyl termini of the GA oligomer and can suppress the depolymerization reaction. The above was solved by adding a diol (e.g. ethylene glycol, propylene glycol, and butylene glycol), which increases the solubility of the glycolic acid oligomer in TGDME and helps the depolymerization reaction system over an extended period of time. When the process is continuous, impurities can accumulate in the reaction system. These impurities can negatively affect the formation of glycolide, since a condensation reaction might compete with the depolymerization reaction. The authors found that when an alcohol is added in the depolymerization reaction system, the formation rate of glycolide is stabilized. They suggested that stoichiometric amounts of the alcohol react or otherwise combine chemically with the organic acid impurities. No explanation is provided for the high selectivity of the added alcohol for the acid impurities.

A. Cationic polymerization

In the late 1960's Chujo et al.[76] reported a ROP of glycolide catalyzed by Brønsted acids such as sulfuric acid and phosphoric acid. This strategy led to brittle and considerably colored polymers. PGA homopolymers and copolymers have been synthesized via ROP with other cationic catalysts such as iron compounds. Dobrzynski et al.[77] for instance produced copolymers with $Fe(acac)_3$ and $Fe(OEt)_3$ as initiators. According to the authors, the produced polymers exhibit similar mechanical properties to analogous copolymers obtained with $Sn(Oct)_2$ as the catalyst. Similarly, Sanina et al.[78] studied the cationic GL polymerization in the melt, catalyzed by antimony trifluoride (SbF_3). The research reported a narrow polymerization temperature window (160-175 °C). At temperatures below 160 °C at low conversion, the polymer was observed to solidify; above 175 °C, a decay of the active species was observed.

Similar thermal behavior was found for the bulk cationic polymerization of PGA catalyzed by a montmorillonite clay catalyst.[79] The cationic ROP mechanism (**Scheme 1.4**) was studied in the presence of Maghnite-H+ at 100 °C for 30 minutes. The authors propose that the GL monomer inserts into the growing chain via the acyl-oxygen bond scission rather than via the breaking of the alkyl-oxygen bond. Furthermore, the effect of temperature on the polymer yield after 3 hours at different weight ratios of Maghnite-H+ was studied. The polymerization of GL reached a maximum yield of about 95% using 15% of Maghnite-H+ content at 140 °C. Above this temperature, after 3 hours, the polymer yield is lower. Although the reported information for cationic ROP of GL is scarce, the studies for other lactones, such as lactide, may be utilized to predict the course of PGA synthesis through this pathway.
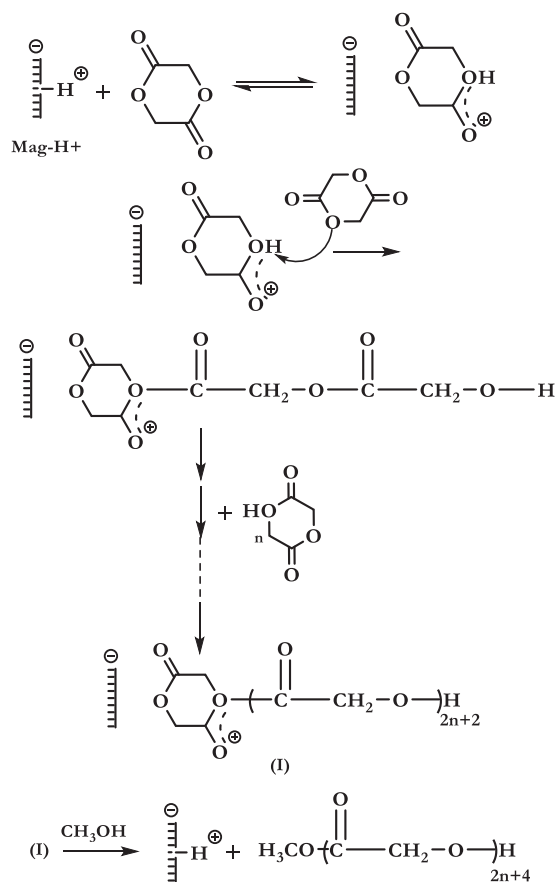
Scheme 1.4 Cationic ROP mechanism of glycolide catalyzed by Maghnite-H+. Adapted from [79].

B. Anionic polymerization

As is the case for lactide, possible initiators for this ROP include alkali metals, alkali metal oxides and alkali metal naphthalenide complexes with crown ethers, among others.[80] The general mechanism (**Scheme 1.5**) consists of initiation by nucleophilic attack of the negatively charged initiator on the carbonyl carbon.[81] Chujo et al.[76] reported that anionic polymerization catalysts, like KOH and pyridine, produce brittle and highly colored PGA with low yields. In a more recent study Baez et al.[82] synthesized nine different PGA oligomers through ROP of glycolide, catalyzed by ammonium decamolybdate $(NH_4)_8[Mo_{10}O_{34}]$ using aliphatic primary alcohols (ROH) as initiators/chain transfer agents at 190 °C for 15 minutes.
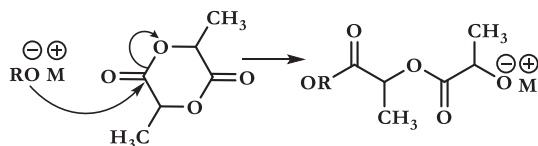
Scheme 1.5 Anionic initiation for PLA. Adapted from [83].

Different molar ratios of GL/ROH in the feed led to the generation of polymers with controlled M_n between 1.3 and 1.8 kg·mol^{-1}. Even with such a low number average molecular weight, the polymers where observed to be insoluble in common solvents like CHCl$_3$, THF, DMF or DMSO. The M_n was determined via NMR analysis in HFIP. The low solubility of PGA polymer in most common solvents complicates characterization. Published information related to anionic ROP of GL is currently limited. However, previous studies on lactones such as PLA may serve as information base to understand possible mechanisms translated to PGA synthesis.

C.   Coordination-insertion mechanism

Certain catalysts can act as coordination polymerization initiators and are capable of producing stereoregular polymers with narrow molecular weight distribution and controlled molecular mass with well-defined endgroups.[51] Some of these commonly used initiators include aluminum and tin alkoxides or carboxylates. The carboxylates are weaker nucleophiles and act more like a catalyst than an initiator when compared to alkoxides.[77] GL metal carboxylates are normally applied together with an active hydrogen compound as co-initiator in a manner analogous to that for PLA.[84] One of the most common catalysts for ring opening polymerization, especially for lactide, is stannous octoate (bis(2-ethylhexanoate)). According to previously reported studies on the topic, it seems that the most suitable explanation to describe the course of the reaction in lactides, is a coordination-insertion mechanism where a hydroxyl group is thought to coordinate to Sn(Oct)$_2$, forming the initiating tin alkoxide.[85] The insertion occurs in two steps, namely nucleophilic attack of the alkoxide on the coordinated lactide followed by ring opening. This leads to the insertion of lactide into the O-H bond of the coordinated alcohol (**Scheme 1.6**).[86]
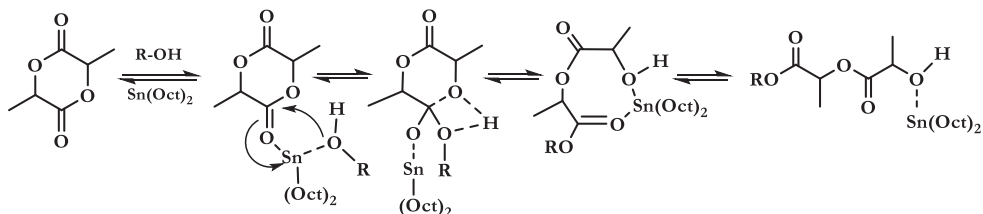
Scheme 1.6 ROP mechanism catalyzed by stannous octoate. Adapted from [87].

According to Kricheldorf et al.[88], the alcohol functionality and the dimer are both coordinated to the $Sn(Oct)_2$ complex during propagation and this coordination step can occur with retention of the octanoate ligands (Equation **(1.1)**) or with the liberation of octanoic acid (Equation **(1.2)**).

$$Sn(Oct)_2 + ROH \rightleftharpoons (ROH)Sn(Oct)_2 \qquad (1.1)$$
$$Sn(Oct)_2 + ROH \rightleftharpoons (RO)Sn(Oct) + OctH \qquad (1.2)$$

It has also been accepted that impurities (e.g. water, lactic acid, alcohols) in the monomer can act as co-initiators, especially when $Sn(Oct)_2$ is used without protic additives.[86] Possible side reactions, like chain transfer, intramolecular chain scission and termination, are still obstacles that can become important when transferring to industrial scale. Intermolecular and intramolecular transesterification reactions can be influenced by temperature, reaction time, type and concentration of catalyst or initiator, and the nature of the lactone.[89] In the case of organometallic initiators, long reaction times and high temperatures favor these reactions.

When using stannous octanoate as the catalyst, the general process for ROP of glycolide requires an initial temperature of approximately 175 °C, which can be gradually increased to 220 °C for a total reaction time of 2 to 6 hours.[90,91] Accurate thermal control is necessary, since the polymer starts degrading above 245 °C. In addition a highly pure acid-free GL is required to obtain high molecular weight polymer. The polymer's low solubility in most practical solvents, combined with the increase in melting point with growth, can easily lead to early polymer precipitation in the molten GL reaction medium at low reaction temperatures. This can limit the reaction yield and the molecular weight, which becomes an even bigger issue when scaling up the manufacturing process.

The complications of the traditional ROP method for PGA at mass production were overcome with a new technology proposed by the Kureha Corporation.[92] Once the pure GL monomer has been obtained, ROP is induced in the molten state and when the GL has completely reacted, the polymer is recovered as a solid to subsequently undergo solid state polymerization. Temperatures used in the process start with the melting point of glycolide (~90 °C) and increase as the polymerization progresses to that of the melting point of high molecular weight PGA (~220 °C). Overall, Kureha's technology allows easy recovery of the obtained polymer, resulting in superior production efficiency with reasonable operational costs.

In a different study, Fisher et al.[93] introduced branching points into the PGA structure. Branching is a specific example of transesterification reaction used for control of molecular architecture. The research combined ROP with condensation of a trifunctional AB_2 monomer, catalyzed by $Sn(Oct)_2$. An example of this is the copolymerization of GL with 2,2-bishydroxymethyl butyric acid (BHB). The authors achieved a structure with linear PGA segments of short average chain length between every branching point. As also observed by Wolf et al.[94] the branching led to a reduction in the degree of crystallinity. In research by

Mhiri et al.[95] two biodegradable PGA networks with different architectures, catalyzed by the same organometallic compound, were studied (**Fig. 1.5**).
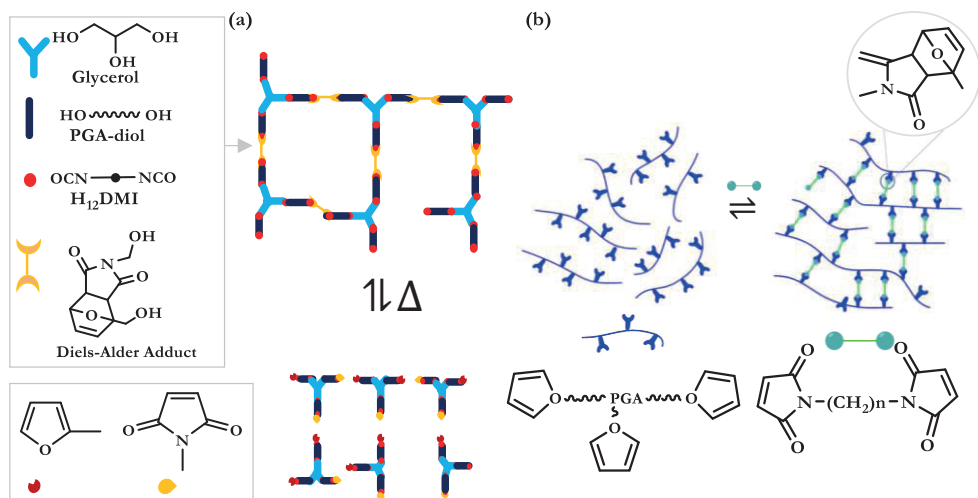
Fig. 1.5 (a) Preparation of first biodegradable network with PGA hydroxyl-telechelic oligomer, a bi-functional Diels-Alder adduct, a polyol and a diisocyanate; **(b)** Synthesis of the second biodegradable network using furan-functionalized prepolymers of GL and a multimaleimide cross-linker. Adapted from[95].

The first (**Fig. 1.5 (a)**) uses a one-step strategy by condensation of a PGA hydroxyl-telechelic oligomer, a bi-functional Diels-Alder adduct (from furfuryl alcohol and N-hydroxymethylmaleimide), polyols (glycerol or pentaerythritol) and a diisocyanate to generate thermoreversible structures; the Diels Alder reaction allows formation of reversible covalent bonds while preserving the possibility of re-processing.[96] The second architecture (**Fig. 1.5 (b)**) was synthesized using furan-functionalized prepolymers of GL and a multimaleimide cross-linker in stoichiometric amounts. Low molar mass networks were generated to facilitate the processing and dynamic rheological analyses were conducted to confirm the polymer's thermoreversibility. Furthermore, the viscoelastic behavior of the material was studied with a creep test. The observed long-term elastic behavior suggests successful formation of a chemically cross-linked network.

Temperature sweep tests were performed between 150 and 50 °C in order to determine cross-linking and decrosslinking temperatures of the systems and to confirm the reversibility of the polymer networks. At 135 °C, before the crosslinking starts, the system is liquid-like. With time and decreasing temperature, the network is gradually developed until densely connected networks are formed at 50 °C. Hence, the authors proposed that the lowest temperature within the studied range is the most suitable temperature to perform the crosslinking step, which occurs through the rebuilding of connections. Since the polymer undergoes gelation (with crosslinker connecting polymer chains) in response to heating/cooling cycles, re-processing is possible within this temperature range.

Furthermore, the influence of temperature on viscoelasticity was investigated with a frequency test. At 50 °C dominant elastic behavior was observed with a storage modulus (G') higher than the loss modulus (G") for all samples. The modulus values remained constant until 80 °C, but above this temperature they decreased until reaching a common value at 135 °C. The performance of these networks shows the potential of tailoring the thermal, mechanical and degradation properties of the polymer.

More recently, Aijun et al.[97] proposed a method for improving the thermal stability of PGA during processing; three dihydrazide metal chelators (**Fig. 1.6**) were synthesized and melt mixed with PGA in a twin screw extruder using stannous chloride (SnCl$_2$) as the catalyst. The chelator N,N-bis(salicyloyl) dodecanedioic acid dihydrazide (**Fig. 1.6 (a)**) showed the highest efficiency in improving the polymer's thermal stability by contributing to catalyst deactivation.
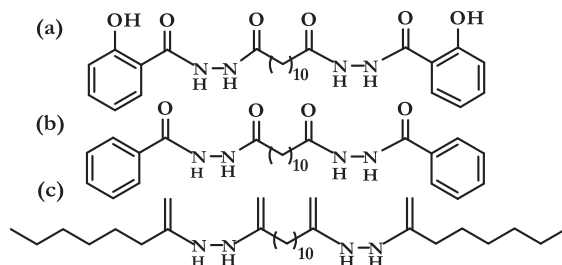
Fig. 1.6 Dihydrazide metal chelators melt mixed with PGA. **(a)** N,N-bis(salicyloyl) dodecanedioic acid dihydrazide; **(b)** N,N-bis(benzoic) dodecanedioic acid dihydrazide; **(c)** N, N-bis(heptyl) dodecanedioic acid dihydrazide.[97]

Polymer degradation studies were carried out at different temperatures (260-320 °C) in the presence and absence of this chelator, where the remaining PGA polymer weight percentage was followed in time. The TGA results (dT/dt= 10 °C·min^{-1}) revealed that at 240 °C the amount of remaining PGA is much higher in the presence of the metal chelator (88.5%) than for pure PGA (23.3%). Above 280 °C the thermal stabilization caused by the metal chelator is less significant. This research contributes to the development of more efficient PGA processing conditions, which could benefit commercial scale production. Nevertheless, the requirements for some of the previous protocols include high temperatures, multistep processes, high vacuum conditions and long reaction times, which are all unfavorable for the implementation at commercial scale. Until now, the majority of studies dealing with the property assessment of PGA (mechanical and barrier properties) have been performed by the Japanese corporation Kureha.

1.3.3   Copolymers with glycolic acid

Copolymerization of GL/GA with other monomers allows, among other advantages, the tailoring of properties by variation in the macromolecular architecture. At small scale, copolymers of PGA with different structures have been prepared mainly via ROP.

Studies have reported the decrease of melting/processing temperatures, improvements in mechanical properties and resistance to hydrolysis of PGA copolymers in comparison to the homopolymer. The effect of monomer sequence on the degradation rate has also been assessed.

1.3.3.1   Poly(lactic-co-glycolic acid)

Copolymerization of GL/GA with lactide has gained significant attention through the years since a wide range of products with modulated properties can be achieved through this approach. Poly(lactic-co-glycolic acid) (PLGA) is an aliphatic polyester of increasing interest for the biomedical field due to its biocompatibility and degradability in vivo. The mechanical and physicochemical properties of this copolymer are strongly determined by the ratio of the monomers.

Lactic acid (LA; 2-hydroxypropionic acid), the constituent unit of poly(lactic acid) (PLA) and one of the monomers for PLGA synthesis, is produced via fermentation or chemical synthesis and it has two enantiomeric forms: *L*- and *D*-lactic acid.[98] Therefore, PLA can be synthesized in three general forms: poly(*L*-lactic acid) (PLLA), poly(*D*-lactic acid) (PDLA), and poly(*D,L*-lactic acid) (PDLLA).[99] Most of the lactic acid produced for commercial purposes is made by the bacterial fermentation of carbohydrates (corn, beet and sugar cane) using homolactic organisms. Homolactic fermentation yields two molecules of lactic acid for every molecule of glucose, whereas heterolactic fermentation also produces CO_2 and ethanol.[100] PLA is currently the leading compostable and bio-based aliphatic polyester with a global production capacity estimated at about 210,000 tons in 2017.[101] Good barrier properties are not typically attributed to this material. Colomines et al.[61] reported an oxygen permeability (OP) of 22 mL·mm·m^{-2}·day^{-1}·bar^{-1} for amorphous PLA films at 23 °C and 0% RH. When compared to high demand fossil-based polymers, PLA has better oxygen barrier properties than the commodity plastic polystyrene (170 mL·mm·m^{-2}·day^{-1}·bar^{-1}) but it performs considerably worse than PET (0.2 mL·mm·m^{-2}·day^{-1}·bar^{-1}).

Most research done on PLA polymerization has focused on the ring opening polymerization of the cyclic lactide dimer. Lactide is obtained by depolymerization of low molecular weight PLA under reduced pressure resulting in *L*-Iactide, *D*-Iactide, or meso-Iactide. The generated percentages of lactide isomers depend on the starting polymer (isomeric form of the lactic acid), catalyst and temperature.[102] Castro-Aguirre et al.[103] reviewed the status of PLA production, processing techniques and applications. Their work also covers methods for tailoring PLA properties and degradation reactions by incorporating GL. In water,

PLGA degrades by hydrolysis of its ester linkages.[104] Because PLA has methyl side groups, it is more hydrophobic than PGA. PLGA copolymers rich in lactide, in consequence, are less hydrophilic and absorb less water, therefore degrading more slowly than PGA.[104] Furthermore, in PLGA copolymers, the degree of crystallinity is lower than in PGA.

PLGA's mechanical strength, swelling behavior and hydrolytic degradation rate are directly influenced by its degree of crystallinity. The latter is dependent on the distribution (random/regular) and molar ratio of glycolide/lactide in the copolymer chain and on the molecular weight of the polymer. Mechanical properties depend on monomer distribution, molecular weight, processing (e.g. 3D printed parts tend to fracture at much lower tensile stresses than injection molded parts[105]), crystallinity and lactide stereochemistry, allowing tuning towards the specific needs of the desired application. Commercial grades of PLGA include Purasorb® (Purac), Lactel® (Birmingham Polymers), Resomer® (BoehringerIngelheim), Medisorb® (Alkermes) and Vicryl rapide™ (Ethicon)[106] which all have different LA/GA monomer ratios: 50/50, 65/35, 75/25, 85/15 and 10/90, respectively.[107] Wang et al.[108] synthesized PLGA polymers with different LA/GA ratios (85/15, 75/25, 65/35 and 50/50) and found T_g values ranging from 27 to 30 °C. The T_g was found to increase with increasing molar percentage of lactide in the copolymer. According to the authors, the methyl group on the lactic acid moiety increases the rigidity of the polymer chain due to the steric hindrance. Increasing lactide content reduces the flexibility of the chains, therefore, increasing the T_g in PLGA. For these copolymers (85/15, 75/25, 65/35 and 50/50) an inherent viscosity between 0.55 and 0.75 dL.g have been reported.[109] Erbetta et al. [110] prepared polymers with 70/30 and 50/50 LA/GA and found amorphous structures for both of the copolymers with T_g's determined at ~35 and ~41 °C, respectively and the copolymers were found to thermally degrade above ~269 °C (PLGA$_{70/30}$) and ~276 °C (PLGA$_{50/50}$).

Sousa et al.[111] studied PLGA membranes for tissue regeneration. The samples were divided into three separate groups to investigate the following variables: heat, humidity and/or the effect of saline water as plasticizer. Plasticizing can augment plastic elongation and reduce brittleness. It can also contribute to reduced processing temperatures, reduced sticking to molds and enhanced wetting. The membranes from the first group were only dried at room temperature. The ones from the second group were plasticized in a saline solution at 55 °C for 10 seconds and then cooled down at room temperature, while the membranes from the third group were additionally cooled down in the saline solution until 10 °C. Tensile strength tests performed on the samples revealed a higher performance for the first group (16.7 MPa) when compared to groups II and III (14.6 MPa and 13.9 MPa, respectively). Although dried membranes showed the highest tensile strength compared to membranes that had only been plasticized or cooled after plasticizing, the differences are not significant enough to confirm that this is the most suitable option in terms of mechanical behavior.

Some of the general properties reported for copolymers with different LA/GA ratios are presented in **Table 1.2**.

Table 1.2 General properties of commercially available PLGA copolymers.

Polymer	T_g (°C)	T_m (°C)	T_d (°C)	σ (Mpa)	ε (%)	Degradation (in water)		Reference
						time (weeks)	T (°C)	
Poly(D,L-lactide-co-glycolide)85/15	50-55	*	n.r	64	3-10	5-6	37	[107,108]
Poly(D,L-lactide-co-glycolide)75/25	38-50	*	260-270	66	3-10	4-5	37	[107,108, 110,112]
Poly(D,L-lactide-co-glycolide)50/50	30-35	*	270-280	50	3-10	1-3	37	[107,108, 110, 112,113]
Poly(D,L-lactide-co-glycolide)10/90	40	205	n.r	111	n.r	6	25	[98]
Poly(glycolic acid)	35	225	280	117	13	2	99	[56]
D,L-poly(lactic acid) 50/50	55-60	*	250	60	10	9	37	[44,114]

* Amorphous; T_d = onset of decomposition; σ = Tensile strength; ε = Elongation at break; n.r = not reported.

1.3.3.1.1 Polymerization techniques

Similar to PGA, two synthetic strategies can be applied to synthesize PLGA. The first is a direct polycondensation reaction of lactic acid with glycolic acid, which tends to result in a low molecular weight polymer.[112] The second is ROP of lactide and glycolide, which allows the synthesis of high molecular weight copolymers with competitive mechanical properties.[72,110] The process parameters for both polymerization routes depend on the comonomer composition. Copolymers with high GL/GA content require temperatures closer to those used for polymerization of PGA. With higher lactide content in the feed, required polymerization temperatures are lower, comparable to those used for PLA synthesis.

A. Direct polycondensation
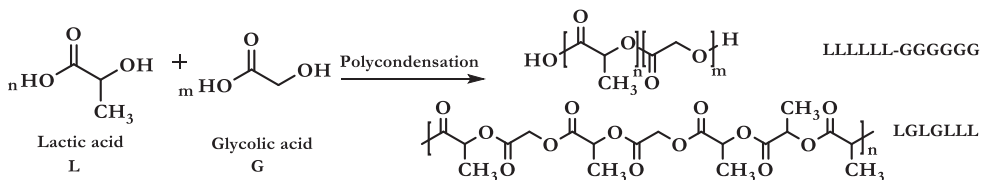
Scheme 1.7 Polycondensation reaction for PLGA production of block and random copolymers.

Ajioka et al.[113] prepared high molecular weight PLGA through a condensation reaction. *L*-lactic acid and glycolic acid were azeotropically dehydrated in diphenyl ether for 20-40 hours at 130 °C in the presence of a tin powder catalyst. Water was removed using a tube packed with molecular sieves mounted on top of the reactor. After the reaction, the mixture was

first concentrated by removing 50% of the volume, followed by chloroform addition. Catalyst was subsequently removed using an HCl solution. The final product, with a M_w of 160 kg·mol^{-1} and a melting point of 135 °C, was obtained after precipitation in methanol, followed by recuperation through decantation. These last purification steps are necessary to eliminate solvent traces, unreacted monomers and catalyst in order to generate a polymer with optimal properties for specific applications. Although high molecular weight polymers can be obtained with this method, the complexity and cost of the process are high compared to other strategies. Given the amount of solvent and anti-solvent this would require, such a process is essentially impossible to commercialize. Furthermore higher M_w fractions are more susceptible to precipitation, skewing the numbers to higher M_w's.

Gao et al.[115] synthesized PLGA (LA/GA 90/10 and 70/30) with high M_w (70 and 45 kg·mol^{-1}, respectively) inspired by a similar procedure of melt polycondensation using azeotropic removal of water. Initial dehydration of LA and GA into oligomers was followed by gradual heating to 180 °C at 130 mbar using equal amounts (0.5 wt%) of SnCl$_2$ and p-toluene sulfonic acid monohydrate (PTSA). Polymerization was maintained under these conditions for twenty hours. Interestingly, the study discusses the effect of GA addition on the racemization of PLA blocks. For this purpose, samples of poly(*D,L*-lactic acid) PDLLA and poly(*L*-lactic acid) PLLA were synthesized with the same process and used as the references of racemization for the microstructural analysis. At high temperature and high vacuum, ROP can induce the racemization of *L*-LA units and transesterification, which increases with initiator basicity and reaction time. This was found by Kricheldorf et al.[116] who studied the influence of various catalysts (metal oxides, carbonates or carboxylates) on the optical purity of poly(*L*-lactide). According to this research, the extent of racemization increases with increasing basicity of the catalyst. The authors suggested that deprotonation of the monomer is the main source of racemization, which is accelerated with increasing temperature. Gao et al.[115] stated that similarly to the ROP, racemization of *L*-LA units can also be induced in polycondensation of PLGA under high temperature and high vacuum. This racemization was found to increase with increasing fraction of glycolic acid. In the melt polymerization of PLLA with Sn(II) catalysts (e.g. SnO, SnCl$_2$) and TSA, the terminal groups of PLLA are coordinated with the catalyst center of Sn(II). TSA is used as a ligand to fill the open coordination sites of the catalyst, so side reactions that can lead to racemization of PLLA are prevented.[117] The authors suggested that in *L*-LA/GA copolymerization, the terminal groups of GA with high reactivity could be preferentially coordinated to the catalyst. Thus, the coordination of *L*-LA and TSA to prevent side reactions could be hindered. Consequently, racemization of PLGA increases with GA fractions.

The authors observed that PLGA's solubility in common organic solvents gradually decreased when the polymerization was carried out for up to six hours. With longer reaction time, the solubility of PLGA was improved. Such behavior suggests higher reactivity of GA, which may lead to PLGA copolymer chains containing GA rich blocks, formed initially and

L-LA rich blocks formed later rather than randomly incorporated sequences obtained when both monomers would have the same reactivity such as for example using *L*- and *D*-lactide.[113] This higher reactivity of GA compared to LA and other monomer combinations has been reported before[72] and can be explained by the fact that GA has a primary alcohol. In addition, GA is less stable and more prone to nucleophilic attack than LA.[118] The authors proposed that randomization via transesterification may reduce both GA and LA block lengths in a gradual manner, which can promote PLGA solubility and lower PLGA crystallinity. PLLGA$_{90/10}$ showed a degree of crystallinity of 25% with smaller crystallites than those of PLLA with 58% degree of crystallinity. Gao et al.[115] explained that the crystal lattice of *L*-LA blocks tends to exclude GA units, and that the incorporation of GA units in the *L*-LA blocks causes lattice defects.

B.   Ring opening polymerization of glycolide and lactide

Although the ROP route involves more steps than direct polycondensation, this is the preferred synthesis method when high molecular weight PLGA is desired (**Scheme 1.8**). Crystallinity and polymer properties can be modulated via the ratio of the monomers and the monomer distribution. Molecular weight control during polymerization is crucial when a specific application is targeted. In order to achieve this, some strategies are available: adjusting polymerization temperature, polymerization time, catalyst type and concentration, the vacuum profile and the addition of molecular weight controllers.[119,120]
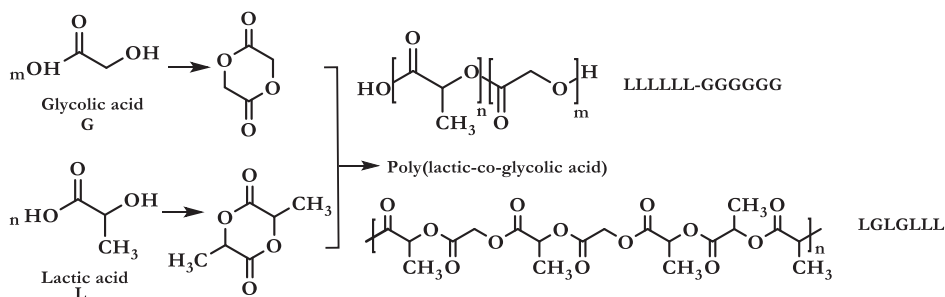
Scheme 1.8 General ROP for PLGA production.

In some cases, under appropriate polymerization conditions, the termination and transfer reactions can be limited to such an extent that the ROP can be treated as living. In a living polymerization, the propagating centers on the growing chains do not terminate and do not undergo chain transfer. When this occurs, a linear dependence between the mean degree of polymerization (DP) and the monomer to initiator molar ratio is observed.[86] As a consequence, controlled molecular weights and narrow distributions are obtained. However, under typical conditions for the copolymerization of glycolide and lactide the incorporation of glycolide induces primary alcohol chain ends, for which transesterification side reactions are likely to take place.[86] This was observed by Gilding et al.[72] when using

stannous octoate (0.3 wt%) as the catalyst at a reaction temperature of ~220 °C. Under these conditions, approximatively 80% of the monomers was converted to polymer within the first 30 minutes of the polymerization. An additional 3½ hours of reaction yielded a further 16% conversion, thus 96% was determined as the limit of the polymerization. The residual 4% consisted of glycolide and lactide in equal amounts. At reaction times over 4 hours, molecular weight distribution broadening was found as a consequence of additional transfer reactions. According to the authors, besides its role as polymerization catalyst, stannous octoate may also be associated with the growing chain in reversible chain transfer reactions. Additionally, temperature control is one of the essential actions in the polymerization process. If the temperature is too high, the reaction is thermodynamically unfavorable and the polymers can undergo depolymerization.[86]

Vacuum control as an alternative parameter to control molecular weight was found to be effective in the PLGA synthesis when keeping the other parameters constant.[119] However, it is not an easy factor to keep constant, especially at high vacuum (below 1 mbar). Other process variables, such as temperature, polymerization time and catalyst concentration, have not proven to affect molecular weight control, mainly when low molecular weight polymers are desired. The use of molecular weight controllers, such as lauryl alcohol ($C_{12}H_{26}O$), is a favorable option to control polymer growth. They react with the carboxylic endgroup of the growing polymer chain, which blocks the reactive group for propagation. Wu et al.[121] studied the effect of lauryl alcohol addition as a molecular weight controller on PLGA synthesis. A linear relationship between the amount of lauryl alcohol incorporated in the PLGA and the molecular weight was observed. These results showed a more accurate control of the polymerization process, which allows for improved reproducibility of the polymer's molecular weight.

Avgoustakis et al.[96] studied the effect of catalyst concentration on the molecular weight at different temperatures for ROP of lactide and glycolide using $Sn(Oct)_2$. At low catalyst concentrations an increase in the molecular weight was observed with increasing catalyst concentration for 130 and 190 °C. Interestingly, this behavior continued until reaching a maximum molecular weight after which a decrease in molecular weight was observed for the highest levels of $Sn(Oct)_2$ catalyst. Above 190 °C, the authors observed polymer decomposition and brown coloration. These results are in line with previous research by Gilding et al.[72], according to whom Sn^{2+} can accelerate both the polymerization and depolymerization rate.

Gorrasi et al.[122] recently reported an anionic mechanism for ROP of glycolide and *L*-lactide, using sodium hydride as the initiator. The synthesis was performed for three hours at 140 °C under inert atmosphere. Here, the sodium hydride did not only act as the initiator but also as reducing agent for the carbonyl groups. Based on the presence of alcohol-functionalized endgroups in the ^{1}H NMR spectra, the authors concluded that a hydride reaction involves cleavage of the acyl-oxygen bond of the cyclic diesters (**Scheme 1.9**).
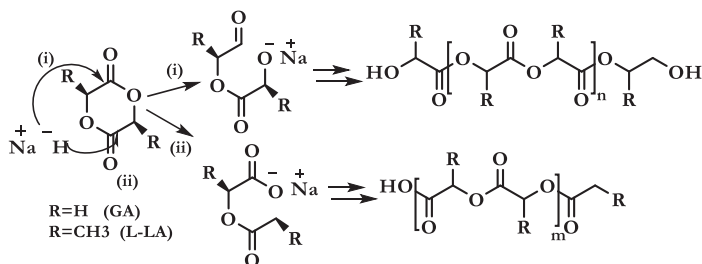
Scheme 1.9 Ring-opening polymerization initiated by NaH. Anionic initiation by cleavage of (i) acyl-oxygen bond and (ii) alkyl-oxygen bond. Adapted from [80].

According to Albertsson et al.[80], anionic polymerization can also occur through alkyl-oxygen cleavage, resulting in both carboxylate and alkoxide endgroups; this was confirmed in the study conducted by Gorrasi, who also observed the appearance of carboxyl endgroups in the MALDI mass spectra. The obtained polymer with random structure evidences the possibility of exploring less harmful, non-toxic catalysts (e.g. metals based on aluminum, zinc, yttrium, calcium, etc.) as alternatives to those generally used for polyester synthesis in general and PLGA synthesis specifically.

1.3.3.1.2   Polymers derived from PLGA

Currently, the majority of studies regarding PLGA copolymers have focused on biomedical applications. Copolymers of PLGA with polyethylene glycol (PEG), forming diblock (AB) or triblock (ABA or BAB) molecules, for instance, have been proposed for drug delivery applications, typically in the form of nanoparticles, hydrogels and micelles. PEG can be used as hydrophilic segment in copolymers with hydrophobic and biodegradable polyesters.[123] The absence of functional groups in PEG's structure prevents interactions with biological components.[124] Currently, polyethylene glycol (PEG) is often covalently bound to a drug or therapeutic protein ("Pegylation") to "mask" the agent from the host's immune system and increase its hydrodynamic size, which prolongs its circulatory time (effectiveness).

Wang et al.[125] reported the synthesis of PEG-PLGA nanoparticles (NPs) as carriers for arsenic trioxide, an effective therapeutic agent for acute promyelocytic leukemia used in medical treatment. The PEG-PLGA copolymer was prepared by ROP using *D,L*-lactide, glycolide (molar ratio 1:1) and methoxy poly(ethylene glycol) (MePEG) in the presence of $Sn(Oct)_2$ as the catalyst. The reaction was carried out at 180 °C for five hours under vacuum, forming a copolymer with a M_w of 16.5 kg·mol^{-1}. Subsequently, the product was used to prepare PEG-PLGA NPs via the emulsification solvent diffusion method. In vitro, the NPs exhibited a release time of more than 26 days. The same synthesis method has been proposed by Liu et al.[123] to produce PLGA-PEG micelles (amphiphilic block copolymers in aqueous solution) using a co-solvent evaporation method with different ratios of PEG, *L*-lactide and glycolide. The copolymer was dissolved in chloroform and the solution was

then mixed with water to induce microphase separation of PEG and PLGA blocks. Finally the solvent was evaporated under stirring and the micellar solution was filtered. Micelles of spherical shape with a diameter of about 50 nm were obtained. Interestingly, besides good compatibility in-vitro, it was observed that the composition and molecular weight of the copolymers do not affect this biocompatibility. In previous work by Tobio et al.[126] it was demonstrated that in a diblock conformation of PLGA-PEG, PEG chains orient themselves towards the external aqueous phase in micelles, surrounding the encapsulated species. The PEG layer acts as a barrier, reducing interactions with foreign molecules by steric and hydrated repulsion, improving the stability and therefore the shelf-life.

This coexistence of hydrophilic and hydrophobic properties within a polymer has been studied extensively for biomedical applications. In fact, an appropriate balance between these two types of blocks can lead to the development of valuable degradable materials as well as the formation of aqueous solutions that are able to generate a gel when exposed to heat (thermogelation).[127] Jeong et al.[128] prepared ABA type biodegradable thermal gels for drug release systems. The ROP of *D,L*-lactide and glycolide initiated by monomethoxypoly(ethylene glycol) led to the generation of a low molecular weight copolymer hydrogel: poly(ethylene glycol-*b*-(*D,L*-lactic acid-co-glycolic acid)) (PEG-PLGA). The diblock polymer was then coupled by hexamethylene diisocyanate to form ABA triblock copolymers. The obtained structures were water soluble, biodegradable, and thermally reversible. Furthermore, they could be injected as liquids and form a highly viscous gel in response to body temperature. For thermally responsive polymers, the PLGA hydrophobic units form associative crosslinks and the hydrophilic units of PEG guarantee that the copolymer molecules stay in solution. At low temperatures, the aqueous solution is dominated by hydrogen bonding between PEG segments and water molecules. With increasing temperature, the hydrogen bonding becomes weaker, while hydrophobic forces involving the hydrophobic PLGA segments are strengthened, leading to the formation of a gel.[104] Evonik (Essen, Germany), commercializes a PEGylated PLGA with a PEG content between 3 and 7 wt%. This product has a $M_w = 33.5$ kg·mol^{-1} and inherent viscosity of 0.93 dL·g^{-1}.[129]

In a different study, Ho Choi et al.[130] prepared degradable elastic matrices for scaffolds in tissue engineering using copolymers with a triblock ABA structure. PLGAs with different LA/GA ratios were used as the A block and PCL as the middle block. Because PCL has a very low T_g (~-58 °C) compared to PLGA (38 °C to 50 °C), it can provide elastic properties to the copolymer. As it exhibits a slower degradation rate than PLGA, the hydrolysis mechanism is slightly affected by this incorporation. For this research, the copolymers were synthesized through ROP using the terminal di-hydroxyl groups in PCL-diol as the initiator for the reaction and Sn(Oct)$_2$ as the catalyst (**Fig. 1.7**).
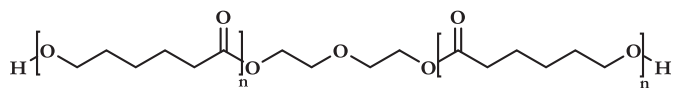
Fig. 1.7 Poly(ε-caprolactone) diol chemical structure.

Copolymers with amounts of LA equal and higher than GA (LA/GA 50/50 and 75/25) exhibited the lowest T_g values of 22 °C and 28 °C for relatively low M_n values of approximately 10.6 and 9.2 kg·mol^{-1}, respectively. It was observed that an increase of the M_n of P(LGA-CL-LGA) up to 40 kg·mol^{-1} caused the T_g values to shift to 35 °C (LA/GA$_{50/50}$) and 44 °C (LA/GA $_{75/25}$). Tensile tests were carried out for these two samples at 20 °C and 50% RH. According to the authors, both copolymers showed an elastic and rubber-like behavior in comparison with PLGA. Although the values observed for mechanical strength of PLGA/PCL 50/50 and 75/25 were considered low (2.4 and 1.9 MPa), the elongation at break reached very favorable values of 401% and 478%, respectively. These copolymers were found to be suitable for making porous elastic scaffolds. PCL, however, is hydrophobic and lacks physiologically active sites, which is unfavorable for cell growth when it comes in contact with the living body.[131] The copolymerization with PLGA may improve in vivo assimilation, but to be implemented, it must also guarantee optimal cell adhesion and proliferation.

1.3.3.2   Other copolymers of PGA

Wolf et al.[94], prepared PGA-based multi-arm star block copolymers containing between 62 and 91 wt% of GA. The structures were prepared through ROP of GL in the melt using a multifunctional hyperbranched polyglycerol (PG) macroinitiator. Hyperbranched copolymers with PGA arms were obtained by varying the initiator/monomer ratio. The resulting PG/PGA copolymers had molecular weights up to 31 kg·mol^{-1} and had a better solubility than PGA. This architecture favors a high molecular weight product with short average arm length. A slight increase in T_g with polymer growth was also observed. Furthermore, a decrease in the T_g and T_m values compared to PGA homopolymers with similar molecular weights was found for the copolymers with 60-76 wt% GA. For copolymers with higher GA content, higher crystallization tendency was observed in the DSC thermogram. The difference in thermal behavior can be translated into lower processing temperatures which in the case of PGA is beneficial given its thermolabile character. The above may also result in lower manufacturing cost. Additionally, with the increased amount of highly reactive endgroups the structure is more prone to hydrolytic degradation, a feature that is potentially beneficial for certain types of packaging and for biomedical applications.

Copolymerization of GL with ε-caprolactone (CL), trimethylene carbonate (TMC) and lactide has been studied (**Scheme 1.10**); Pack et al.[132] performed detailed research on microstructure, thermal properties and crystallinity of GL and CL copolymerized in bulk by

ROP at temperatures between 150 and 210 °C. Stannous octoate was used as the catalyst and various reaction temperatures, times, and comonomer feed ratios were investigated. The results showed that glycolide was polymerized preferentially in the first stage and the CL was incorporated later. After ten hours of reaction, the comonomer composition in the product was identical to that of the monomer feed.
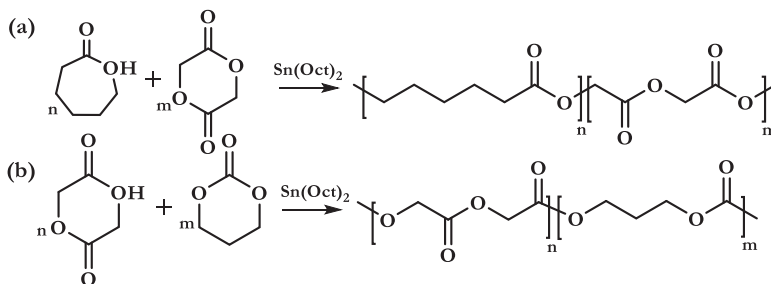
Scheme 1.10 ROP of GL with PCL and TMC catalyzed by Sn(Oct)$_2$.[132]

GL/CL$_{50/50}$ copolymers with an M$_n$ of 81 kg·mol^{-1} (by GPC) were reported.[132] The resultant reactivity ratios of the caproyl and glycolyl units (defined as the ratios of the propagation rate constants kCC/kCG and kGG/kGC) were calculated as 0.13 and 6.84, respectively. This confirms the highly reactive character of GL reported in other work. In terms of thermal properties, the crystalline phase of polyglycolide was observed to have ordered block characteristics and was not significantly affected by the contributions of internal defects with respect to T$_m$ decrease. The sequence length calculated from the reactivity ratios showed that copolymers with a random distribution are produced at GL content of 50% and lower. Furthermore, it was found that the nature of the sequence distribution also has an effect on the T$_m$ of GL/CL copolymers, together with the composition.

Later, Dobrzynski et al.[133] and Li et al.[134] reported a series of studies where the same copolymer was prepared through ROP using various compositions of monomers with Sn(Oct)$_2$ or zirconium(IV) acetylacetonate Zr(Acac)$_4$ as initiators. The structure-property relationships for the polymer degradation mechanism were reported. Results showed that transesterification is enhanced when high temperatures are used and when Zr(Acac)$_4$ is used as initiator instead of Sn(Oct)$_2$. The copolymers synthesized at low temperature (100 °C) had a more or less blocky chain structure that according to the authors can be attributed to the high reactivity difference between the two monomers GL and CL and the limited transesterification reactions during/after polymerization under low temperature conditions. Increasing the reaction temperature to 150 °C significantly changed the copolymer microstructure, leading to a reduced average block length and a higher degree of randomness because of an increase in transesterification reactions. It was observed that the degradation rate also depends on the chain microstructure and crystallinity rather than only on the copolymer composition. The crystallinity of each compositional component in the

copolymer is associated with the block length. Because in general copolymers with a high degree of randomness showed a short average block length and an amorphous structure, their degradation rate was faster than the degradation rate observed for copolymers with a more blocky chain microstructure. The authors state that glycolidyl sequences (GG) can undergo bond cleavage as a result of transesterification reactions, which lead to the formation of sequences with odd numbers of glycolyl (G) units, such as -CGC- and -CGGGC-. Usually, copolymers with a high degree of randomness exhibit fast degradation However, in this study it was found that unexpectedly these sequences showed more resistance to hydrolysis than C-C sequences showed more resistance to hydrolysis than C-C sequences and in consequence the degradation residues at the latest stages of degradation were composed in their majority of sequences linked by -CGC- and -CGGGC-units.

Copolymers with improved mechanical properties can be obtained by combining the stiffness of highly crystalline polyglycolide with the elastomeric characteristics of poly(trimethylene carbonate) (PTMC). A copolymer constituted of both elements (65% GL and 35% TMC) is currently commercialized under the trademark Maxon™ as a bioabsorbable monofilament suture. Celorio et al.[135,136] have synthesized copolymers with variable TMC architectures and compositions (close to 32.5% TMC as in the case of Maxon™) through ROP and reported the influence of the microstructure on the final properties. The synthesis proceeds in two steps: first, a middle soft segment with a theoretically random distribution of the two monomer units is prepared by copolymerization of GL and TMC. This is followed by incorporation of two hard segments (60 wt% of the total content) at each end of the middle segment by polymerization of glycolide. Although significant transesterification was observed during the first step of the process, the addition of the hard blocks did not influence the transesterification percentage. Good miscibility of the two monomers was observed and a strong influence of the length of the polyglycolide hard segments on the thermal properties was demonstrated.

According to the thermogravimetric analyses, all the synthesized copolymers degrade in a similar fashion upon heating, despite the differences in microstructure, ranging from a random to a blocky monomer distribution. It was reported that microstructure did not have a strong influence on thermal degradation temperature, since a maximum weight loss was observed close to 344 °C for all samples in the TGA thermogram ($dT/dt = 10$ °C·min^{-1}). This suggested transesterification reactions during the heating run, which can lead to a random microstructure independently of the initial monomer distribution or also, a possible stabilizing effect caused by the presence of polyglycolide units. According to the authors the degradation mechanism proceeded via a non-radical backbiting ester interchange.

1.4   Oxalic acid and its polyesters

1.4.1   Oxalic acid

Numerous methods for oxalic acid synthesis are known in the art, but only some of them are utilized at commercial scale while the others are still at the research stage. Asia is estimated to be the largest consumer of oxalic acid in the world by volume with China as a major consumer, producer and exporter.[137] In 2016, the total production of oxalic acid in China exceeded 200 kilo tons.[138] Some other major players in the oxalic acid market include Ube industries in Japan, Oxaquim S.A in Spain and Indian Oxalate.

Oxalic acid can be commercially produced via the oxidation of carbohydrates, such as glucose, sucrose, starch, dextrin and cellulose, with nitric acid in the presence of sulfuric acid and a catalyst, such as vanadium pentoxide or other vanadium compounds, molybdenum or manganese.[139-141] The process is highly exothermic with large amounts of heat generated, especially during the first stages of the reaction. Since the reaction is very sensitive to temperature, a controlled range between 65 and 70 °C is required to avoid side reactions and thus optimize oxalic acid yield.[141] Other commercial processes, such as the ethylene glycol process, propylene process dialkyl oxalate process and sodium formate process have been reviewed by Sawada et al.[142]

Some setbacks of the initial nitric acid based synthesis methods were mainly related to the high cost of recovery of oxides of nitrogen formed in the reaction. This situation was addressed later by other researchers. Fuchs et al.[140] for example, proposed a process where the nitrogen oxides that escape the reaction medium are led to an absorption system to be oxidized in nitrogen dioxide, which can be recirculated to the reactor with the mother liquor.

Another reported strategy is the oxidation of propylene with nitric acid or with a mixture of sulphuric and nitric acids.[143] The intermediate oxidation products α-nitratolactic acid and lactic acid subsequently reacted in the presence of oxygen to produce oxalic acid. Suitable catalysts include sulfite, nitrate, chloride or phosphate salts of iron, aluminum, chromium, tin or bismuth, ferrous oxide and ferric oxide. Continuous research and improvement of the production techniques have been crucial to large-scale oxalic acid production. In 1971 the Japanese company Mitsubishi patented a method for oxalic acid production that is still used today. The process starts from oxidizing ethylene glycol or glycolic acid in an atmosphere of molecular oxygen with nitric acid and/or sulphuric acid, using a vanadium compound as the catalyst.[144] In conventional processes, gases such as nitrogen monoxide or molecular nitrogen which are not converted to nitric acid, are formed during oxidation. In the proposed process, the formation of those by-products is prevented. Furthermore, when nitrogen oxides are oxidized with oxygen containing gas and absorbed in water for producing nitric acid, the gases and the water require cooling for a sufficient oxidation rate and absorption efficiency to make it an efficient process. If the water contains sulfuric acid,

the efficiency of absorption is significantly decreased, and a large absorber is required. Since such absorber can become more expensive than the main reactor, this represents an important economical drawback. With the above, the new process eliminates the need for large absorbers for the generated nitrogen oxides and results in a yield of 90-94%.

Another successful process, using carbon monoxide (CO) to prepare a diester of oxalic acid (starting material for oxalic acid production), was reported by the Japanese company UBE Industries.[145-147] The synthesis utilizes a co-catalyst in order to increase selectivity and catalyst lifetime compared to the conventional processes using CO reported before.[148] Traditionally, the mechanism consists of reacting CO with an ester of nitrous acid in the gas phase at a temperature between 80 and 150 °C at 1-5 bar pressure (Equation **(1.3)**). This improved process is carried out in the presence of a heterogeneous catalyst. The oxidative carbonylation generates nitric oxide as a byproduct, which is recirculated through reaction with an alcohol. This, together with the oxygen fed in the reaction medium, leads to the formation of nitric esters.

$$2CO + 2RONO \rightarrow \begin{array}{c} COOR \\ | \\ COOR \end{array} + 2NO \quad R = alkyl\ or\ cycloalkyl \quad (1.3)$$
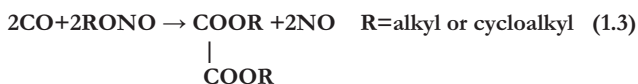
More recently, new technologies to produce oxalic acid from carbon dioxide (CO_2) by electrochemical reduction have emerged. The goal of mitigating harmful CO_2 emissions by converting them into economically valuable materials such as fuels and industrial chemicals, is currently gaining relevance for many industries. This so-called Carbon Capture and Utilization (CCU) is a superior long term solution than the costly Carbon Capture and Storage (CCS). The former company Liquid Light, now part of Avantium in Amsterdam, developed a process to convert CO_2 to formate and formate to oxalate at the start of the decade. The process involved the electrocatalytic reduction of CO_2 in an electrochemical cell. The formate is subsequently passed through a thermal reactor in the presence of a base catalyst to produce oxalate. Oxalate is then converted into oxalic acid by a membrane-based electrochemical acidification process. In a collaboration with Liquid Light, Lakkaraju optimized the formate to oxalate coupling reaction and elaborated on the reaction mechanism.[149] An alternative strategy consists of reacting CO_2 with a metal hydroxide, which generates a stream of metal bicarbonate ($MHCO_3$), which can be reduced to formate. The Shell Oil Company utilizes a similar process where formate is generated by reacting $MHCO_3$ with hydrogen.[150]

1.4.1.1 Polymerization techniques

In 1996 Pinkus et al.[151] patented a process to produce a poly(methylene oxalate) (PMO). The polymer was prepared by dissolving bis(tetrabutylammonium) oxalate in chlorobenzene and methylene bromide (CH_2Br_2). The solution was refluxed for about 6 hours and then

cooled to room temperature. Subsequently, the precipitate formed was recovered by centrifugation and washed with methanol. The product was nonflammable, resistant to high temperatures (above 430 °C) and insoluble in common organic solvents. According to the authors, this material would be suitable for applications that require light weight and exposure to elevated temperatures (e.g. structural material in air craft and space vehicles).

One of the first established methods for the synthesis of polyoxalates was proposed by Carothers et al. in 1930[152] and later reported again by the same authors, in a simplified manner. The methodology consisted of the preparation of linear condensation polymers with high molecular weight, capable of being drawn into fibers. Subsequent studies adopted this method for polyoxalate synthesis[153,154]: the general protocol involves a two step melt polycondensation of an oxalic acid diester and a diol (**Scheme 1.11**), with an initial pre-polymerization reaction taking place in a reactor under inert atmosphere.
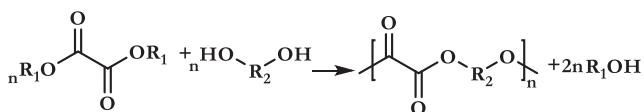
Scheme 1.11 Polycondensation of an oxalic acid diester with a diol.

The reaction mixture is gradually heated above 100 °C and the reaction pressure is first maintained at atmospheric pressure while allowing the resulting alcohol to distill off as the prepolymer is obtained. As for the PGA-based polymers discussed previously, rigorous control of the water content, especially at the start of the reaction, is important to obtain a high molecular weight polymer. Preferred catalysts for the first polymerization stage include titanium alkoxides like titanium tetrabutoxide, antimony compounds like antimony trioxide, and tin compounds such as butylindilaurate.[154] Once the alcohol has ceased to distill at the first stage of the reaction, the second stage, where the principal polymerization occurs is executed. At this point, the pressure in the reactor is reduced, combined with suitable continuous heating under a nitrogen atmosphere. The reaction proceeds with the removal of the remaining excess alcohol. The final product is cooled gradually to room temperature.[154] This approach has also been used for the synthesis of poly(alkylene oxalates) with diols such as ethylene glycol, 1,3-propanediol,1,4-butanediol or 1,6-hexanediol in combination with diethyl oxalate or dimethyl oxalate.[153,155-157]

Different methods have been proposed for producing high molecular weight polyoxalates (POX). Synthesis via ROP of a cyclic oxalate monomer has been reported exclusively for the preparation of poly(ethylene oxalate). The cyclic monomer can be obtained by heating oligo(ethylene oxalate) with subsequent depolymerization under nitrogen atmosphere.[158-160] The depolymerization is performed at 190-220 °C and a pressure of 0.03-13.5 mbar. This is followed by purification of the cyclic monomer by recrystallization.[160] The ROP is conducted by heating the cyclic monomer to a temperature lower than 200 °C in the presence of a catalyst at ambient pressure under an inert atmosphere. An alternative process

for the preparation of the cyclic ethylene oxalate consists of preparing a mixture of ethylene oxalate oligomer dissolved in a high boiling solvent (285-420 °C), which is subsequently heated to a temperature (235-245 °C) at which depolymerization of the oligomer occurs. This additional heating of the solution leads to the formation of the cyclic monomer, which is then distilled out together with the polar organic solvent.[158] A POX with a density of about 1.48 g·cm^{-3} measured in amorphous state and a melt viscosity of 30 Pa·s (determined at 190 °C and a shear rate of 1000 sec^{-1}) was claimed to result from this synthesis method.

Some of the mentioned polyester resins have been produced using oxalic acid as starting material.[44,152,161,162] Alksnis et al.[161] reported a two-step polycondensation reaction for the production of high molecular weight PEOX from ethylene glycol and oxalic acid in the presence of benzene and thorium carbonate as the catalyst. The process was initiated with oligomer synthesis at low temperature (below 80 °C) followed by a second stage where the oligo (ethylene oxalate) was subjected to transesterification in the melt at 170-180 °C for six hours under argon flow. The thermal conditions were selected in view of the melting temperature (170 °C) and the decomposition temperature (230 °C) of PEOX. Temperature regulation is crucial for this synthesis, since it has been reported that oxalic acid can decarboxylate to CO_2 and formic acid when heated above 140 °C. In fact, this decarboxylation may occur at lower temperatures, influenced by the reaction medium (e.g. solvent, water content, oxalic acid concentration etc.). This also influences the degradation pathway, as there are several ways oxalic acid can decompose.[163] Furthermore, the presence of formic acid leads to blocking of the polyester's hydroxy groups.[13] Decomposition to formate seems to increase steadily until no more free oxalic acid/oxalic acid ester endgroups are present. This shows that even if oxalic acid reacts once with an alcohol to form the ester, there is still the possibility for decomposition at temperatures above 140 °C.[163]

1.4.1.2 Oxalate based polymers

Oxalate based polymers were first introduced in the 1970's for suture coating purposes. According to the type, they may provide easy control of physicochemical properties such as biodegradability, crystallinity and mechanical strength.[164] Linear polyesters of oxalic acid and diols have been reported as materials with, among others, a high melting point, soluble in a wide range of solvents, capable of forming biaxially or uniaxially oriented films and fibers.[153,158] Interestingly, the hydrophobicity of this family of polymers has been registered between that of PGA and PLA.[165]

Reports on the thermal and mechanical behavior of certain polyoxalates (POX) have led to revealing the promising potential of these types of materials for applications where tailored degradation after use of the products would be favorable to implement. Poly(alkylene oxalates), a group of polymers derived from aliphatic diols with oxalic acid, have been studied for biomedical applications and reported to be absorbable with minimal adverse

tissue reaction. Good mechanical properties and ease of processability have also been attributed to this polymer type used for surgical devices. In the late 1970's Ethicon[153] patented the use of poly(alkylene oxalates) as fibers for synthetic absorbable sutures. These fibers exhibited a tensile strength of about 237-344 MPa, a Young's modulus of 1.2-1.3 GPa and 32-39% elongation at failure. This is comparable to Vicryl 2.0 , an absorbable polymer typically used for sutures, derived from lactide and glycolide (tensile strength of 262 MPa).[166] Later, Kim et al.[167] synthesized and characterized a semicrystalline polymer of this type, intended for biomedical applications. The resulting product was composed of a flexible linear aliphatic chain, which exhibited a T_c and T_m of 90 and 160 °C, respectively.
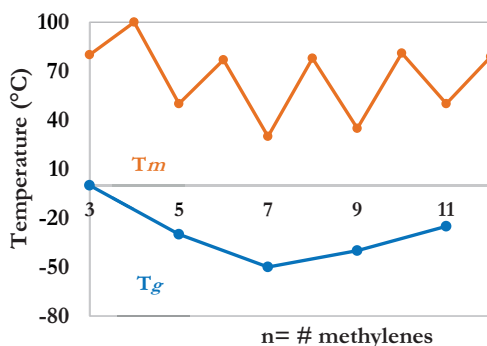
Fig. 1.8 Glass transition temperatures and melting temperatures for poly(alkylene oxalates) with an increasing number of methylene units (n=3-12).[168]

A more recent study on poly(alkylene oxalates)[168] revealed that different thermal behavior occurs as a function of the number of methylene units in the diol (n). Polymers with a higher T_m were found for an even number of methylene units n, compared to those with an odd n (**Fig. 1.8**). For polymers with an even n, the T_g could not be measured. The same study established that rigidity, T_g and T_m of the structure can be increased by including rigid comonomers, such as aromatic diols, into the polymer backbone.

Resorcinol bis(hydroxyethyl) ether (RBHE) or hydroquinone bis(hydroxyethyl) ether (HBHE) and the aliphatic diol 1,10-decanediol (**Fig. 1.9**) were investigated. The polymer's T_m decreased with increasing aromatic comonomer content up to 40%. Above 50% aromatic comonomer content, the T_m increased steadily with increasing aromatic comonomer content. The behavior encountered initially is presumably due to the aromatic units functioning as chain defects in the poly(decylene oxalate).[168] Although poly(alkylene oxalates) offer sufficient mechanical behavior, in general a significant limitation for certain applications is related to the unsatisfactory thermal properties.

(a)

(b)

(c)
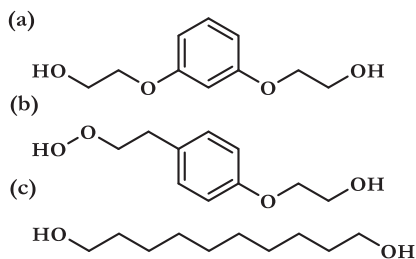
Fig. 1.9 Chemical structures of (a) Resorcinol bis(hydroxyethyl)ether; (b) hydroquinone bis(hydroxyethyl)ether; (c) 1,10-decanediol.

Alksnis et al.[161] synthesized and reported a poly(ethylene oxalate) (PEOX) with fiber forming properties and a T_g and T_m of about 32 °C and 178 °C, respectively. Later, Shiiki et al.[158] claimed the production of a PEOX with the same molecular weight, crystalline properties, excellent behavior for melt processability and good degradability in soil. The authors tested the mechanical properties of some biaxially oriented PEOX films. A tensile strength of 240 MPa, a modulus in tension of 5.2 GPa and a 75% elongation at break were found when the films were stretched at 40-45 °C. More satisfying mechanical behavior was observed for filaments stretched at 50-55 °C, with a modulus in tension of 100 GPa, a tensile strength of 500 MPa and a 30% elongation at break.
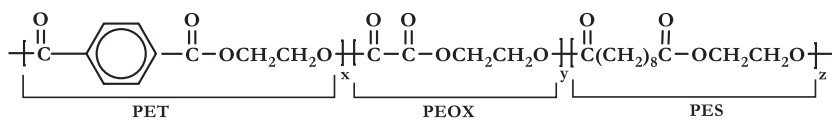
Fig. 1.10 Structure of poly(ethylene terephthalate-co-oxalate-co-sebacate) (PETOXS).[169]

Zhao et al.[169] investigated materials derived from diethylene oxalate (DEOX), poly(ethylene sebacate) (PES) and PET (**Fig. 1.10**). The resulting poly(ethylene terephthalate-co-oxalate-co-sebacate) (PETOXS) showed an augmentation on the Young's modulus and a maximum tensile stress with increasing content of PEOX in aliphatic units: 60/24/16 PET/PEOX/PES had a tensile strength of 7.6 MPa and a modulus in tension of 0.039 GPa, while 60/32/8 PET/PEOX/PES showed a tensile strength of 23.6 MPa and a Young's modulus of 0.584 GPa. A contrary result was found for the elongation at break, which decreased from 478% to 170% for the above-mentioned copolymers.

A thermal stability up to ~390 °C was reported for this polymer. Higher melting and crystallization temperatures were observed for the sample with a higher PEOX content. According to the authors, the effect of PETOXS composition in the crystallization mechanism is not straight forward, as it can act in two ways. On the one hand, the aromatic repeating unit of PET and the aliphatic unit of PEOX are more rigid than the aliphatic unit of PES, which may favor easier formation of regular crystalline entities. On the other hand, when the flexible units of PES are added to the main chain, segments of copolyesters tend

to have improved mobility, which can lead to rearrangements, therefore increasing the crystallinity. In another study, interesting barrier properties have been found for films made of PEOX blended with PLA;[154] an oxygen permeation of 4.8 mL·mm·day^{-1}·bar^{-1} was observed at 23 °C and 65% RH and a water vapor permeation of 1.6 g·mL·m^{-2}·day^{-1} was measured at 40 °C and 90% RH. This is comparable to PVC, which shows an oxygen permeation of 2-8 mL·mm·day^{-1}·bar^{-1} and a water vapor permeation of 1-2 g·mL·m^{-2}·day^{-1} at 23 °C and 85% RH.

The crystallization mechanism and microstructure of another POX derivate, poly(butylene oxalate) (PBO), was studied by Kuo et al.[155] The DSC analysis for different PBO crystals revealed T$_m$ ranging from 99.8 °C to 102.2 °C at crystallization temperatures between 70 °C and 85 °C. Furthermore, a morphological study showed the formation of thicker crystalline layers at the highest crystallization temperatures. Independently, the thermal behavior of PBO copolymerized with azelaic acid (nonanedioic acid) was studied;[170] The copolymers were found to be partially crystalline and thermally stable up to ~290 °C. At room temperature, all the synthesized samples appeared as semicrystalline, with the same crystal structure as the PBO polymer. According to the authors, the main effect of the copolymerization was a decrease in T$_m$ and T$_g$ with respect to PBO. Furthermore, T$_g$ values decreased with increasing butylene azelate unit content, notably due to the increased presence of methylene groups, which contribute more flexibility to the polymeric chain. The reported thermal properties for some of the previously discussed polymers are presented in **Table 1.3**.

Table 1.3 Thermal properties of some polyoxalates of interest.

Polymer	T$_g$ (°C)	T$_m$ (°C)	Reference
PEOX	32	178	[158,161]
Poly(butylene oxalate) (PBO)	-32	99-102	[155,170]
PBO-Butylene azelate $_{70/30}$	-47	62	[170]

1.5   Polymer degradation pathways

Polymer degradation can be defined as "a deleterious change in the chemical structure, physical properties, or appearance of a polymer, which may result from chemical cleavage of the macromolecules forming a polymeric item, regardless of the mechanism of chain cleavage".[171]

From the physical angle, cleavage of the backbone can occur in a heterogeneous or homogeneous fashion.[172] In homogeneous (or bulk) degradation, via hydrolysis for example, water penetrates the interior of the matrix and hydrolysis of the ester bonds of the interior chains lead to uniform backbone cleavage. There is minimal loss of mass until the molecular weight reaches a threshold value, below which the sample is rapidly decomposed.

The rate of backbone cleavage for heterogeneous (or surface) degradation, on the other hand, is much faster than the rate of penetration of water into the matrix. Therefore, hydrolysis is concentrated on the polymer surface and a gradual decrease in mass and size of the sample occurs with time.[173]

The main process involved in the degradation of glycolic acid and oxalic acid based polyesters is hydrolysis. A decrease in molecular weight and the release of soluble oligomers and monomers result from cleavage of the ester groups. In general, the mechanism leads to an increase in the number of carboxylic acid chain ends, known to autocatalyze ester hydrolysis with the subsequent release of soluble oligomers from the matrix, as shown for PLA in **Scheme 1.12**. Some of these oligomers (closer to the surface) can be leached out while those in the core of the matrix remain entrapped.
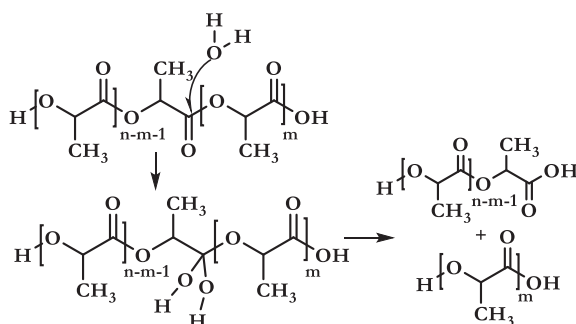
Scheme 1.12 Hydrolytic degradation of PLA. Adapted from [174].

For PLA for example, degradation of the amorphous portions into lactic acid leads to a gradual increase of the acidity.[175-176] Subsequently, the hydrolytic degradation of PLA continues through chain cleavage, preferentially in the amorphous regions, which leads to an increase in the polymer's crystallinity during this stage.[177] A similar mechanism has been observed for all the polyesters reviewed in this document.

PGA degradation and the in vitro toxicity of the degradation products have been previously studied.[178] Hydrolysis of PGA was found to be catalyzed by certain enzymes, especially those with esterase activity.[179] Similar to the PLA case, bulk degradation of PGA via hydrolysis is detrimental to the mechanical properties, due to decreasing molecular weight and the eventual generation of the monomer, glycolic acid. Despite the fact that glycolic acid is resorbable at high concentrations, it has been reported that for some biomedical applications the acid catalyzed hydrolytic degradation can lead to tissue damage.[178] Kuredux®, the PGA resin from the Kureha Corporation, is claimed to degrade into CO_2 and water under composting conditions within one month.[64] However, no support for this statement has been published and the lack of results from compostability tests makes the confirmation of PGA's bio-compostable character under standard backyard conditions difficult. With a similar mechanism, hydrolytic PLGA degradation involves complete

solubilization of oligomer fragments. As in the case of the previously discussed polymers (PLA and PGA), the formation of an acidic microclimate within the matrix[180] has been reported to cause issues for some biomedical applications, notably for protein stability during preparation and storage for controlled release systems.[181]

In general, the rate of the hydrolytic degradation is primarily temperature and humidity dependent[26], although degradation of glycolic acid and oxalic acid based polyesters has been found to also depend on additional factors such as molecular weight, crystallinity, purity, pH, the presence of terminal carboxyl or hydroxyl groups and water permeability. Additives acting catalytically, like bacteria (through the use of enzymes), inorganic fillers and metal residues also contribute to this mechanism.[90,182] Furthermore, the polymer's degradation can be induced by several natural factors besides hydrolysis, such as oxidation, light and heat.[183]

Miller et al.[184] tested resorbable implants in vivo and observed a half-life of 6.6 months for the ones made of PLA, compared to 5 months for those prepared with PGA. Later, Song et al.[185] reviewed the composting of different biodegradable packaging materials under backyard composting conditions. PLA can be classified as a slow biodegradation rate plastic with an observed mass loss of only 5% after 90 days and no visual evidence of microbial breakdown after 180 days. Under industrial composting conditions (60 °C and 63% RH) Kale et al.[114] demonstrated in a different study that PLA degrades completely within 30-45 days. In the same way as PLA and PGA, PLGA can undergo in vivo degradation by non-enzymatic hydrolysis and through enzymes. The degradation time can vary from several months to several years, depending on the molecular weight, copolymer ratio, chain composition, hydrophobic/hydrophilic balance and crystallinity.[176] From the commercial copolymers of PLGA (D,L-lactide/glycolide) (50/50, 65/35, 75/25, 80/20 and 10/90), Vicryl rapide™ (PLGA $_{10/90}$) has the fastest hydrolysis rate with a degradation time of 42 days at room temperature. The most widely used composition for biomedical applications (50/50) has a degradation time of about 50-60 days in vivo. Other compositions, such as 65/35, 75/25 and 80/20, have progressively longer in vivo lifetimes.[181] Houchin et al.[180] studied the effect of moisture on certain properties of PLGA films subjected to storage at 70 °C and up to 95% RH. Following a similar mechanism as PLA and PGA, increasing moisture levels led to a decrease in the molecular weight and thereafter, reduction of the T_g.

In a different study, Li et al.[186] demonstrated that the monomer distribution influences the hydrolysis degradation kinetics of PLGA: random polymer degrades quicker than analog-sequenced PLGA. In this same research, materials with highly controlled sequences and stereochemistry were obtained using 1,3-diisopropyl carbodiimide (DIC) and 4-(dimethylamino)pyridinium p-toluenesulfonate (DPTS) as catalysts. The different tacticities allowed tuning of the hydrolysis rate. Although in principle, these results were considered by the authors as potentially useful for drug delivery systems, it can be inferred that agricultural and packaging applications could also benefit from this tailored degradation. With the previous information in mind, it becomes clear that the PLA/PGA copolymers

offer an undeniable advantage of hydrolysis rate tailoring. This is important for any type of application as it ultimately allows controlling the lifetime of the polymeric material.

Oxalate based polymers degrade in a similar fashion through hydrolytic cleavage of oxalate ester linkages in their backbone (ester hydrolysis). Their degradation in vivo typically generates nontoxic low molecular weight substances that can be easily excreted such as diols and oxalic acid, both considered biocompatible.[164,187] Additionally, polymers with aromatic rings adjacent to oxalate ester linkages are rapidly hydrolyzed by water.[51] This suggests that poly(alkylene) oxalates derived from 1,4-cyclohexanedimethanol, which have poor electron-withdrawing properties, exhibit increased stability for microparticle and nanoparticle formation and drug encapsulation in the aqueous environment compared to other oxalate containing polymers. According to Kim et al.[187] polyoxalate nanoparticles synthesized using 1,4-cyclohexanedimethanol can be degraded by hydrogen peroxide and water faster than PLGA nanoparticles. Their half-life in water at 37 °C and pH 7.4 was 6.5 days. In a different study, microparticles prepared with the same composition also showed a half-life of 6.5 days at similar conditions (pH 7.4 and 5).[187]

In addition to the above, all the polyesters discussed previously are prone to thermal degradation during processing. Jamshidi et al.[188] conducted research on this topic with a focus on polylactides. According to the authors, transesterification reactions are involved in this process (**Scheme 1.13**).
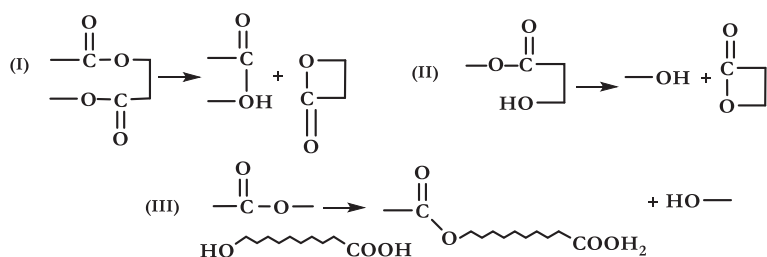
Scheme 1.13 Reactions involved in thermal degradation of PLA. Adapted from [188].

The first two are intramolecular transesterifications that result in the formation of cyclic oligomers, catalyzed by the residual polymerization catalyst. Both of these reactions can lead to the generation of low molecular weight compounds that may evaporate at high temperatures resulting in a gradual reduction of the polymer's weight. The third transesterification reaction involves random chain scission with a possible sharp drop in molecular weight. This indicates that polymerization catalysts will have a strong effect in lowering the molecular weight of lactides at high temperature.

Because the onset of thermal degradation of PGA begins 30 °C above the T_m (230 °C), it is more vulnerable to thermal conditions than PLA and therefore a more rigorous control of processing temperatures is required. Erbetta et al.[110] determined the temperature at which thermal degradation starts for PLGA copolymers with two LA/GL built-in ratios, 50/50

and 70/30. According to the authors, a single stage weight loss of close to 100% is shown at temperatures between 261 and 283 °C.

Essentially, in summary, all the polyesters discussed in this review show hydrolytic degradation through cleavage of ester linkages in their backbone. From the group reviewed, PLA has the highest T_g and the slowest hydrolytic degradation rate when compared under similar temperature and pressure conditions. As a consequence PGA exhibits a faster hydrolytic degradation than PLA and this behavior is accentuated with increasing temperature and moisture. Furthermore, copolymerizing LA and GA or lactide and glycolide allows a tailored degradation profile through variation in the constituent ratios of each monomer. Although the biomedical field is the one dominating its implementation, packaging and agricultural applications would certainly also benefit from the material's tunable biodegradability. Additionally, polyoxalates can be conceived to degrade at a faster rate than PLGA according to their functional requirements, as has already been demonstrated with microparticles and nanoparticles by Kim et al. and Lee et al.[187,189]

1.6   Applications

The strong barrier properties of PGA, accompanied by its biodegradability, make it a good candidate for the packaging industry. Polymer grade PGA is commercialized for packaging applications under the registered trademark Kuredux® by Kureha Corporation, which runs the world's first industrial-scale PGA manufacturing facility. Their bi-axially oriented film exhibits a tensile strength of about 380 MPa and tensile modulus of 7 GPa, both higher than those of some engineering polymers, including PET (σ=230 MPa, E=3.9 GPa) and PA6 (σ=206 MPa, E=1.5 GPa).[56] In addition to the abuse resistance, the material provides excellent barrier integrity, making it suitable for flexible packaging and various industrial films.

Despite the evident potential, PGA is a costly material facing severe difficulty in its large-scale commercialization, which creates challenges for its implementation in a broad range of application areas. Although glycolide is also produced in pilot scale quantities by companies other than Kureha, the current commercial production cost is €5-10 per kilo, which is still high compared to other monomers used in the production of renewable polymers (e.g. lactide production cost €2-3 per kilo[190]). In 2014, the Kureha company held a market share of nearly 84% and was the only commercial producer of PLGA for non-biomedical applications. Although other players, such as Teleflex, DuPont and Huizhou Foryou Medical Devices are also active in the field as providers for medical and biomedical applications, Kureha is still expected to maintain the monopolistic landscape for 2018-2023.[191] In 2015, the corporation stated that the current focus of PGA commercialization is on downstream businesses with a high margin such as shale gas extraction.[192] In fact, downhole tools with nontoxic and biodegradable character using PGA resin have been patented in the past years.[193-194]

Extraction-molded bars form the basic structures for "frac plugs" used in shale oil and gas extraction. Interestingly, shale gas extraction accounted for over 35% of the global demand for poly(glycolic acid) in 2014.[191]

Despite the aforementioned downsides related to the packaging applications, utilization of PGA has been reported for packaging components. Multilayer polymeric systems for containers and films for food contact, using at least one layer of PGA have been made.[195] Improved performance regarding gas permeability and adhesion between layers was reported. However, it was difficult to obtain satisfactory mechanical strength under molding conditions. A similar multilayer container, claimed to be potentially useful for, among others, carbonated fruit juices, dairy products, beers, wines and soups, showed improved heat resistance, capable of withstanding hot filling at 93 °C for 20 seconds. The container was composed of a PGA intermediate layer (Kuredux resin) and another thermoplastic polyester resin (PET or Polyethylene naphthalene, PEN), forming an inner and outer layer. The element was manufactured by a co-injection stress blow molding production process. Good moldability, transparency and durability, accompanied by enhanced barrier properties were achieved.[196] Other similar multilayer systems using PGA have been reported for packaging applications.[197-199] Although multilayer systems with PET or PEN improve valuable properties for the packaging industry, they are not expected to biodegrade or to be compostable and therefore waste disposal remains an issue. The possibility of tailoring PLGA´s mechanical, thermal and optical properties place it among the biodegradable polyesters with a promising performance in the packaging industry.

Oxidation can be a spontaneous process or can be induced by environmental and catalytic systems, such as light, temperature, enzymes, metals, metalloproteins and micro-organisms. To deal with this, the addition of antioxidants is common practice in polymer applications. The release of antioxidants from $PLGA_{50/50}$ films into milk powder products was studied by Van Aardt et al.[200] For this purpose 2% α-tocopherol and 1% butylated hydroxytoluene (BHT), combined with 1% butylated hydroxyanisole (BHA), were used as antioxidants in the PLGA. Biodegradation tests were performed in the presence of water and oil. Lipid oxidation in fat-containing foods that are high in phospholipids is a major cause of deterioration during processing and storage. NMR analysis conducted for the study showed a decrease in the antioxidant content of PLGA films over 4 weeks of storage and a subsequent increase in the antioxidant content in the whole milk powder. Migration of antioxidants from antioxidant loaded films into dry milk products, with a water content lower than 4.60%, was found to be driven by volatilization and surface contact rather than by hydrolytic degradation of $PLGA_{50/50}$ when the dairy products were exposed to light. Apparently, as a response to this contact, the milk fat in the products was partially stabilized. Interestingly, BHT was found to be the only antioxidant that was released through diffusion and hydrolytic degradation of the polymer when stored in water at room temperature for 8 weeks. Volatile compounds (hexanal, pentanal and heptanal) may serve as an indicator of lipid oxidation. The authors were not able to confirm complete control of the formation of

these compounds under the conditions applied for the study. Yet, the potential for these degradable films on the protection of milk quality was acknowledged.

Ube Industries patented PEOX films copolymerized with lactic acid[154] that exhibit good performance for food packaging, medicines, cosmetics, precision machines, and home electric appliances. The inventors claimed that the resin composition can also be employed for multi-layered films in agriculture for compost bags, seed tapes, and germination sheets. High molecular weight PEOX with enhanced processability has also been claimed in a different invention as a suitable material for food packaging, and wrapping for electronic items in the form of films and heat sealing sheets.[158] A different polyester derived from PEOX and glycolic acid oligomers was patented by Alskins et al.[201] The claimed polymer with below 5 mol% of glycolic acid units had a Tm of about 170 °C and a Td close to 210°C (heating rate was not specified). According to the authors, this material shows can be formed into films and fibers and could be used for packaging applications in the food and medical industry.

The published information currently available suggests that a process for large-scale production of PLGA and the discussed polyoxalates is still not well developed. Available information on related studies for packaging applications is scarce. Overall, it seems that further optimization of the synthesis process and complete techno-economical assessments need to be conducted before conclusions can be drawn with respect to the feasibility of these materials for applications where well-established commodity polymers are currently utilized.

1.6.1 Agricultural applications

Plastic films are widely used in agriculture. The world's growing population leads to an increasing demand for food with an accompanying increase in the use of agricultural plastics. Films for greenhouses, silage and mulching are among those in high demand, with Asia as the fastest growing market. The latter accounted for over 40% of the total plastic films used in agriculture in 2012.[19] Some of the advantages offered by mulch films include insect and weed control, increase in air and soil temperature, minimization of soil erosion and reduced water evaporation.[202] These plastics are contaminated with soil after use and therefore not collected by most recycling facilities[21], leading to higher costs for landfilling. Since this is a growing market and recycling does not appear to be a viable option, the need for replacement with biodegradable plastics becomes apparent. Considering that hydrolysis is the major degradation mechanism, it is important to assess the fate of the monomers and their impact on soil productivity and other environments where depolymerization may occur. For PLA, the degradation pathway and degradation products have been studied. However, for other systems, for example multilayer systems containing PET, which degrades very slowly via hydrolysis[203-204], the effect of the monomer terephthalic acid has not been assessed yet.

The use of PLA as homopolymer in agriculture has been limited due to its mechanical and thermal properties not always being suitable for all applications. For the production of commercial mulch films it is usually blended with other biodegradable polyesters and plasticizers. BASF offers ecovio® F Mulch, consisting of the copolyester ecoflex® (polybutylene adipate terephthalate) blended with PLA.[205] The improved strength of this material allows its use in other applications, such as silage and cover film. In 2012 Showa Denko launched a completely biodegradable resin under the trademark Bionolle Starcla. This material, which consists of different PLA grades blended with poly(ethylene/butylene succinate), demonstrated suitability for mulching films.[206] Furthermore, the previously mentioned Ingeo™ PLA is widely used for this same application and also to manufacture pots, yard waste bags, tomato clips and pegs, among others.[207] Other Ingeo™ based derivatives include BI-OLP, a biodegradable film by Oerlemans Plastics, mainly used in greenhouses and DS Technical Nonwovens with HortaFlex®, a mulch matting and weed control product.[208]

The need for more efficient fertilizer technology in the agrochemical sector to control the dosage and avoid excessive local concentration levels of nutrients is evident. Strategies to deal with this situation have involved the use of biodegradable PLA. Jintakanon et al.[209] studied the suitability of poly(lactic acid-co-ethylene terephthalate) as a coating material for controlled release of urea, a common source of nitrogen nutrition for plants. The urea granules were first coated with commercial PLA and PLA/poly(lactic acid-co-ethylene terephthalate) synthesized by the authors. The release properties were assessed by monitoring the urea concentration through measurement of the refractive index in a rotating bottle of water, containing the coated urea granules. The release was found to be a function of the applied coating percentage, which was shown to depend directly on the molecular weight and nature of the polymer coating and concentration of the polymer solution. Additionally, it was concluded that the morphology of the coating's surface influenced the release. Later, Calabria et al.[210] reported a slow release fertilizer system with blends of soy protein isolate (SPI) and PLA plasticized with triacetin (TA) to be used as a matrix for nitrogen, phosphorus and potassium (NPK) fertilizer. Sustained release of nutrients was achieved with the composite material, forming a highly ordered porous matrix of SPI with homogeneous dispersion of the NPK salts. Additional systems for successful control of fertilizer release rate have been reported[209,211], using a double layer granular urea fertilizer coated with PLA and other lactic acid oligomers. A second exterior coating (sealant) can be applied to decrease the water permeability. To the best of our knowledge, commercialization of polyoxalates or PGA derived polymers for the agrochemical industry has not been reported yet. Based on both PGA and PLGA polymer's general properties and the possibility of tailoring them, it could be very beneficial to the agrochemical industry.

Currently, some players in the agricultural market, such as Bayer CropScience AG (Germany), BASF SE (Germany) and Germains Seed Technology (UK), commercialize polymer seed coatings. New regulations for coating materials are forcing manufacturers to look for more sustainable (degradable) polymer solutions. Often, these sustainable options

(e.g. PGA copolymers) are more expensive; increasing cost of raw material causes higher production cost and therefore higher prices in the market. With this in mind, the potential of the polyesters mentioned in this review for seed coatings does not depend exclusively on the technical requirements. The use of coated seeds needs to increase, for the most common human consumption products (e.g. grains, vegetables, fruits). This would lead to a marked growth in the demand for new polymer coatings, which should affect scale and thus increase the efficiency of monomer production, benefiting price and availability.

1.6.2 Biomedical applications

The biomedical field is the most extensively studied application area for the polymers reviewed in this document. Numerous investigations have been published using PLA, PGA, PLGA or polyoxalates for purposes related to this field. However, this review aims to focus on other applications and therefore it will only be treated briefly.

An extensive increase has been reported regarding the use of PLA for biomedical applications where specific chemical, mechanical, physical, biological and degradation properties are required. Some uses include: stents[212], surgical sutures[213], plates and screws for craniomaxillofacial bone fixation, interference screws in ankle, knee, and hand; tacks and pins for ligament attachment, anchors, spinal cages, soft-tissue implants, tissue engineering scaffolds, tissue cultures, drug delivery devices.[214-216] Craniofacial augmentations in plastic surgery are also part of the potential applications.[213] A limitation related to the use of PLA involves the viscoplastic flow that can lead to premature failure at stress magnitudes that are significantly lower than the yield strength and the ultimate tensile strength of the material. This behavior can lead to creep rupture or fatigue failure; this is an issue since it means that for some applications, device failure can occur long before the material is estimated to fail due to degradation in vivo.[217] 3D printing is already used for some of the aforementioned devices. However, the generation of complex tissues such as bone, cartilage, muscles, vessels and organs with intricate 3D microarchitecture (liver, lymphoid organs), presents several technical limitations related to the balance between physical/mechanical properties and biodegradation kinetics.[218]

For biomedical applications, PGA appears attractive since the polymer's biodegradation generates glycolic acid, a natural metabolite.[90] One of the first industrial applications of PGA was proposed in 1962 by the former American Cyanamid Company now part of Pfizer. The company developed the first absorbable surgical sutures with the trademark Dexon®, which benefited from the good mechanical strength and biodegradable character of PGA.[219] Surgical sewing threads formed from braided multifilaments of this PGA exhibit a 50% breaking strength loss within 21 days.[220] Absorbable sutures are widely commercialized these days by different corporations under registered marks such as Trisorb®[221] and Safil®[222]. Efforts for enhancing its mechanical performance have resulted in some proposed

core and shell filament structures composed of the fast absorbing polymer PGA and for example a slow absorbing polymer like poly(caprolactone). These models allow prolonged mechanical strength by delaying bioabsorption. Resorba successfully commercializes this type of surgical suture as Glycolon™.[223]

Scaffolds constituted of fibers are a pioneering application of PGA in tissue engineering.[67] Although melt spinning and extrusion represent the most widely reported processes for PGA fiber manufacturing, different fabrication techniques using PGA fibers and fillers have been reported to obtain highly porous scaffolds with an increased surface area to incentivize cell attachment. Fiber bonding[68], gas foaming and phase separation emulsification[224] are among them. Additionally, prosthetic structures with PGA, such as reinforcing pins[55], plates and screws[225], have also been formulated. You et al.[226] prepared porous ultrafine PGA fibers by electrospinning (PGA/PLA) (30/70) fibers and then removing the PLA via a selective dissolution technique with chloroform. Three-dimensionally interconnected pores with narrow size distribution and circular shape with average diameters ranging from 200 to 500 nm were obtained. The product was recognized to be potentially useful for nanofiltration and functional nanotubes.

Combined applications in the packaging and medical fields are also of potential interest for PGA. A multilayer film for the production of pouching systems in ostonomy applications with about 4 to 80 wt% of PGA, in combination with a noise dampening polymer resin, was reported by Bekele et al.[227] Pouches are typically made of poly(vinylidene chloride) PVDC or copolymers of vinylidene chloride; both hazardous to the environment when disposed of by open-air incineration (still a common practice in many countries) or in combustion systems where some fractions escape unburned and other portions are converted into new organic compounds (e.g. dioxins). Pouches require good odor and moisture barrier properties, softness, heat or radio frequency sealability, skin compatibility, comfort and oxygen and moisture vapor impermeability. In addition, such pouches should not emit noise during use. The obtained packaging device with the highest composition of PGA proved to fulfill the aforementioned criteria with an oxygen transmission rate (OTR) of less than 60 $cm^3 \cdot m^{-2} \cdot day^{-1} \cdot bar^{-1}$ at 23 °C at 100% of relative humidity. Nylon 6 coated with PVDC at the same temperature and 90% RH exhibits an OTR of 10 $cm^3 \cdot m^{-2} \cdot day^{-1} \cdot bar^{-1}$.[228] Another very competitive gas and aroma barrier material, PVDC-coated BOPP (biaxially oriented polypropylene), has an OTR of 13 $cm^3 \cdot m^{-2} \cdot day^{-1} \cdot bar^{-1}$ at 23 °C at 0% RH.[229]

Studies have extensively investigated the potential of PLGA for biomedical applications, including sutures, fibers, micro- and nanostructures for controlled release and scaffolds for tissue engineering. During the late 1960s and early 1970s, successful research in terms of tissue compatibility on absorbable suture materials opened the door to the use of biodegradable polymer implants for other clinical applications.[230-232] Ethicon became the first company developing and commercializing a multifilament suture of PLGA today

known as Vicryl™ (polyglactin 910), made from 90% glycolide and 10% *L*-lactide. The copolymer, synthesized by ROP of lactide and glycolide is initially made in the form of pellets. The pellets are melted and the material is extruded as filaments that are subsequently strengthened by stretching to allow molecular alignment. The filaments are braided and once again submitted to a stretching process to increase their tensile strength. Complete absorption by hydrolysis of the resulting suture occurs in approximately 80 days.[232] Currently, surgical sutures are combined with bioactive materials. Vicryl Plus (10:90 LA/GA) coated with triclosan is an available commercial example that offers the ability to inhibit bacterial growth on the suture.[233] Vicryl rapide, a suture with the same LA/GA composition, provides a faster breakdown by hydrolysis (42 days).

Other applications for PLGA include scaffolds for tissue engineering[234-236], bone tissue engineering[237], and drug delivery systems.[1331-238] Limitations for other biomedical applications are related to the common inflammatory response triggered by the acid catalyzed in vivo degradation.[124,239] Composites of PLGA with fillers such as calcium phosphates[240], magnesium[241,242] and iron oxide particles[243], TiO_2 nanotube[244] and hydroxyapatite[245-246] have been reported for biomedical applications that include tissue engineering and preparation of scaffolds. According to these studies, the addition of one of these elements in the dispersed phase, enhances the physical and biological properties of the matrix. Although in most cases this incorporation improved the mechanical properties of the composite allowing better performance, this showed high dependency on the filler content and fabrication processes (e.g. electrospinning, encapsulation, supercritical gas foaming and phase separation).

Another component reported in the last years for the synthesis of PLGA composites is chitosan. Boukari et al.[247] prepared a scaffold composite system made of porous PLGA and protein loaded PLGA-chitosan microspheres. Different studies for the same application have also incorporated alginate in the PLGA matrix.[248,249] The addition of chitosan and alginate in the dispersive phase, has been reported to retain cytocompatibility and increase the encapsulation efficiency. Furthermore, it preserves the release function of the antibody in the microspheres since it helps preventing initial burst release of the protein, a challenging aspect according to the encapsulated substance. Although certain advantages related to biocompatibility, encapsulation efficiency and mechanical performance have been reported by the preparation of PLGA composites, issues remain to be addressed for a wider utilization of these materials at least in clinical applications. Inflammation in vivo, degradation profile tuning, optimization of filler amount and scaling up are the most relevant aspects that still need further research.

Despite its versatile potential, biomedicine is the field where POX has received the most attention, while utilization for packaging or agricultural applications has been scarcely reported. Biodegradable nanoparticles and microparticles have been synthesized for targeted drug delivery of therapeutic agents.[164,187,250,251] For poly(alkylene) oxalates one of

the first reported applications still in use exploits their good tensile strength for in vivo degradable surgical sutures[252] and coatings for multifilament sutures.[142] Scaffolds and other surgical devices have also been studied as applications. Reports on composites containing POX are very scarce and only studied for the biomedical field. Phromviyo et al.[239] studied a biodegradable polyoxalate blended with poly(vinyl alcohol) to create composite nanofibers for controlled release of drugs. The release was found to occur with a diffusion stage followed by degradation. The drug release rate for the composite nanofibers was found to depend on the POX content, being the slowest for high POX amounts. This is reasonable since the hydrophilicity of the system is affected by the hydrophobic contribution of the POX. Overall, some contributions to the drug delivery field can be subtracted from this research. Yet, in vivo studies to confirm the biocompatibility and cytotoxicity of this system still have to be performed in order to draw more realistic conclusions.

1.7   Concluding remarks

The increasing government norms and regulations for the reduction of plastic waste have boosted the demand for new materials. Europe leads the shift to renewable polymers in major industries such as the pharmaceutical, textile, cosmetics and packaging industries. The Asia Pacific region is becoming more relevant in the sustainable polymer market with some of the major producers of glycolide and oxalic acid in China, India and Japan. Opportunities for polyesters to contribute to a circular economy are definitely promising.

CO_2 is a valuable feedstock since it is naturally abundant, nontoxic, inexpensive, a non-oxidant and renewable. Currently, transformation of CO_2 into building blocks for materials is a promising option with environmental benefit for production of the polyesters discussed in this review. A relevant example of this technology has been developed by Liquid Light Inc., now part of Avantium. The process is based on an electrochemical reduction of CO_2 to formic acid derivatives that can subsequently be converted into useful monomers such as oxalic acid and glycolic acid. The development of this kind of technology targets future monomer production costs that can at scale compete with fossil counterparts (€1-2/kg). This will allow the development of a promising landscape for new polyesters, especially taking into account the required transition from fossil feedstocks to renewable resources. However, significant research is still required to optimize and deal with the challenges related to upscaling of these production processes with a focus on further reduction of the manufacturing costs. Further optimization of these processes after initial commercialization will be necessary in terms of selectivities and yields as well as with respect to the energy demand in all unit operations and reduced sensitivities to feedstock specifications. In order to start using glycolic acid derived polyesters in large-scale applications (e.g. for degradable drinking straws, degradable barrier films, degradable seed/fertilizer coatings, etc.) it is necessary to develop both extremely efficient monomer and polymer production routes as

well as developing the market by matching of the novel polymer properties to current unmet market needs in various applications.

1.8   Outline of this thesis

The research discussed in this thesis is part of the OCEAN (EU Horizon 2020 Spire program) project in which a new route was investigated for producing polymers, using CO_2 as circular feedstock. At the center of this route are oxalic acid and glycolic acid and their role as polyester monomers. We investigated the synthesis of oxalic acid and glycolic acid based polyesters and their properties. The structural characterization of the resulting materials was typically done with ^{1}H NMR and the molecular weight distribution was determined with GPC. The thermal transitions and stability where assessed with DSC and TGA. Permeability studies were carried out with compression molded films to evaluate the barrier properties. Findings regarding the degradability of these polyesters are also presented. Initial assessments on their application potential were based on the outcome of the utilized characterization techniques.

The aim of **chapter 2** is to understand the structure-property relationships for the mostly unexplored glycolic acid rich poly(lactide-co-glycolide) (PLGA) copolymer series, synthesized via ring opening polymerization and to assess their potential as barrier materials. Application on bulk scale, such as in films for packaging, is promising due to the combination of exceptional barrier properties, potential future production from CO_2, (chemical) recyclability and biodegradability.

In **chapter 3** copolyesters of degradable polyoxalates and polyglycolic acid (PGA) and PLA are explored. This includes synthesis strategies, physical characterization and degradability assessment via a hydrolysis study. The resulting copolyesters showed faster hydrolysis rates than the respective homopolymers they were made from and the barrier properties were favored by increasing PGA content, while the thermal stability was increased with higher polyoxalate content. Possible application in single-use packaging, as coatings for controlled release in agriculture and even in the medical field, are suggested.

Production of PLGA polyesters via ring opening polymerization is still very costly, particularly considering the still high cost of glycolide compared to lactide. Therefore, in **chapter 4,** we propose a new synthesis route to prepare PLGA copolymers with high glycolic acid content through direct polycondensation of glycolic acid and lactic acid.

This is done in the presence of p-cresol or guaiacol as reactive solvent at a scale of up to 35 g. The resulting molecular weight values attained with this method represent an approximate threefold improvement compared to the values achieved in a typical direct polycondensation starting from both acids in the absence of solvents. Also, this strategy

requires less time than other reported routes to increase the molecular weight of similar type of polymers and it allows for solvent recycling for reuse.

The same synthesis route was applied in **chapter 5** on PLA synthesis. Although this strategy was not as efficient for molecular weight improvement in PLA as in PLGA, it could be used as an alternative for lactide production. This would require further optimization to determine its potential in comparison with the methods already used industrially. In the last chapter the ongoing efforts to scale up the direct polycondensation synthesis route for PLGA copolymers, presented in **chapter 4**, from the 35 g to 1 kg scale is discussed. Although initial work revealed that guaiacol is the most suitable solvent for this process, preferred over p-cresol, significant work is still required to ensure a high enough molecular weight copolymer for subsequent processing and application assessment.

1.9   References

(1)   Paris Agreement, Clim. Action - Eur. Comm. (2016). https://ec.europa.eu/clima/policies /international/negotiations/paris_en (accessed January 16, 2019).

(2)   Kember, M. R.; Buchard, A.; Williams, C. K. Catalysts for CO_2/epoxide copolymerization. *Chem. Commun.* **2010**, *47* (1), 141-163. https://doi.org/10.1039/C0CC02207A.

(3)   Plastics-the Facts 2016. An Analysis of European plastics production, demand and waste data. *Plastics Europe*. Belgium 2016.

(4)   European Commission - press release-Single-use plastics: New EU rules to reduce marine litter. http://europa.eu/rapid/press-release_IP-18-3927_en.htm?locale= EN (accessed August 15, 2018).

(5)   Mrowiec, B. Plastics in the circular economy (CE). *Environ. Prot. Nat. Resour. J. Inst. Environ. Prot.-Natl. Res. Inst.* **2018**, *29* (4), 16-19. https://doi.org/10.2478/oszn-2018-0017.

(6)   Neufeld, L.; Stassen, F.; Sheppard, R.; Gilman, T.; Eds. The new plastics economy: rethinking the future of plastics. https://ellenmacarthurfoundation.org/the-new-plastics-economy-rethinking-the-future-of-plastics (accessed January 05, 2019)

(7)   Patel, M.; von Thienen, N.; Jochem, E.; Worrell, E. Recycling of plastics in Germany. *Resour. Conserv. Recycl.* **2000**, *29* (1), 65–90. https://doi.org/10.1016/S0921-3449(99)00058-0.

(8)   Garcia, J. M.; Robertson, M. L. The future of plastics recycling. *Science* **2017**, *358* (6365), 870-872. https://doi.org/10.1126/science.aaq0324.

(9)   Hopewell, J.; Dvorak, R.; Kosior, E. Plastics recycling: challenges and opportunities. *Philos. Trans. R. Soc. B Biol. Sci.* **2009**, *364* (1526), 2115-2126. https://doi.org/10.1098/rstb.2008.0311.

(10)   European Commission - Press release - Single-use plastics: New EU rules to reduce marine litter http://europa.eu/rapid/press-release_IP-18-3927_en.htm?locale=EN (accessed Aug 15, 2018).

(11)   Müller, R.-J. Biodegradability of polymers: regulations and methods for testing. In *Biopolymers Online*; American Cancer Society, 2005. https://doi.org/10.1002/3527600035.bpola012.

(12)   Laycock, B.; Nikolić, M.; Colwell, J. M.; Gauthier, E.; Halley, P.; Bottle, S.; George, G. Lifetime prediction of biodegradable polymers. *Prog. Polym. Sci.* **2017**, *71*, 144-189. https://doi.org/10.1016 /j.progpolymsci.2017.02.004.

(13)   Agarwal, S. 5.15 - Biodegradable polyesters. *Polymer Science: A Comprehensive Reference.* 2012; pp 333-361. https://doi.org/10.1016/B978-0-444-53349-4.00145-X.

(14)   Gross, R. A.; Kalra, B. Biodegradable polymers for the environment. *Science* **2002**, *297* (5582), 803-807. https://doi.org/10.1126/science.297.5582.803.

(15)   Touchaleaume, F.; Martin-Closas, L.; Angellier-Coussy, H.; Chevillard, A.; Cesar, G.; Gontard, N.; Gastaldi, E. Performance and environmental impact of biodegradable polymers as agricultural mulching films. *Chemosphere* **2016**, *144*, 433-439. https://doi.org/10.1016/j.chemosphere.2015. 09.006

(16) Bilck, A. P.; Grossmann, M. V. E.; Yamashita, F. Biodegradable mulch films for strawberry production. *Polym. Test.* **2010**, *29* (4), 471-476. https://doi.org/10.1016/j.polymertesting.2010.02. 007.

(17) Guilbert, S.; Gontard, N. 16 - Agro-polymers for edible and biodegradable films: review of agricultural polymeric materials, physical and mechanical characteristics. *Innov. Food Packag.* Academic Press, London, 2005; pp. 263-276. https://doi.org/10.1016/B978-012311632-1/50048-6.

(18) BioBag - Compostable products. https://biobagworld.com/ (accessed Apr 3, 2018).

(19) Agricultural Films Market- Global Industry Analysis, Growth, Trends, Forecast, 2013-2019, Transpar. Mark. Res. (2013). https://www. transparencymarketresearch.com/agricultural-film.html (accessed February 2, 2018).

(20) Gu, X.-B.; Li, Y.-N.; Du, Y.-D. Biodegradable film mulching improves soil temperature, moisture and seed yield of winter oilseed rape (Brassica Napus L.). *Soil Tillage Res.* **2017**, *171*, 42-50. https://doi.org/10.1016/j.still.2017.04.008.

(21) Sintim, H. Y.; Flury, M. Is biodegradable plastic mulch the solution to agriculture's plastic problem? *Environ. Sci. Technol.* **2017**, *51* (3), 1068–1069. https://doi.org/10.1021/acs.est.6b06042.

(22) Trenkel, M. E. Slow- and controlled-release and stabilized fertilizers: an option for enhancing nutrient use efficiency in agriculture. International Fertilizer Industry Association (IFA); Paris, France, (2010).

(23) Trinh, T. H.; KuShaari, K. Dynamic of water absorption in controlled release fertilizer and its relationship with the release of nutrient. *Procedia Eng.* **2016**, *148*, 319–326. https://doi.org/10.1016/j.proeng.2016.06.444.

(24) Akelah, A. Novel utilizations of conventional agrochemicals by controlled release formulations. *Mater. Sci. Eng. C* 1996, *4* (2), 83–98. https://doi.org/10.1016/0928-4931(96)00133-6.

(25) Kaufman, G. Seed coating: a tool for stand establishment; a stimulus to seed quality. *Hort Technology* **1991**, *1* (1), 98–102.

(26) Lunt, J. Marketplace opportunities for integration of biobased and conventional plastics. *Minn. Corn Res. Counc.* 2014, 116.

(27) Siracusa, V.; Rocculi, P.; Romani, S.; Dalla Rosa, M. Biodegradable polymer for food packaging: a review. *Trends Food Sci. Technol.* **2008**, *19*, 634–643. https://doi.org/10.1016/j.tifs.2008.07.003.

(28) Briassoulis, D.; Dejean, C.; Picuno, P. Critical review of norms and standards for biodegradable agricultural plastics part II: composting. *J Polym Environ.* **2010**, *18,* 364–383. https://doi.org/10.1007/s10924-010-0168-1.

(29) Dai, Z.; Middleton, R.; Viswanathan, H.; Fessenden-Rahn, J.; Bauman, J.; Pawar, R.; Lee, S.-Y.; McPherson, B. An integrated framework for optimizing CO_2 sequestration and enhanced oil recovery. *Environ. Sci. Technol. Lett.* **2014**, *1* (1), 49–54. https://doi.org/10.1021/ez4001033.

(30) Aresta, M., Forti, G., Eds. *Carbon dioxide as a source of carbon: biochemical and chemical uses*; Nato Science Series C. Springer Netherlands, 1987.

(31) Troschl, C.; Meixner, K.; Fritz, I.; Lechner, K.; Palacios Romero, A.; Kovalcik, A.; Sedlacek, P.; Drosg, B. Pilot-scale production of poly-β-hydroxybutyrate with the Cyanobacterium Synechocytis Sp. CCALA192 in a non-sterile tubular photobioreactor. *Algal Res.* **2018**, *34*, 116–125. https://doi.org / 10.1016/j.algal.2018.07.011.

(32) Higuchi-Takeuchi, M.; Morisaki, K.; Toyooka, K.; Numata, K. Synthesis of high-molecular-weight polyhydroxyalkanoates by marine photosynthetic purple bacteria. *PloS One.* **2016**, *11* (8), e0160981. https://doi.org/10.1371/journal.pone.0160981.

(33) Markl, E.; Grünbichler, H.; Lackner, M. Cyanobacteria for PHB bioplastics production: a review, *Algae;* London: IntechOpen, 2018. https://doi.org/10.5772/intechopen.81536.

(34) Alper, E.; Yuksel Orhan, O. CO_2 utilization: developments in conversion processes. *Petroleum.* **2017**, *3* (1), 109–126. https://doi.org/10.1016/j.petlm.2016.11.003.

(35) W. J. Meerendonk, V. CO_2 as a monomer for the phosgene-free synthesis of new polycarbonates : catalyst development, mechanistic investigations and monomer screening. Ph.D. thesis, Technische Universiteit Eindhoven, 2005. https://doi.org/10.6100/IR596016.

(36) Meerendonk, W. J. van; Duchateau, R.; Koning, C. E.; Gruter, G.-J. M. High-throughput automated parallel evaluation of zinc-based catalysts for the copolymerization of CHO and CO_2 to polycarbonates. *Macromol. Rapid Commun.* **2004**, *25* (1), 382–386. https://doi.org/10.1002 / marc. 200300255.

(37) van Meerendonk, W. J.; Duchateau, R.; Koning, C. E.; Gruter, G.-J. M. Unexpected side reactions and chain transfer for zinc-catalyzed copolymerization of cyclohexene oxide and carbon dioxide. *Macromolecules*. **2005**, *38* (17), 7306–7313. https://doi.org/10.1021/ma050797k.

(38) Duchateau, R.; van Meerendonk, W. J.; Yajjou, L.; Staal, B. B. P.; Koning, C. E.; Gruter, G.-J. M. Ester-functionalized polycarbonates obtained by copolymerization of ester-substituted oxiranes and carbon dioxide: A MALDI-ToF-MS analysis study. *Macromolecules* **2006**, *39* (23), 7900–7908. https://doi.org/10.1021/ma0610313.

(39) Muthuraj, R.; Mekonnen, T. Recent progress in carbon dioxide (CO_2) as feedstock for sustainable materials development: co-polymers and polymer blends. *Polymer*. **2018**, *145*, 348–373. https://doi.org/ 10.1016/j.polymer.2018.04.078.

(40) Ganesh, I. Electrochemical conversion of carbon dioxide into renewable fuel chemicals – the role of nanomaterials and the commercialization. *Renew. Sustain. Energy Rev.* **2016**, *59*, 1269–1297. https://doi.org/10.1016/j.rser.2016.01.026.

(41) Palm, E.; Nilsson, L. J.; Åhman, M. Electricity-based plastics and their potential demand for electricity and carbon dioxide. *J. Clean. Prod.* **2016**, *129*, 548–555. https://doi.org/ 10.1016/ j.jclepro.2016.03.158.

(42) European commission. A Roadmap for moving to a competitive low carbon economy in 2050. Brussels, March 2011. http://europa.eu/rapid/press-release_MEMO-11-150_en.htm?locale=en.

(43) Brown, W. H.; Iverson, B. L.; Anslyn, E.; Foote, C. S. *Organic Chemistry*; Cengage Learning, 2013.

(44) Agarwal, S. Functional (bio)degradable polyesters by radical ring-opening polymerization. *Biodegrad, Polyesters*. **2015**, 25–45. https://doi.org/10.1002/9783527656950.ch2.

(45) Larson, A. T. Process for the preparation of glycolic acid. US2153064A, April 4, 1939.

(46) DiCosimo, R.; Payne, M. S.; Panova, A.; Thompson, J.; O'Keefe, D. P. Enzymatic production of glycolic acid. US7198927B2, April 3, 2007.

(47) Kataoka, M.; Sasaki, M.; Hidalgo, A. R.; Nakano, M.; Shimizu, S. Glycolic acid production using ethylene glycol-oxidizing microorganisms. *Biosci. Biotechnol. Biochem.* **2001**, *65* (10), 2265–2270. https://doi.org/10.1271/bbb.65.2265.

(48) He, Y.-C.; Xu, J.-H.; Su, J.-H.; Zhou, L. Bioproduction of glycolic acid from glycolonitrile with a new bacterial isolate of alcaligenes Sp. ECU0401. *Appl. Biochem. Biotechnol.* **2010**, *160* (5), 1428–1440. https://doi.org/10.1007/s12010-009-8607-y.

(49) Nancucheo, I.; Johnson, D. Production of glycolic acid by chemolithotrophic iron- and sulfur-oxidizing bacteria and its role in delineating and sustaining acidophilic sulfide mineral-oxidizing consortia. *Appl. Environ. Microbiol.* **2009**, *76*, 461–467. https://doi.org/10.1128/AEM.01832-09.

(50) Falbe, J. *Carbon Monoxide in Organic Synthesis*; Springer Science & Business Media, 2013; pp 123-146.

(51) Carothers, W. H.; Dorough, G. L.; Natta, F. J. van. Studies of polymerization and ring formation. x. the reversible polymerization of six-membered cyclic esters. *J. Am. Chem. Soc.* **1932**, *54* (2), 761–772. https://doi.org/10.1021/ja01341a046.

(52) Lowe, C. E. Preparation of high molecular weight polyhydroxyacetic ester. US2668162A, February 2, 1954.

(53) Gorth, D.; J Webster, T. 10 - Matrices for tissue engineering and regenerative medicine. *Biomater. Artif. Organs,* Woodhead Publishing, Woodhead Publishing. 2011, pp. 270-286. https://doi.org/ 10.1533/9780857090843.2.270.

(54) Smith, R. *Biodegradable Polymers for Industrial Applications*; CRC Press, 2005; pp 3-32.

(55) Yamane, K.; Miura, H.; Ono, T.; Nakajima, J.; Itoh, D. Crystalline polyglycolic acid, polyglycolic acid composition and production process thereof. US20030125508A1, July 3, 2003.

(56) Kureha America - Product Groups - PGA http://www.kureha.com/product-groups/pga.htm (accessed 2018 -07 -24).

(57) Abe, S. Sequentially biaxially-oriented polyglycolic acid film, production process thereof and multi-layer film. US20110027590A1, February 3, 2011.

(58) Schmitt, E. E.; Polistina, R. A. Surgical dressings of absorbable polymers. US3875937A, April 8, 1975.

(59) Kawakami, Y.; Sato, N.; Hoshino, M.; Kouyama, T.; Shiiki, Z. Polyglycolic acid sheet and production process thereof. EP0805176A1, November 5, 1997.

(60) Kawakami, Y.; Sato, N.; Hoshino, M.; Kouyama, T.; Shiiki, Z. Oriented polyglycolic acid film and production process thereof. US5853639A, December 29, 1998.

(61) Colomines, G.; Domenek, S.; Ducruet, V.; Guinault, A. Influences of the crystallisation rate on thermal and barrier properties of polylactide acid (PLA) food packaging films. *Int. J. Mater. Form.* **2008**, *1*, 607–610. https://doi.org/10.1007/s12289-008-0329-0.

(62) Lange, J.; Wyser, Y. Recent innovations in barrier technologies for plastic packaging—a review. *Packag. Technol. Sci.* **2003**, *16* (4), 149–158. https://doi.org/10.1002/pts.621.

(63) Mokwena, K. K.; Tang, J. Ethylene vinyl alcohol: a review of barrier properties for packaging shelf stable foods. *Crit. Rev. Food Sci. Nutr.* **2012**, *52* (7), 640–650. https://doi.org /10.1080/10408398. 2010.504903.

(64) Yamane, K.; Sato, H.; Ichikawa, Y.; Sunagawa, K.; Shigaki, Y. Development of an industrial production technology for high-molecular-weight polyglycolic acid. *Polym. J.* **2014**, *46* (11), 769–775. https://doi.org/10.1038/pj.2014.69.

(65) Montes de Oca, H.; Ward, I.; Klein, P. G.; Ries, M.; Rose, J.; Farrar, D. Solid state nuclear magnetic resonance study of highly oriented poly(glycolic acid). *Polymer.* **2004**, *45*, 7261–7272. https://doi.org /10.1016 / j.polymer.2004.08.028.

(66) Yu, C.; Bao, J.; Xie, Q.; Shan, G.; Bao, Y.; Pan, P. Crystallization behavior and crystalline structural changes of poly(glycolic acid) investigated: via temperature-variable WAXD and FTIR analysis. *CrystEngComm.* **2016**, *18,* 7894-7902. https://doi.org/10.1039/C6CE01623E.

(67) G. Mikos, A.; Temenoff, J. Formation of highly porous biodegradable scaffolds for tissue engineering. *Electron. J. Biotechnol.* **2000**, *3*, 23–24. https://doi.org/10.4067/S0717-34582000 000200003.

(68) Mikos, A. G.; Bao, Y.; Cima, L. G.; Ingber, D. E.; Vacanti, J. P.; Langer, R. Preparation of poly(glycolic acid) bonded fiber structures for cell attachment and transplantation. *J. Biomed. Mater. Res.* **1993**, *27* (2), 183–189. https://doi.org/10.1002/jbm.820270207.

(69) Higgins, N. A. Condensation polymers of hydroxyacetic acid. US2676945A, April 27, 1954.

(70) Takahashi, K.; Taniguchi, I.; Miyamoto, M.; Kimura, Y. Melt/solid polycondensation of glycolic acid to obtain high-molecular-weight poly(glycolic acid). *Polymer.* **2000**, *41* (24), 8725–8728. https://doi.org/10.1016/S0032-3861(00)00282-2.

(71) Gädda, T.; Pirttimaa, M.; Harlin, A.; Härkönen, M. Glycolic acid polymers and method of producing the same. EP2994496A4, November 2, 2016.

(72) Gilding, D. K.; Reed, A. M. Biodegradable polymers for use in surgery—polyglycolic/poly(lactic acid) homo- and copolymers: 1. *Polymer.* **1979**, *20* (12), 1459–1464. https://doi.org/10.1016/0032-3861(79)90009-0.

(73) Bhatia, K. K. Continuous process for rapid conversion of oligomers to cyclic esters. US5023349A, June 11, 1991.

(74) Thayer, C. A.; Bellis, H. E. Process for the synthesis of lactide or glycolide from lactic acid or glycolide acid oligomers. US5374743A, December 20, 1994.

(75) Yamane, K.; Kawakami, Y. Glycolide production process, and glycolic acid oligomer for glycolide production. US7235673B2, June 26, 2007.

(76) Chujo, K.; Kobayashi, H.; Suzuki, J.; Tokuhara, S.; Tanabe, M. Ring-opening polymerization of glycolide. *Makromol. Chem.* **1967**, *100* (1), 262–266. https://doi.org/10.1002/macp.1967.021000128.

(77) Dobrzynski, P.; Kasperczyk, J.; Janeczek, H.; Bero, M. Synthesis of biodegradable glycolide/l-lactide copolymers using iron compounds as initiators. *Polymer.* **2002**, *43* (9), 2595–2601. https: //doi.org/10.1016/S0032-3861(02)00079-4.

(78) Sanina, G. S.; Fomina, M. V.; Khomyakov, A. K.; Livshits, V. S.; Savin, V. A.; Lyudvig, Ye. B. Cationic polymerization of glycolide in the presence of antimony trifluoride. *Polym. Sci. USSR* **1975**, *17* (12), 3133–3140. https://doi.org/10.1016/0032-3950(75)90344-5.

(79) Amine, H.; Karima, O.; Amine, B. M. E.; Belbachir, M.; Meghabar, R. Cationic ring opening polymerization of glycolide catalysed by a montmorillonite clay catalyst. *J. Polym. Res.* **2005**, *12* (5), 361–365. https://doi.org/10.1007/s10965-004-0004-1.

(80) Albertsson, A.-C.; Varma, I. K. Recent developments in ring opening polymerization of lactones for biomedical applications. *Biomacromolecules.* **2003**, *4* (6), 1466–1486. https://doi.org/10.1021 /bm034247a.

(81) Dubois, P.; Coulembier, O.; Raquez, J.-M. *Handbook of Ring-Opening Polymerization*; John Wiley & Sons, 2009; pp. 379-398.

(82)   Kaplan, D. L. *Biopolymers from Renewable Resources*; Springer Science & Business Media, 2013; pp. 367-405.

(83)   Báez, J.; Marcos-Fernández, A. A simple and rapid preparation of poly(glycolide) (PGA) oligomers catalyzed by decamolybdate anion in the presence of aliphatic alcohols. *Int. J. Polym. Anal. Charact.* **2011**, *16*, 269–276. https://doi.org/10.1080/1023666X.2011.570288.

(84)   Singh, V.; Tiwari, M. Structure-processing-property relationship of poly(glycolic acid) for drug delivery systems 1: synthesis and catalysis. *Int. J. Polym. Sci.* 2010. https://doi.org/ 10.1155/2010/ 652719.

(85)   Stridsberg, K. M.; Ryner, M.; Albertsson, A.-C. Controlled ring-opening polymerization: polymers with designed macromolecular architecture. In *Degradable Aliphatic Polyest.* **2002**, 41–65. https://doi. org/10.1007/3-540-45734-8_2.

(86)   Dechy-Cabaret, O.; Martin-Vaca, B.; Bourissou, D. Controlled ring-opening polymerization of lactide and glycolide. *Chem. Rev.* **2004**, *104* (12), 6147–6176. https://doi.org/10.1021/cr040002s.

(87)   Sedush, N. G.; Chvalun, S. N. Kinetics and thermodynamics of l-lactide polymerization studied by differential scanning calorimetry. *Eur. Polym. J.* **2015**, *62*, 198–203. https://doi.org/10.1016/ j.eurpolymj.2014.11.038.

(88)   Kricheldorf, H. R.; Kreiser-Saunders, I.; Stricker, A. Polylactones 48. SnOct$_2$-initiated polymerizations of lactide: a mechanistic study. *Macromolecules.* **2000**, *33* (3), 702–709. https://doi. org /10.1021/ma991181w.

(89)   Bourissou, D.; Martin-Vaca, B.; Dumitrescu, A.; Graullier, M.; Lacombe, F. Controlled cationic polymerization of lactide. *Macromolecules.* **2005**, *38* (24), 9993–9998. https://doi.org /10.1021/ ma051646k.

(90)   Gunatillake, P. A.; Adhikari, R. Biodegradable synthetic polymers for tissue engineering. *Eur. Cell. Mater.* **2003**, *5*, 1–16.

(91)   Kaihara, S.; Matsumura, S.; Mikos, A. G.; Fisher, J. P. Synthesis of poly(l-lactide) and polyglycolide by ring-opening polymerization. *Nat. Protoc.* **2007**, *2* (11), 2767–2771. https://doi.org/10.1038/ nprot.2007.391.

(92)   Sato, H.; Akutsu, F.; Kobayashi, F. Polyglycolic acid resin composition. US8362158B2, January 29, 2013.

(93)   Fischer, A. M.; Frey, H. Soluble hyperbranched poly(glycolide) copolymers. *Macromolecules.* **2010**, *43* (20), 8539–8548. https://doi.org/10.1021/ma101710t.

(94)   Wolf, F. K.; Fischer, A. M.; Frey, H. Poly(glycolide) multi-arm star polymers: improved solubility via limited arm length. *Beilstein J. Org. Chem.* **2010**, *6*, No. 67. https://doi.org/10.3762/bjoc.6.67.

(95)   Mhiri, S.; Mignard, N.; Abid, M.; Prochazka, F.; Majeste, J.-C.; Taha, M. Thermally reversible and biodegradable polyglycolic-acid-based networks. *Eur. Polym. J.* **2017**, *88*, 292–310. https://doi.org /10.1016/j.eurpolymj.2017.01.020.

(96)   Avgoustakis, K.; Nixon, J. R. Biodegradable controlled release tablets 1: preparative variables affecting the properties of poly(lactide-co-glycolide) copolymers as matrix forming material. *Int. J. Pharm.* **1991**, *70* (1), 77–85. https://doi.org/10.1016/0378-5173(91)90166-L.

(97)   Aijun, C.; Shihan, X.; Mingyang, H.; Jian, X.; Qun, C. The effects on thermal stability of polyglycolic acid by adding dihydrazide metal chelators. *Polym. Degrad. Stab.* **2017**, *137,* 238-243. https:// doi.org/10.1016/j.polymdegradstab.2017.01.016.

(98)   Lunelli, B. H.; Andrade, R. R.; Atala, D. I. P.; Wolf Maciel, M. R.; Maugeri Filho, F.; Maciel Filho, R. Production of lactic acid from sucrose: strain selection, fermentation, and kinetic modeling. *Appl. Biochem. Biotechnol.* **2010**, *161* (1–8), 227–237. https://doi.org/10.1007/s12010-009-8828-0.

(99)   Pivsa-Art, S.; Tong-ngok, T.; Junngam, S.; Wongpajan, R.; Pivsa-Art, W. Synthesis of poly(d-lactic acid) using a 2-steps direct polycondensation process. *Energy Procedia* **2013**, *34*, 604–609. https:// doi.org/10.1016/j.egypro.2013.06.791.

(100)   Thomas, T. D.; Ellwood, D. C.; Longyear, V. M. Change from homo- to heterolactic fermentation by streptococcus lactis resulting from glucose limitation in anaerobic chemostat cultures. *J. Bacteriol.* **1979**, *138* (1), 109–117. https://doi.org/10.1128/jb.138.1.109-117.1979.

(101)   EUBIO_Admin, Market, Eur. Bioplastics EV. https://www.european-bioplastics.org/market/ (accessed April 22, 2018).

(102)   Azimi, B.; Nourpanah, P.; Rabiee, M.; Arbab, S. Poly (lactide -co- glycolide) fiber: an overview. *J. Eng. Fibers Fabr.* **2014**, *9* (1), 20.

(103) Castro-Aguirre, E.; Iñiguez-Franco, F.; Samsudin, H.; Fang, X.; Auras, R. Poly(lactic acid)—mass production, processing, industrial applications, and end of life. *Adv. Drug Deliv. Rev.* **2016**, *107*, 333–366. https://doi.org/10.1016/j.addr.2016.03.010.

(104) Makadia, H. K.; Siegel, S. J. Poly lactic-co-glycolic acid (PLGA) as biodegradable controlled drug delivery carrier. *Polymers.* **2011**, *3* (3), 1377–1397. https://doi.org/10.3390/polym3031377.

(105) Kaynak, C.; Varsavas, S. D. Performance comparison of the 3d-printed and injection-molded PLA and its elastomer blend and fiber composites. *J. Thermoplast. Compos. Mater.* **2019**, *34(4)*, 501-210. https://doi.org /10.1177/0892705718772867.

(106) Coated VICRYL® (polyglactin 910) Suture | Ethicon, https://www.ethicon.com/na/products /wound-closure/absorbable-sutures/coated-vicryl-polyglactin-910-suture (accessed July 24, 2018).

(107) Singh, G.; Tanurajvir, K.; Ravinder, K.; Kaur, A. recent biomedical applications and patents on biodegradable polymer-PLGA. *Int. J. Pharmacol. Pharm. Sci.* **2014**, *1*, 30–42.

(108) Wang, N.; Wu, X. S.; Li, C.; Feng, M. F. Synthesis, characterization, biodegradation, and drug delivery application of biodegradable lactic/glycolic acid polymers: I. synthesis and characterization. *J. Biomater. Sci. Polym. Ed.* **2000**, *11* (3), 301–318.

(109) Ansary, R.; Awang, M.; Rahman, M. Biodegradable poly(d,l-lactic-co-glycolic acid)-based micro/nanoparticles for sustained release of protein drugs - a review. *Trop. J. Pharm. Res.* **2014**, *13*, 1179–1190. https://doi.org/10.4314/tjpr.v13i7.24.

(110) Erbetta, C. Synthesis and characterization of poly(d,l-lactide-co-glycolide) copolymer. *J. Biomater. Nanobiotechnology.* **2012**, *03*, 208–225. https://doi.org/10.4236/jbnb.2012.32027.

(111) Sousa, B. G. B. de; Pedrotti, G.; Sponchiado, A. P.; Cunali, R. S.; Aragones, Á.; Sarot, J. R.; Zielak, J. C.; Ornaghi, B. P.; Leão, M. P. analysis of tensile strength of poly(lactic-coglycolic acid) (PLGA) membranes used for guided tissue regeneration. *RSBO Online,* **2014**, *11* (1), 59–65.

(112) Fukuzaki, H.; Yoshida, M.; Asano, M.; Kumakura, M. Synthesis of copoly(d,l-lactic acid) with relatively low molecular weight and in vitro degradation. *Eur. Polym. J.* **1989**, *25* (10), 1019–1026. https://doi.org/10.1016/0014-3057(89)90131-6.

(113) Ajioka, M.; Suizu, H.; Higuchi, C.; Kashima, T. Aliphatic polyesters and their copolymers synthesized through direct condensation polymerization. *Polym. Degrad. Stab.* **1998**, *59* (1), 137–143. https://doi.org/10.1016/S0141-3910(97)00165-1.

(114) Kale, G.; Auras, R.; Singh, S. P. Degradation of commercial biodegradable packages under real composting and ambient exposure conditions. *J. Polym. Environ.* **2006**, *14,* 317–334. https://doi.org/10.1007/s10924-006-0015-6.

(115) Gao, Q.; Lan, P.; Shao, H.; Hu, X. Direct synthesis with melt polycondensation and microstructure analysis of poly(l-lactic acid-*co*-glycolic acid). *Polym. J.* **2002**, *34* (11), 786–793. https://doi.org/ 10.1295/polymj.34.786.

(116) Kricheldorf, H. R.; Serra, A. Polylactones 6. Influence of various metal salts on the optical purity of poly(l-lactide). *Polym. Bull.* **1985**, *14* (6), 497–502. https://doi.org/10.1007/BF00271606.

(117) Moon, S. I.; Lee, C. W.; Miyamoto, M.; Kimura, Y. Melt polycondensation of L-lactic acid with Sn(ii) catalysts activated by various proton acids: a direct manufacturing route to high molecular weight poly(L-lactic acid). *J. Polym. Sci. Part Polym. Chem.* **2000**, *38* (9), 1673–1679. https://doi.org/10.1002/(SICI)1099-0518(20000501)38:9<1673::AID-POLA33>3.0.CO;2-T.

(118) Whitmore, F. C. *Organic Chemistry, Volume One: Part I: Aliphatic Compounds Part II: Alicyclic Compounds*; Courier Corporation, 2012.

(119) Hyon, S.-H.; Jamshidi, K.; Ikada, Y. Synthesis of polylactides with different molecular weights. *Biomaterials.* **1997**, *18* (22), 1503–1508. https://doi.org/10.1016/S0142-9612(97)00076-8.

(120) Nieuwenhuis, J. Synthesis of polylactides, polyglycolides and their copolymers. *Clin. Mater.* **1992**, *10* (1), 59–67. https://doi.org/10.1016/0267-6605(92)90086-9.

(121) Wu, X. S.; Wang, N. Synthesis, characterization, biodegradation, and drug delivery application of biodegradable lactic/glycolic acid polymers. Part II: biodegradation. *J. Biomater. Sci. Polym. Ed.* **2001**, *12* (1), 21–34. https://doi.org/10.1163/156856201744425.

(122) Gorrasi, G.; Meduri, A.; Rizzarelli, P.; Carroccio, S.; Curcuruto, G.; Pellecchia, C.; Pappalardo, D. Preparation of poly(glycolide-co-lactide)s through a green process: analysis of structural, thermal, and barrier properties. *React. Funct. Polym.* **2016**, *109*, 70–78. https://doi.org/10.1016 /j.reactfunctpolym. 2016.10.002.

(123) Liu, X.; Shen, X.; Sun, X.; Peng, Y.; Li, R.; Yun, P.; Li, C.; Liu, L.; Su, F.; Li, S. Biocompatibility evaluation of self-assembled micelles prepared from poly(lactide-co-glycolide)-poly(ethylene glycol) diblock copolymers. *Polym. Adv. Technol.* **2018**, *29* (1), 205–215. https://doi.org/10.1002/pat.4104.

(124) Yang, A.; Yang, L.; Liu, W.; Li, Z.; Xu, H.; Yang, X. Tumor necrosis factor alpha blocking peptide loaded peg-plga nanoparticles: preparation and in vitro evaluation. *Int. J. Pharm.* **2007**, *331* (1), 123–132. https://doi.org/10.1016/j.ijpharm.2006.09.015.

(125) Wang, Z.; Liu, W.; Xu, H.; Yang, X. Preparation and in vitro studies of stealth pegylated plga nanoparticles as carriers for arsenic trioxide. *Chin. J. Chem. Eng.* **2007**, *15* (6), 795–801. https://doi.org/10.1016/S1004-9541(08)60005-1.

(126) Tobío, M.; Gref, R.; Sánchez, A.; Langer, R.; Alonso, M. J. Stealth PLA-PEG nanoparticles as protein carriers for nasal administration. *Pharm. Res.* **1998**, *15* (2), 270–275. https://doi.org/10.1023/a:1011922819926.

(127) Thermogelation of PLGA-block-PEG-block-PLGA Copolymers, Sigma-Aldrich. https://www.sigmaaldrich.com /technical-documents/articles/materials-science/thermogelation.html (accessed February 12, 2018).

(128) Jeong, B.; Bae, Y. H.; Kim, S. W. Drug release from biodegradable injectable thermosensitive hydrogel of PEG–PLGA–PEG triblock copolymers. *J. Controlled Release* **2000**, *63* (1), 155–163. https://doi.org/10.1016/S0168-3659(99)00194-7.

(129) Babos, G.; Biró, E.; Meiczinger, M.; Feczkó, T. Dual drug delivery of sorafenib and doxorubicin from PLGA and PEG-PLGA polymeric nanoparticles. *Polymers.* **2018**, *10*, 895. https://doi.org/10.3390/polym10080895.

(130) Ho Choi, S.; Gwan Park, T. Synthesis and characterization of elastic PLGA/PCL/PLGA tri-block copolymers. *J. Biomater. Sci. Polym. Ed.* **2002**, *13*, 1163–1173. https://doi.org /10.1163/156856202320813864.

(131) Gao, J.; Chen, S.; Tang, D.; Jiang, L.; Shi, J.; Wang, S. Mechanical properties and degradability of electrospun PCL/PLGA blended scaffolds as vascular grafts. *Trans. Tianjin Univ.* **2019**, *25* (2), 152–160. https://doi.org/10.1007/s12209-018-0152-8.

(132) Pack, J. W.; Kim, S. H.; Cho, I.-W.; Park, S. Y.; Kim, Y. H. Microstructure analysis and thermal property of copolymers made of glycolide and ϵ-caprolactone by stannous octoate. *Polym. Sci Part A Polym. Chem.* **2002**, 544–554. https://doi.org/10.1002/pola.10123.

(133) Dobrzynski, P.; Li, S.; Kasperczyk, J.; Maciej, B.; Gasc, F.; Vert, M. Structure−property relationships of copolymers obtained by ring-opening polymerization of glycolide and ε-caprolactone. Part 1. Synthesis and characterization. *Biomacromolecules.* **2005**, *6*, 483–488. https://doi.org/10.1021/bm0494592.

(134) Li, S.; Piotr, D.; Kasperczyk, J.; Maciej, B.; Gasc, F.; Vert, M. Structure−property relationships of copolymers obtained by ring-opening polymerization of glycolide and ε-caprolactone. Part 2. influence of composition and chain microstructure on the hydrolytic degradation. *Biomacromolecules.* **2005**, *6*, 489–497. https://doi.org/10.1021/bm049458+.

(135) Celorio, E.; Franco, L.; Rodriguez-Galan, A.; Puiggalí, J. Synthesis of glycolide/trimethylene carbonate copolymers: influence of microstructure on properties. *Eur. Polym. J.* **2012**, *48*, 60-73. https://doi.org/10.1016/j.eurpolymj.2011.10.014.

(136) Celorio, E.; Franco, L.; Rodriguez-Galan, A.; Puiggalí, J. Study on the hydrolytic degradation of glycolide/trimethylene carbonate copolymers having different microstructure and composition. *Polym. Degrad. Stab.* **2013**, *98*, 133–143. https://doi.org/10.1016/j.polymdegradstab.2012.10.019.

(137) Oxalic Acid Market - Global Industry Analysis, Size and Forecast, 2016 to 2026 https://www.futuremarketinsights.com/reports/oxalic-acid-market (accessed July 24, 2018).

(138) Global Oxalic Acid Market 2018 Consumption, high demand, manufacturing process, revenue, raw materials, suppliers, traders and product scope till 2025 – Reuters. https://www.reuters.com/brandfeatures/venture-capital/article?id=47167 (accessed December 10, 2018).

(139) Brooks, M. J. Manufacture of oxalic acid. US2322915A, June 29, 1943.

(140) Fuchs, G. H.; Watson, W. E. Manufacture of oxalic acid. US3536754A, October 27, 1970.

(141) Stevens, S. G. Method of producing oxalic acid. US2057119A, October 13, 1936.

(142) Sawada, H.; Murakami, T. Oxalic Acid. *Kirk-Othmer Encycl. Chem. Technol.* American Cancer Society, 2000. https://doi.org/10.1002/0471238961.1524011219012301.a01.

(143) Duroux, J. M.; Elie, L. M. Manufacture of oxalic acid. US3549696A, December 22, 1970.

(144) Yonemitsu, E.; Isshika, T.; Suzuki, T.; Sanada, A. Process for producing oxalic acid. US3691232A, September 12, 1972.

(145) Miyazaki, H.; Shiomi, Y.; Fujitus, S.; Masunaga, K.; Yanagisawa, H. Process for preparing oxalic acid diesters using platinum group metals supported on alumina. US4410722A, October 18, 1983.

(146) Miyazaki, H.; Shiomi, Y.; Fujitus, S.; Masunaga, K.; Yanagisawa, H. Process for the preparation of oxalic acid diesters. US4384133A, May 17, 1983.

(147) Miyazaki, H.; Shiomi, Y.; Fujitus, S.; Masunaga, K.; Yanagisawa, H. Process for the production of a diester of oxalic acid. US4507494A, March 26, 1985.

(148) Nishimura, K.; Fujii, K.; Nishihira, K.; Matsuda, M.; Uchiumi, S. Process for preparing a diester of oxalic acid in the gaseous phase. US4229591A, October 21, 1980.

(149) Lakkaraju, P. S.; Askerka, M.; Beyer, H.; Ryan, C. T.; Dobbins, T.; Bennett, C.; Kaczur, J. J.; Batista, V. S. Formate to oxalate: a crucial step for the conversion of carbon dioxide into multi-carbon compounds. *ChemCatChem.* **2016**, *8* (22), 3453–3457. https://doi.org/10.1002/cctc.201600765.

(150) Meurs, J. H. H. Method of preparing oxalic acid. WO2016124646A1, August 11, 2016.

(151) Pinkus, A. G.; Hariharan, R. Poly(methylene oxalate), a new composition of matter. US5561212A, October 1, 1996.

(152) Carothers, W. H. Linear condensation polymers. US2071250A, February 16, 1937.

(153) Shalaby, S. W.; Damiolkowski, D. D. Synthetic absorbable surgical devices of poly(alkylene oxalates). US4140678A, February 20, 1979.

(154) Okushita, H.; Kurachi, K.; Tanaka, S.; Adachi, F.; Tanaka, H.; Fujiwara, Y.; Yoshida, Y. Polyoxalate resin and shaped articles and resin compositions comprising same. US20050027081A1, February 3, 2005.

(155) Kuo, P.-C.; Lo, C.-T.; Chen, C.-Y. Crystallization and microstructure of poly(butylene oxalate). *Polymer.* **2013**, *54* (24), 6654–6662. https://doi.org/10.1016/j.polymer.2013.10.015.

(156) Yoshikawa, S.; Yamada, T. Polyoxalates and a process for the production thereof. US20170002135A1, January 5, 2017.

(157) Shalaby, S. W.; Jamiolkowski, D. D. Poly(alkylene oxalate) absorbable coating for sutures. US4105034A, August 8, 1978.

(158) Shiiki, Z.; Kawakami, Y. Poly(ethylene oxalate), product formed of molded therefrom and production process of poly(ethylene oxalate). US5688586A, November 18, 1997.

(159) Ballistreri, A.; Garozzo, D.; Giuffrida, M.; Impallomeni, G.; Montaudo, G. Primary thermal fragmentation processes in poly(ethylene oxalate) investigated by mass spectrometry. *Polym. Degrad. Stab.* **1988**, *21* (4), 311–321. https://doi.org/10.1016/0141-3910(88)90018-3.

(160) Cline, W. K. Polyethylene oxalate process. US3197445A, July 27, 1965.

(161) Alksnis, A.; Deme, D.; Surna, J. Synthesis of oligoesters and polyesters from oxalic acid and ethylene glycol. *J. Polym. Sci. Polym. Chem. Ed.* **1977**, *15* (8), 1855–1862. https://doi.org/10.1002/pol.1977.170150807.

(162) Bader, A. R. Preparation of esters of oxalic acid. US2693478A, November 2, 1954.

(163) Chattaway, F. D. XX.-Interaction of glycerol and oxalic acid. *J. Chem. Soc. Trans.* **1914**, *105* (0), 151–156. https://doi.org/10.1039/CT9140500151.

(164) Hong, D.; Song, B.; Kim, H.; Kwon, J.; Khang, G.; Lee, D. Biodegradable polyoxalate and copolyoxalate particles for drug-delivery applications. *Ther. Deliv.* **2011**, *2* (11), 1407–1417.

(165) Holland, S. J.; Tighe, B. J.; Gould, P. L. Polymers for biodegradable medical devices. 1. the potential of polyesters as controlled macromolecular release systems. *J. Control. Rel.* **1986**, *4* (3), 155–180. https://doi.org/10.1016/0168-3659(86)90001-5.

(166) Najibi, S.; Banglmeier, R.; Matta, J.; Tannast, M. Material properties of common suture materials in orthopaedic surgery. *Iowa Orthop. J.* **2010**, *30*, 84–88.

(167) Kim, S.; Park, H.; Song, Y.; Hong, D.; Kim, O.; Jo, E.; Khang, G.; Lee, D. Reduction of oxidative stress by p-hydroxybenzyl alcohol-containing biodegradable polyoxalate nanoparticulate antioxidant. *Biomaterials.* **2011**, *32* (11), 3021–3029. https://doi.org/10.1016/j.biomaterials. 2010.11.033.

(168) Garcia, J. J.; Miller, S. A. Polyoxalates from biorenewable diols via oxalate metathesis polymerization. *Polym. Chem.* **2013**, *5* (3), 955–961. https://doi.org/10.1039/C3PY01185B.

(169) Zhao, Y. H.; Xu, G. H.; Yuan, X.-B.; Sheng, J. Novel degradable copolyesters containing poly(ethylene oxalate) units derived from diethylene oxalate. *Polym. Degrad. Stab.* **2006**, *91* (1), 101–107. https://doi.org/10.1016/j.polymdegradstab.2005.04.023.

(170) Finelli, L.; Lotti, N.; Munari, A. Thermal properties of poly(butylene oxalate) copolymerized with azelaic acid. *Eur. Polym. J.* **2002**, *38* (10), 1987–1993. https://doi.org/10.1016/S0014-3057(02)00089-7.

(171) Pickett, J. E.; Coyle, D. J. Hydrolysis kinetics of condensation polymers under humidity aging conditions. *Polym. Degrad. Stab.* **2013**, *98* (7), 1311–1320. https://doi.org/10.1016/j.polymdegradstab.2013.04.001.

(172) Qi, X.; Ren, Y.; Wang, X. New advances in the biodegradation of poly(lactic) acid. *Int. Biodeterior. Biodegrad.* **2017**, *117*, 215–223. https://doi.org/10.1016/j.ibiod.2017.01.010.

(173) Hwang, N. H. C.; Woo, S. L.-Y. *Frontiers in Biomedical Engineering: Proceedings of the World Congress for Chinese Biomedical Engineers*; Springer Science & Business Media, 2003.

(174) Lunt, J. Large-scale production, properties and commercial applications of polylactic acid polymers. *Polym. Degrad. Stab.* **1998**, *59* (1), 145–152. https://doi.org/10.1016/S0141-3910(97)00148-1.

(175) Tsuji, H. Poly(lactic Acid) stereocomplexes: a decade of progress. *Adv. Drug Deliv. Rev.* **2016**, *107*, 97–135. https://doi.org/10.1016/j.addr.2016.04.017.

(176) Vert, M.; Mauduit, J.; Li, S. Biodegradation of PLA/GA polymers: increasing complexity. *Biomaterials* **1994**, *15* (15), 1209–1213. https://doi.org/10.1016/0142-9612(94)90271-2.

(177) Elsawy, M. A.; Kim, K.-H.; Park, J.-W.; Deep, A. Hydrolytic degradation of polylactic acid (PLA) and its composites. *Renew. Sustain. Energy Rev.* **2017**, *79*, 1346–1352. https://doi.org/10.1016/j.rser.2017.05.143.

(178) Taylor, M. S.; Daniels, A. U.; Andriano, K. P.; Heller, J. Six bioabsorbable polymers: in vitro acute toxicity of accumulated degradation products. *J. Appl. Biomater.* **1994**, *5* (2), 151–157. https://doi.org/10.1002/jab.770050208.

(179) Williams, D. F.; Mort, E. Enzyme-accelerated hydrolysis of polyglycolic acid. *J. Bioeng.* **1977**, *1* (3), 231–238.

(180) Houchin, M. L.; Topp, E. M. Chemical degradation of peptides and proteins in PLGA: a review of reactions and mechanisms. *J. Pharm. Sci.* **2008**, *97* (7), 2395–2404. https://doi.org/10.1002/jps.21176.

(181) Mundargi, R. C.; Babu, V. R.; Rangaswamy, V.; Patel, P.; Aminabhavi, T. M. Nano/micro technologies for delivering macromolecular therapeutics using poly(d,l-lactide-co-glycolide) and its derivatives. *J. Controlled Release* **2008**, *125* (3), 193–209. https://doi.org/10.1016/j.jconrel.2007.09.013.

(182) Park, K. I.; Xanthos, M. A Study on the degradation of polylactic acid in the presence of phosphonium ionic liquids. *Polym. Degrad. Stab.* **2009**, *94* (5), 834–844. https://doi.org/10.1016/j.polymdegradstab.2009.01.030.

(183) Tokiwa, Y.; Calabia, B. P. Biodegradability and biodegradation of poly(lactide). *Appl. Microbiol. Biotechnol.* **2006**, *72* (2), 244–251. https://doi.org/10.1007/s00253-006-0488-1.

(184) Miller, R. A. Degradation rates of oral resorbable implants (polylactates and polyglycolates) : rate modification with changes in PLA/PGA copolymer ratios. *J Biomed Mater Res.* **1977**, *11*, 711–719. https://doi: 10.1002/jbm.820110507

(185) Song, J. H.; Murphy, R. J.; Narayan, R.; Davies, G. B. H. Biodegradable and compostable alternatives to conventional plastics. *Philos. Trans. R. Soc. Lond. B Biol. Sci.* **2009**, *364* (1526), 2127–2139. https://doi.org/10.1098/rstb.2008.0289.

(186) Li, J.; Stayshich, R. M.; Meyer, T. Y. Exploiting sequence to control the hydrolysis behavior of biodegradable PLGA copolymers. *J. Am. Chem. Soc.* **2011**, *133* (18), 6910–6913. https://doi.org/10.1021/ja200895s.

(187) Kim, S.; Seong, K.; Kim, O.; Kim, S.; Seo, H.; Lee, M.; Khang, G.; Lee, D. Polyoxalate nanoparticles as a biodegradable and biocompatible drug delivery vehicle. *Biomacromolecules.* **2010**, *11* (3), 555–560. https://doi.org/10.1021/bm901409k.

(188) Jamshidi, K.; Hyon, S.-H.; Ikada, Y. Thermal characterization of polylactides. *Polymer.* **1988**, *29* (12), 2229–2234. https://doi.org/10.1016/0032-3861(88)90116-4.

(189) Lee, E.; Kim, S.; Seong, K.; Park, H.; Seo, H.; Khang, G.; Lee, D. A biodegradable and biocompatible drug-delivery system based on polyoxalate microparticles. *J. Biomater. Sci. Polym. Ed.* **2011**, *22* (13), 1683–1694. https://doi.org/10.1163/092050610X519480.

(190) Sustainable Bioplastics Council of Maine. The Business Case for Commercial Production of Bioplastics in Maine. Https://Www.Ourhealthyfuture.Org/Sites/ Default/Files/Pdfs

/The_business_case_for_commercial_production_of_bioplastics_ in_maine_final.Pdf. (2010)

(191) Growing Demand for Absorbable Sutures to Create Growth Opportunities for Polyglycolic Acid Market, reports TMR https://www.transparencymarketresearch.com/pressrelease/polyglycolic-acid-market.htm (accessed July 24, 2018).

(192) Kureha news release http://www.kureha.co.jp/en/release/pdf/20150203-en.pdf (accessed January 21,2018).

(193) Frazier, W. L. dissolvable downhole tools comprising both degradable polymer acid and degradable metal alloy elements. US20170234103A1, August 17, 2017.

(194) Frazier, W. L.; Frazier, G.; Frazier, D. Downhole tools having non-toxic degradable elements and their methods of use. US9587475B2, March 7, 2017.

(195) Barbee, R. B.; Jr, T. H. W. Polyester containers having improved gas barrier properties. US4426512a, January 17, 1984.

(196) Nakajima, J.; Kato, T.; Matsukura, Y. Multilayer container of polyglycolic acid and polyester and blow molding production process. US7713464B2, May 11, 2010.

(197) Hokari, Y.; Yamane, K.; Wakabayashi, J.; Suzuki, T. Polyglycolic acid resin-based layered sheet and method of producing the same. US20090081396A1, March 26, 2009.

(198) Schrenk, W. J.; Shastri, R. K.; Roehrs, H. C.; Ayres, R. E. Method for producing injection molded multilayer articles. US5202074A, April 13, 1993.

(199) Shiiki, Z.; Kawakami, Y.; Sato, N.; Hoshino, M.; Kouyama, T. Gas-barrier composite film. US6245437B1, June 12, 2001.

(200) Aardt, M. V.; Duncan, S. E.; Marcy, J. E.; Long, T. E.; O'Keefe, S. F.; Sims, S. R. Release of antioxidants from poly(lactide-co-glycolide) films into dry milk products and food simulating liquids. *Int. J. Food Sci. Technol.* 42 (11), 1327–1337. https://doi.org/10.1111/j.1365-2621.2006.01329.x.

(201) Alksnis, A.; Vilsone, D.; MISĀNE, M. Método de obtención de un polímero fibroso biodegradable a partir de ácido oxálico. LV11902B, May 20, 1998.

(202) Gu, J.-D. Microbiological deterioration and degradation of synthetic polymeric materials: recent research advances. *Int. Biodeterior. Biodegrad.* **2003**, *52* (2), 69–91. https://doi.org/10.1016/S0964-8305(02)00177-4.

(203) Fotopoulou, K. N.; Karapanagioti, H. K. Degradation of various plastics in the environment. *Hazard. Chem. Assoc. Plast. Mar. Environ.* The Handbook of Environmental Chemistry; Springer International Publishing: Cham, 2017, pp 71–92. https://doi.org/10.1007/698_2017_11.

(204) Kint, D. P. R.; Martínez de Ilarduya, A.; Muñoz-Guerra, S. Hydrolytic degradation of poly(ethylene terephthalate) copolymers containing nitrated units. *Polym. Degrad. Stab.* **2003**, *79* (2), 353–358. https://doi.org/10.1016/S0141-3910(02)00299-9.

(205) ecovio® F Mulch C2311 Biodegradable compound for agricultural film. https://www.plasticsportal.net/wa/plasticsEU~de_DE/function/conversions:/publish/common/upload/biodegradable_plastics/Ecovio_F_Mulch_C2311.pdf?doc_lang=   en_GB (accessed January 22, 2018).

(206) Starcla - Bio-based Bionolle resin, Showa Denko eur. GmbH Shap. Ideas. https://www.showa-denko.com/news/starcla-bio-based-bionolle-resin/ (accessed July 24, 2018).

(207) Nature Works | Landscape and Agriculture. https://www.natureworksllc.com/ Ingeo-in-Use/ Landscape-and-Agriculture (accessed January 7, 2018).

(208) NatureWorks | Hortifair 2009 Showcases Innovative Ingeo Bioplastic Products https://www.natureworksllc.com/News-and-Events/Press-Releases/2009/10-13-09-Hortifair (accessed July 24, 2018).

(209) Jintakanon, N.; Opaprakasit, P.; Petchsuk, A.; Opaprakasit, M. Controlled-release materials for fertilizer based on lactic acid polymers. *Adv. Mater. Res.* **2008**, *55–57*, 905–908. https://doi.org/10.4028 /www.scientific.net/AMR.55-57.905.

(210) Calabria, L.; Vieceli, N.; Bianchi, O.; Boff de Oliveira, R. V.; do Nascimento Filho, I.; Schmidt, V. Soy protein isolate/poly(lactic acid) injection-molded biodegradable blends for slow release of fertilizers. *Ind. Crops Prod.* **2012**, *36* (1), 41–46. https://doi.org/10.1016/j.indcrop.2011.08.003.

(211) Pursell, T.; Jr, A. R. S.; Cochran, K. D.; Miller, J. M.; Holt, T. G.; Peeden, G. S. Controlled release fertilizer with biopolymer coating and process for making same. US9266787B2, February 23, 2016.

(212) Wiebe, J.; Nef, H. M.; Hamm, C. W. Current status of bioresorbable scaffolds in the treatment of coronary artery disease. *J. Am. Coll. Cardiol.* **2014**, *64* (23), 2541–2551. https://doi.org/10.1016/j.jacc.2014.09.041.

(213) Dejong, E. S.; DeBerardino, T. M.; Brooks, D. E.; Judson, K. In vivo comparison of a metal versus a biodegradable suture anchor. *Arthrosc.* **2004**, *20* (5), 511–516. https://doi.org/10.1016/j.arthro.2004.03.008.

(214) Saini, P.; Arora, M.; Kumar, M. N. V. R. Poly(lactic acid) blends in biomedical applications. *Adv. Drug Deliv. Rev.* **2016**, *107*, 47–59. https://doi.org/10.1016/j.addr.2016.06.014.

(215) Armentano, I.; Bitinis, N.; Fortunati, E.; Mattioli, S.; Rescignano, N.; Verdejo, R.; Lopez-Manchado, M. A.; Kenny, J. M. Multifunctional nanostructured pla materials for packaging and tissue engineering. *Prog. Polym. Sci.* **2013**, *38* (10), 1720–1747. https://doi.org/10.1016/j.progpolymsci.2013.05.010.

(216) Yang, J.; Yamato, M.; Kohno, C.; Nishimoto, A.; Sekine, H.; Fukai, F.; Okano, T. Cell sheet engineering: recreating tissues without biodegradable scaffolds. *Biomaterials.* **2005**, *26* (33), 6415–6422. https://doi.org/10.1016/j.biomaterials.2005.04.061.

(217) Bergström, J. S.; Hayman, D. An overview of mechanical properties and material modeling of polylactide (PLA) for medical applications. *Ann. Biomed. Eng.* **2016**, *44* (2), 330–340. https://doi.org/10.1007/s10439-015-1455-8.

(218) Farah, S.; Anderson, D. G.; Langer, R. Physical and mechanical properties of PLA, and their functions in widespread applications — a comprehensive review. *Adv. Drug Deliv. Rev.* **2016**, *107*, 367–392. https://doi.org/10.1016/j.addr.2016.06.012.

(219) Duffy, R. J.; Maria, F. D. Method for tanning absorbable surgical sutures. US3483286A, December 9, 1969.

(220) McClain, J. Surgical sutures having increased strength. *U.S. Patent 8,636,767 B2.* January 28, 2014.

(221) Trisorb®-Samyang Biopharmaceuticals https://www.samyangbiopharm.com/eng/ProductIntroduce/medical_device02 (accessed July 24, 2018).

(222) Safil Absorbable Surgical Suture | Aesculap USA https://www.aesculapusa.com/products/wound-closure/absorbable-sutures/safil-absorbable (accessed July 24, 2018).

(223) Resorba® Sutures Glycolon™ Absorbable Monofilament Suture, Osteogenics Biomedical https://www.osteogenics.com/v/product-group/Glycolon-Absorbable-Monofilament-Suture/10f/ (accessed July 24, 2018).

(224) Whang, K.; Thomas, C. H.; Healy, K. E.; Nuber, G. A novel method to fabricate bioabsorbable scaffolds. *Polymer.* **1995**, *36* (4), 837–842. https://doi.org/10.1016/0032-3861(95)93115-3.

(225) Rose, J. High strength bioresorbable containing poly-glycolic acid. US7455674B2, November 25, 2008.

(226) You, Y.; Youk, J. H.; Lee, S. W.; Min, B.-M.; Lee, S. J.; Park, W. H. Preparation of porous ultrafine PGA fibers via selective dissolution of electro spun PGA/PLA blend fibers. *Mater. Lett.* **2006**, *60* (6), 757–760. https://doi.org/10.1016/j.matlet.2005.10.007.

(227) Bekele, S. Polyglycolic acid-based film. EP2782531A2, October 1, 2014.

(228) Solovyov, S.; Goldman, A. *Mass Transport & Reactive Barriers in Packaging: Theory, Applications, & Design*; DEStech Publications, Inc, 2008.

(229) EVAL™ https://www.kuraray.eu/produkte/sortiment/evaltm/ (accessed August 22, 2018).

(230) Cutright, D. E.; Beasley, J. D.; Perez, B. Histologic comparison of polylactic and polyglycolic acid sutures. *Oral Surg. Oral Med. Oral Pathol.* **1971**, *32* (1), 165–173. https://doi.org/10.1016/0030-4220(71)90265-9.

(231) Pillai, C. K. S.; Sharma, C. Absorbable polymeric surgical sutures: chemistry, production, properties, biodegradability, and performance. *J. Biomater. Appl.* **2010**, *25* (4), 291–366. https://doi.org/10.1177/0885328210384890.

(232) Conn, J.; Oyasu, R.; Welsh, M.; Beal, J. M. Vicryl (polyglactin 910) synthetic absorbable sutures. *Am. J. Surg.* **1974**, *128* (1), 19–23. https://doi.org/10.1016/0002-9610(74)90228-1.

(233) Plus Antibacterial Sutures Evidence Summary https://www.ethicon.com/na/system/files/2017-08/034874-170106_PlusSuture_Evidence_Summary_r5.pdf (accessed January 12, 2018).

(234) Zhao, W.; Li, J.; Jin, K.; Liu, W.; Qiu, X.; Li, C. Fabrication of functional PLGA-based electrospun scaffolds and their applications in biomedical engineering. *Mater. Sci. Eng. C* **2016**, *59*, 1181–1194. https://doi.org/10.1016/j.msec.2015.11.026.

(235) Zhao, X.; Han, Y.; Li, J.; Cai, B.; Gao, H.; Feng, W.; Li, S.; Liu, J.; Li, D. BMP-2 Immobilized PLGA/hydroxyapatite fibrous scaffold via polydopamine stimulates osteoblast growth. *Mater. Sci. Eng. C Mater. Biol. Appl.* **2017**, *78*, 658–666. https://doi.org/10.1016/j.msec.2017.03.186.

(236) Heo, M.; Lee, S. J.; Heo, D. N.; Lee, D.; Lim, H.-N.; Moon, J.-H.; Kwon, I. K. Multilayered co-electro spun scaffold containing silver sulfadiazine as a prophylactic against osteomyelitis: characterization and biological in vitro evaluations. *Appl. Surf. Sci.* **2018**, *432*, 308–316. https://doi.org/10.1016/j.apsusc.2017.04.147.

(237) Gentile, P.; Chiono, V.; Carmagnola, I.; Hatton, P. V. An overview of poly(lactic-co-glycolic) acid (PLGA)-based biomaterials for bone tissue engineering. *Int. J. Mol. Sci.* **2014**, *15* (3), 3640–3659. https://doi.org/10.3390/ijms15033640.

(238) Cerqueira, B. B. S.; Lasham, A.; Shelling, A. N.; Al-Kassas, R. Development of biodegradable plga nanoparticles surface engineered with hyaluronic acid for targeted delivery of paclitaxel to triple negative breast cancer cells. *Mater. Sci. Eng. C Mater. Biol. Appl.* **2017**, *76*, 593–600. https://doi.org/10.1016/j.msec.2017.03.121.

(239) Ceonzo, K.; Gaynor, A.; Shaffer, L.; Kojima, K.; Vacanti, C. A.; Stahl, G. L. Polyglycolic acid-induced inflammation: role of hydrolysis and resulting complement activation. *Tissue Eng.* **2006**, *12* (2), 301–308. https://doi.org/10.1089/ten.2006.12.301.

(240) Zhou, H.; Lawrence, J. G.; Bhaduri, S. B. Fabrication aspects of PLA-CaP/PLGA-CaP composites for orthopedic applications: a review. *Acta Biomater.* **2012**, *8* (6), 1999–2016. https://doi.org/10.1016/j.actbio.2012.01.031.

(241) Xu, T. O.; Kim, H. S.; Stahl, T.; Nukavarapu, S. P. Self-neutralizing PLGA/magnesium composites as novel biomaterials for tissue engineering. *Biomed. Mater.* **2018**, *13* (3), 035013. https://doi.org/10.1088/1748-605X/aaaa29.

(242) Brown, A.; Zaky, S.; Ray, H.; Sfeir, C. Porous magnesium/PLGA composite scaffolds for enhanced bone regeneration following tooth extraction. *Acta Biomater.* **2015**, *11*, 543–553. https://doi.org/10.1016/j.actbio.2014.09.008.

(243) Ayyanaar, S.; Kesavan, M. P.; Sivaraman, G.; Maddiboyina, B.; Annaraj, J.; Rajesh, J.; Rajagopal, G. A novel curcumin-loaded PLGA micromagnetic composite system for controlled and PH-responsive drug delivery. *Colloids Surf. Physicochem. Eng. Asp.* **2019**, *573*, 188–195. https://doi.org/10.1016/j.colsurfa.2019.04.062.

(244) Eslami, H.; Azimi Lisar, H.; Jafarzadeh Kashi, T. S.; Tahriri, M.; Ansari, M.; Rafiei, T.; Bastami, F.; Shahin-Shamsabadi, A.; Mashhadi Abbas, F.; Tayebi, L. Poly(lactic-co-glycolic acid)(PLGA)/TiO$_2$ nanotube bioactive composite as a novel scaffold for bone tissue engineering: in vitro and in vivo studies. *Biol. J. Int. Assoc. Biol. Stand.* **2018**, *53*, 51–62. https://doi.org/10.1016/ j.biologicals. 2018.02.004.

(245) Jiang, L.-X.; Jiang, L.-Y.; Ma, C.; Han, C.-T.; Xu, L.-J.; Xiong, C.-D. Preparation and characterization of nano-hydroxyapatite/PLGA composites with novel surface-modified nano-hydroxyapatite. *Wuji Cailiao XuebaoJournal Inorg. Mater.* **2013**, *28*, 751–756. https://doi.org/10.3724 /SP.J.1077.2013.12502.

(246) Xin, X.; Guan, Y.; Yao, S. Bi-/Multi-modal pore formation of PLGA/hydroxyapatite composite scaffolds by heterogeneous nucleation in supercritical CO$_2$ foaming. *Chin. J. Chem. Eng.* **2018**, *26* (1), 207–212. https://doi.org/10.1016/j.cjche.2017.04.005.

(247) Boukari, Y.; Qutachi, O.; Scurr, D. J.; Morris, A. P.; Doughty, S. W.; Billa, N. A dual-application poly (dl-lactic-co-glycolic) acid (PLGA)-chitosan composite scaffold for potential use in bone tissue engineering. *J. Biomater. Sci. Polym. Ed.* **2017**, *28* (16), 1966–1983. https://doi.org/10.1080/ 09205063.2017.1364100.

(248) Behera, T.; Swain, P. Alginate–chitosan–PLGA composite microspheres induce both innate and adaptive immune response through parenteral immunization in fish. *Fish Shellfish Immunol.* **2013**, *35* (3), 785–791. https://doi.org/10.1016/j.fsi.2013.06.012.

(249) Zhai, P.; Chen, X. B.; Schreyer, D. J. PLGA/alginate composite microspheres for hydrophilic protein delivery. *Mater. Sci. Eng. C.* **2015**, *56*, 251–259. https://doi.org/10.1016/j.msec.2015.06.015.

(250) Phromviyo, N.; Swatsitang, E.; Chompoosor, A. Effect of a surface stabilizer on the formation of polyoxalate nanoparticles and their release profiles. *Vacuum.* **2014**, *107*, 208–212. https://doi.org/10.1016/j.vacuum.2014.02.004.

(251) Höcherl, A.; Jäger, E.; Jäger, A.; Hrubý, M.; Konefał, R.; Janoušková, O.; Spěváček, J.; Jiang, Y.; Schmidt, P. W.; Lodge, T. P.; Štěpánek, P. One-Pot Synthesis of Reactive Oxygen Species (ROS)-

Self-Immolative Polyoxalate Prodrug Nanoparticles for Hormone Dependent Cancer Therapy with Minimized Side Effects. *Polym. Chem.* **2017**, *8* (13), 1999–2004. https://doi.org/10.1039/C7PY00270J.

CHAPTER 2

PLGA barrier materials from CO₂. The influence of lactide comonomer on glycolic acid polyesters

Abstract

The combination of the predicted polymer market growth and the emergence of new feedstocks creates a fantastic opportunity for novel sustainable polymers. To replace fossil-based feedstock, there are only three alternative sustainable carbon sources: biomass, CO_2 and existing plastics (via mechanical and/or chemical recycling). The ultimate circular feedstock would be CO_2: it can be electrochemically reduced to formic acid derivatives that subsequently can be converted into useful monomers such as glycolic acid. This work is part of the European Horizon 2020 project "Ocean" in which the steps from CO_2 to glycolic acid are developed. Polyglycolic acid (PGA) and poly(lactic-co-glycolic) (PLGA) copolyesters with high lactic acid (LA) content are well known. PGA is very difficult to handle due to its high crystallinity. On the other hand, PLGA's with high LA content lack good oxygen and moisture barriers. The aim of this work is to understand the structure-property relationships for the mostly unexplored glycolic acid rich PLGA copolymer series and to assess their suitability as barrier materials. Thus, PLGA copolymers with between 50 and 91 mol% of glycolic acid were synthesized and their properties were evaluated. Increased thermal stability was observed with increasing glycolic acid content. Only those containing 87 and 91 mol% glycolic acid were semicrystalline. A crystallization study under non-isothermal conditions revealed that copolymerization reduces the crystallization rate for PLGA compared to polylactic acid (PLA) and PGA. While PGA homopolymer crystallizes completely when cooled at 10 °C·min^{-1}, the copolymers with 9 and 13% lactic acid show almost 10 times slower crystallization, which is a huge advantage vis-à-vis PGA for processing. The kinetics of this process, modeled with the Jeziorny-modified Avrami method, confirmed those observations. Barrier property assessment revealed great potential for these copolymers for application in barrier films. Increasing glycolic acid content in PLGA copolymers enhances the barrier to both oxygen and water vapor. At room temperature and a relative humidity below 70% the PLGA copolymers with high glycolic acid content outperform the barrier properties of polyethylene terephthalate (PET).

2.1   Introduction

Poly(lactic-co-glycolic acid) (PLGA) are aliphatic polyesters of increasing interest for the biomedical field due to their biocompatibility and degradability in vivo.[1] High molecular weight PLGA can only be produced via Ring Opening Polymerization (ROP) of lactide (LAC) and glycolide (GL) and not via the monomers LA and GA.[2] ROP has shown to be a very useful route to produce polymers of industrial importance at commercial scale. These polyester syntheses can be carried out via different mechanisms such as anionic, cationic, enzymatic and coordination-insertion polymerization.[3,4] Because of its solubility in various lactones, high catalytic activity, low toxicity and ability to give high molecular weight polymers, tin(II) 2-ethylhexanoate $Sn(Oct)_2$ has been the most widely used and studied catalyst for lactide and glycolide polymerization.[5] According to Ryner et al.,[6] the most

accepted ROP mechanism involves a coordination-insertion mechanism initiated by the hydroxyl group of an added alcohol which coordinates to SnOct$_2$, forming an initiating tin alkoxide complex. The rate-determining step of the ROP is then the nucleophilic attack of the alkoxide on the carbonyl carbon of the monomer.

The mechanical and physicochemical properties of PLGA are strongly determined by the ratio of the monomers. Most commercial PLGA grades currently available contain mainly lactide (between 50 and 95 mol%)[7,8] with the exception of the absorbable suture material brand Vicryl (90% glycolide) from Ethicon.[9] Copolymers with between 50 and 85 mol% of lactide exhibit a tensile strength (σ) between 41.4 and 55.2 MPa and a tensile modulus *(E)* between 1 and 4.3 GPa.[10] These values tend to be close to those reported for PLA (σ=60.4 MPa and E=3.54 GPa[11]) and considerably lower than those for PGA, especially the tensile strength (σ=117 MPa and E=7.6 GPa[12]). Furthermore, materials with high contents of lactide exhibit an amorphous microstructure with glass transition temperatures (T$_g$) between 31 and 51 °C and thermal stability up to 240 °C.[13,14] They have also shown longer degradation time with increasing lactide content and improved hydrophobicity.[15] Studies for copolymers with higher glycolic acid content are scarce[16,17] and important properties (e.g. barrier properties, thermal stability and crystallization behavior) useful for determining their potential for a wider range of applications have not been reported yet. In 1979, Gilding et al. published work on PLGA copolymers with high glycolide content.[16] To the best of our knowledge, this is the only published research thus far that has focused on these types of materials. Although valuable observations concerning the reaction mechanism and their characterization have been provided, many important aspects of these copolymers are still unknown. The PLA and PLGA data reported in that paper and references used for comparison all deal with *L*-lactic acid or *L*-lactide based polymers.

Research on polymer crystallization is very relevant since it can influence properties such as permeability, transparency, toughness and elasticity. For semicrystalline materials, these properties are affected by size, orientation, shape and regularity of the crystallites, as well as by the degree of crystallinity.[18] Crystallization behavior of pure PLA has been reported frequently.[18-20] For PGA, however, studies on crystallization behavior are scarce. Yu et al. investigated the spherulitic morphology,[21] crystalline structure and structural evolution of PGA in the crystallization and melting processes by time-resolved wide-angle X-ray diffraction (WAXD) and Fourier transform Infrared (FTIR) spectrometry. According to the authors, PGA exhibits very fast crystallization from the melt and it completely crystallizes under fast cooling conditions (dT/dt = 10 °C·min^{-1}). A unique morphology during crystallization, consisting of hedrites, was observed. This differs from the normal characteristic spherulites found for PLA and other aliphatic polyesters with similar chemical structures. Furthermore, Chen et al. studied different composites with a PLA matrix and PGA fibers as fillers.[22] The results showed that PGA fiber addition accelerates the

crystallization of PLA under isothermal conditions. This trend however, was not strongly affected by the fiber content.

For semicrystalline PLGA copolymers, the influence of glycolide content on the crystallization process has not been reported. Understanding such behavior is very relevant since it can provide valuable insight for material processing and application assessment.

Another very relevant property for PLGA copolymers, which is affected by the glycolide content, is the barrier for water vapor and oxygen. Common oxygen barrier polymers include PET, ethylene vinyl alcohol (EVOH), polyvinylidene chloride (PVDC), polyvinyl alcohol (PVOH), polyacrylonitrile (PAN), nylons and nylon-MXD6.[23] In some cases, they are used in multilayer systems with good water barrier polymers such as polypropylene (PP) and polyethylene (PE). These materials, consumed massively in different applications, are fossil based and not degradable, which means that when leaked into ecosystems, irreversible accumulation of polymers will occur. For this reason, the use of single-use packaging is under increasing pressure.

The barrier properties of PLA have been frequently studied and reviewed.[24-30] PLA alone does not exhibit a good enough water vapor barrier to compete with commonly used packaging materials such as PET and polystyrene (PS). In terms of oxygen barrier, PLA shows a lower permeability coefficient than PS and a higher one than PET.[31] Because of the aforementioned limitations regarding barrier, PLA use in packaging has been restricted to short shelf life products. Nevertheless, the growing environmental awareness of consumers has contributed to increasing and ongoing interest for this polymer in the packaging industry. [32,33]

PGA, on the other hand, possesses very good barrier properties. The company Kureha has used it for the production of containers, pouches and mono-[34] and multilayer[35,36] sheets. According to Kureha, a PGA film of 20 µm thickness possesses an oxygen transmission rate (OTR) of about 1 $cm^3 \cdot m^{-2} \cdot day^{-1}$ (measured at 30 °C and 80% relative humidity (RH)) and a water vapor transmission rate (WVTR) of about 10 $g \cdot m^{-2} \cdot day^{-1}$ at the same conditions. [37] This performance is superior to that of most commercially available barrier polymers.

Nevertheless, PGA is also a very brittle material (linked to its high degree of crystallinity), with very limited solubility and difficult processability. The latter is related to its thermal properties. PGA exhibits a relatively small difference between its melt T_m (222 °C) and crystallization temperature (T_c = 192-198 °C). [38] For extrusion of items such as films and sheets this fast crystallization upon cooling from the melt, complicates obtaining amorphous preforms. Consequently, transparent products are difficult to achieve. PGA also displays a small difference between its T_g (40-45 °C) and cold crystallization temperature (T_{cc} =75 °C). [39] This is problematic for stretching (of films, sheets, fibers, etc.) or stretch blow molding, since this is limited to a narrow temperature range. Furthermore, PGA has been reported to generate gasses upon melt processing, which have been attributed to low-molecular weight products produced in the molten state.

Lastly, PGA is limited in its application due to its very fast degradation rate[12] (2 weeks by hydrolysis at 99 °C). Taking into account the aforementioned limitations, copolymerization with low amounts of lactic acid/lactide is an attractive strategy for enhancing processability and solubility properties while also tuning the material properties (e.g. degradation rate).

Here, we report on our studies regarding the effects of glycolic acid content on the properties of copolymers derived from glycolide and lactide. Copolymers containing from 50 to 91 mol% of glycolide were synthesized via ROP and characterized in terms of structure, density, thermal stability and molecular weight distribution. For semicrystalline copolymers, the crystallization behavior was studied under non-isothermal crystallization conditions. Furthermore, the potential of PLGA copolymers as barrier materials was assessed by measuring the oxygen and water permeability at 30 °C and 70% RH, using hot pressed films. In addition, the effect of relative humidity and temperature on the water permeability was assessed for the two copolymers with higher glycolic acid content.

2.2   Experimental section

2.2.1   Materials

Lactide and glycolide were acquired from Corbion (the Netherlands). $Sn(Oct)_2$ was purchased from Alfa Aesar (96% purity) and 1-dodecanol was obtained from Merck (98%). Toluene was purchased from Acros (99.8% purity). Deuterated chloroform was obtained from Eurisotop and hexafluoroisopropanol-d_2 was acquired from Sigma Aldrich.

2.2.2   Copolymer synthesis

A series of lactide and glycolide copolymers was prepared on 20 gram scale by ring opening polymerization using the following general procedure.

Prior to polymerization, the glassware was cleaned and dried at 120 °C in an oven overnight. Lactide and glycolide were weighed in a 250 mL three neck round bottom flask, equipped with a mechanical stirrer. Subsequently, the system was evacuated under vacuum and flushed three times with nitrogen for 5 minutes, each time at room temperature. Then, 0.060 g (0.03 wt.% relative to the monomer feed) of catalyst $Sn(Oct)_2$ and 0.020 g (0.01 wt% relative to the monomer feed) of initiator 1-dodecanol were added to the flask (prepared separately as a toluene solution). The toluene was removed under reduced pressure (10 mbar). The flask was heated in a silicone oil bath initially at 180 °C under nitrogen atmosphere. The temperature was gradually increased to 200 °C and then stirred at 100 rpm for 4 hours. The product was recovered, grinded and dried for about 12 hours at 40 °C in a vacuum oven (10 mbar).

Copolymers with increasing glycolide content (50, 60, 70, 80, 85 and 90 mol%) were prepared using this procedure (see **Table 2.4** in Appendix for detailed reaction conditions). While the concentration of catalyst and initiator were kept constant for all syntheses, the reaction temperature was increased gradually up to 220 °C for the copolymers with 85 and 90 mol% of glycolide. Furthermore, the reaction time was reduced to 3 hours for 80 and 85% glycolide and to 2 hours for 90 mol% of glycolide. Under these conditions, both monomers reached high conversion with little discoloration of the final product. As was observed in prior experiments, longer reaction times for these three samples led to additional transesterification side-reactions, broader molecular weight distributions and strong polymer discoloration. PLA and PGA were synthesized as reference materials according to the protocol described by Kaihara et al.[40]

2.2.3 Structure and thermal stability of PLGA copolymers

2.2.3.1 Nuclear Magnetic Resonance (NMR)

^{1}H NMR spectroscopy was used to determine the built-in ratio of LA and GA in the copolymer for each sample. The measurements were performed on a Bruker AMX 400 (^{1}H, 400.13 MHz). Samples with less than 70 mol% of glycolide content were dissolved in deuterated chloroform. The remaining samples were dissolved in deuterated hexafluoroisopropanol.

2.2.3.2 Gel Permeation Chromatography (GPC)

Gel permeation chromatography was used to determine the molecular weight, relative to poly(methyl methacrylate) (PMMA) calibration standards, for all samples. A Merck-Hitachi LaChrom HPLC system, equipped with two PL gel 5 µm MIXED-C (300×7.5 mm) columns using hexafluoroisopropanol as mobile phase, was used. Calculation of the molecular weight was done with the Cirrus™ PL DataStream software package.

2.2.3.3 Thermogravimetric Analysis (TGA)

Thermogravimetric analyses were performed to determine the thermal stability and mass loss as a function of temperature increase. The measurements were carried out on a TGA/DSC 3+ STAR[e] system from Mettler Toledo. Approximatively 7 mg of each sample was introduced in a sealed aluminum sample vessel (40 µm). The test was subsequently conducted at a heating rate of 10 °C·min^{-1} from room temperature to 400 °C under nitrogen atmosphere with a flow rate of 50 mL·min^{-1}.

2.2.3.4 Differential Scanning Calorimetry (DSC)

The thermal transitions were determined using a differential scanning calorimeter DSC 3+ STAR^e system from Mettler Toledo. Samples with a mass of approximatively 5 mg were introduced in sealed aluminum pans (40 μm). Two scans were carried out. First, each sample was heated from room temperature to 230 °C (dT/dt = 10 °C·min⁻¹). Subsequently they were cooled to room temperature at the same rate, and finally heated again to 230 °C at 10 °C·min⁻¹. The T_g, T_{cc} and melting temperature were recorded from the second scan. The percentage of crystallinity for the semicrystalline samples was calculated according to Equation **(2.1)**. [28]

$$\% \, X_c = 100 \times \frac{\Delta H_m - \Delta H_{cc}}{\Delta H_m^C} \qquad \qquad (2.1)$$

Here ΔH_m represents the enthalpy of fusion, ΔH_{cc} is the enthalpy of cold crystallization and ΔH_m^C is the heat of melting of the purely crystalline sample.

2.2.4   Crystallization behavior of semicrystalline copolymers

To study the effect of glycolide content on the crystallization process, a non-isothermal crystallization test of all PLGA copolymers containing 80 mol% or more glycolic acid was carried out using DSC. Each copolymer sample was first heated from 0 to 230 °C (dT/dt = 10 °C·min⁻¹) and maintained at that temperature for 3 minutes to remove the thermal history. Subsequently, the samples were cooled down at different cooling rates (10, 7, 5, 3, 1 and 0.5 °C·min⁻¹) to 0 °C. The T_c and enthalpy of crystallization (ΔH_c) were recorded. Finally, samples were heated for a second time from 0 °C to 230 °C (dT/dt = 10 °C·min⁻¹). For comparison, a similar method was carried out for PLA and PGA synthesized in the laboratory. PLA and PGA were first heated from 0 to 190 °C and 240 °C, respectively at 10 °C·min⁻¹. PLA and PGA were respectively kept at these temperatures for 3 minutes and then cooled down at the different cooling rates mentioned before. In the second heating scan, PLA and PGA were heated to 190 and 240 °C, respectively, at 10 °C·min⁻¹. All measurements were performed under nitrogen atmosphere, using a flow of 50 mL·min⁻¹.

The effect of glycolide content on the spherulitic growth and morphology of the semicrystalline samples was observed with a polarized optical microscope (Olympus BX53) mounted with an Olympus DP26 camera and equipped with a Linkam Hotstage HFSX350. The grinded samples were first sandwiched between two glass slides and molten at 240 °C for 3 minutes. They were subsequently cooled to 40 °C at 10 °C·min⁻¹. The crystalline morphology was recorded during this process.

2.2.5   Measurement of barrier properties from PLGA films

PLGA films were prepared via compression molding using a thermal press (Carver Auto Four/3015-NE,H). The polymer powder was first dried (12 hours at 40 ºC) and kept under vacuum until processing. The polymer was subsequently sandwiched between two polytetrafluoroethylene (PTFE) films (0.14 mm thickness) and 2 aluminum plates (3 mm thickness each). For copolymers with 50, 60, 70 and 80 mol% of glycolide, the sandwich was held for 1 minute at 180 ºC with a force of 0.5 ton to guarantee complete melting of the material. Subsequently, a pressure of 1 ton was applied for 30 seconds and finally the pressure was increased to 5 tons for another 30 seconds. For copolymers with 85 and 90 mol% mol glycolic acid the same procedure was used, except with a pressing temperature between 210 and 220 ºC. The films were cooled down by putting the PTFE sandwich in contact with two cold aluminum plates. Sample thickness was measured with an electronic micrometer at 12 different points and an average of these values was taken as the film thickness. Films with a thickness between 170 μm (for copolymers with up to 70 mol% glycolide) and 100 μm (for copolymers with between 80 and 90 mol% glycolide) were tested for oxygen and moisture barrier.

Because PGA has a very high barrier to both oxygen and water, it would be necessary to prepare film samples below 50 μm thickness to be able to detect permeant. However, sufficiently thin PGA films could not be made using this technique as compression molded films prepared with such a highly crystalline material exhibit high brittleness and tend to crack very easily during demolding. This is accompanied by other microdefects (e.g. bubbles, pinholes) that are prone to appear in thinner films. For this reason, the oxygen permeability (OP) and the water permeability (WP) values for commercial PGA were used as a comparison.

The OP was determined using a Totalperm (Permtech s.r.l) instrument (see Appendix 2.6.2 and **Fig. 2.8** for explanation and schematic representation of the measuring cell). Calibration of the system was carried out with a standard PET film provided by Permtech (Italy), according to the ASTM F1927-14 standard. In this study, the series of glycolide and lactide copolymers was tested at 30 °C and 70% RH. The measurements were done in duplicates and each one concluded when the collected data had reached a tolerance level of 0.5%. The system reports the Oxygen Transmission Rate (OTR) at the established conditions; these values were normalized by the film thickness (x) to determine the oxygen permeability as follows:[24]

$$\mathbf{OTR = \frac{\text{volume of O}_2}{\text{area·day}} = \frac{\text{cm}^3}{\text{m}^2 \cdot 24\ \text{h}}} \quad (2.2) \qquad \mathbf{OP = OTR\left(\frac{\text{cm}^3}{\text{m}^2 \cdot 24\ \text{h}}\right) \cdot \frac{1}{\Delta P} \cdot x} \qquad (2.3)$$

The water permeability (WP) was measured using the same Totalperm (Permtech s.r.l) instrument calibrated for water vapor according to the ASTM E96/E96M-15 standard. The test concludes once the variation between the recorded results reaches a tolerance level of

0.5%. Initially, the samples were tested at 30 °C and 70% RH. Subsequently, the influence of temperature on the WP was studied at 30 °C and 40 °C for the films with the highest content of glycolic acid (80 and 90%). Similarly, the effect of RH was tested at 10, 50, 70 and 90% RH for these samples. The measured WVTR was normalized by the film thickness (x) to calculate the water permeability as follows:[24]

$$\text{WTR} = \frac{\text{weight of H}_2\text{O}}{\text{area}\cdot\text{day}} = \frac{\text{gr}}{\text{m}^2\cdot 24\text{ h}} \quad (2.4) \qquad\qquad \text{WP=WTR}\left(\frac{\text{gr}}{\text{m}^2\cdot 24\text{ h}}\right)\cdot\frac{1}{\Delta P}\cdot x \quad (2.5)$$

2.2.6 Density determination of PLGA films by a density gradient column

The measurements were carried out in a density gradient column using a column filler and sweeper from H&D Fitzgerald Ltd, according to the ASTM D1501-10 standard. The column was filled by mixing two miscible liquids of known densities creating a density gradient. The "heavy liquid" is a calcium nitrate tetrahydrate/water solution (ϱ=1503 kg·m^{-3}) and the "light liquid" is Milli-Q purified water (ϱ=997.5 kg·m^{-3}). The density of the solution was measured with a density meter for liquids (Mettler Toledo DM40). Calibrated glass floats of known density were used as reference material for the column calibration. All the measurements were taken at room temperature (21 ± 1 °C).

Two density columns with different ranges were used: the first one between 1477 kg·m^{-3} and 1428 kg·m^{-3} and the second one between 1440 kg·m^{-3} and 1349 kg·m^{-3}. These ranges were chosen by testing various samples of each copolymer in calcium nitrate tetrahydrate/water solutions with different densities. Following the ASTM D1505-10 standard the columns were calibrated with a correlation factor (R^2) of 0.9929 and 0.9956, providing a density measurement with good accuracy. The polymer films were first cut in small triangles, immersed in water for about 3 minutes and then carefully introduced in the density column. Measurements were taken after 1 hour. The test for each copolymer was done in triplicate.

2.3   Results and discussion

2.3.1   Effect of glycolide content on structure and thermal stability of PLGA copolymers

Each copolymer composition was measured by NMR spectroscopy. Samples with an initial glycolic acid content of 70 mol% and higher were not soluble in any of the deuterated organic solvents commonly used in the laboratory. For this reason hexafluoroisopropanol-d_2 (HFIP) was used.[41] Unfortunately, as (deuterated) HFIP is an expensive and harmful solvent its general use in several analytical techniques is limited. Therefore, chloroform-d was used as solvent for the remaining samples (see **Fig. 2.9** in Appendix for ^{1}H NMR

example). The ratio of glycolide to *L*-lactide in the copolymer was determined by the integral of the peaks corresponding to the methylene group hydrogens (CH_2) of glycolide and the area under the peaks of the methyl group hydrogens (CH_3) or the methine group (CH) of the lactide according to Equations **(2.6)** and **(2.7)** (see **Table 2.5** in Appendix for ^{1}H NMR chemical shifts and integrals).

$$\% \text{ Glycolide in polymer} = 100 \times \frac{\frac{\text{Integral peak}(CH_2)}{2}}{\frac{\text{Integral peak}(CH_3)}{3} + \frac{\text{Integral peak}(CH_2)}{2}} \quad (2.6)$$

$$\% \text{ Lactide in polymer} = 100 \times \frac{\frac{\text{Integral peak}(CH_3)}{3}}{\frac{\text{Integral peak}(CH_3)}{3} + \frac{\text{Integral peak}(CH_2)}{2}} \quad (2.7)$$

The determined ratio between lactic and glycolic acid in the copolymers is shown in **Table 2.1**. In a previous work, Gilding et al.,[16] reported the synthesis of polyglycolic acid using $Sn(Oct)_2$ as a catalyst. According to their research, when glycolide is polymerized over 3-4 hours (94-96%), the molecular weight distribution broadens significantly due to transesterification reactions between the existing polymer chains. This dual polymerizing and depolymerizing effect with $Sn(Oct)_2$ when used at temperatures above 200 °C has been reported before.[42] In line with the previous remarks, 4 h was selected as the maximum reaction time for the PLGA copolymers reported in this work. At longer reaction time, also dark brown coloration was observed.

Table 2.1 GL/LAC built-in ratios, molecular weight distribution and thermal transitions for PLGA copolymers, PLA and PGA.

GL in feed (mol%)	LAC in feed (mol%)	GL in copo (mol%)	LAC in copo (mol%)	M_n (kg·mol⁻¹)	PDI	T_g (°C)	Micro structure	T_{cc} (°C)	T_m (°C)	X_c (%)
50	50	52	48	23.6	2.2	44	amorphous	-	-	-
60	40	61	39	29.3	2.6	43		-	-	-
70	30	72	28	27.2	2.7	43		-	-	-
80	20	82	18	33.1	3.5	42		-	-	-
85	15	87	13	28.9	2.9	41	semi crystalline	133	190	5
90	10	91	9	35.9	3.4	41		113	199	29
0	100	0	100	35.8	2.0	58		103	174	25
100	0	100	0	-	-	41		-	222	48

As shown in **Table 2.1**, there is a common trend for higher incorporation of glycolide in the copolymer with respect to the designed amount in the feed. This is in line with previous reports and results from the much higher reactivity of glycolide compared to lactide in ROP. From literature[14,43] it is known that the polymerization of these two monomers starts with the most reactive monomer polymerizing preferentially with itself: a glycolide ended

growing chain will tend to add another glycolide unit, while a lactide ended chain will also tend to add a glycolide unit. As the reaction progresses, lactide is built into the polymer chains that are rich in glycolide. In the end some unreacted lactide remains. This means that the resulting copolymers are likely richer in glycolide than the initial monomer mixture would suggest, as can be seen in **Table 2.1**. In addition, broad composition ranges within the initially formed chains and those formed towards the end are more expected due to the significant reactivity difference between glycolide and lactide. For all cases, the glycolide conversion reached 99%. In the case of lactide however, copolymers with initial feeds of 50, 60 and 70 mol% showed a maximum conversion of 96%. For the remaining copolymers, a small fraction of residual lactide was found (between 1 and 2%) together with some oligomer formation. Under similar reaction conditions, higher addition of glycolide induces broadening of the molecular weight distribution. Although the reaction time was reduced for these high glycolic acid containing copolymers (above 70 mol% of glycolide in the feed), the required temperatures for polymerization (up to 220 °C) seem to promote chain transfer reactions when using $Sn(Oct)_2$ as a catalyst.

Although both PLA and PGA are semicrystalline, copolymerization induces a loss of crystallinity and as a consequence materials obtained from glycolide between 50 and 80 mol% in the feed are amorphous according to DSC, when submitted to 10 °C·min^{-1} heating and cooling cycles. The samples with 87 and 91 mol% of built-in glycolic acid showed a crystalline phase in the thermogram with a T_α at 133 and 113 °C and a T_m of 190 and 199 °C, respectively. The degree of crystallinity was calculated using Equation **(2.1)**, taking 191.3[44] and 93.7 J·g^{-1} [45] as the heats of melting for purely crystalline samples (ΔH_m^C) of PGA and PLA, respectively. At these conditions the degree of crystallinity is higher for the copolymer with greater glycolide content. However, when compared to the degree of crystallinity of PGA, it is observed that a small incorporation of lactide units can reduce the ability for the polymer chains to adopt an ordered configuration and, therefore, delay the formation of crystalline regions. Furthermore, the broad molecular weight distribution determined for PLGA$_{13/87}$ and PLGA$_{9/91}$ implies high heterogeneity in chain length. This can also influence the crystallization process, since long and short chains tend to crystallize at different rates. The TGA curves of PLA, PGA and the PLA/PGA copolymers, scanned under nitrogen atmosphere, are shown in **Fig. 2.1**. For all the samples, the thermal degradation occurred in a single-stage process.

All PLGA copolymers were thermally stable up to 250 °C and they show increasing resistance to thermal degradation with increasing content of glycolide. A mass loss of 5% occurs between 271 and 292 °C and the maximum degradation rate occurs between 364 and 385 °C. Of all the copolymers, the highest temperature values correspond to PLGA$_{9/91.}$ This is not unexpected since semicrystalline materials tend to be more thermally stable than their amorphous counterparts. In a highly ordered state, the mobility of the polymer chains is more restricted. PGA for example, possesses the most ordered molecular packaging (relative

to degree of crystallinity) and thus requires higher temperatures to transform to an unordered fluid state and consequently to decompose (see **Table 2.6** in Appendix for specific temperatures at different mass loss percentages).
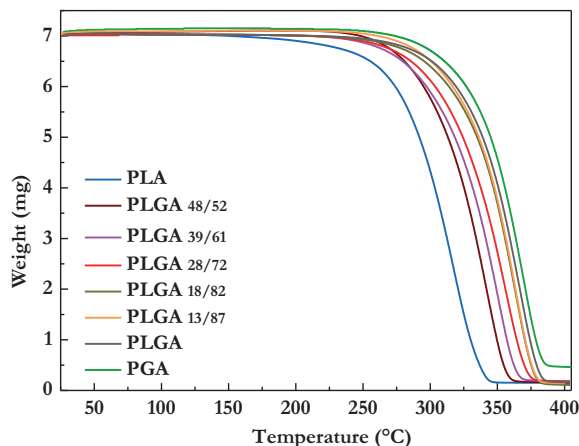
Fig. 2.1 TGA thermogram for PLGA copolymers, PGA and PGA using a heating rate of 10 °C·min⁻¹.

2.3.2   Crystallization behavior of semi crystalline PLGA copolymers

The exothermic effects recorded for $PLGA_{13/87}$ and $PLGA_{9/91}$ during the first cooling cycle are shown in **Table 2.2**. The crystallization range for $PLGA_{13/87}$ narrows as the cooling rate decreases. This is accompanied by a shift of the T_c toward higher values. Also, an increase in exothermic enthalpy change is observed with slower cooling of the samples. For this copolymer, the degree of crystallinity increases from 5 to 25% when cooled at between 10 and 0.5 °C·min⁻¹. Although a similar trend is observed for $PLGA_{9/91,}$ the exothermic range is narrower and at 10 °C·min⁻¹ the sample already exhibits 29% crystallinity. With decreasing cooling rate (ϕ), the crystallinity reaches 34% at 0.5 °C·min⁻¹. Other parameters, such as T_c and onset temperature of crystallization (T_o), are also shown in **Table 2.2**. As expected, under all cooling conditions, the copolymers crystallize at temperatures within the crystallization range of PGA and PLA individually.

PGA showed complete crystallization at a cooling rate of 10 °C·min⁻¹, with a ΔH_c that remained fairly constant with different cooling rates. These observations are in agreement with data previously reported for PGA.[12,21] When comparing the crystallization temperatures of semicrystalline PLGA samples with PGA, it becomes apparent that with a small inclusion of lactide, the resulting copolymers not only crystallize at lower temperatures, but also in a broader temperature range. These thermal variations will have an impact on material processing. The difference between T_m and the onset crystallization temperature for $PLGA_{13/87}$ and $PLGA_{9/91}$ cooled at 10 °C·min⁻¹ (45-46 °C) is higher than

that of PGA (26.3°C). Due to this broader range, obtaining transparent items (films, sheets, etc.) upon extrusion of PLGA$_{13/87}$ and PLGA$_{9/91}$ would be easier. As mentioned before, this is still very challenging for PGA.
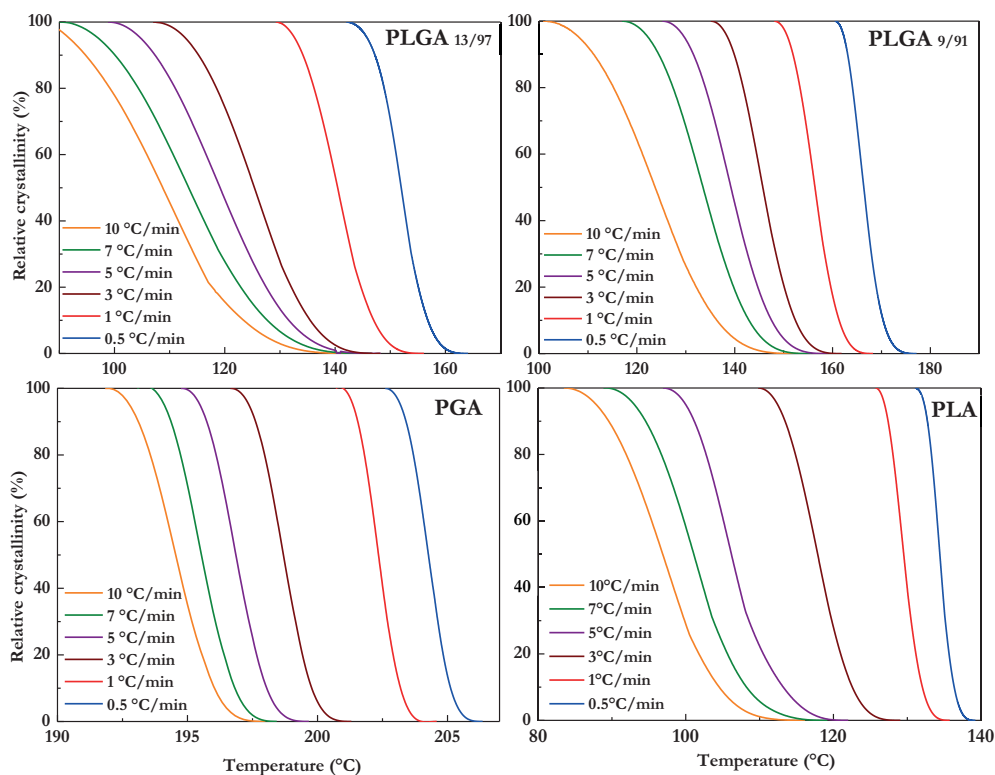
Table 2.2 Crystallization temperatures of PLGA, PLA and PGA samples at different cooling rates.

Sample	ϕ (°C·min^{-1})	T_o (°C)	T_c (°C)	Sample	ϕ (°C.min^{-1})	T_o (°C)	T_c (°C)
PLGA$_{13/87}$	10	145	117	PGA	10	198	196
	7	147	119		7	198	196
	5	148	124		5	200	198
	3	148	130		3	201	199
	1	152	143		1	205	203
	0.5	164	154		0.5	206	205
PLGA$_{9/91}$	10	153	129	PLA	10	116	101
	7	156	137		7	119	103
	5	159	142		5	122	108
	3	162	148		3	129	120
	1	168	158		1	136	130
	0.5	177	167		0.5	139	135

To better understand the non-isothermal crystallization mechanism, the relative crystallinity (X) as a function of temperature was calculated. Using Equation **(2.8)**, the exothermic events during cooling can be integrated along the crystallization range. Here, T$_\infty$ corresponds to the end temperature of crystallization and H$_c$ is the enthalpy of crystallization.[46]

$$\frac{\int_{T_o}^{T} \left(\frac{dH_c}{dT} \right) dT}{\int_{T_o}^{T_\infty} \left(\frac{dH_c}{dT} \right) dT} \qquad (2.8)$$

Fig. 2.2 shows the relative crystallinity evolution as function of temperature at different cooling rates for PLGA$_{13/87}$, PLGA$_{9/91}$, PGA and PLA. Both copolymers PLGA$_{13/87}$ and PLGA$_{9/91}$ clearly exhibit broader crystallization ranges with increasing cooling rate. The glycolide content in the copolymers has a significant influence in the crystallization mechanism. As shown, with this small difference in glycolide content, the crystallization temperatures for PLGA$_{13/87}$ and PLGA$_{9/91}$ are increased from 117 to 154 °C at 10 °C·min^{-1} and from 129 to 177 °C at the slowest cooling rate of 0.5 °C·min^{-1}. For PGA, the crystallization range broadness remains constant despite the cooling rate, while for PLA it narrows with slower cooling. Nevertheless, this effect for PLA is less significant than for the copolymers.

Fig. 2.2 Evolution of relative degree of crystallinity as function of temperature for non-isothermal crystallization of $PLGA_{13/87}$, $PLGA_{9/91}$, PGA and PLA at different cooling rates.

As mentioned before, crystal formation for PGA was similar under all tested cooling conditions. This differs from PLA, which shows a behavior closer to that of the copolymers: the degree of crystallization is enhanced with the decreasing cooling rate.

The progression of the relative degree of crystallinity as a function of time can be determined using Equation **(2.9)**.[18] Here, T represents the crystallization temperature at time t and ϕ is the cooling rate in °C·min^{-1}.

$$t=(T_o-T)/\phi \qquad (2.9)$$

Fig. 2.3 illustrates the resulting plots for the copolymers and PLA and PGA homopolymers. PLA and PGA homopolymers exhibit a higher crystallization rate than both $PLGA_{13/87}$ and $PLGA_{9/91}$ copolymers. This difference is more significant for PGA, which crystallizes very rapidly even at the highest cooling rates. Overall, higher crystallization temperatures induced by slower cooling rates, are a consequence of slow crystallization. For each sample individually, the crystallization rate does not seem to be highly impacted by the cooling rate between 10 and 3 °C·min^{-1}. However, there was a substantial delay in crystallization when samples were cooled down at 1 and 0.5 °C·min^{-1}. This trend was common for all samples.

Importantly, the much longer crystallization times for PLGA$_{13/87}$ and PLGA$_{9/91}$ in comparison to those for PLA and PGA confirm that small inclusions of lactic acid in glycolic acid rich samples, have a detrimental effect on their ability to crystallize. This effect becomes more significant with increasing lactic acid content (from 20 mol%) leading to amorphous copolymers.
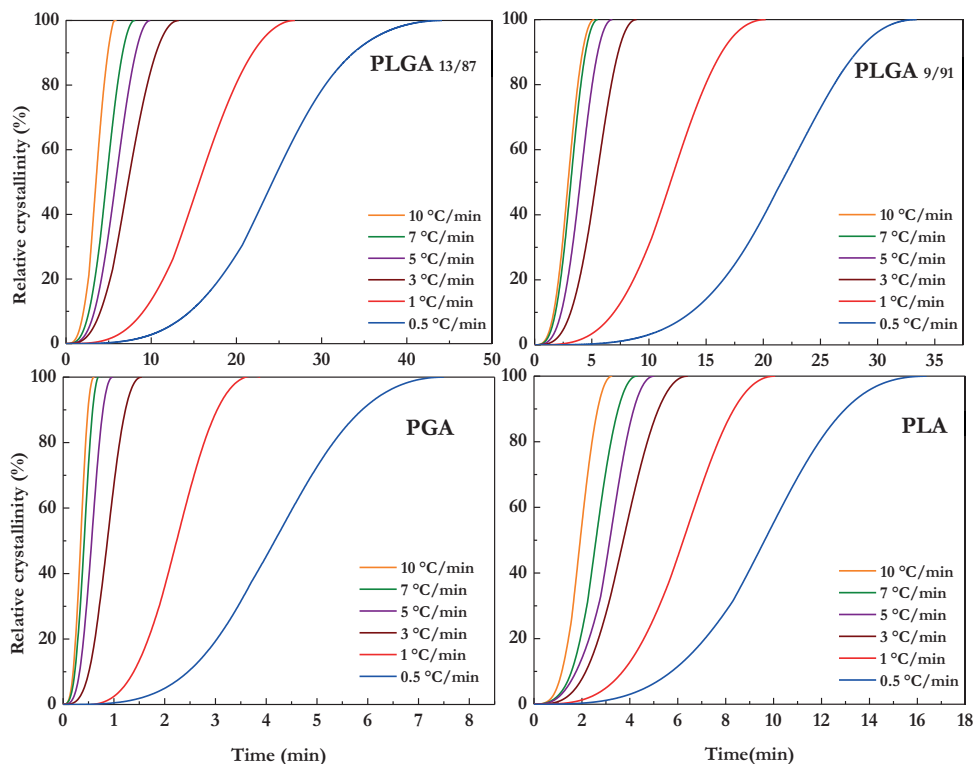
Fig. 2.3 Evolution of relative degree of crystallinity as function of time for non-isothermal crystallization of PLGA$_{13/87}$, PLGA$_{9/91}$, PGA and PLA at different cooling rates.

Spherulitic behavior and morphology were observed during non-isothermal crystallization from the melt at 10 °C·min^{-1} for both PLGA samples (**Fig. 2.4**). According to the polarized optical microscopy images, PLGA$_{13/87}$ starts crystallizing at lower temperatures than PLGA$_{9/91}$ and both temperature ranges remain below the crystallization temperature of PGA. These results support the crystallization data obtained by DSC. Yu et al. reported the formation of hedrites with a high degree of complexity during isothermal crystallization of PGA.[21] This unique morphology differs from other polyesters with comparable chemical structure, such as PLA, which shows well-defined spherulites during crystallization.[20] As shown in the images of **Fig. 2.4**, both copolymers exhibit a spherulitic morphology that resembles to that of PLA. This is an unexpected observation, since both samples contain a very high amount of glycolide and yet no hedrite like crystals are observed. While PLGA$_{9/91}$

exhibits higher spherulite size than $PLGA_{13/87}$, the latter shows denser growth. In both cases, amorphous areas with no spherulite formation remained.
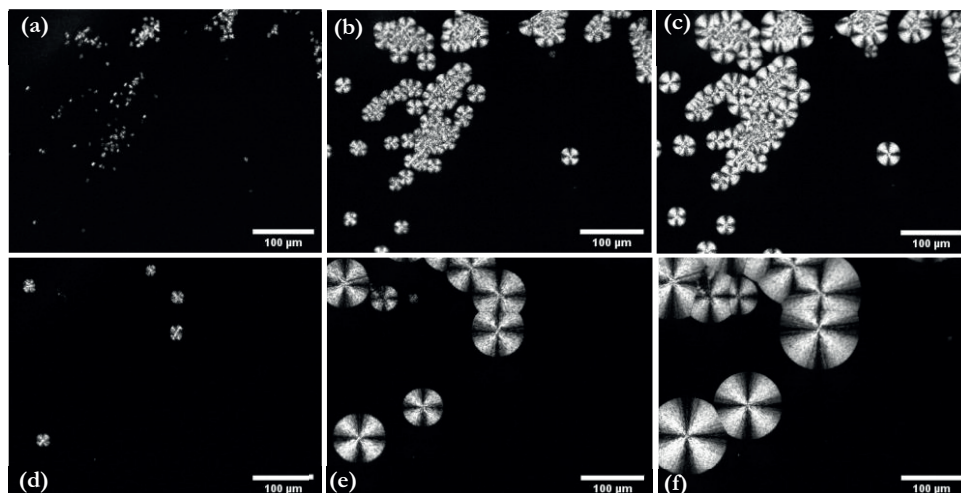

Fig. 2.4 Optical micrograms taken for $PLGA_{13/87}$ cooled down from the melt at 10 °C·min^{-1} at: **(a)** 145 °C; **(b)** 115 °C; **(c)** 85 °C and for $PLGA_{9/91}$ at **(d)** 155 °C; **(e)** 130 °C; **(f)** 100 °C.

2.3.2.1   Non isothermal crystallization kinetics

The crystallization kinetics were studied with the Jeziorny modified Avrami model.[47] This method has been previously applied and reported for studying polymer crystallization under non-isothermal conditions.[48-51]

Typically, the Avrami model alone is used to analyze crystallization kinetics under isothermal conditions according to Equation **(2.10)**, with X_t the relative crystallinity as function of time, K the Avrami (crystallization) rate constant, n the Avrami exponent and t the crystallization time.

$$X_t = 1 - \exp(-Kt^n) \qquad (2.10)$$

Equation **(2.10)**, can be modified for non-isothermal conditions, leading to the Jeziorny-modified Avrami model, which includes a correction for the cooling rate:

$$\log\left[-\ln(1-X_t)\right] = n\log t + \log K \qquad (2.11)$$

$$\log K_c = \frac{\log K}{\phi} \qquad (2.12)$$

Here n is related to the type of nucleation and growth mechanism and K is a rate constant that takes into account nucleation and growth rate parameters. In addition, K can be corrected (K_c) for variable cooling rates. Equation **(2.11)** implies that n and K can be

determined from the slope and intercept of the resulting (linearized) plot of $\log\left[-\ln(1-X_t)\right]$ vs $\log t$ (**Fig. 2.5**).[18,52]
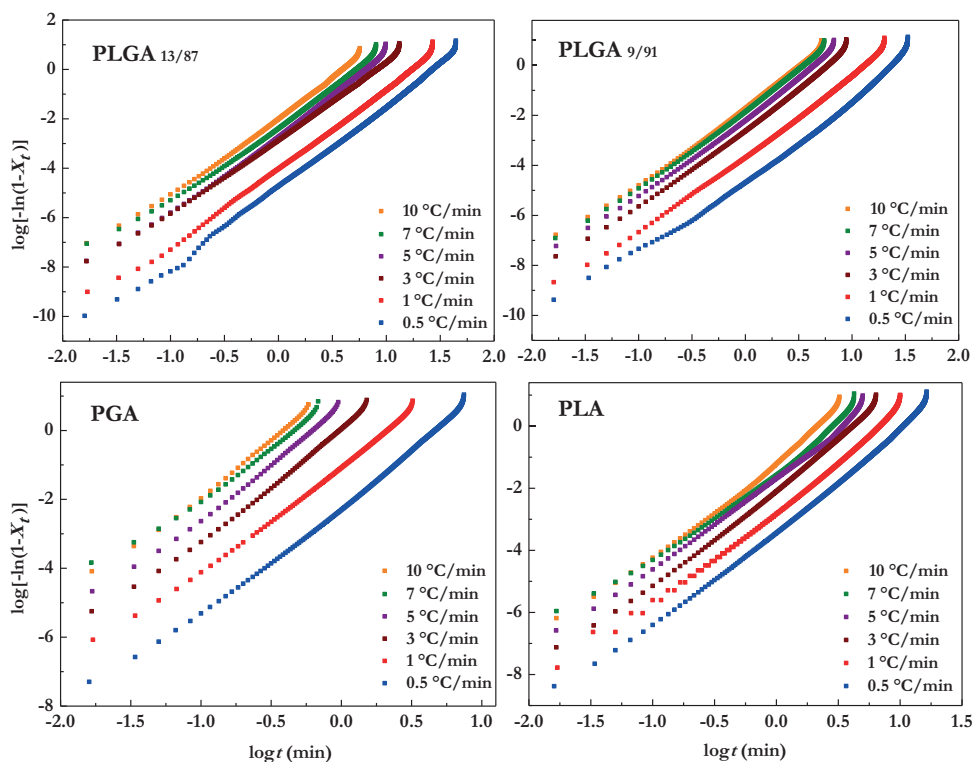
Fig. 2.5 Avrami plots for $\log\left[-\ln(1-X_t)\right]$ as a function of $\log t$ at different heating rates for $PLGA_{13/87}$, $PLGA_{9/91}$, PLA and PGA.

For all curves some non-linearity is observed. This was typically observed below 1% and above 90% relative crystallinity. Because of this, the area between both values was selected as the range to fit the Avrami linear model. **Table 2.3** presents the calculated n, K, Kc and the R^2 correlation coefficient using the Jeziorny-modified Avrami method. As shown, for both copolymers the n values stay within a similar range (3.3-3.6). This could suggest a similar crystallization mechanism. However, a consistent trend was not identified for all evaluated samples, which makes it difficult to draw conclusions on the nature of a general crystallization process.

For K_c, a steady trend was identified for all the samples. K_c decreases with decreasing cooling rate, which implies that crystallization takes longer when the cooling rate is lowered. Furthermore, K_c values for $PLGA_{13/87}$ are lower than those for $PLGA_{9/91}$ and both are below the values determined for PLA and PGA. This is also in line with the DSC analysis where PGA and PLA showed faster crystallization compared with the copolymers.

Table 2.3 Parameters for non-isothermal crystallization kinetics of $PLGA_{13/87}$, $PLGA_{9/91}$, PLA and PGA obtained from Jeziorny-modified Avrami model.

Sample	ϕ (°C·min⁻¹)	n	K (min⁻¹)	K_c (min⁻¹)	R^2
$PLGA_{13/87}$	10	3.42	0.13	0.82	0.99
	7	3.35	$8.8×10^{-3}$	0.71	0.99
	5	3.39	$63×10^{-3}$	0.58	1.00
	3	3.16	$551×0^{-3}$	0.38	0.99
	1	3.32	$16×10^{-3}$	$16×10^{-3}$	0.99
	0.5	3.62	$5.6×10^{-3}$	$3.16×10^{-5}$	0.99
$PLGA_{9/91}$	10	3.34	0.18	0.84	1.00
	7	3.41	0.15	0.77	1.00
	5	3.48	0.11	0.64	0.99
	3	3.53	0.07	0.40	0.99
	1	3.49	0.02	$20×10^{-3}$	0.99
	0.5	3.59	$6.7×10^{-3}$	$4.52×10^{-5}$	0.99
PLA	10	3.67	0.30	0.88	0.99
	7	3.45	0.20	0.80	0.99
	5	3.11	0.18	0.71	0.99
	3	3.41	0.12	0.49	0.99
	1	3.55	0.05	$51×10^{-3}$	0.99
	0.5	3.56	0.02	$7×10^{-4}$	0.99
PGA	10	2.97	2.73	1.10	0.99
	7	3.19	2.92	1.16	0.99
	5	3.41	2.01	1.15	0.99
	3	3.41	1.04	1.01	0.99
	1	4.09	0.20	0.20	0.99
	0.5	3.52	0.09	$9.1×10^{-3}$	0.99

2.3.3 Effect of glycolide content on density and barrier properties of PLGA films

Fig. 2.6 (a) shows the densities for PLGA films as a function of glycolide percentage in the copolymer. The reported values are averages of measurements performed in triplicate. The measured density increases with glycolide content: from 1.38 g.cm⁻³ for PLA to 1.50 g.cm⁻³ for $PLGA_{9/91}$. Nevertheless, the results remain within the expected density range between PLA and PGA (1.2-1.7 g.cm⁻³). All copolymers have a density higher than 1, which implies that they would sink when/if leaked into marine ecosystems. Because PLGA plastics are expected to degrade through hydrolysis as a first step, it is important to understand their degradation mechanism (see Appendix 2.6.4 for hydrolysis study) and the effect of their degradation products on aquatic media/ecosystems. For this group of copolymers a tailored degradation can be achieved by tuning the lactide content.

Specific barrier properties are required for polyesters, depending on the intended application. In the packaging industry, for example, oxygen and water vapor permeability are key properties, as water and oxygen often have a large impact on product shelf-life. For PLA and PGA these properties have been studied.[31,37] Although these barrier properties are important performance characteristics of PLGA copolymers, no reports on this topic were found so far. The compression molded films were analyzed by DSC using the same method described before. Although the films were cooled down rapidly using cold aluminum plates, a degree of crystallinity between 2 and 10% was measured for $PLGA_{13/87}$, and $PLGA_{9/91}$, respectively. Obtaining this information is very relevant, since crystallinity is well known to influence barrier properties of polymers. Furthermore, T_m of the same semicrystalline samples remained unaffected by the processing, but T_g decreased with respect to the unprocessed polymers (34.5 and 35.7 °C respectively). High temperature and pressure during compression molding can induce thermal degradation of the polymer. For the amorphous copolymers, films showed a decrease in T_g during the first heating scan (T_g between 43 and 37 °C) compared to that of the unprocessed material.
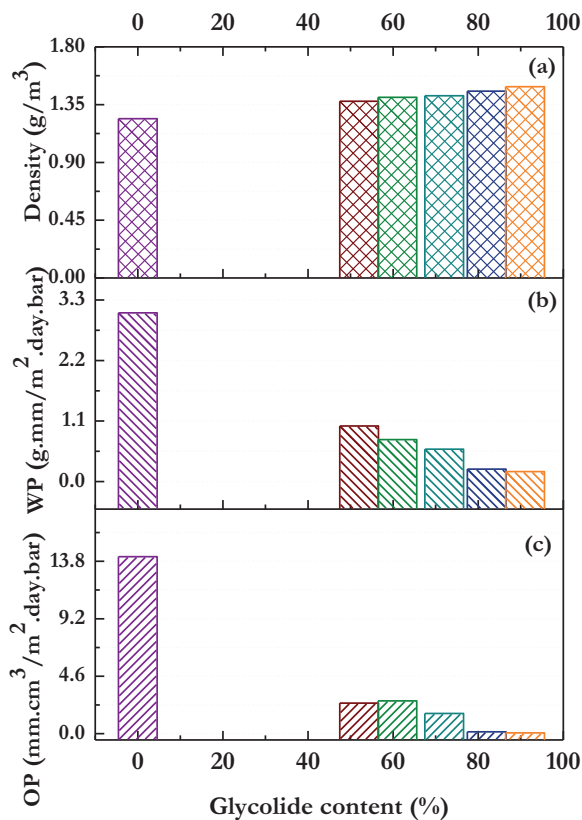
Fig. 2.6 (a) Density, **(b)** oxygen permeability and **(c)** water permeability (measured at 70% RH and 30 °C) as a function of glycolide content in PLGA copolymers.

Panels **(b)** and **(c)** of **Fig. 2.6** show the oxygen and water permeability, respectively, for copolymers with between 52 and 91 mol% of glycolic acid content, at 30 °C and 70% RH. For comparison, a PLA film prepared with the same compression molding protocol was also tested. The results obtained for WP and OP for PLA match with those reported by Siró et al. for commercial PLA (Biophan® 111) measured under similar conditions.[53]

PLA has a much higher OP than the other tested samples and copolymerization with glycolide significantly improves the barrier to both oxygen and water vapor. PLGA films with between 52 and 72 mol% glycolic acid exhibit similar OP and WP values, with a slight decrease for those with increased glycolic acid content. This trend becomes more evident at the highest glycolic acid contents, with both OP and WP below 1.0. When compared to values for PGA reported by the Kureha company (OP = 0.013 mm·cm³·m⁻²·day⁻¹·bar⁻¹ at 20 °C and 80% RH; WP= 0.165 g·mm·m²·day⁻¹·bar⁻¹ at 40 °C and 90% RH), PLGA copolymers exhibit a higher transmission for both permeants. The negative effect of lactic acid introduction on the barrier properties was expected, since PLA alone has much higher permeability coefficients for water and oxygen than PGA.

The transport of a gas or vapor through a polymer film depends on both its solubility within the polymer matrix and the ability of the gas or vapor to diffuse though the matrix.[54] It has been demonstrated before that crystallinity influences both the solubility and the diffusion coefficient. Crystalline regions tend to be much more dense and well-arranged than amorphous regions, which helps to prevent penetrant sorption and reduces penetrant solubility.[55] This is in line with the much better WP of $PLGA_{9/91}$ compared to the amorphous samples. The crystalline regions act as barriers to diffusion and force the water molecules to go through a more tortuous path compared to the more permeable amorphous regions. In the case of commercial PGA, the much higher crystallinity in comparison to the tested copolymers (45–55%) contributes to this trend, which leads to superior performance.

PLGA copolymers perform really well as barrier to oxygen and water as compared to PET, a common barrier polymer. PET films (10% degree of crystallinity) were prepared with compression molding and tested with the same protocol described here for PLGA films. They showed an OP of 4.5 mm·cm³·m⁻²·day⁻¹·bar⁻¹ and a WP of 0.83 g·mm·m⁻²·day⁻¹·bar⁻¹ at 30 °C and 70% RH. These values are higher than those reported for commercial PET, for which typically chain orientation is induced during the stretching process. This processing induces lower permeability coefficients. The non-oriented PET shows higher WP than the entire range of PLGA copolymers studied in this work. The OP, however, is improved in comparison to PLLA but only superior to PET for the samples with richer glycolide content. Since PET is a very high demand polymer in the packaging industry, the fact that PLGA copolymers, depending on the composition, have a comparable or improved barrier to oxygen and water suggests good potential for this application field. It

is, however, important to consider that PET exhibits higher T_g (60-80 °C) and T_m (253-255 °C) than PLGA, which allows it to retain its properties over a wider temperature range.

Furthermore, PET is known for its high mechanical strength and good flexibility. A commercial PET film (23 μm), for example, displays a tensile strength (σ) of 200 MPa, a tensile modulus *(E)* of 3.9 GPa and elongation of 30%.[56] Less flexibility is displayed by PGA films (20 μm) with elongation of 40%, σ=380 MPa and E=7 GPa.[12] When comparing both PET and PGA with a commercial PLA film (100 μm), higher elongation at break is reported (180%), but both σ (103 MPa) and E (3.44 GPa) are inferior.[57] Although mechanical properties for the series of copolymers here studied have not been determined, a behavior between that of PGA and PLA, depending on the lactide to glycolide ratio, should be expected. Furthermore PET, even in its partly bio-based form (Coca-Cola's 'plant-bottle' PET), is neither degradable nor compostable.[2] Therefore, using PLGA copolymers (bio- and CO_2-based and (bio)degradable) for applications such as packaging can avoid the infinite accumulation of plastics such as PET that leak into the environment (an estimated 8 million tons per year). In addition, composting of food wastes contaminated with (bio)degradable plastic packaging is a much better end-of-life option than (open air) burning, which is often the only solution for food contaminated non-degradable plastics in areas without a waste collection infrastructure.

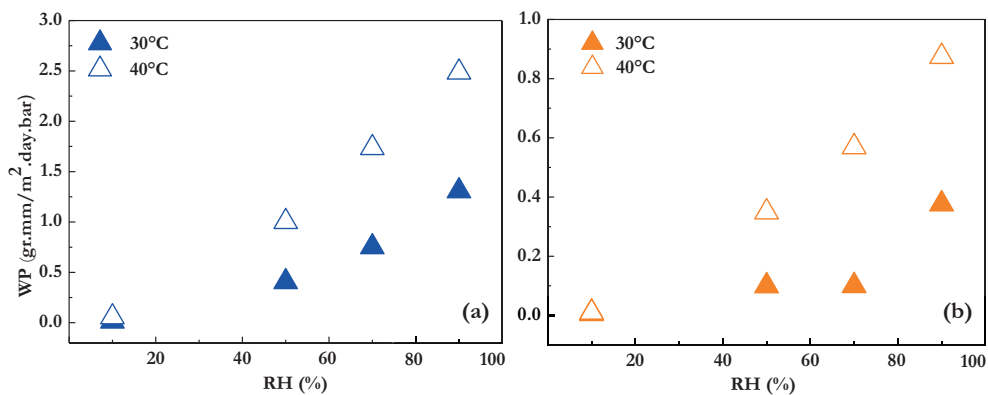### 2.3.4 Effect of temperature and relative humidity on WP of glycolic acid rich copolymers

Fig. 2.7 Water permeability vs. relative humidity at 30 and 40 °C for **(a)** PLGA$_{13/87}$, **(b)** PLGA$_{9/91}$.

Barrier properties of plastics are affected by different factors, which include: fractional free volume, chemical structure, chain orientation, crystallinity, temperature, and relative humidity. This section of the study focuses on water permeability, because PLA and PGA are known to degrade preferentially through hydrolysis. PGA particularly, has shown a faster degradation rate than PLA.[58,59] Therefore, it is important to evaluate how the water barrier performance of glycolic acid rich copolymers is affected by different moisture conditions

and temperature changes (close to the T_g). **Fig. 2.7** shows the water permeability for PLGA$_{13/87}$ and PLGA$_{9/91}$ vs the relative humidity (between 10 and 90%) at 30 and 40 °C.

As observed in **Fig. 2.7**, the rate of moisture sorption is very dependent on temperature and relative humidity. As a general trend, more water is permeated through the film with increasing RH and temperature. For 30 °C this growth is gradual and at the highest RH, the barrier to water is still very good. Clearly, an increase in temperature (closer to the T_g) is detrimental for barrier performance and the increase in WP with increasing relative humidity, is much more important. For PLGA$_{13/87}$ for example, more than double the amount of water is permeated at 40 °C under equal RH conditions (above 10% RH) compared to 30 °C. PLGA$_{9/91}$ also takes up more moisture at higher temperature.

For comparison, the thermo-compressed commercial PET was tested under the same temperature and RH conditions. At 40 °C and 90% RH it showed a WP of 1.8 g·mm·m^{-2}·day^{-1}·bar^{-1}. When compared to the WP of PLGA$_{13/87}$ (2.5 g·mm·m^{-2}·day^{-1}·bar^{-1}) it is clear that from a practical point of view, PET performs better at high temperatures. Evidently, PLGA$_{13/87}$ does not perform well at a service life temperature close to or above 40 °C. In contrast, PLGA$_{9/91}$ exhibits lower WP (0.87 g·mm·m^{-2}·day^{-1}·bar^{-1}) than PET at the same conditions (1.8 g·mm·m^2·day^{-1}·bar^{-1}), demonstrating that even at temperatures close to the T_g and at high moisture content, it performs better as barrier to water.

2.4   Conclusions

While previous publications have focused on lactic acid rich PLGA copolymers, this study focused on mapping the structure-property relationships for glycolic acid rich PLGA copolymers. For this purpose, PLGA copolymers with between 50 and 91 mol% of glycolide were synthesized by ROP. The higher reactivity of glycolide compared to lactide resulted in slightly higher glycolide content than the feed ratio would suggest. An increased thermal stability was observed with increasing glycolic acid content, although the differences were small. The density increased with increasing glycolic acid content. In all cases, the densities were significantly higher than that of water (1.0).

The PLGA copolymers show significantly different crystallization behavior than both PLA and PGA homopolymers, which exhibit a semicrystalline structure as observed in DSC when heated and cooled down at 10 °C·min^{-1}. The samples with 87 and 91 mol% of glycolic acid were semicrystalline, whereas those with 50-80% glycolide content were amorphous. A crystallization study under non-isothermal conditions revealed that copolymerization reduces the crystallization rate for PLGA copolymers almost 10 times compared to PLA and PGA homopolymers at 10 °C·min^{-1} cooling rate. This is an advantage vis-à-vis PGA for processing into, among others, films. The kinetics of this process, modeled with the Jeziorny-modified Avrami method, were in line with the more difficult crystallization for these copolymers. The crystallization rate decreased with decreasing cooling rates. Furthermore, the crystal morphology

observed by polarization optical microscopy revealed spherulite like crystals, the structure of which is more closely related to that of PLA.

Finally, the barrier property assessment revealed that increasing glycolic acid content has a beneficial effect on the barrier to both oxygen and water vapor. At room temperature and a relative humidity below 70%, these copolymers outperform non-oriented PET. At 40 °C, only PLGA$_{9/91}$ remains less permeable than PET. In all cases, the water permeability was highly dependent on the temperature and relative humidity conditions. Their great potential as barrier polymers and their possible future production from CO_2, as well as the fact that these materials are (chemically) recyclable and biodegradable, make these materials very interesting for future applications in areas such as films for packaging. Currently, however, glycolide, the main monomer for the production of high GA content PLGA materials, is expensive and is produced at limited scale. It is for this reason that we are developing a cheaper route from CO_2 in this European Ocean Program.

2.5   Acknowledgments

2.6   Appendix

2.6.1   Additional experimental conditions

Table 2.4 Reaction conditions of PLGA copolymers.

| LA feed (mol%)	GL feed (mol%)	LA feed (g)	LA feed (mol)	GL feed (g)	GA feed (mol)	T (°C)	time (hours)
50	50	11.1	7.72×10^{-2}	8.87	7.64×10^{-2}	180-205	4
40	60	9.10	6.31×10^{-2}	10.9	9.38×10^{-2}	180-205	4
30	70	6.99	4.85×10^{-2}	13.0	1.12×10^{-2}	180-205	4
20	80	4.77	3.31×10^{-2}	15.2	1.31×10^{-2}	180-205	3
15	85	3.62	2.51×10^{-2}	16.4	1.41×10^{-2}	190-220	3
10	90	2.44	1.69×10^{-2}	17.6	1.51×10^{-2}	190-220	2
100	0	20.0	1.38×10^{-1}	0	0	140-195	10
0	100	0	0	20.0	1.72×10^{-1}	195-230	1

2.6.2 Functioning principle of the Totalperm for barrier property testing

For all measurements, the sample was initially inserted into a chamber where a system of O-rings fixes the film in position, avoiding leakage. In this chamber, the surface area exposed to the permeant is 50 cm². The upper chamber has an atmosphere that can be specified according to the required measurement (e.g. oxygen, water, CO_2), while the lower chamber contains the detection sensor. In addition, the absolute pressure on both sides of the film is maintained equivalent (atmospheric pressure).

To test the oxygen barrier the chamber was purged to remove any residual oxygen with a gas mixture of nitrogen/hydrogen 98/2 (mol%) after sample insertion. This conditioning was done for up to 24 hours for all samples prior to testing. Eventually, the penetrant flow became linear as a function of time, which indicated that the system had reached a steady state. Pure oxygen was then introduced in the upper chamber. The oxygen permeating through the sample to the lower chamber was swept by the carrier gas (nitrogen/hydrogen mixture) to the sensor which measured the concentration of oxygen in the nitrogen. Once the temperature and RH conditions of each test are set, they are controlled and maintained constant automatically.

To test the water barrier, the sample was inserted in the same chamber as explained above and conditioned in a similar manner for up to 24 hours. The upper chamber had a saturated atmosphere (according to the specified RH) maintained by a small reservoir containing distilled water. Dry nitrogen mixture flowed from the upper to the lower chamber while the infrared detector measured the water concentration in the carrier gas. Once the temperature and RH conditions of each test are set, they are controlled and maintained constant automatically.
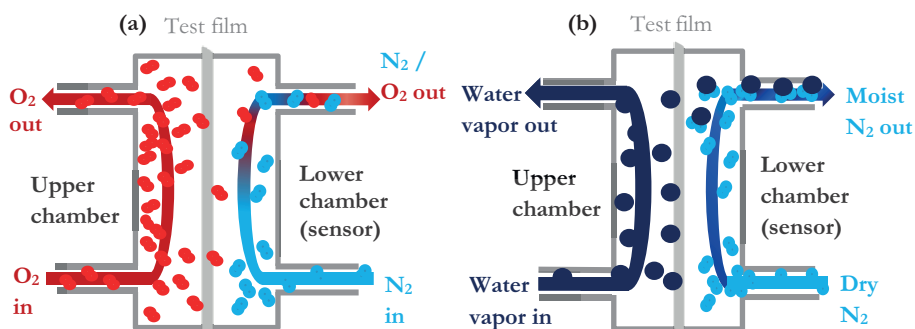
Fig. 2.8 Schematic representation of the cell for **(a)** oxygen and **(b)** water vapor permeability measurements.
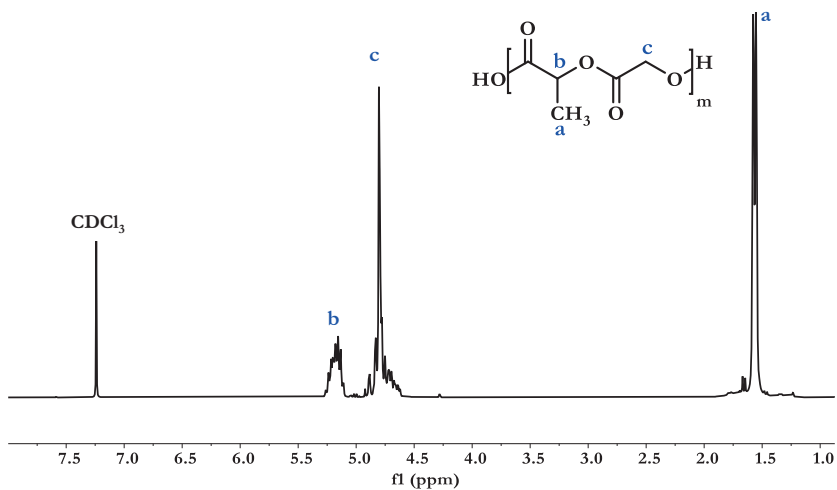
2.6.3   Copolymer characterization

Fig. 2.9 ^{1}H NMR spectra of PLGA$_{48/52}$ in CDCl$_3$.

Table 2.5 Chemical shifts of PLGA copolymers and integrals in ^{1}H NMR spectra.

Chemical shifts of PLGA copolymers (ppm)					Integral		
LA feed (mol%)	GL feed (mol%)	CH$_3$	CH$_2$	CH	CH$_3$	CH$_2$	CH
50	50	1.55-1.59	4.62-4.92	5.11-5.28	2.99	2.17	1
40	60	1.55-1.58	4.59-4.92	5.12-5.28	3.13	3.19	1
30	70	1.62-1.67	4.87-4.94	5.28-5.39	2.18	3.64	0.72
20	80	1.65-1.70	4.87-4.97	5.28-5.42	1.89	5.92	0.66
15	85	1.64-1.73	4.90-4.97	5.33-5.39	0.71	3.24	0.22
10	90	1.64-1.69	4.89-4.99	5.33-5.43	0.56	3.76	0.19

Table 2.6 Mass loss of 5 wt.% ($T_{5\%}$) and 70 wt.% ($T_{70\%}$) of each PLGA sample and the temperature of maximum degradation rate (T_{max}).

| Sample	$T_{5\%}$ (°C)	$T_{70\%}$ (°C)	T_{max} (°C)
PLGA$_{48/52}$	271	341	364
PLGA$_{39/61}$	271	348	369
PLGA$_{28/72}$	277	355	373
PLGA$_{18/82}$	287	362	378
PLGA$_{13/87}$	292	363	381
PLGA$_{9/91}$	292	366	385
PLA	244	320	344
PGA	304	370	391

2.6.4 Biodegradation and non-enzymatic hydrolysis of poly(lactic-co-glycolic acid) (PLGA$_{12/88}$ and PLGA$_{6/94}$)

A degradability study with PLGA copolymers rich in glycolic acid (GA) content synthesized within the OCEAN project, was performed by Yue Wang from our research group.[60] An overview of the experimental protocols and the results is presented below.

In this research, the degradability of PLGA$_{12/88}$ and PLGA$_{6/94}$ synthesized by polycondensation of glycolic acid and lactic acid was studied in parallel using two strategies. In the first, the biodegradability in soil of the copolymers and monomers was monitored using a parallel automated respiration platform called Respicond. The second studied the non-enzymatic hydrolysis of both copolymers using NMR and D₂O.

2.6.4.1 Biodegradation in soil of PLGA$_{12/88}$ and PLGA$_{6/94}$ and its monomers

One of the phases of plastic biodegradation under aerobic conditions involves conversion of the polymer-derived carbon into CO_2 (mainly) and biomass by the action of microbia.[61-63] In this research, this CO_2 evolution was followed with the Respicond, which consists of 95 vessels and each one represents a closed system. A hydroxide solution inside of them traps the CO_2 generated from polymer degradation which converts the hydroxide into carbonate causing change on the conductivity (Reaction **(I)**).[64] This allows for calculation of the absorbed CO_2 (mg). The schematic set up of an individual vessel is depicted in **Fig. 2.10**.
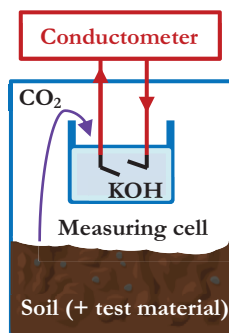
$$2OH^-(aq)+CO_2(g)\rightarrow CO_3^{2-}(aq)+H_2O(l) \quad (I)$$
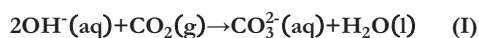
Fig. 2.10 Measuring unit of the parallel respirometer

$PLGA_{12/88}$ and $PLGA_{6/94}$ synthesized by polycondensation and PLA prepared via ring opening polymerization were assessed for biodegradation in soil together with glycolic acid, lactic acid and lactide. Cellulose was also tested as reference material. For this, the non-soluble polymers were ground and mixed with dry soil and the moisture was then adjusted to a pH of 5.9 by adding a mineral salt solution. The soluble monomers were instead first dissolved in the mineral salt solution prior to mixing with soil. Afterwards, 15 g of (wet) soil mixture was added in 250 mL vessels which corresponds to about 62.5 mg of organic carbon from the test substance in each one. For the non-soluble samples, the test was performed in five replicates, while for the soluble ones it was done in triplicates. Additionally, five blanks were included in the test. The close vials were kept at 25 °C during the entire test period.

The amount of generated CO_2 determined by the Respicond's software (CO_{2_sample}) was then used to calculate the relative amount of substrate from each sample converted into CO_2 at determined time, designated as degree of biodegradation (D_t,%) (Equation (**2.13**)).[65] This was done by subtracting the average CO_2 contribution from the blank (CO_{2_blank}) and taking into account the maximum theoretical amount of CO_2 ($ThCO_2$) that could be generated from the material considering the amount of organic carbon initially added.

$$D_t = \frac{CO_{2\_sample} - CO_{2_{blank}}}{ThCO_2} \times 100 \qquad (2.13)$$

Fig. 2.11 (a) presents the evolution of biodegradation in soil over time for all the tested samples. After 53 days, the copolymers $PLGA_{6/94}$ and $PLGA_{12/88}$ with a $53(\pm9)\%$ and $37(\pm2)\%$ respectively converted into CO_2, degraded faster than cellulose and PLA. $PLGA_{6/94}$ exhibited the fastest degradation followed by $PLGA_{12/88}$ which showed a similar trend than cellulose. The slowest degradation in this timeframe was shown by PLA ($<5\%$), which was to be expected based on what is known from literature.[66] These results imply that the degradation rate of PLGA copolymers is favored by increasing amount of glycolic acid in their composition.
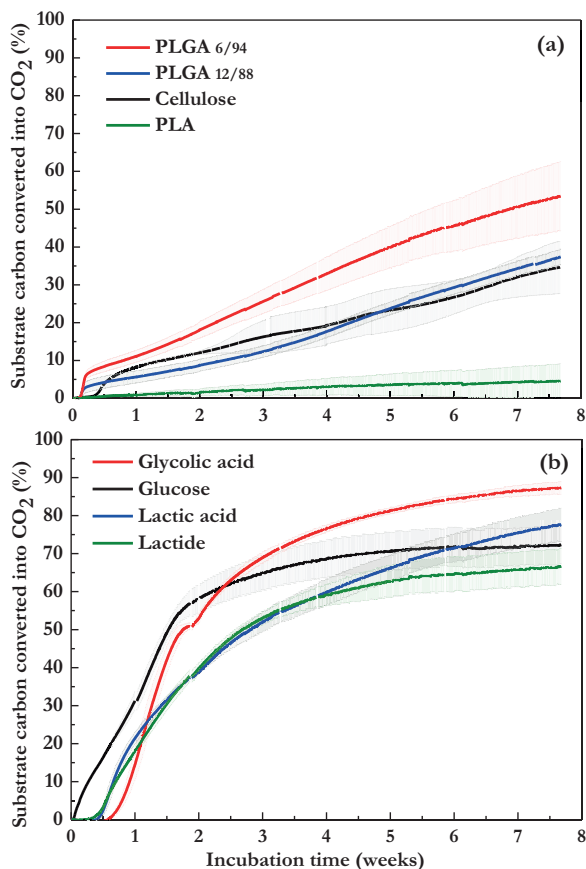
Fig. 2.11 53-Day biodegradation curves of **(a)** PLA, PLGA$_{12/88}$, PLGA$_{6/94}$ and cellulose (references) and **(b)** glycolic acid, lactic acid, lactide and glucose (building blocks) with approximately 5 mg (substrate) carbon g^{-1} dry soil at 25 °C. Mean biodegradation (lines) were plotted. The shaded area represents the standard deviation (calculated per point) of at least three replicates, except for glucose, in which case it represents the range of the duplicates.

Fig. 2.11 (b) shows the biodegradation in soil over time for glycolic acid, lactic acid and lactide together with glucose for comparison. The monomers exhibit a similar degradation rate to that of glucose and as expected they degraded much faster than the polymers. This supports the theory according to which the rate limiting step for the biodegradation of polyesters in soil is the hydrolysis of the ester bonds.[67] Furthermore, a longer lag phase was observed for the monomers compared to the polymers. It was suggested that due to their acidity, high initial concentration of the acidic monomers could have inhibited biological activity.

2.6.4.2 Non-enzymatic PLGA hydrolysis

Hydrolysis in nature can, in principle, occur via non-enzymatic and enzymatic pathways. Enzymatic hydrolysis requires specific hydrolases, which are typically present in fungi and bacteria. Here, experiments were carried out to obtain better understanding of the role of non-enzymatic hydrolysis in the biodegradation of $PLGA_{12/88}$, $PLGA_{6/94}$ and PLA. For this, approximately 10 mg of ground and sieved (425 μm screen) polymer were added to 1 mL of D_2O with 2 mg·mL^{-1} of deuterated DMSO as standard in a 5 mm NMR tube. The tubes were then sealed by melting and stored at controlled temperature of 25 °C. The tests were performed in triplicates over a period of 116 weeks.

Glycolic acid (GA) and lactic acid (LA) generated from the hydrolysis of the polymers are soluble in D_2O and could therefore be measured and quantified by ^1H NMR in an Bruker AMX 400 (^1H, 400.13 MHz) using Equation **(2.14)**. Here, I represents the peak area, N the number of protons from the integrated peak(s) and C (μmol) the amount of a specific hydrolysis product (x, i.e., LA or GA) or DMSO (internal standard).

$$C_x = \frac{I_x}{I_{DMSO}} \times \frac{N_{DMSO}}{N_x} \times C_{DMSO} \qquad (2.14)$$

The degree of hydrolysis Y (%), which represents the total yield of hydrolysis products after multiplying each one by their respective proportion was calculated according to Equation **(2.15)**. Here, Cx (μmol) is the amount of monomer released, f corresponds to its molar fraction incorporated in the polymer and ThC (μmol) the theoretical amount of monomer upon complete hydrolysis.

$$Y = \sum_x \frac{C_x f_x}{ThC_x} \times 100 \qquad (2.15)$$

The amount of dissolved LA or GA relative to the total amount of hydrolyzed monomers (Fx) was calculated with Equation **(2.16)**, where I represents the ^1H NMR peak area and N the number of protons corresponding to the integrated peak(s) (x, i.e., LA or GA).

$$F_x = \frac{\dfrac{I_x}{N_x}}{\dfrac{I_{LA}}{3} + \dfrac{I_{GA}}{2}} \times 100 \qquad (2.16)$$

Initially, the samples were measured once per week and in the latter stages once per month. Also, at the end of the experiment, a sodium deuteroxide solution (over 100 mg) was added in the tube to force complete hydrolysis. The calculated degree of hydrolysis for all the samples as a function of time is presented in **Fig. 2.12**. Both copolymers hydrolyzed much faster than PLA with $PLGA_{6/94}$ initially exhibiting faster formation of GA and LA than $PLGA_{12/88}$. In literature, this behavior is attributed to the higher steric hindrance for hydrolysis of lactate ester groups compared to glycolate ester groups, which could reduce the accessibility to water.[68]
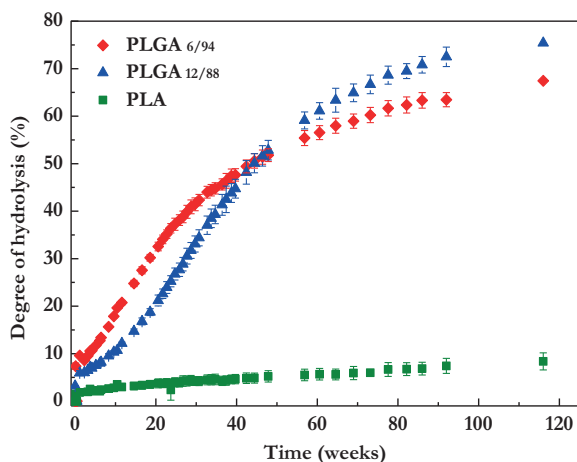
Fig. 2.12 Degree of hydrolysis for $PLGA_{6/94}$, $PLGA_{12/88}$ and PLA as a function of time over 116 weeks at 25 °C in D_2O. The points correspond to the averages of triplicate experiments, with the error bars representing the standard deviation.

The results presented in **Fig. 2.11** and **2.12** indicate that under ambient conditions the hydrolysis of PLGA copolymers in water is slower than their biodegradation in soil: in 7 weeks 12-16% of $PLGA_{6/94}$ hydrolyzed to soluble monomers and oligomers in water, while 50% conversion of $PLGA_{6/94}$ to CO_2 was registered in soil. From this it was concluded that although non-enzymatic hydrolysis could play a role in PLGA soil biodegradation, enzymatic hydrolysis is much faster and thus more relevant in PLGA biodegradation.

The individual yields relative to their maximum theoretical yield **(a)** and the absolute amounts **(b)** of glycolic acid and lactic acid for all polymer hydrolysis experiments at 25 °C in D_2O are presented in **Fig. 2.13**. According to **Fig. 2.13 (a)**, and taking into account the incorporated ratio in the polymers, a higher amount of LA and lower amount of GA than expected is released. Based on this, it appears that GA–LA ester bonds are more prone to hydrolysis than GA–GA ester bonds. Because of the known slow hydrolysis of PLA and low content, LA–LA ester bonds are not expected to have an effect on this outcome. The low absolute amounts relative to the total amount of monomers are thought to have affected the accuracy, leading to the overestimation of LA yield observed in **Fig. 2.13 (a)**. The fact that this outcome is more apparent for $PLGA_{6/94}$ supports this theory. **Fig. 2.13 (b)** shows that after about 20 weeks the amount of LA from $PLGA_{12/88}$ started increasing relative to that of $PLGA_{6/94}$. For GA, after about 50 weeks, the released amount from $PLGA_{12/88}$ exceeds that of $PLGA_{6/94}$. A lack of GA-LA ester bonds by this time could have caused this rate decrease of $PLGA_{6/94}$.
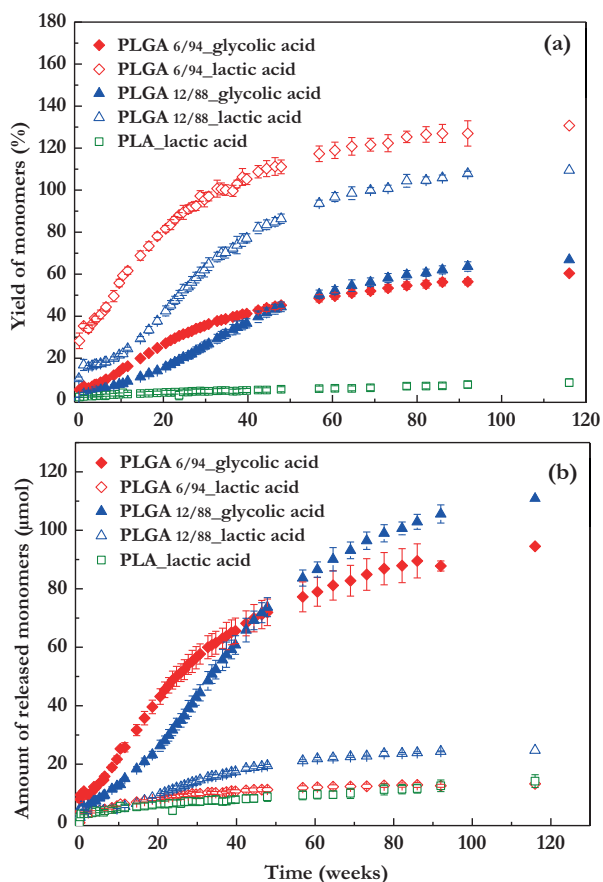
Fig. 2.13 Individual **(a)** yields and **(b)** amounts of monomers (glycolic acid and lactic acid) versus time from hydrolysis of $PLGA_{6/94}$, $PLGA_{12/88}$ and PLA at 25 °C in D_2O. The points correspond to the averages of triplicate experiments, with the error bars representing the standard deviation.

Fig. 2.14 presents the percentage of released GA and LA (including dimers and trimers) relative to their sum (i.e., GA/(GA + LA) or LA/(GA + LA)) over time from hydrolysis of both PLGA copolymers. It is striking that initially the values for LA are much higher than the relative content in the polymer, and consequently the opposite can be said for GA. The consequence of this is that the amount of GA in the remaining polymer increases, possibly also favoring an increase in the degree of crystallinity, which slows down hydrolysis.[69-71] According to **Fig. 2.12**, a decrease in hydrolysis rate was observed after around 20 weeks for $PLGA_{6/94}$ and after about 40 weeks for $PLGA_{12/88}$.
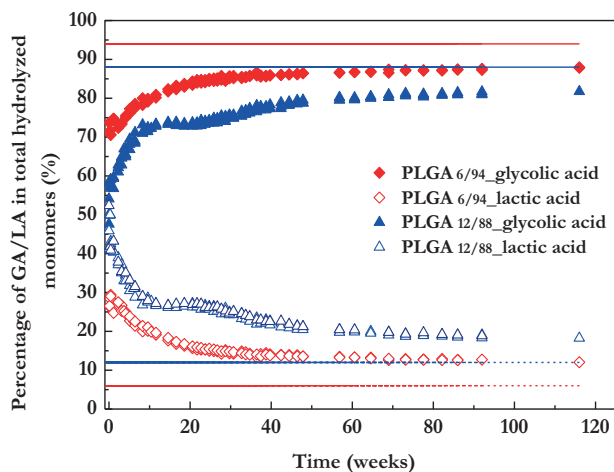
Fig. 2.14 Percentages of dissolved glycolic acid and lactic acid relative to the total amount of hydrolyzed monomers in time for PLGA12/88 and PLGA6/94. Triplicates were plotted. The lines show the starting composition of the polymer.

The percentage of GA slowly increased in time, nearing the feed ratio for synthesis, although it did not reach the same ratio found after forcing complete hydrolysis. For PLGA$_{6/94}$ for example, the 6/94 ratio was determined after complete hydrolysis while in the test the GA/LA composition evolved until 89/11. A higher content of GA built in the copolymer can be expected due to the known higher reactivity of GA over LA and possible evaporation of the latter at the synthesis conditions. Overall, the relative hydrolysis rate of PLGA (rich in GA) appears to be determined by two competing factors: one is the lower hydrophilicity caused by higher LA content, which is mostly relevant at the early stages of hydrolysis; the other relates to crystalline regions in the copolymers with higher GA content, which appear to delay the hydrolysis in the latter stages. The authors concluded that a high quality study for the biodegradability of novel polymers can be performed with a high-throughput platform in a time-efficient way. PLGA copolyesters rich in glycolic acid show the potential to degrade into CO_2 and biomass within months. Considering this, in addition to their outstanding barrier properties, food packaging would be an interesting application to further explore.

2.7   References

(1)   Silva, A.; Cardoso, B.; Silva, M.; Freitas, R.; Sousa, R. Synthesis, characterization, and study of PLGA copolymer in vitro degradation. *J. Biomater. Nanobiotechnol.* **2015**, *06,* 8-19. https://doi.org /10.4236/jbnb.2015.61002.
(2)   Murcia Valderrama, M. A.; van Putten, R.-J.; Gruter, G.-J. M. The potential of oxalic - and glycolic acid based polyesters (review). towards CO_2 as a feedstock (Carbon Capture and Utilization - CCU). *Eur. Polym. J.* **2019**, *119*, 445-468. https://doi.org/10.1016/j.eurpolymj.2019.07.036.
(3)   Kricheldorf, H. Syntheses and application of polylactides. *Chemosphere.* **2001**, *43,* 49−54. https:// doi.org /10.1016/S0045-6535(00)00323-4.

(4)   Storey, R.; Mullen, B.; Desai, G.; Sherman, J.; Tang, C. Soluble Tin(II) macroinitiator adducts for the controlled ring-opening polymerization of lactones and cyclic carbonates. *J. Polym. Sci. Part A: Polym. Chem.* **2002**, *40*, 3434-3442. https://doi.org/10.1002/pola.10448.

(5)   Kaplan, D. L. *Biopolymers from Renewable Resources*; Springer Science & Business Media, 2013.

(6)   Ryner, M.; Stridsberg, K.; Albertsson, A.-C.; von Schenck, H.; Svensson, M. Mechanism of ring-opening polymerization of 1,5-dioxepan-2-one and l-lactide with stannous 2-ethylhexanoate. A theoretical study. *Macromolecules.* **2001**, *34* (12), 3877-3881. https://doi.org/10.1021/ma002096n.

(7)   Chu, C. C. 11 - Materials for absorbable and nonabsorbable surgical sutures. In *Biotextiles as Medical Implants.* **2013**, 275-334. https://doi.org/10.1533/9780857095602.2.275.

(8)   Singh, G.; Tanurajvir, K.; Ravinder, K.; Kaur, A. Recent biomedical applications and patents on biodegradable polymer-PLGA. *Int. J. Pharmacol. Pharm. Sci.* **2014**, *1*, 30-42.

(9)   Plus antibacterial sutures evidence summary. Technical, clinical, and economic data supporting triclosan-coated sutures. https://www.jnjmedicaldevices.com/sites/default/files/user_uploaded_assets/pdf_assets/2019-06/103240-181127_Plus_EvidenceSummary_192_CA.pdf (accessed June 20, 2020).

(10)   Van de Velde, K.; Kiekens, P. Biopolymers: overview of several properties and consequences on their applications. *Polym. Test.* **2002**, *21*, 433-442. https://doi.org/10.1016/S0142-9418(01)00107-6

(11)   Phuong, V. T.; Coltelli, M.-B.; Cinelli, P.; Cifelli, M.; Verstichel, S.; Lazzeri, A. Compatibilization and property enhancement of poly(lactic acid)/polycarbonate blends through triacetin-mediated interchange reactions in the melt. *Polymer.* **2014**, *55* (17), 4498-4513. https://doi.org/10.1016/j.polymer.2014.06.070.

(12)   About Kuredux| Kureha Corp., Tokyo, Japan, http://www.kuredux.com/en/about/index.html(accessed Jun 20, 2020).

(13)   Wang, N.; Wu, X. S.; Li, C.; Feng, M. F. Synthesis, characterization, biodegradation, and drug delivery application of biodegradable lactic/glycolic acid polymers: I. Synthesis and characterization. *J Biomater Sci Polym Ed.* **2000**, *11* (3), 301-318. https://doi.org/10.1163/ 156856200743715.

(14)   D'Avila Carvalho Erbetta, C.; Alves, R. J.; Resende, J. M.; Fernando de Souza Freitas, R.; Geraldo de Sousa, R.. Synthesis and characterization of poly(D,L-Lactide-Co-Glycolide) copolymer. *J. Biomater. Nanobiotechnol.* **2012**, *03*, 208-225. http://dx.doi.org/10.4236/jbnb.2012.32027

(15)   Vargha-Butler, E. I.; Kiss, E.; Lam, C. N. C.; Keresztes, Z.; Kálmán, E.; Zhang, L.; Neumann, A. W. Wettability of biodegradable surfaces. *Colloid Polym. Sci.* **2001**, *279*, 1160-1168. https://doi.org/10.1007/s003960100549

(16)   Gilding, D. K.; Reed, A. M. Biodegradable polymers for use in surgery—polyglycolic/poly(lactic acid) homo- and copolymers: 1. *Polymer.* **1979**, *20* (12), 1459–1464. https://doi.org/10.1016/0032-3861(79)90009-0.

(17)   Gorrasi, G.; Meduri, A.; Rizzarelli, P.; Carroccio, S.; Curcuruto, G.; Pellecchia, C.; Pappalardo, D. Preparation of poly(glycolide-co-lactide)s through a green process: analysis of structural, thermal, and barrier properties. *React. Funct. Polym.* **2016**, *109*, 70–78. https://doi.org/10.1016/j.reactfunctpolym.2016.10.002.

(18)   Chen, Y.; Yao, X.; Gu, Q.; Pan, Z. Non-isothermal crystallization kinetics of poly (lactic acid)/graphene nanocomposites. journal of polymer engineering. *J. Polym. Eng.* **2013**, *33*. 163-171. https://doi.org/10.1515/polyeng-2012-0124.

(19)   Kawai, T.; Rahman, N.; Matsuba, G.; Nishida, K.; Kanaya, T.; Nakano, M.; Okamoto, H.; Kawada, J.; Usuki, A.; Honma, N.; Nakajima, K.; Matsuda, M. Crystallization and melting behavior of poly (l-lactic acid). *Macromolecules.* **2007**, *40* (26), 9463-9469. https://doi.org/10.1021/ma070082c.

(20)   Liu, Y.; Wang, L.; He, L.; Fan, Z.; Li, S.-M. Non-Isothermal Crystallization Kinetics of Poly(L-Lactide). *Polym. Int.* **2010**, *59*, 1616-1621. https://doi.org/10.1002/pi.2894.

(21)   Yu, C.; Bao, J.; Xie, Q.; Shan, G.; Bao, Y.; Pan, P. Crystallization behavior and crystalline structural changes of poly(glycolic acid) investigated: via temperature-variable WAXD and FTIR analysis. *CrystEngComm.* **2016**, *18*, 7894-7902. https://doi.org/10.1039/C6CE01623E.

(22)   Chen, H.; Ma, C.; Bai, W.; Chen, D.; Xiong, C. Isothermal crystallization and melting behavior of composites composed of poly(l-lactic acid) and poly(glycolic acid) fibers. *J. Macromol. Sci., Part B: Phys.* **2014**, *53*, 1715-1725. https://doi.org/10.1080/00222348.2014.898998.

(23)   Finnigan, B. Barrier polymers. In *The Wiley Encyclopedia of Packaging Technology*; 3ʳᵈ ed.; John Wiley & Sons, Inc.: New York, 2009, pp. 305-309. https://doi.org/10.1002/9780470541395.

(24) Karkhanis, S. S.; Stark, N. M.; Sabo, R. C.; Matuana, L. M. Water vapor and oxygen barrier properties of extrusion-blown poly(lactic acid)/cellulose nanocrystals nanocomposite films. *Composites, Part A.* **2018**, *114*, 204-211. https://doi.org/10.1016/j.compositesa.2018.08.025.

(25) Sonchaeng, U.; Iñiguez-Franco, F.; Auras, R.; Selke, S.; Rubino, M.; Lim, L.-T. Poly(lactic acid) mass transfer properties. *Prog. Polym. Sci.* **2018**, *86*, 85-121. https://doi.org/10.1016/j.progpolymsci.2018.06.008.

(26) Arrieta, M. P.; Fortunati, E.; Dominici, F.; Rayón, E.; López, J.; Kenny, J. M. PLA-PHB/Cellulose based films: mechanical, barrier and disintegration properties. *Polym. Degrad. Stab.* **2014**, *107*, 139-149. https://doi.org/10.1016/j.polymdegradstab.2014.05.010.

(27) Courgneau, C.; Domenek, S.; Lebossé, R.; Guinault, A.; Avérous, L.; Ducruet, V. Effect of crystallization on barrier properties of formulated polylactide. *Polym. Int.* **2012**, *61* (2), 180-189. https://doi.org/10.1002/pi.3167.

(28) Colomines, G.; Ducruet, V.; Courgneau, C.; Guinault, A.; Domenek, S. Barrier properties of poly(lactic acid) and its morphological changes induced by aroma compound sorption. *Polym. Int.* **2010**, *59* (6), 818-826. https://doi.org/10.1002/pi.2793.

(29) K. Holm, V.; Ndoni, S.; Risbo, J. The stability of poly(lactic acid) packaging films as influenced by humidity and temperature. *J. Food Sci.* **2006**, *71*, E40-E44. https://doi.org/10.1111/j.1365-2621.2006.tb08895.x

(30) Lehermeier, H. J.; Dorgan, J. R.; Way, J. D. Gas permeation properties of poly(lactic acid). *J. Membr. Sci.* **2001**, *190* (2), 166-172. https://doi.org/243–251. 10.1016/j.memsci.2006.08.021.

(31) Auras, R. A.; Singh, S. P.; Singh, J. J. Evaluation of oriented poly(lactide) polymers vs. existing PET and oriented PS for fresh food service containers. *Packag. Technol. Sci.* **2005**, *18* (4), 207-216. https://doi.org/10.1002/pts.692.

(32) Pandey, K.; Antil, R.; Saha, S.; Jacob, J.; Balavairavan, B. Poly(lactic acid)/thermoplastic polyurethane/wood flour composites: evaluation of morphology, thermal, mechanical and biodegradation properties. *Mater. Res. Express.* **2019**, *6* (12), 125306.

(33) Mullapudi, S. S.; Pandey, K.; Maiti, S. N.; Saha, S. PLA/EVA/teak wood flour biocomposites for packaging application: evaluation of mechanical performance and biodegradation properties. *J. Package Technol. Res.* **2018**, *2* (3), 191-201. https://doi.org/10.1007/s41783-018-0037-2.

(34) Kawakami, Y.; Sato, N.; Hoshino, M.; Kouyama, T.; Shiiki, Z. Oriented polyglycolic acid film and production process thereof. US5853639 A, December 29, 1998.

(35) Hokari, Y.; Yamane, K.; Wakabayashi, J.; Suzuki, T. Polyglycolic acid resin-based layered sheet and method of producing the same.US 20090081396 A1, March 26, 2009.

(36) Yamane, K.; Kato, R.; Tobita, H. Method for producing multilayer stretch-molded article. EP 1674240 B1, December 17, 2008.

(37) Yamane, K.; Sato, H.; Ichikawa, Y.; Sunagawa, K.; Shigaki, Y. Development of an industrial production technology for high-molecular-weight polyglycolic acid. *Polym. J.* **2014**, *46* (11), 769-775. https://doi.org/10.1038/pj.2014.69.

(38) Kawakami, Y.; Sato, N.; Hoshino, M.; Kouyama, T.; Shiiki, Z. Polyglycolic acid sheet and production process thereof. EP0805176A1, November 5, 1997.

(39) Yamane, K.; Miura, H.; Ono, T.; Nakajima, J.; Itoh, D. Crystalline polyglycolic acid, polyglycolic acid composition and production process thereof. US20030125508A1, July 3, 2003.

(40) Kaihara, S.; Matsumura, S.; Mikos, A. G.; Fisher, J. P. Synthesis of poly(l-lactide) and polyglycolide by ring-opening polymerization. *Nat. Protoc.* **2007**, *2* (11), 2767-2771. https://doi.org/10.1038/nprot.2007.391.

(41) Ayyoob, M.; Lee, D. H.; Kim, J. H.; Nam, S. W.; Kim, Y. J. Synthesis of poly(glycolic acids) via solution polycondensation and investigation of their thermal degradation behaviors. *Fibers Polym.* **2017**, *18* (3), 407-415. https://doi.org/10.1007/s12221-017-6889-1.

(42) Avgoustakis, K.; Nixon, J. R. Biodegradable controlled release tablets 1: preparative variables affecting the properties of poly(lactide-co-glycolide) copolymers as matrix forming material. *Int. J. Pharm.* **1991**, *70* (1), 77-85. https://doi.org/10.1016/0378-5173(91)90166-L.

(43) Grijpma, D. W.; Nijenhuis, A. J.; Pennings, A. J. Synthesis and hydrolytic degradation behavior of high-molecular-weight l-lactide and glycolide copolymers. *Polymer.* **1990**, *31* (11), 2201-2206. https://doi.org/10.1016/0032-3861(90)90096-H.

(44) Chu, C. C. Differential scanning calorimetric study of the crystallization kinetics of polyglycolic acid at high undercooling. *Polymer.* **1980**, *21* (12), 1480-1482. https://doi.org/10.1016/0032-3861(80)90153-6.

(45) Fischer, E. W.; Sterzel, H. J.; Wegner, G. Investigation of the structure of solution grown crystals of lactide copolymers by means of chemical reactions. *Kolloid Z. Z. Polym.* **1973**, *251* (11), 980-990. https://doi.org/10.1007/BF01498927.

(46) Hay, J. N.; Sabir, M. Crystallization kinetics of high polymers. polyethylene oxide—part ii. *Polymer.* **1969**, *10*, 203-211. https://doi.org/10.1016/0032-3861(69)90031-7.

(47) Jeziorny, A. Parameters characterizing the kinetics of the non-isothermal crystallization of poly(ethylene terephthalate) determined by d.s.c. *Polymer.* **1978**, *19* (10), 1142-1144. https://doi.org/10.1016/0032-3861(78)90060-5.

(48) Sun, Z.; Wang, X.; Guo, F.; Jiang, C.; Pan, Q. Isothermal and nonisothermal crystallization kinetics of bio-sourced nylon 69. *Chin. J. Chem. Eng.* **2016**, *24* (5), 638-645. https://doi.org/10.1016/j.cjche.2015.12.021.

(49) Coburn, N.; Douglas, P.; Kaya, D.; Gupta, J.; McNally, T. Isothermal and non-isothermal crystallization kinetics of composites of poly(propylene) and MWCNTs. *Adv Ind Eng Polym Res.* **2018**, *1* (1), 99-110. https://doi.org/10.1016/j.aiepr.2018.06.001.

(50) Zeng, Y.; Liu, Y.; Wang, L.; Huang, H.; Zhang, X.; Liu, Y.; Min, M.; Li, Y. Effect of silver nanoparticles on the microstructure, non-isothermal crystallization behavior and antibacterial activity of polyoxymethylene. *Polymers.* **2020**, *12* (2), 424. https://doi.org/10.3390/polym12020424.

(51) Courgneau, C.; Ducruet, V.; Avérous, L.; Grenet, J.; Domenek, S. Nonisothermal crystallization kinetics of poly(lactide)—effect of plasticizers and nucleating agent. *Polym. Eng. Sci.* **2013**, *53* (5), 1085-1098. https://doi.org/10.1002/pen.23357.

(52) Li, J.; Wang, Y.; Wang, X.; Wu, D. Development of polyoxymethylene/polylactide blends for a potentially biodegradable material: crystallization kinetics, lifespan prediction, and enzymatic degradation behavior. *Polymers.* **2019**, *11* (9), 1516. https://doi.org/10.3390/polym11091516.

(53) Siró, I.; Plackett, D.; Sommer-Larsen, P. A Comparative study of oxygen transmission rates through polymer films based on fluorescence quenching. *Packag. Technol. Sci.* **2010**, *23* (6), 301-315. https://doi.org/10.1002/pts.895.

(54) Miller, K. S.; Krochta, J. M. Oxygen and aroma barrier properties of edible films: a review. *Trends Food Sci. Technol.* **1997**, *8* (7), 228-237. https://doi.org/10.1016/S0924-2244(97)01051-0.

(55) Dhoot, S. N.; Freeman, B. D.; Stewart, M. E. Barrier polymers. *Encyclopedia of polymer science and technology*; American Cancer Society, 2002.

(56) Engineers, N. B. of C. &. *Handbook on pet film and sheets, urethane foams, flexible foams, rigid foams, speciality plastics, stretch blow moulding, injection blow moulding, injection and co-injection preform technologies.* Asia pacific business press Inc., 2018.

(57) Ford, L. Ingeo Biopolymer 4032D. https://www.natureworksllc.com/~/media/Technical_Resources/Technical_Data_Sheets/TechnicalDataSheet_4032D_films_pdf. (accessed May 10, 2020).

(58) Elsawy, M. A.; Kim, K.-H.; Park, J.-W.; Deep, A. Hydrolytic degradation of polylactic acid (PLA) and its composites. *Energy Rev.* **2017**, *79*, 1346-1352. https://doi.org/10.1016/j.rser.2017.05.143.

(59) Williams, D. F.; Mort, E. Enzyme-accelerated hydrolysis of polyglycolic acid. *J Bioeng.* **1977**, *1* (3), 231-238. PMID: 210160.

(60) Wang, Y.; Valderrama, M. A. M.; Putten, R.-J. van; Davey, C. J. E.; Tietema, A.; Parsons, J. R.; Wang, B.; Gruter, G.-J. M. Biodegradation and non-enzymatic hydrolysis of poly(lactic-co-glycolic acid) (PLGA12/88 and PLGA6/94). *Polym.* **2022**, *14*, 15. https://doi.org/10.3390/POLYM14010015.

(61) Badia, J. D.; Gil-Castell, O.; Ribes-Greus, A. Long-term properties and end-of-life of polymers from renewable resources. *Polym. Degrad. Stab.* **2017**, *137,* 35-57. https://doi.org/10.1016/J.POLYMDEGRADSTAB.2017.01.002.

(62) Krzan, A.; Hemjinda, S.; Miertus, S.; Corti, A.; Chiellini, E. Standardization and certification in the area of environmentally degradable plastics. *Polym. Degrad. Stab.* **2006**, *91 (12)*, 2819-2833. https://doi.org/10.1016/J.POLYMDEGRADSTAB.2006.04.034.

(63) Krueger, M. C.; Harms, H.; Schlosser, D. Prospects for microbiological solutions to environmental pollution with plastics. *Appl. Microbiol. Biotechnol.* **2015**, *99 (21),* 8857-8874. https://doi.org/10.1007/S00253-015-6879-4.

(64) Chapman, S. B. A Simple conductimetric soil respirometer for field use. **1971**, *22 (3)*, 348. https://doi.org/10.2307/3543857.

(65) Smirnova, N.; Demyan, M. S.; Rasche, F.; Cadisch, G.; Müller, T. Calibration of CO_2 trapping in alkaline solutions during soil incubation at varying temperatures using a Respicond VI. *Open J. Soil Sci.* **2014**, *04 (05)*, 161-167. https://doi.org/10.4236/OJSS.2014.45019.

(66) Karamanlioglu, M.; Preziosi, R.; Robson, G. D. Abiotic and biotic environmental degradation of the bioplastic polymer poly(lactic acid): a review. *Polym. Degrad. Stab.* **2017**, *137,* 122-130. https://doi.org/10.1016/J.POLYMDEGRADSTAB.2017.01.009.

(67) Sander, M. Biodegradation of polymeric mulch films in agricultural soils: concepts, knowledge gaps, and future research directions. *Environ. Sci. Technol.* **2019**, *53 (5),* 2304-2315. https://doi.org/10.1021/ACS.EST.8B05208.

(68) Pitt, C.; Gu, Z.-W. Modification of the rates of chain cleavage of poly (e-caprolactone) and related polyesters in the solid state. *J. Controlled Release.* **1987**, *4*, 283-292. https://doi.org/10.1016/0168-3659(87)90020-4.

(69) Schliecker, G.; Schmidt, C.; Fuchs, S.; Wombacher, R.; Kissel, T. Hydrolytic degradation of poly(lactide-co-glycolide) films: effect of oligomers on degradation rate and crystallinity. *Int. J. Pharm.* **2003**, *266 (1–2),* 39-49. https://doi.org/10.1016/S0378-5173(03)00379-X.

(70) Park, T. G. Degradation of poly(lactic-co-glycolic acid) microspheres: effect of copolymer composition. *Biomaterials.* **1995**, *16 (15),* 1123-1130.https://doi.org/10.1016/0142-9612(95)93575-X.

(71) Muthu, M. S. Nanoparticles based on PLGA and its co-polymer: an overview. *Asian J. Pharm.* **2009**, *3 (4),* 266-273. https://doi.org/10.4103/0973-8398.59948.

CHAPTER 3

Synthesis and properties of degradable blends and copolyesters of polyoxalates and PGA/PLA
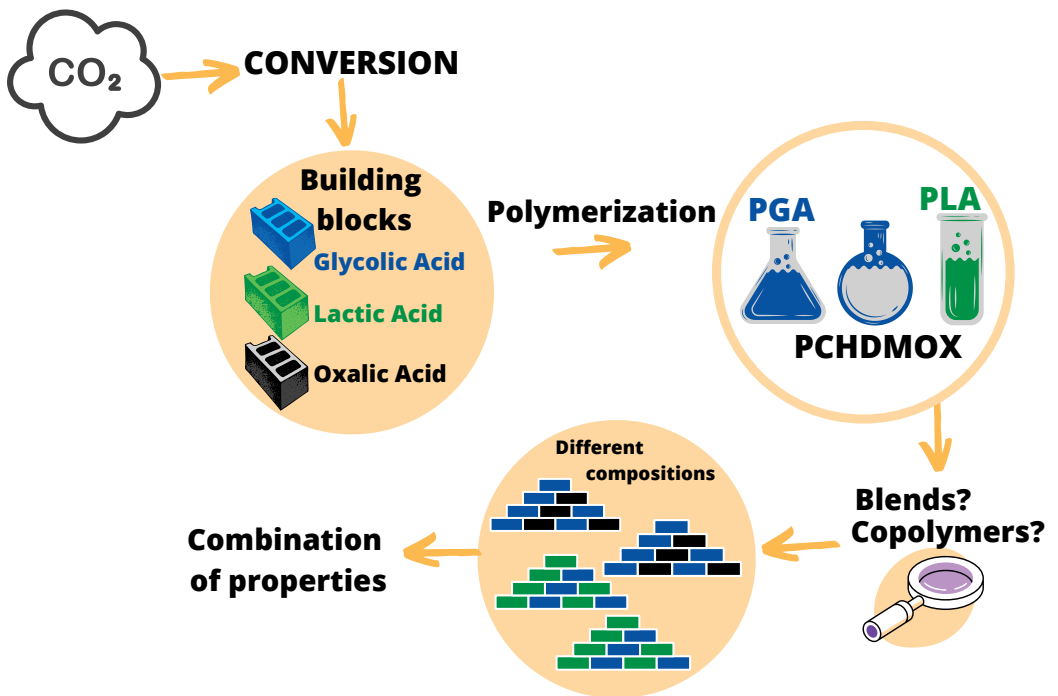
Abstract

Previously we reported on the very good mechanical and thermal properties of polyoxalates and on the outstanding oxygen barrier properties of PGA/PLGA. Both classes of materials were found to be biodegradable, the rate of which depends on the composition. In this study the potential of copolyesters in which the structural features of both polyoxalates and PGA/PLA are combined is researched, with the purpose of evaluating if and how the remarkable barrier performance of PGA could be integrated with the high thermal stability and fast hydrolysis of poly(1,4-cyclohexanedimethanol oxalate) (PCHDMOX). As a comparison PLA was also assessed. Different feed ratios of either PGA, glycolide (GL), PLA and lactide (LAC) were copolymerized with PCHDMOX (50/50 and 30/70 wt%). In general, higher PCHDMOX incorporation favored the thermal stability while higher GL/PGA content improved the barrier to oxygen and water vapor. As expected, the barrier to water vapor of PCHDMOX was negatively affected by copolymerization with PLA/LAC. Copolyesters from PCHDMOX and PGA/GL showed lower T_g, higher thermal stability, better barrier properties and faster hydrolysis rate than those prepared with PLA/LAC. All copolyesters hydrolyzed at a faster rate than the respective homopolymers they were made from. Essentially, these materials could cover a similar application range to that of PGA/PLGA/PLA/PCHDM, where low T_g (below 50 °C) would be suitable and the possibility of tunning specific material properties and accelerating their decomposition is desired.

3.1   Introduction

Currently, there is no alignment between the plastic production rate and adequate plastic waste management. Plastic can leak into the environment not only through consumer usage and disposal but also during production and transport. This mismanaged plastic waste causes unprecedented harm to ecosystems. About 12 million tons (Mt) per year of plastic currently leak into the oceans[1] and it is estimated that by 2040 a total of about 12,000 Mt of this plastic will have ended up discarded in landfills or in the natural environment.[2] Moreover, the rising plastic demand involves increasing requirement of fossil fuel, energy and therefore higher carbon emissions by the industry. The total plastics footprint was 0.86 Gt in 2019 and is expected to grow to 2.8 Gt in 2050 if the volume growth continues at 3.5% annually and we continue to produce our plastics from fossil resources.[3] The aforementioned issues prompt the need to rethink the entire plastic value chain. Especially since most plastics produced presently are fossil based.

Polyesters are one of the most promising families of polymers based on renewable resources, because of their tunable performance in combination with their potential towards reuse, recycle and biodegradability.[4]

Currently various monomers, such as FDCA (2,5-Furandicarboxylic acid), bio-MEG (mono ethylene glycol), 1,3-PDO (propane diol), 1,4-BDO (butanediol), glycolic acid, lactic acid, oxalic acid, succinic acid and isosorbide, stand out as available building blocks for polyester production. Monomers used in this study, glycolic and oxalic acid, can be derived from electrochemical reduction of CO_2[5] and lactic acid from biomass. Glycolic acid derived polymers have shown to be biocompatible and degradable.[6,7] Both features are also common with polyesters from oxalic acid. Some polyoxalates for example, have been reported to degrade almost completely (81-92% M_n reduction) after 13 months under atmospheric conditions.[8] Commercial PGA tested under different environmental conditions has been claimed to take one month to degrade in compost and between 2 to 3 weeks in vivo.[9] Degradability is a valuable feature not only for the biomedical field: it can also be an advantageous property for specific applications where plastic recovery and recycling is difficult or impossible and there is an increased chance of leakage into the environment, for instance for certain packaging (specifically paper coating), agricultural films and cosmetics.[10] Polyoxalates have shown excellent melt processability, very good thermal stability and mechanical properties,[8,11-13] including high tensile strength. Similarly, PGA has significantly higher tensile strength than that of some engineering polymers[14], but it also exhibits high crystallinity, which results in brittleness and poor solubility. Still, its outstanding barrier properties are of great interest.[15]

Making polymers directly from oxalic acid (OA) using melt polymerization is difficult, since it undergoes decarboxylation into CO_2 and formic acid[16] starting at about 140 °C. Therefore, derivatives such as dimethyl oxalate[8,16], diethyl oxalate[18], ethylene oxalate[19], diphenyl oxalate[20-22], etc. have been used for the production of polyoxalates.[7] Glycolic acid (GA), on the other hand, can be polymerized into PGA through polycondensation. However, the resulting polymer has too low molecular weight as a consequence of the equilibrium reaction between the forming PGA and glycolide (GL), the cyclic diester of GA.[23] Although some strategies to circumvent this problem have been reported[23-25], polymer grade PGA and other related polymers are currently produced through ring opening (ROP) of glycolide. This route does not require any solvents, nor does it release side products, and high molecular weight polymers with good mechanical properties can be achieved. Nevertheless, glycolide is still a relatively expensive monomer, making PGA and its copolymers very costly materials, which complicates large-scale commercialization.[7]

With ongoing technological development and increasing availability of renewable feedstocks, easier access to CO_2 based monomers such as glycolic acid and oxalic acid could be expected. At the same time, CO_2-based polymers result in so-called negative emissions, which will be very important towards the net zero emissions targets (as zero emissions will not be possible, net zero emissions can be obtained by compensating with negative emissions). Given the demand for sustainable materials regarding CO_2 emissions and plastic waste reduction, combined with the promising properties observed for P(L)GAs and

polyoxalates, it is interesting to study if the properties of these polymers can be combined. Nevertheless, little has been reported on materials combining both OA and GA building blocks. Alksnis et al.[26] synthesized degradable polyester fibers based on oxalic acid, modified with up to 13 mol% of glycolic acid. For this purpose, an oligoester of ethylene glycol and oxalic acid was reacted with different amounts of a glycolic acid oligoester using Tin(II) chloride dehydrate as catalyst under reduced pressure (1 mbar). Since no characterization was provided, potential applications of these materials cannot be identified. Something similar is the case for polyoxalates. Because most research has focused on the biomedical field, information on its potential in other application fields, where degradability could also be a desired property, is limited.

The opposite can be said of lactic acid. Numerous research efforts have been dedicated to this monomer, as it is used (via its cyclic diester lactide) to produce polylactic acid (PLA), the leading biobased polyester commercially available. Although PLA is considered (industrially) compostable, its degradation takes much longer than that of polyoxalates and PGA. Rigid films take up to 70 days to disintegrate in a composting environment (rich in organic matter) at 50-60 °C.[27] On this basis, it is also of interest to study polyesters derived from polyoxalates and lactic acid. It may help not only to determine the effect of this combination in the final properties of the material, but also to acquire more insight regarding the use of oxalic acid derivatives as comonomers.

In this study copolyesters derived from poly(1,4-cyclohexanedimethanol oxalate) (PCHDMOX) and PGA or PLA were synthesized and evaluated. Additional experiments were performed in which PGA or PLA was replaced by glycolide or lactide, respectively. Their structure, thermal transitions and stability and molecular weight distribution will be reported. A barrier property assessment carried out using thermocompressed films will be presented and finally the degradability of the synthesized samples monitored via a hydrolysis study will be analyzed.

3.2   Experimental section

3.2.1   Materials

All chemicals were used without further purification. Diphenyl oxalate 98% was acquired from TCI chemicals, glycolic acid (GA) 99% and *L*-lactic acid (LA) 90% solution (in water) were purchased from ACROS organics. 1,4-Cyclohexanedimethanol (CHDM) 99% (mixture of 70% trans-, 30% cis-isomers) and butyltin hydroxide oxide (BuSnO(OH)) 97% were acquired from Sigma-Aldrich, as well as deuterated chloroform (CDCl$_3$). Finally, glycolide and lactide were purchased from Purac (Corbion).

3.2.2   Prepolymer synthesis

3.2.2.1 PCHDMOX (poly(1,4-cyclohexanedimethanol oxalate)) prepolymer

In a typical batch, equimolar amounts of diphenyl oxalate (97.4 g, 0.40 moles) and CHDM (58.4 g, 0.40 moles) were placed in a three-necked round bottom flask equipped with a mechanical stirrer, a nitrogen inlet and a distillation head. The system was first flushed with nitrogen gas for 5 minutes at room temperature and then immersed in an oil bath at 120 °C in the presence of BuSnO(OH) as catalyst (0.07 mol% based on the oxalate). The mixture was stirred at 100 rpm under nitrogen atmosphere with a gradual temperature increase to 200 °C over 6 hours. The monomer conversion was tracked with ^{1}H NMR. Subsequently, starting at atmospheric pressure, the pressure was halved every 15 minutes until 1 mbar and kept at 1 mbar for 45 minutes. During this stage, the temperature was increased up to 220 °C. Finally, the prepolymer was recovered, crushed and dried under vacuum for 24 hours at 30 °C.

3.2.2.2 Glycolic acid or *L*-lactic acid prepolymers

The same basic setup as described in 3.2.2.1 was used for this procedure. 60 g of glycolic acid (0.78 moles) was introduced in a 250 mL round bottom flask under nitrogen atmosphere with 0.03 mol% of BuSnO(OH) as catalyst. The reactor was initially immersed in an oil bath and the temperature was increased to 200 °C and subsequently maintained during 4 hours at atmospheric pressure and 100 rpm. The water produced was recovered in the receiver. Next, the pressure was reduced to 10 mbar over 3 hours while the temperature was increased to 235 °C. The resulting polyglycolic acid (PGA) was allowed to cool down in the reactor, where it formed a single white solid that was crushed and subsequently dried under vacuum at 40 °C.

A similar procedure was performed with *L*-lactic acid (70 g of 90% L-LA in water, 0.70 moles). The reaction was conducted at between 175 and 195 °C over 18 hours. A final increment to 200 °C was accompanied by a pressure reduction to 10 mbar over 3 hours. The resulting PLA was recovered, crushed and dried under vacuum.

3.2.3   PCHDMOX and PGApp / PLApp blends

Polymers derived from PGA_{pp} or PLA_{pp} (pp = prepolymer) and PCHDMOX were prepared using different blend compositions (50/50 and 30/70 wt%).

3.2.3.1   Blends with PGA

For one set of products, 3.6 or 6 g of the PGA prepolymer was weighed in a 250 mL three-neck round bottom flask and molten at 230 °C under nitrogen flow. Subsequently, 8.4 or 6 g of PCHDMOX was added to the reactor, adding up to a combined mass of 12 g, and the mixture was mechanically stirred for 30 minutes at 90 rpm at a constant temperature (230 °C). The resulting products PCHDMGA-*co*-OX$_{50/50}$ and PCHDMGA-*co*-OX$_{30/70}$ were recovered, ground and dried under vacuum.

3.2.3.2   Blends with PLA

For PCHDMLA-*co*-OX$_{50/50}$ and PCHDMLA-*co*-OX$_{30/70}$, a similar procedure was used. The required amounts of PCHDMOX and PLA prepolymer, for a total of 15 g of product, were added in the reactor at the same time. The mixture was stirred at 90 rpm and 200 °C for 1 hour under nitrogen flow.

3.2.4   PCHDMDOX and glycolide (GL) or lactide (LAC) copolyesters

The PCHDMGA-*co*-OX and PCHDMLA-*co*-OX type samples were prepared using PCHDMOX with glycolide and with lactide with two compositions each: 50/50 and 30/70 wt%. Prior to use, a 250 mL reactor equipped with a mechanical stirrer and nitrogen inlet was initially vacuum (1 mbar) and nitrogen flushed twice in cycles of 5 minutes. Subsequently, the required amounts of PCHDMOX and cyclic dimer, for a total mass of 12 g, were loaded into the reactor. No additional catalyst was added. The system was flushed with nitrogen for 5 minutes before being immersed in an oil bath. For the blends containing glycolide, the initial oil bath temperature was 200 °C, which was subsequently increased to 235 °C within 15 minutes. The pressure was then reduced to 400 mbar and the stirring speed was set to 90 rpm. After 20 minutes at 235 °C the product was recovered, ground and dried under vacuum. For the copolyesters with lactide the reaction was conducted at 200 °C (oil bath) for 60 minutes at 400 mbar and 90 rpm.

3.2.5   Analytical techniques and other measurements

3.2.5.1 ^{1}H NMR, DSC and TGA

The progression of all reactions and the structure of the final products were studied with ^{1}H NMR spectroscopy on a Bruker AMX 400 (^{1}H, 400.13 MHz) using CDCl$_3$ as solvent. The thermal transitions were determined using a differential scanning calorimetry (DSC) 3+ STAR^{e} system from Mettler Toledo. For all samples, approximatively 5 mg of sample was introduced in sealed aluminum pans (40 μm) and heated from 0 up to 200 °C (dT/dt = 10 °C·min^{-1}) except for the PGA$_{PP}$, which was heated to 240 °C. The samples were maintained

at that temperature for 2 minutes and subsequently cooled down to 0 °C at the same rate. A second heating scan was recorded under the same conditions. The reported glass transition temperature T_g and melting temperature T_m were determined from the last scan. The thermal stability was determined using a TGA/DSC 3+ STARe system from Mettler Toledo. For this purpose, about 7 mg of copolymer was introduced in a sealed aluminum sample vessel (40μm). Subsequently, the samples were heated from room temperature to 400 °C (dT/dt = 10 °C·min⁻¹) under nitrogen flow (50 mL·min⁻¹). The molecular weight distribution was determined by Gel Permeation Chromatography (GPC). The measurements were conducted in a Merck-Hitachi LaChrom HPLC system, equipped with two PL gel 5 μm MIXED-C (300×7.5 mm) columns using hexafluoroisopropanol as mobile phase and poly(methyl methacrylate) (PMMA) as calibration standards. The reported molecular weights were calculated with the software package Wyatt Astra 6.1.

3.2.5.2 Thermocompression of films for gas barrier assessment

Samples of the PCHDMOX prepolymer and representative copolyesters were compressed into films using a thermal press (Carver AutoFour/3015-NE, H). Prior to processing, the polymer powders were dried under vacuum. Subsequently, they were sandwiched between two PTFE films (0.14 mm thickness) and two aluminum plates (3 mm thickness each). Once pressed, the films were cooled down by putting the PTFE sandwich in contact with two cold aluminum plates. For all samples, a pressure ramp of 0.5 ton for 1 minute, followed by 1 ton for 30 seconds and finally 5 tons for 30 seconds was applied. The compression temperature was fixed at 185 °C for all samples. Finally, the sample thickness was determined by measuring twelve different points with an electronic micrometer and reporting an average of these values. Films of between 100 and 110 μm thickness were evaluated for oxygen and water vapor barrier. A film of PLA (synthesized via ROP) and a commercial PET, both also prepared via compression molding, were evaluated at the same conditions for comparison.

The films were assessed using a Totalperm (Permtech s.r.l) instrument calibrated with a standard PET film according to the ASTM F1927-14 and ASTM E96/E96M-15 standard. The measurement is based on diffusion of oxygen gas or moisture through the surface area of a film fixed in a chamber.[15] The measurements were done in duplicates at 30 °C and 70% RH and the resulting barrier properties are reported in terms of oxygen (OP) and water permeability (WP). The OP, expressed in cm³·mm·m⁻² ·day⁻¹·atm⁻¹, represents the rate at which O_2 passes through the film, normalized for the thickness and pressure. The WP indicates the volume of water vapor that passes through the film and is normalized similarly, given in g·mm·m⁻² ·day⁻¹·atm⁻¹.

3.2.6 Hydrolysis study

The degradation via hydrolysis was studied for copolyesters derived from PCHDMOX and PLA and PGA prepolymers. For this, polymers were ground into powder and sieved with a 425 μm screen. About 10 mg of polymer was added to 1 mL D_2O with 2 mg·mL^{-1} DMSO as a standard in a 5 mm NMR tube (Wilmad). The tubes were subsequently stored at a controlled temperature of 25 °C. A Bruker AMX 400MHz NMR spectrometer was used to measure (^{1}H NMR) soluble hydrolysis products over time during a period of 215 days. GA, LA and CHDM resulting from polymer hydrolysis are soluble in D_2O and can be quantified (Equation **(3.1)**), allowing determination of the degree of hydrolysis (Equation **(3.2)**).

$$C_x = \frac{I_x}{I_{DMSO}} \times \frac{N_{DMSO}}{N_x} \times C_{DMSO} \qquad (3.1)$$

Here I represents the integral area, N the number of protons corresponding to the integrated peak(s) and C (μmol) the concentration of the compound of interest(x) and DMSO (internal standard, $N_{DMSO} = 6$, $C_{DMSO} = 25.5$ mM).

The degree of hydrolysis Y of the polymer, corresponding to the sum of yields of individual hydrolysis products after multiplying by corresponding proportions, was calculated according to Equation **(3.2)**.

$$Y = \sum_x \frac{C_x f_x}{ThC_x} \qquad (3.2) \qquad\qquad F_x = \frac{I_x/N_x}{I_{LA} + I_{GA}/2 + I_{CHDM}/4} \times 100 \qquad (3.3)$$

Here, C (μmol) represents the amount of monomer released, f the molar fraction of said monomer incorporated in the polymer and ThC (μmol) the theoretical amount of monomer upon complete hydrolysis. The amount of dissolved LA, GA or CHDM relative to the total amount of hydrolysed monomers (F_x) was calculated according to Equation **(3.3)**. Here, I represents the ^{1}H NMR peak area and N the number of protons corresponding to the integrated peak(s) (x, i.e., LA or GA or CHDM).

3.3   Results and discussion

To make blends of PCHDMOX and either PGA or PLA, the prepolymers of each type were first synthesized separately. Due to the known instability of oxalic acid at higher temperatures, diphenyl oxalate was used as the monomer for the preparation of the polyoxalate prepolymer. As it is shown in **Scheme 3.1**, this interaction results in a product with different possible endgroups.

Previous research has demonstrated that oxalic acid can decarboxylate to CO_2 and formic acid when heated above 170 °C, or even at lower temperatures (140 °C) depending on the reaction medium (catalyst, solvent, water content, etc.).[26] This decomposition to formate can continue during the reaction until no more free oxalic acid/oxalic acid ester endgroups

are present. As a result, low molecular weight products are obtained. In contrast, using diphenyl oxalate allows the synthesis of higher molecular weight products for two reasons: esterification stabilizes the oxalate, allowing higher reaction temperatures (diphenyloxalate: $T_m = 136\ °C$, $T_b = 337\ °C$), and phenols are good leaving groups, which increases the rate of transesterification and therefore increases the molecular weight. Dimethyl and diethyl oxalate were evaluated as alternatives to diphenyl oxalate and as expected the resulting molecular weight was inferior to that attained with the latter. Moreover, CHDM was selected as the diol since it is known to provide rigidity to polyester chains, which limits mobility and leads to T_g increase.[28] Other (linear) diols tested in this work (2,2-Dimethyl-1,3-propanediol, 1,5 pentanediol) lead to very low T_g polymers with gel like consistency at room temperature.
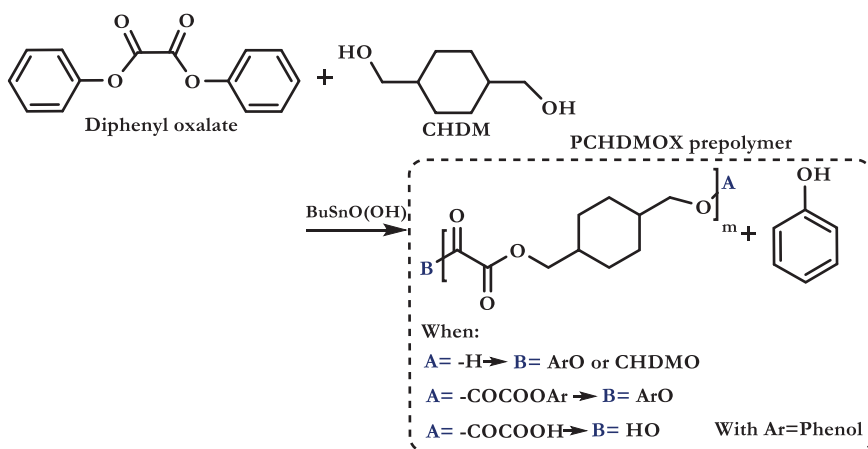
Scheme 3.1 PCHDMOX prepolymer synthesis.

Here, ester linkages are generated from the transesterification reaction between the oxalate ester and a hydroxyl group of CHDM. Phenol, which is formed as a side product, is efficiently evaporated from the reaction mixture. Since its reactivity is lower than that of water and primary alcohols, the backwards reaction is less likely to occur and the equilibrium can be driven towards chain growth. **Fig. 3.1** shows the ^{1}H NMR spectra of PCHDMOX in deuterated chloroform. The spectra clearly shows the protons of the cis- and trans- form of the CHDM repeating unit connected to the oxalate at 4.10 and 4.19 ppm, respectively. The difference in peak intensities evidences a cis- trans- ratio of 30/70 in the resulting prepolymer. Similarly, the sequence of peaks between 1.07 and 2.01 ppm, were assigned to the cis- and trans- protons of the cyclohexane ring in the repeating unit. Traces of residual CHDM (below 0.05 mol%), were observed between 3.46 and 3.56 ppm. Signals corresponding to bound or free phenol were usually not observed in the region between 6.82 and 7.38 ppm in the NMR spectra.
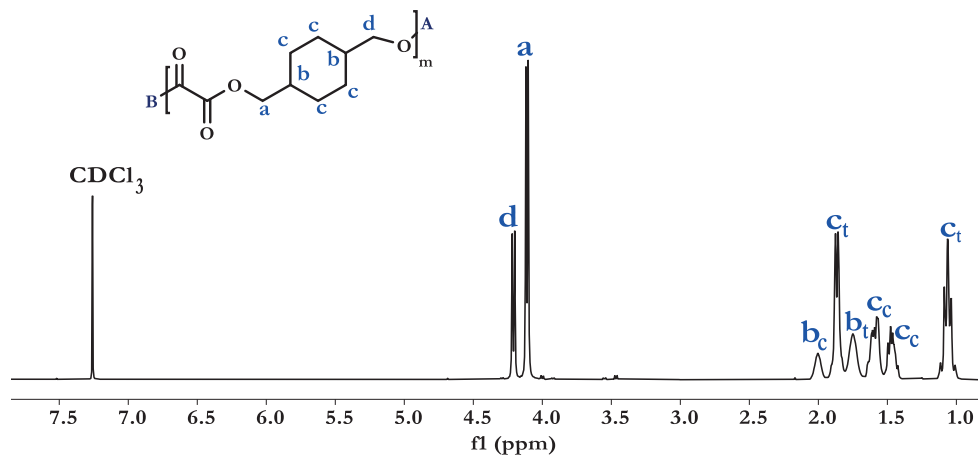
Fig. 3.1 ^{1}H NMR spectra of PCHDMOX in CDCl$_3$.

Polycondensation of lactic (LA) and glycolic acid (GA) typically involves molecular weight limitations. This is related to the water formed as byproduct which can cause chain-transfer reactions and subsequently lactide or glycolide formation. Therefore, efficient water removal is critical to shift the equilibrium to the product side. Industrially, glycolide (GL) and lactide (LAC) are used to synthesize high M_n products via ring opening polymerization processes. However, this makes the overall process more costly. Here, the polycondensation method was initially used to produce low molecular weight products that are referred to as prepolymers (**Scheme 3.2**). These prepolymers were meant to be used together with the previously synthesized PCHDMOX to prepare blends of different compositions.
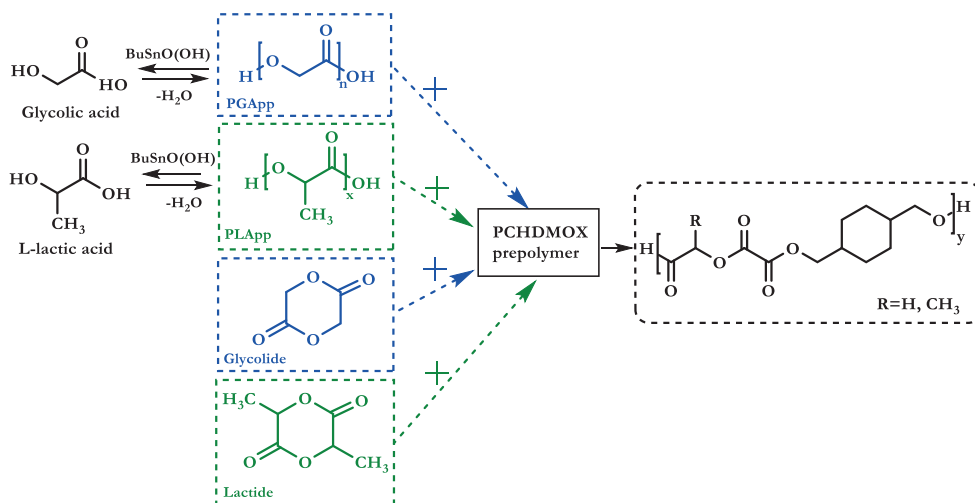


Scheme 3.2 Synthesis route for PCHDMOX and PGA/PLA.

Table 3.1. Thermal transitions, stability and molecular weight distribution of prepolymers and copolyesters with different compositions.

Prepolymer	T_m (°C)	ΔH_m (J·g⁻¹)	T_g (°C)	Microstructure	$T_{5\%}$ (°C)	$T_{50\%}$ (°C)	$T_{70\%}$ (°C)	M_n (kg·mol⁻¹)	M_w (kg·mol⁻¹)
PCHDMOX	164	28	38	semicrystalline	333	368	377	15.2	32.2
PGA$_{pp}$	214	86	39	semicrystalline	287	353	364	10.1	25.2
PLA$_{pp}$	-	-	49	amorphous	253	297	305	10.6	23.8

Copolyesters

	PCHDMOX	Product	T_g (°C)	Microstructure	$T_{5\%}$ (°C)	$T_{50\%}$ (°C)	$T_{70\%}$ (°C)	M_n (kg·mol⁻¹)	M_w (kg·mol⁻¹)
PGA$_{pp}$	50/50	PCHDMGA-*co*-OX$_{50/50}$	28	amorphous	297	360	370	11.4	25.9
	30/70	PCHDMGA-*co*-OX$_{30/70}$	27	amorphous	311	356	365	11.5	25.1
Glycolide	50/50	PCHDMGA-*co*-OX$_{50/50}$	40	amorphous	313	364	375	24.3	50.0
	30/70	PCHDMGA-*co*-OX$_{30/70}$	38	amorphous	323	366	377	19.3	38.8
PLA$_{pp}$	50/50	PCHDMLA-*co*-OX$_{50/50}$	40	amorphous	279	353	364	10.5	22.3
	30/70	PCHDMLA-*co*-OX$_{30/70}$	40	amorphous	308	357	366	12.5	26.1
Lactide	50/50	PCHDMLA-*co*-OX$_{50/50}$	46	amorphous	280	356	371	21.6	43.4
	30/70	PCHDMLA-*co*-OX$_{30/70}$	39	amorphous	288	361	374	14.0	28.4

The effect of replacing the GA and LA prepolymer directly for GL and LAC was evaluated later. The resulting copolyesters prepared with different compositions are presented in **Table 3.1** along with an overview of their thermal transitions, stability and molecular weight distribution. Independent on the type of composition, all resulting products showed an amorphous structure even though some of the prepolymers (e.g. PGA_{pp} and PCHDMOX) are semicrystalline. It is also observed that blends of PCHDMOX with PGA_{pp} or PLA_{pp}, have lower M_n and M_w than copolyesters with GL or LAC. This is also reflected by the resulting T_g: while PCHDMGA-*co*-OX copolyester from glycolide exhibits a T_g of 38 and 40 °C for the 50/50 and 30/70 wt% composition, respectively, a T_g of 27 °C was observed for both compositions obtained from PGA_{pp}. For the copolyesters PCHDMLA-*co*-OX from lactide and from lactic acid differences in T_g were less significant, except for PCHDMLA-*co*-OX$_{50/50}$ from lactide, with a T_g of 46 °C versus a T_g of 39-40 °C for the other compositions.

The combination of each prepolymer from direct polycondensation of GA and LA with the polyoxalate (PCHDMOX) (**Scheme 3.2**) was achieved via reactive blending. Oil temperatures of 230 and 200 °C were required for the full melting of the initial components in the blends PCHDMGA-*co*-OX and PCHDMLA-*co*-OX respectively. This temperature, together with the catalyst already present in the prepolymers, showed to be sufficient to promote transesterification between the terminal groups in both cases.

The occurrence of transesterification was first concluded based on the solubility of the resulting products. Chloroform is a good solvent for PLA_{pp} and PCHDMOX, but not for PGA_{pp}. In fact, PGA even at low molecular weights is known to be soluble only in highly fluorinated solvents (e.g. Hexafluoroisopropanol). Here, the blends containing 30 and 50 wt % of PGA_{pp} were readily soluble in CDCl$_3$ for NMR analysis. Subsequently, the ^{1}H NMR spectra (**Fig. 3.2**) showed additional peaks that were not observed in any of the spectra from the prepolymers.
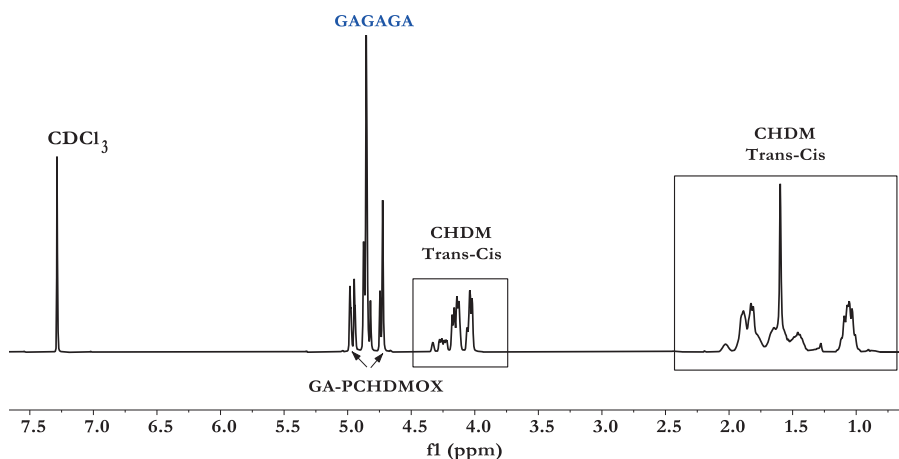
**Fig. 3.2** ^{1}H NMR spectra of GA-PCHDMOX$_{50/50}$ blend in CDCL$_3$.

Accurate peak assignment and integration was not possible, since in both ^{1}H and ^{13}C NMR spectra multiple peaks in the regions of interest overlap. Still, general observations were made from additional 2D NMR experiments. Specifically in the region between 3.95 and 4.39 ppm of **Fig. 3.2** extra peaks appear, overlapping with those corresponding to the cis- and trans- isomers of CHDM in the repeating unit of PCHDMOX. These peaks correspond to the CHDM cis- and trans- from CHDM of PCHDMOX connected to a GA moiety. The peaks in this region are also correlated with those between 1.05 and 2.02 ppm. Here, besides the protons from the CHDM ring in the PCHDMOX repeating unit, additional overlapping peaks, which correspond to the CHDM ring protons of PCHDMOX connected to a GA moiety, are observed. Furthermore, the peak attributed to the CH_2 protons in the PGA$_{pp}$ repeating unit (GAGAGA) is identified at 4.85 ppm. In the same region, the remaining peaks between 4.72 and 4.98 ppm are attributed to different CH_2 units connected to PCHDMOX on the oxalate side (e.g. CHDMGAOX; CHDMGAGA; GAGAOX with both cis- and trans CHDM).

An almost identical ^{1}H NMR spectrum was obtained when preparing the copolyester with GL instead of with PGA$_{pp}$. At the beginning of the copolyester synthesis from PCHDM and GL, the glycolide starts polymerizing into PGA at 200 °C, which is the temperature required to fully melt the PCHDMOX. Consequently, the reaction temperature is increased to 235 °C and within 30 minutes a miscible mixture is observed with higher viscosity in the melt than the products prepared with PGA$_{pp}$, a clear sign of a higher molecular weight. This is to be expected when using the cyclic dimers LAC and GL. Furthermore, it is important to consider the effect of the reaction temperature on the microstructure of the resulting reactive blends. For those with GA, a more randomized structure was probably promoted at 235 °C for the sample richer in PCHDMOX. This would result in higher density of GA-CHDMOX units for PCHDMGA-*co*-OX$_{30/70}$ than for PCHDMGA-*co*-OX$_{50/50}$. For the latter, with higher PGA$_{pp}$ content, less randomization is expected to occur since the reaction temperatures are closer to the melting point of PGA$_{pp}$ (214 °C). Consequently, compared to PCHDMGA-*co*-OX$_{30/70}$, a structure with more GA-GA blocks in between GA-CHDMOX units could be expected.

For the PCHDMLA-*co*-OX blends, accurate identification of each signal in the ^{1}H NMR spectra (see **Fig. 3.11** and **3.12** in Appendix for spectra) is not possible, since the region between 0.92 and 2.10 ppm contains multiple overlapping peaks that correspond to the protons from the CHDM ring (in PCHDMOX) and the CH proton of the PLA$_{pp}$ repeating unit (normally seen between 1.49 and 1.66 ppm). Extra peaks correlated to PLA$_{pp}$ connected to PCHDMOX are therefore not distinguishable in that region. However, the spectra showed small additional overlapping peaks between 3.98 and 4.06 ppm, close to those of the cis- and trans- protons from the CHDM in PCHDMOX. This suggested that transesterification did take place under the blending conditions, although more likely at a lower extend than for PGA$_{pp}$ due to the decreased reactivity of the PLA$_{pp}$ endgroups containing on one side a pending CH_3.

3.3.1 Thermal properties of PCHDMGA-*co*-OX or PCHDMLA-*co*-OX copolyesters

DSC measurements (dT/dt = 10 °C·min⁻¹) showed that the only materials that exhibit semi-crystallinity are PCHDMOX and PGA$_{pp}$ (**Fig. 3.3**). The low molecular weight PLA$_{pp}$ curve only shows a small endotherm between 105 and 127 °C but no crystallization peak was observed during cooling at the same rate.
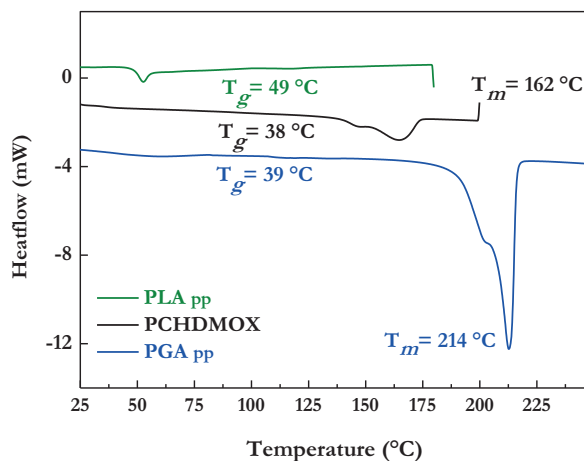
**Fig. 3.3** DSC thermograms (10 °C·min⁻¹) of prepolymers PCHDMOX, PGA and PLA.

In general, the copolyesters are amorphous at the measured conditions (**Fig. 3.4 (a) and (b)**). In the case of PGA, having amorphous products is more beneficial. This is because one of the known issues regarding PGA processing is its fast crystallization (T$_m$=220 °C, T$_c$=200 °C for commercial PGA) which complicates the manufacture of transparent products. In **Fig. 3.4 (a)** and **(b)**, a clear endothermic transition corresponding to the T$_g$ can be observed. The absence of endotherms corresponding to the melt supports the observations from NMR that discard just a physical blend between two miscible polyesters. The latter would normally have led to two distinct T$_g$ peaks and in this case one or two melting peaks depending on the type of blend. In fact, the mentioned physical blend was observed by the authors when preparing both prepolymers (e.g. PCHDMOX and PGA) without adding any catalyst with posterior blending at the same temperatures as indicated here (230 °C for the referred prepolymers). **Fig. 3.4 (a)** presents a comparison between the blends prepared from PCHDMOX and the prepolymers from lactic and glycolic acid PGA$_{pp}$/PLA$_{pp}$ with two different compositions.

The T$_g$ for the copolyesters with GL are in the same range as the T$_g$ of the separate prepolymers at around 40 °C, which is also the known value for high molecular weight PGA. When LAC was used, the 70/30 copolyester showed a T$_g$ of 39 °C, which is close to

the 38 °C measured for the PCHDMOX. For the 50/50 wt% PCHDMLA-*co*-OX from lactide the T_g increased significantly to 46 °C. This is not surprising, given that PLA has a higher T_g. The resulting T_g for blends containing the PGA_{PP} is much lower than for their initial prepolymers, independent of the composition (**Fig. 3.4 (b)**). Higher T_g values are observed for the blends from PLA_{PP} compared to PGA and its blends. The influence of molecular weight changes on the T_g is evident here. Higher M_n and M_w are achieved when starting from the cyclic dimers in comparison to the acids. Consequently, the T_g is increased by up to 12 °C, for example in the PGA_{PP} blend PCHDMGA-*co*-OX$_{50/50}$ compared to glycolide copolyester PCHDMGA-*co*-OX$_{50/50}$.
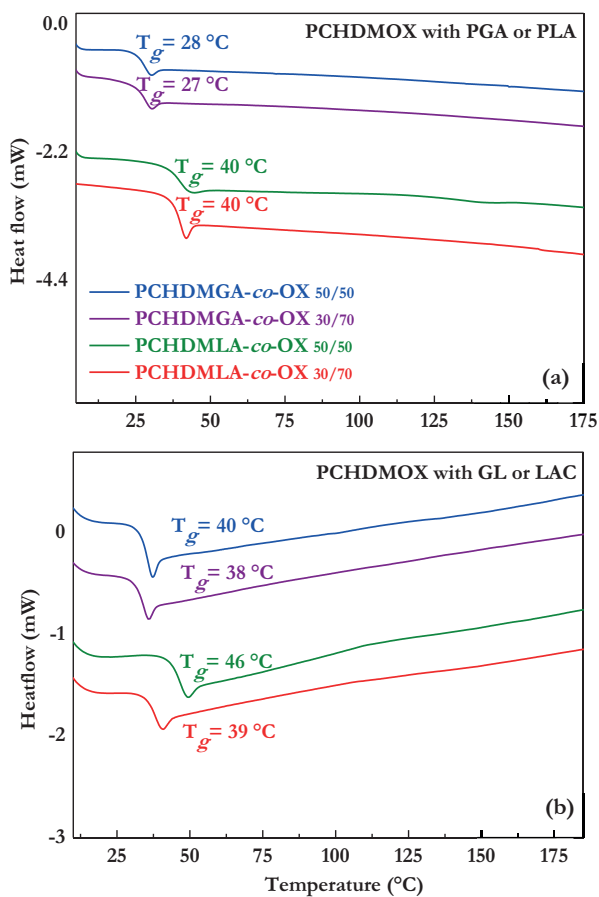
Fig. 3.4 Comparison of DSC thermograms (10 °C·min⁻¹) of blends derived from 50 or 70 wt% of PCHDMOX and **(a)** PLApp and PGApp and **(b)** copolyesters from PCHDMOX with glycolide (GL) or lactide (LAC).

The mass loss percentage with increasing temperature measured with TGA was already presented in **Table 3.1**. The TGA thermograms for both types on blends derived from GA

and LA and their respective prepolymers are shown in **Fig. 3.5**. In all cases, thermal decomposition occurs in a single stage.
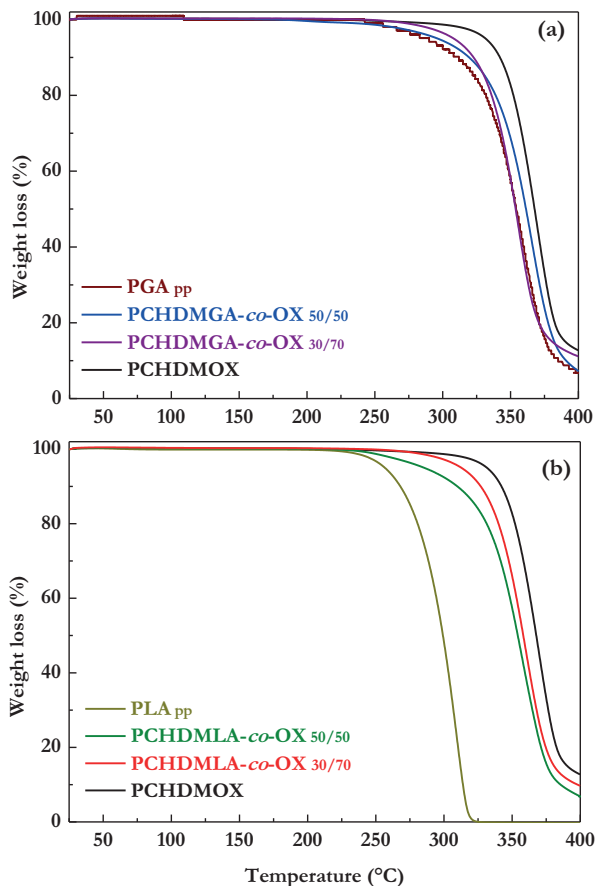

Fig. 3.5 Weight loss evolution with increasing temperature for **(a)** blends obtained from PGA_{pp} and **(b)** blends derived from PLA_{pp}.

PCHDMOX exhibits the highest thermal stability amongst the tested samples, reaching a 5% weight loss only at 333 °C. For PGA_{pp} the same weight loss occurs at 287 °C and for PLA_{pp} already at 253 °C. In general, all the reported copolyesters are thermally stable up to at least 279 °C. Importantly, copolymerizing with PCHDMOX improves the thermal stability, especially of LA derived polymers (**Fig. 3.5 (b)**). As it can be observed, blends derived from PLA_{pp} show faster mass loss than the ones from PGA_{pp} at the initial stages of degradation. With increasing temperature, the mass loss occurs at comparable rate for most blends without major differences for the variable compositions.

3.3.2 Barrier property assessment

Reported information on barrier properties of polymers derived from oxalates, is somewhat scarce. Although some patents state the usability as barrier materials of some of these polymers, they do not always report quantitative measurements. In the cases where this information is available, it is observed that barrier properties highly vary depending on the type and amount of diol and other comonomers (if used) in the polymerization.[29,30] Here, the barrier to oxygen and moisture was studied for copolyesters of PCHDMOX with GL/LAC at two different compositions: 50/50 and 70/30 wt%. **Fig. 3.6** shows the oxygen permeability (OP) measured at 30 °C and 70% RH for films with a film thickness between 100 and 110 μm.
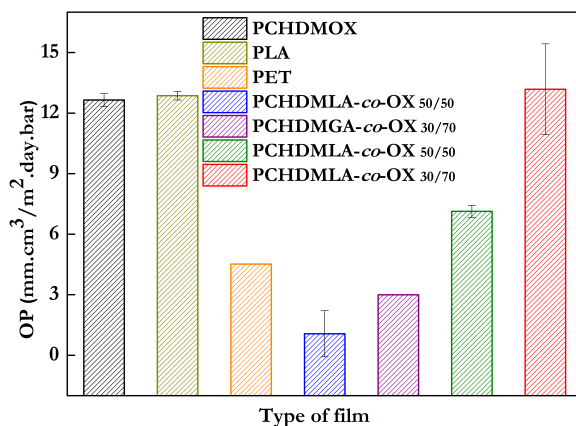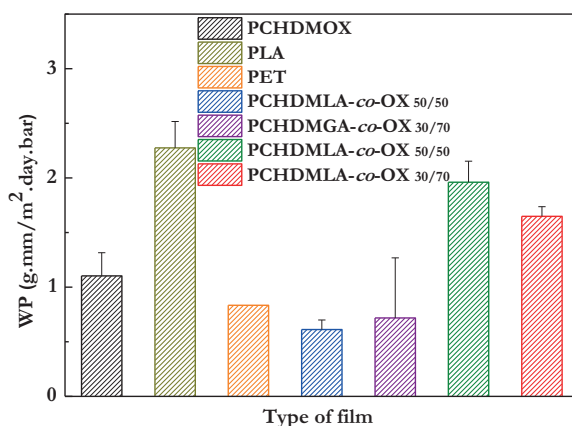

Fig. 3.6 Oxygen permeability at 30 °C and 70% RH for PCHDMGA-*co*-OX and PCHDMLA-*co*-OX copolyesters and reference polymers PLA and PET.

The low barrier of PLA is already known to be a limitation specifically for certain food packaging applications. The PCHDMOX film shows a similar oxygen permeability to that of a PLA film with the same thickness (OP = 12.6 $cm^3 \cdot mm \cdot m^{-2} \cdot day^{-1} \cdot bar^{-1}$ and OP = 12.9 $cm^3 \cdot mm \cdot m^{-2} \cdot day^{-1} \cdot bar^{-1}$, respectively). However, when PCHDMOX is reacted with GL, an improvement is observed even with an incorporation of 30 wt% (OP = 2.9 $cm^3 \cdot mm \cdot m^{-2} \cdot day^{-1} \cdot bar^{-1}$). A more significant enhancement is observed for PCHDMGA-*co*-OX$_{50/50}$, with an OP of 1.1 $cm^3 \cdot mm \cdot m^{-2} \cdot day^{-1} \cdot bar^{-1}$. This performance is superior to that of PET (RAMA, non-oriented, 10% degree of crystallinity) measured at the same conditions (OP = 4.6 $cm^3 \cdot mm \cdot m^{-2} \cdot day^{-1} \cdot bar^{-1}$). For the LAC containing samples no improvement was registered with 30 wt% in the blend. This was expected, considering that the molecular weights were close to that of the constituting prepolymers and that both exhibited similar OP. Differently, for the copolyester with 50 wt% of LAC, a lower OP of 7.1 $cm^3 \cdot mm \cdot m^{-2} \cdot day^{-1} \cdot bar^{-1}$ was found. This interaction could be connected to the higher M_n and M_w of this blend compared to PCHDMLA-*co*-OX$_{70/30}$ and PCHDMOX alone, since molecular weight

distribution also plays a role in polymer permeability. Yet, the permeability is higher than that of the copolyesters containing GA and of PET.

The barrier to water vapor is shown in **Fig. 3.7**. The prepolymer PCHDMOX exhibits a better barrier to moisture (1.10 g·mm·m^{-2} ·day^{-1}·bar^{-1}) than PLA, (2.27 g·mm·m^{-2}·day^{-1}·bar^{-1}). In consequence, copolymerizing with either 30 or 50 wt% of LAC has a detrimental effect on the moisture barrier, with a slightly more pronounced effect for the highest LAC containing copolyester. As expected, the opposite was observed for both copolyesters derived from GL, which show a decrease in WP compared to the PCHDMOX prepolymer, with WP= 0.61 (PCHDMGA-*co*-OX$_{50/50}$) and 0.72 g·mm·m^{-2} ·day^{-1}·atm^{-1} (PCHDMGA-*co*-OX$_{30/70}$). In the latter cases, the blends even perform slightly better than PET under the same conditions.


Fig. 3.7 Water permeability at 30 ºC and 70% RH for PCHDMGA-*co*-OX and PCHDMLA-*co*-OX copolyesters and reference polymers PLA and PET.

3.3.3   Hydrolytic degradation

The hydrolytic degradation of PGA, PLA and PCHDMOX was followed in time by quantifying their monomer release. **Fig. 3.8** shows the total monomer yield (glycolic acid, lactic acid or CHDM) measured over time. It is important to notice that even though the PLA used for this study had been stored for a prolonged time in a capped glass vial, soluble monomer was already detected since the first day of exposure to D$_2$O. A more detailed study on the hydrolysis of this individual sample has been previously reported.[6] For PGA, glycolic acid is released starting from the initial days at a rather constant rate, while PCHDMOX exhibited a prolonged lag phase with no CHDM identified until day 59. This type of behavior has been observed before for other oxalate derived polymers.[31]

Between 60 and 75 days, a sudden CHDM release was detected, which subsequently slowed down to a hydrolysis rate similar to that for PGA. Surprisingly, PGA and PLA reached a similar degree of hydrolysis (5%) by the end of the testing period.

This was an unexpected outcome considering the findings reported in a previous research of our group, where a poly(lactic-co-glycolic acid) copolymer with 94 mol% of GA exhibited a degree of hydrolysis of about 40% at the same time and under equivalent testing conditions.[6] The high degree of crystallinity of PGA together with the fact that GA-GA bonds are presumably less prone to hydrolytic cleavage than GA-LA bonds, are thought to be the main reasons behind this behavior.
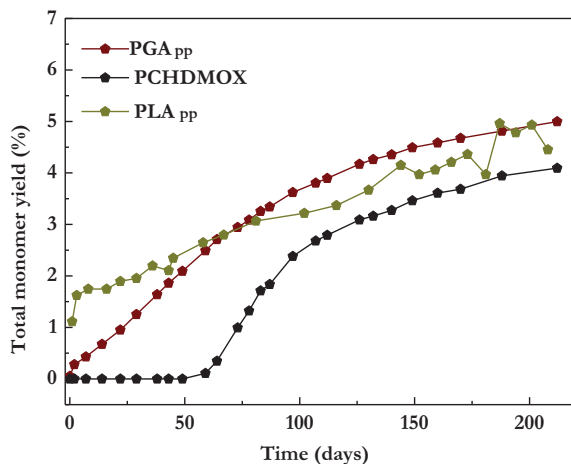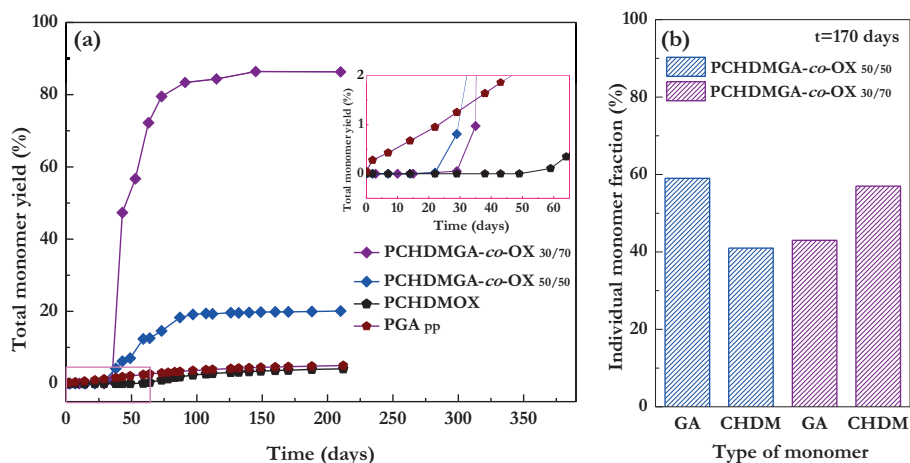

Fig. 3.8 Total monomer yield released over time for PGA, PLA and PCHDMOX until day 215.

For the two semicrystalline samples (PGA and PCHDMOX) it seems that many factors, such as the molecular weight difference (higher M_n and M_w for PCHDMOX), hydrophilicity (higher for PGA than for PCHDMOX) and the degree of crystallinity (higher for PGA) played a role in the hydrolysis process. As a consequence, PCHDMOX and PGA show a similar hydrolysis rate, while in fact oxalate-based polymers have been reported to exhibit faster hydrolytic degradation kinetics than PLA, PGA and PLGA. More specifically, polyoxalates display fast hydrolysis (faster than that of PLGA copolymers), which makes them suitable for drug delivery systems[32,33] and fast absorption (quicker than that of PGA), which is useful for degradable sutures.[34] Importantly, polyoxalates with similar structure have been reported to hydrolyze rapidly in water.[35] The possible instability from using diphenyl oxalate in this present work was expected to be reduced to some extent by the use of CHDM, which has poor electron-withdrawing properties.

Faster hydrolysis was observed for PCHDMGA-*co*-OX obtained from PGA and PCHDMOX than for their prepolymers (**Fig. 3.9 (a)**). This suggested that the ester bond linking GA-CHDMOX units is initially more prone to undergoing hydrolytic cleavage than the bond GA-GA or CHDMOX-CHDMOX. Also, crystalline regions, which are predominant in the prepolymers, are expected to be more hydrolysis resistant than amorphous regions. Notably, both PCHDMGA-*co*-OX$_{50/50}$ and PCHDMGA-*co*-OX$_{30/70}$ blends exhibited a lag phase until about 20-30 days, which was reduced in comparison to

the 49 days shown for PCHDMOX. After this lag phase, a remarkably fast monomer release was recorded for the blend containing 30 wt% of the PGA_{PP}, which reached a plateau towards the last part of the study. By day 215, up to 86% of CHDM and glycolic acid combined had hydrolyzed. Although at first glance PCHDMGA-*co*-OX$_{50/50}$ was expected to be the fastest degrading sample, assuming a statistical distribution, only about 20% of the monomers was released by the end of the test. Also, the release of CHDM and GA became slow and almost constant since day 97.
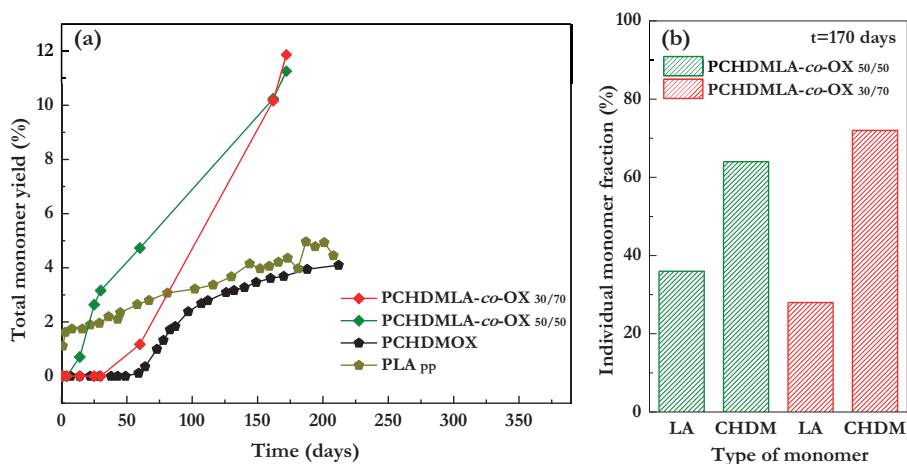

Fig 3.9 (a) Total monomer yield over time for blends derived from PGA and PCHDMOX with a close-up of the lag phase in the right upper corner and **(b)** fraction of each degradation product released after 170 days.

The blends derived from PGA_{PP} and PCHDMOX exhibited an amorphous microstructure with similar molecular weight distributions and T_g (M_n=11.4 and 11.5 kg·mol^{-1}, M_w=25.9 and 25.1 kg·mol^{-1}, T_g=38 and 39 °C for PCHDMGA-*co*-OX$_{50/50}$ and PCHDMGA-*co*-OX$_{30/70}$, respectively). Therefore, the significant difference in hydrolysis rate between both samples could not be due to any of those factors. It was already mentioned that a more randomized structure and therefore higher density of GA-CHDMOX units is expected for PCHDMGA-*co*-OX$_{30/70}$ over PCHDMGA-*ox*-OX$_{50/50}$ as result of the reaction temperature (235 °C). This supports the faster degradation of PCHDMGA-*co*-OX$_{30/70}$ based on GA-CHDMOX units being more prone to hydrolysis than GA-GA or CHDMOX-CHDMOX units. In connection to this a slower hydrolysis for the blend PCHDMGA-*co*-OX$_{50/50}$ could also be explained by a higher density of GA-GA bonds, which when cleaved may lead to oligomer chains with high mobility that can crystallize and as result of this microstructural change, delay the water penetration in the polymer backbone.

Fig. 3.9 (b) presents the individual fraction of released monomers relative to the total amount of monomers found after 170 days of hydrolysis. At this time, a total monomer yield of about 20% was registered for PCHDMGA-c*o*-OX$_{50/50}$, of which 41% corresponded to CHDM and 59% to GA.

Based on the monomer released over time for the prepolymers (**Fig. 3.9 (a)**), it is feasible that the remaining part of PCHDMGA-c*o*-OX$_{50/50}$ to be hydrolyzed after 170 days is composed of sequences of only PGA and PCHDMOX. For PCHDMGA-*co*-OX$_{30/70}$, with a total monomer yield of about 84%, higher CHDM release (57%) was found compared to GA (43%). The remaining part is expected to be predominantly PCHDMOX.

The copolymers derived from PLA$_{pp}$ (**Fig. 3.10 (a)**) displayed a somewhat faster hydrolysis than their prepolymers, but slightly slower in comparison with those derived from PGA$_{pp}$. units. This is different for the PLA$_{pp}$ blends in connection to the presence of the methyl group attached to the PLA backbone conferring a less hydrophilic character. Also for these blends lag phases were observed: 14 days for PCHDMLA-*co*-OX$_{50/50}$ and 25 days for PCHDMLA-*co*-OX$_{30/70}$. The latter hydrolyzed at a faster rate once the lag phase was overcome. By day 162 both blends reached similar yields of degradation products. After 170 days 12% of the monomers had been released from PCHDMLA-*co*-OX$_{30/70}$ compared to 11% from PCHDMLA-*co*-OX$_{50/50}$. For PCHDMLA-*co*-OX$_{30/70}$ and PCHDMLA-*co*-OX$_{50/50}$ the differences in released amounts of each type of monomer are much more apparent than in the PGA$_{pp}$ with PCHDMOX blends.

Fig. 3.10 (a) Total monomer yield over time for blends derived from PLA and PCHDMOX compared to their respective prepolymers; **(b)** fraction of each degradation product released after 170 days.

Overall, there is a consistently higher release of CHDM throughout time compared to lactic acid. After 170 days a total monomer yield of about 11% was measured for both PCHDMLA-*co*-OX$_{50/50}$ and PCHDMLA-*co*-OX$_{30/70}$. For PCHDMLA-*co*-OX$_{50/50}$ 36% of monomer released was lactic acid and 64% CHDM. For PCHDMLA-*co*-OX$_{30/70}$ the released monomer ratio was close to the polymer composition: 72% CHDM and 28% LA. Overall, this suggests easier ester bond cleavage for LA-CHDMOX units followed by CHDMOX-CHDMOX units and finally LA-LA units.

3.4　Conclusion

Two strategies for preparing copolyesters derived from glycolic acid or lactic acid with poly(1,4-cyclohexanedimethanol oxalate) (PCHDMOX) were successfully applied, using different feed ratios (50/50 and 30/70 wt%). For both approaches the prepolymer PCHDMOX was synthesized from diphenyl oxalate and CHDM. This was combined with either PGA or PLA made by polycondensation ($M_n \approx 10$ kg·mol^{-1}), or by copolymerization with glycolide or with lactide. The latter resulted in products with higher molecular weight and higher T_g in comparison to those prepared from the polycondensated hydroxy-acids. Overall, copolyesters from PCHDMOX and glycolic acid/ glycolide showed lower T_g, higher thermal stability, better barrier to oxygen and moisture and faster hydrolysis rate than those prepared with lactic acid/lactide. Improvement in the barrier to oxygen and water of PCHDMOX was observed with higher GL content. Importantly, for both compositions the barrier performance was superior to that of non-oriented PET at the same conditions. In contrast, for the combinations with lactide a detrimental effect was observed, specifically in the barrier to water. Nevertheless, the water permeability for these blends was still lower than that of pure PLA. All the samples hydrolyzed at a faster rate than the respective homopolymers they were made from. The fastest rate was recorded for those derived from glycolic acid and PCHDMOX with a degree of hydrolysis of up to 86% after 215 days for the sample with 30 wt% of glycolic acid. Essentially, these materials could cover a similar application range to that of PGA/PLGA/PLA/PCHDM, where low Tg (below 50 °C) would be suitable and the possibility of tunning specific material properties and accelerating their decomposition is desired. The results obtained in this research initially suggest that copolymers from α-hydroxyacids and oxalates have potential for application in coatings for controlled release, single-use packaging not suitable for recycle or even the medical field.

3.5　Appendix

3.5.1　PCHDMOX and PGApp / PLApp blends

In **Fig. 3.11**, the region between 0.92 and 2.10 ppm contains overlapping peaks that correspond to the CH$_3$ protons from PLA$_{pp}$ and the protons from the CHDM ring (in PCHDMOX). Signals corresponding to LA moieties connected to the polyoxalate are also likely to be in that region. Between 3.98 and 4.06 ppm, besides the peaks from the cis- and trans- protons from the CHDM in PCHDMOX, the small overlapping peaks at between 3.96 and 4.11 ppm, are an indication of transesterification between PCHDMOX and PLA. Also, the peak corresponding to the CH proton from the repeating unit of PLA between 5.15 and 5.29 ppm, shows some broadening and the presence of small new peaks on the higher frequency side, which can be attributed to the interaction between LA moieties and PCHDMOX. Something similar is observed in the ^{1}H NMR spectra of PCHDMLA-co-

OX$_{30/70}$ in **Fig. 3.12** but in this case contributions from PCHDMOX are more apparent in the mixture.
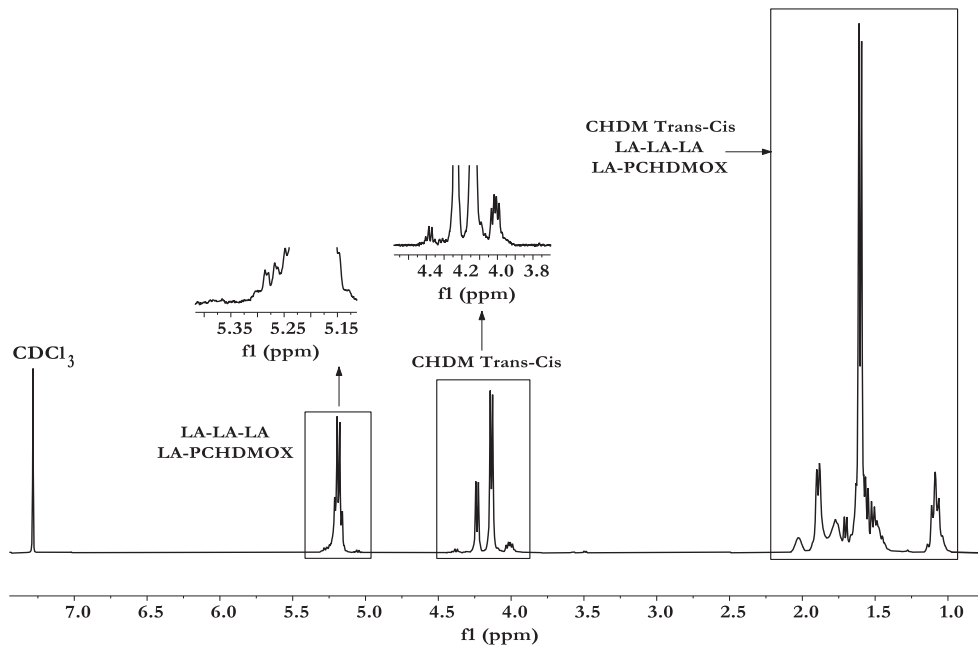

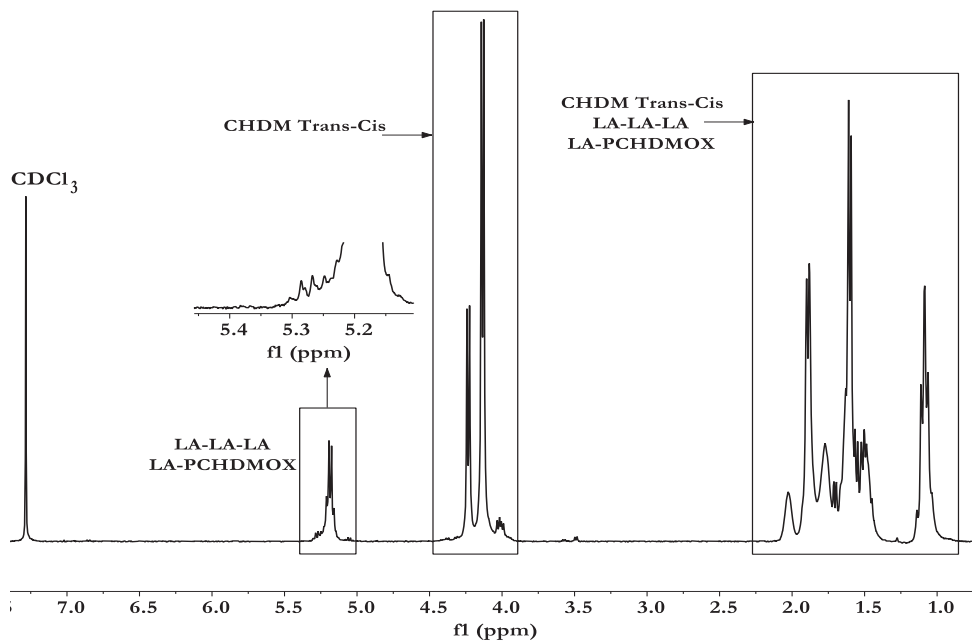**Fig. 3.11** ^{1}H NMR spectra of PCHDMLA-co-OX$_{50/50}$ copolyester in CDCl$_3$.

Fig. 3.12 ^{1}H NMR spectra of PCHDMLA-co-OX$_{30/70}$ copolyester in CDCl$_3$.
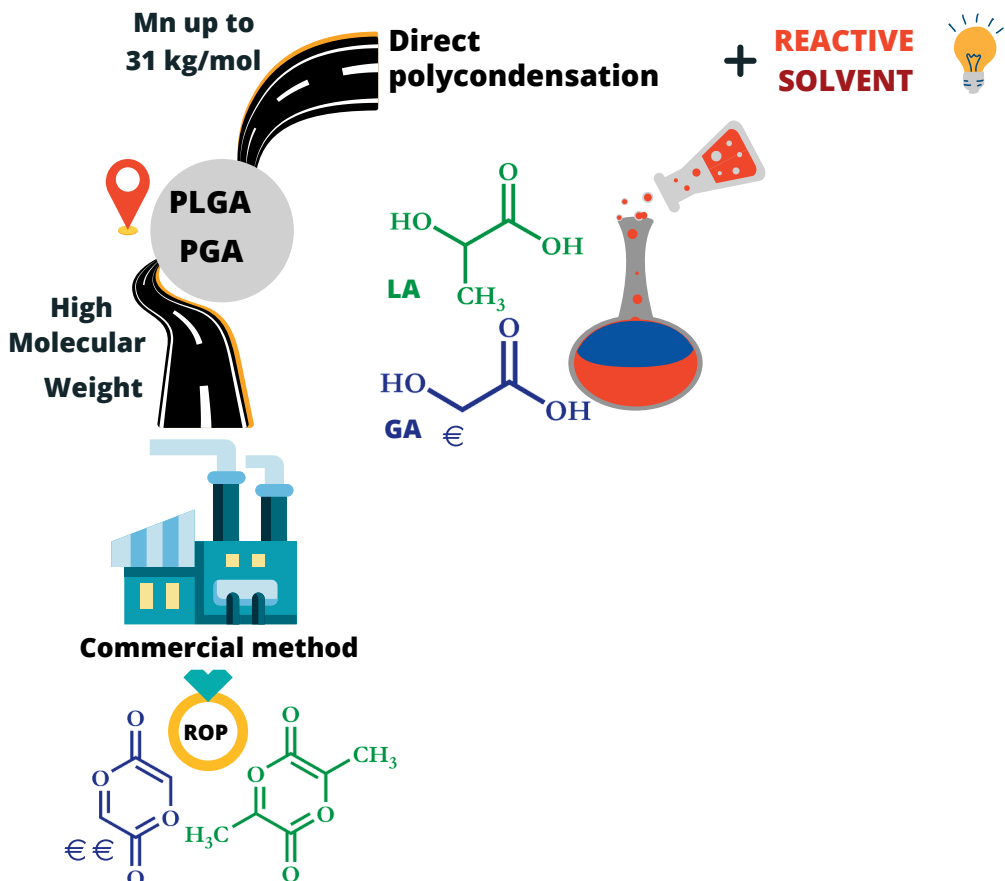
3.6   References

(1)   Boucher, J.; Billard, G.; Simeone, E.; Sousa, J. *The Marine Plastic Footprint;* IUCN, International Union for Conservation of Nature, 2020. https://doi.org/10.2305/iucn.ch.2020.01.en.

(2)   Geyer, R.; Jambeck, J. R.; Law, K. L. Production, use, and fate of all plastics ever made. *Sci. Adv.* **2017**, *3 (7)*. e1700782 https://doi.org/10.1126/sciadv.1700782.

(3)   L.A., H.; S, F. Plastic & Climate: The Hidden Costs of a Plastic Planet (May 2019) - Center for International Environmental Law https://www.ciel.org/reports/plastic-health-the-hidden-costs-of-a-plastic-planet-may-2019/ (accessed December 21, 2021).

(4)   Vilela, C.; Sousa, A. F.; Fonseca, A. C.; Serra, A. C.; Coelho, J. F. J.; Freire, C. S. R.; Silvestre, A. J. D. The quest for sustainable polyesters-insights into the future. *Polym. Chem.* **2014**, *5*, 3119-3141. https://doi.org/10.1039/c3py01213a.

(5)   Philips, M. F.; Gruter, G. J. M.; Koper, M. T. M.; Schouten, K. J. P. Optimizing the electrochemical reduction of CO_2 to formate: a state-of-the-art analysis. *ACS Sustain. Chem. Eng.* **2020**, *8 (41)*, 15430-15444. https://doi.org/10.1021/ACSSUSCHEMENG.0C05215.

(6)   Wang, Y.; Valderrama, M. A. M.; Putten, R.-J. van; Davey, C. J. E.; Tietema, A.; Parsons, J. R.; Wang, B.; Gruter, G.-J. M. Biodegradation and non-enzymatic hydrolysis of poly(lactic-co-glycolic acid) (PLGA12/88 and PLGA6/94). *Polym.* **2022**, *14*, 15. https://doi.org/10.3390/ POLYM14010015.

(7)   Murcia Valderrama, M. A.; van Putten, R.-J.; Gruter, G.-J. M. The potential of oxalic – and glycolic acid based polyesters (review). towards CO_2 as a feedstock (Carbon Capture and Utilization – CCU). *Eur. Polym. J.* **2019**, *119*, 445-468. https://doi.org/10.1016/j.eurpolymj.2019.07.036.

(8)   Garcia, J. J.; Miller, S. A. Polyoxalates from biorenewable diols via oxalate metathesis polymerization. *Polym. Chem.* **2014**, *5 (3)*, 955-961. https://doi.org/10.1039/c3py01185b.

(9)   Gorth, D.; Webster, T. J. Matrices for tissue engineering and regenerative medicine. In *Biomaterials for artificial organs*; Elsevier Inc., 2010, pp. 270-286. https://doi.org/10.1533/9780857090843.2.270.

(10)   Hatti-Kaul, R.; Nilsson, L. J.; Zhang, B.; Rehnberg, N.; Lundmark, S. *Designing biobased recyclable polymers for plastics. trends in biotechnology*. Elsevier Ltd, 2020, pp. 50–67. https://doi.org/10.1016/ j.tibtech.2019.04.011.

(11)   Shiiki, Z.; Kawakami, Y. Poly(ethylene oxalate), product formed of molded therefrom and production process of poly(ethylene oxalate). EP0749997A3, August 27, 1997.

(12)   Kale, G.; Auras, R.; Singh, S. P. Comparison of the Degradability of Poly(Lactide) Packages in Composting and Ambient Exposure Conditions. *Packag. Technol. Sci.* **2007**, *20* (1), 49–70. https://doi.org/10.1002/pts.742.

(13)   Zhao, Y. H.; Xu, G. H.; Yuan, X. B.; Sheng, J. Novel degradable copolyesters containing poly(ethylene oxalate) units derived from diethylene oxalate. *Polym. Degrad. Stab.* **2006**, *91 (1)*, 101-107. https://doi.org/10.1016/j.polymdegradstab.2005.04.023.

(14)   Yamane, K.; Sato, H.; Ichikawa, Y.; Sunagawa, K.; Shigaki, Y. Development of an industrial production technology for high-molecular-weight polyglycolic acid. *Polymer Journal.* **2014**, *46,* 769–775. https://doi.org/10.1038/pj.2014.69.

(15)   Murcia Valderrama, M. A.; van Putten, R.-J.; Gruter, G.-J. M. PLGA Barrier materials from CO_2. The influence of lactide comonomer on glycolic acid polyesters . *ACS Appl. Polym. Mater.* **2020**, *7*, 2706-2718. https://doi.org/10.1021/acsapm.0c00315.

(16)   Wang, H. Y.; Zheng, H. F. Research on raman spectra of oxalic acid during decarboxylation under high temperature and high pressure. *Spectr. Anal.* **2012**, *32 (3)*, 669–672. https://doi.org/10.3964/ j.issn.1000-0593(2012)03-0669-04.

(17)   Finelli, L.; Lotti, N.; Munari, A. Thermal properties of poly(butylene oxalate) copolymerized with azelaic acid. *Eur. Polym. J.* **2002,** *38*, 1987-1993. https://doi.org/10.1016/S0014-3057(02)00089-7.

(18)   Shalaby, W. S.; Jamiolkowski, D. D. Synthetic absorbable surgical devices of poly(alkylene oxalates). US4205399A. June 3, 1978.

(19)   Cline, W. K. Polyethylene oxalate process. US3197445A. July 27, 1965.

(20)   Wang, B.; Gruter, G.-J. M. Polyester copolymer . WO2018211132A1, November 22, 2018.

(21)   Wang, B.; Gruter, G.-J. M. Polyester copolymer. WO2018211133A1, November 22, 2018.

(22) Wang, B.; Gruter, G.-J. M.; Putten, R.-J.; Weinland, D. H. Process for the production of one or more polyester copolymers, method for the preparation of one or more oligomers, oligomer composition and polyester copolymer. WO2020106144A1, May 28, 2020.

(23) Takahashi, K.; Taniguchi, I.; Miyamoto, M.; Kimura, Y. Melt/solid polycondensation of glycolic acid to obtain high-molecular- weight poly(glycolic acid). *Polymer*. **2000**, *41 (24),* 8725-8728. https://doi.org/10.1016/S0032-3861(00)00282-2.

(24) Ayyoob, M.; Lee, D. H.; Kim, J. H.; Nam, S. W.; Kim, Y. J. Synthesis of poly(glycolic acids) via solution polycondensation and investigation of their thermal degradation behaviors. *Fibers Polym.* **2017**, *18 (3)*, 407-415. https://doi.org/10.1007/s12221-017-6889-1.

(25) Sanko, V.; Sahin, I.; Aydemir Sezer, U.; Sezer, S. A versatile method for the synthesis of poly(glycolic acid): high solubility and tunable molecular weights. *Polym. J.* **2019**, *51 (7),* 637-647. https://doi.org/10.1038/s41428-019-0182-7.

(26) Alksnis, A.; Deme, D.; Surna, J. Synthesis of oligoesters and polyesters from oxalic acid and ethylene glycol. *J. Polym. Sci. Polym. Chem. Ed.* **1977**, *15 (8),* 1855-1862. https://doi.org/10.1002/pol.1977.170150807.

(27) Sikorska, W.; Musiol, M.; Nowak, B.; Pajak, J.; Labuzek, S.; Kowalczuk, M.; Adamus, G. Degradability of polylactide and its blend with poly[(r,s)-3-hydroxybutyrate] in industrial composting and compost extract. *Int. Biodeterior. Biodegrad.* **2015**, *101*, 32-41. https://doi.org/ 10.1016/j.ibiod.2015.03.021.

(28) Chen, T.; Jiang, G.; Li, G.; Wu, Z.; Zhang, J. Poly(ethylene glycol-co-1,4-cyclohexanedimethanol terephthalate) random copolymers: effect of copolymer composition and microstructure on the thermal properties and crystallization behavior. *RSC Adv.* **2015**, *5 (74)*, 60570-60580. https://doi.org/10.1039/c5ra09252c.

(29) Kurachi, K.; Shimokawa, M. Poly(isosorbide oxalate), WO2005103111A1. November 3, 2005.

(30) Okushita, H.; Kurachi, K.; Tanaka, S.; Adachi, F.; Youtaro, F.; Yoshida, Y. Polyoxalate resin and shaped articles and resin compositions comprising same. US20050027081A1. March 2, 2005.

(31) Wang, Y.; Davey, C. J. E.; van der Maas, K.; van Putten, R. J.; Tietema, A.; Parsons, J. R.; Gruter, G. J. M. Biodegradability of novel high T_g poly(isosorbide-co-1,6-hexanediol) oxalate polyester in soil and marine environments. *Sci. Total Environ.* **2022**, *815*, 152781. https://doi.org/10.1016/J.SCITOTENV.2021.152781.

(32) JC, S.; G, S.; SC, Y.; M, B.; T, O.; S, D.; N, M.; ME, D. Sustained release of a p38 inhibitor from non-inflammatory microspheres inhibits cardiac dysfunction. *Nat. Mater.* **2008**, *7 (11),* 863-869. https://doi.org/10.1038/NMAT2299.

(33) Hong, D.; Song, B.; Kim, H.; Kwon, J.; Khang, G.; Lee, D. Biodegradable polyoxalate and copolyoxalate particles for drug-delivery applications. *Ther Deliv.* **2011**, *2(11)*, 1407-1417. https://doi.org/10.4155/tde.11.113.

(34) Holland, S. J.; Tighe, B. J.; Gould, P. L. Polymers for biodegradable medical devices. 1. The potential of polyesters as controlled macromolecular release systems. *J. Control. Release.* **1986**, *4 (3)*, 155-180. https://doi.org/10.1016/0168-3659(86)90001-5.

(35) S, K.; K, S.; O, K.; S, K.; H, S.; M, L.; G, K.; D, L. Polyoxalate nanoparticles as a biodegradable and biocompatible drug delivery vehicle. *Biomacromolecules.* **2010**, *11 (3)*, 555-560. https://doi.org/ 10.1021/BM901409K.

CHAPTER 4

PLGA and PGA synthesis via polycondensation using aromatic solvents

Mn up to 31 kg/mol

Direct polycondensation

+ REACTIVE SOLVENT

PLGA PGA

High Molecular Weight

LA

GA

Commercial method

ROP

Abstract

Polyglycolic acid (PGA) and poly(lactide-co-glycolide) (PLGA) with high glycolic acid content are very interesting biobased polyesters, namely due to their degradability, biocompatibility and remarkable barrier properties. Commercially, they are produced via ring opening polymerization (ROP) of glycolide and lactide, the cyclic dimers of glycolic acid and lactic acid, respectively. However, this is still a costly process and the increasing demand for more sustainable polymers urges the need for cheaper production routes. In this research, a new polycondensation route for the production of PGA and PLGA copolymers directly from glycolic and _L_-lactic acid in the presence of p-cresol or guaiacol as reactive solvent was studied. This was done at a scale between 20 and 35 g. For copolymers with an initial amount of 80 and 90 mol% of glycolic acid, M_n values as high as 27.2 and 31.5 kg·mol^{-1} respectively were achieved. Films prepared with these copolymers exhibited a superior performance regarding water and oxygen permeability in comparison to PLA and PET. Lastly, SSP was evaluated as a feasible option to further improve the molecular weight of these copolymers. The synthesis route assessed in this research involves less time than other reported approaches to increase the molecular weight of similar type of polymers and it allows for solvent recycling for reuse.

4.1   Introduction

Polyglycolic acid (PGA), polylactic acid (PLA) and their copolymers poly(lactide-co-glycolide) (PLGA), are linear aliphatic polyesters of great interest for the ongoing transition towards more sustainable plastic alternatives.[1] PGA has been mostly used in biomedical applications due to its biocompatibility and degradability. Although it exhibits outstanding barrier properties[2], its high crystallinity, thermal instability and limited solubility restrict its use for a wider range of applications (e.g. packaging). When copolymerized with lactic acid (LA), the material properties can be tuned and the aforementioned issues can be circumvented to some extent.[3] Commercially, these polyesters and copolyesters are produced via ring opening polymerization (ROP) of glycolide and/or lactide, the cyclic dimers of glycolic acid (GA) and lactic acid, respectively. Although high molecular weights can be achieved with this synthetic strategy, the intermediary steps involved in the overall process lead to a costly production, especially considering the still high cost of glycolide compared to lactide.

A direct polycondensation of GA or GA and LA could be a more cost efficient route for homo- and copolymerization. This polymerization process, however, involves two equilibrium reactions that limit the resulting molecular weight of the polymer.[4] One reaction concerns the dehydration equilibrium for esterification and the other the ring-chain equilibrium involving depolymerization to glycolide[5] or lactide. As the reaction proceeds and oligomers are formed, high temperatures and high vacuum are required for water

removal. Under these conditions, depolymerization reactions are favored and glycolide and lactide are formed. Since this limits the molecular weight of the polymer, which results in poor mechanical properties, this method is not used to produce PGA or PLGA at commercial scale. Nevertheless, the increasing demand for more sustainable polymers urges the need for cheaper production routes. Therefore, the polycondensation approach is still explored as an alternative for producing these polyesters at industrial scale.

PGA prepared from glycolic acid with a M_n of up to 45 kg·mol^{-1} has been reportedly obtained by Takahashi et al., through a 2 step process consisting of initial melt-polycondensation followed by solid-state polycondensation.[5] Alternatively, Sanko et al.[6] prepared PGA with a M_n and M_w as high as 32.0 and 40.3 kg·mol^{-1} via azeotropic distillation of water with anisole and a Dean Stark apparatus. Both processes, however, required between 20 and 30 hours to be completed and the latter process uses a large excess of 15 mL solvent per gram of GA for the reaction. High molecular weight PLGA copolymers, produced directly from the α-hydroxy acids, have been hardly reported. In fact, the majority of the research for PLGA or PGA polycondensation copolymers comprises low molecular weight products with M_n bellow 14 kg·mol^{-1}.[7,8] These are suitable for biomedical applications (e.g. drug delivery systems) but not for a wider range of purposes where mechanical properties are also relevant. Also, the majority of research has focused on the copolymers rich in lactic acid rather than those with higher glycolic acid content.

In a previous publication from our group the strong performance, especially as gas barrier to water vapor and oxygen of PLGA copolymers with high glycolide content, prepared via ROP, was reported.[3] This, together with their degradability and easier processability than PGA, implies potential for PLGA copolymers in, for example, the packaging industry. However, in order to extend their applicability, less expensive synthesis routes than those currently used commercially to produce high molecular weight products are required. Consequently, this work focuses on a synthesis route to prepare PLGA copolymers with high GA content through direct polycondensation of GA and LA. In other polyester synthesis, especially when dealing with secondary diol incorporation, it was proven that phenol and substituted phenols facilitate the polycondensation, leading to molecular weights that were previously only obtainable with reactive diester monomers (phenyl diesters) or diacid chlorides.[9] This automatically led to the idea of applying this strategy to PGA and PLGA synthesis. The polycondensation of GA and LA was thus performed in the presence of guaiacol (2-methoxyphenol) or p-cresol.

4.2 Experimental section

4.2.1 Materials

All chemicals were used without further purification. Glycolic acid (99%) and lactic acid solution (90% in water) were purchased from Acros Organics. Butyl stannoic acid (BuSnO(OH)) (97%), 1,4-dimethoxy benzene and p-cresol (99%) were acquired from Sigma Aldrich and Acros Organics, respectively. Tin (II) 2-ethylhexanoate (Sn(Oct)$_2$), Tin(II) chloride (SnCl$_2$), p-Toluenesulfonic acid (pTSA), Titanium butoxide (Ti(OBu)$_4$), Ytterbium(III) trifluoromethanesulfonate (Yb(OTf)$_3$) were purchased from Sigma Aldrich. Guaiacol (99%), deuterated dimethyl sulfoxide (DMSO-d$_6$) and Hexafluoroisopropanol (HFIP-d$_2$) were also obtained from Sigma Aldrich.

4.2.2 Synthesis of PLGA$_{10/90}$ and PLGA$_{20/80}$ from polycondensation of GA and LA

The general synthesis strategy applied in this work is presented in **Scheme 4.1**. In a typical experiment 20 g of monomer (90 or 80 mol% glycolic acid and 10 or 20 mol% lactic acid) was used in the presence of catalyst and a substituted phenol or inert solvent. The types and amounts of catalyst and solvent were varied according to the experiment (**Table 4.1**). Experiments in the absence of catalyst or solvent were also performed. All loadings for catalyst and solvent are mol% relative to the monomer loading.
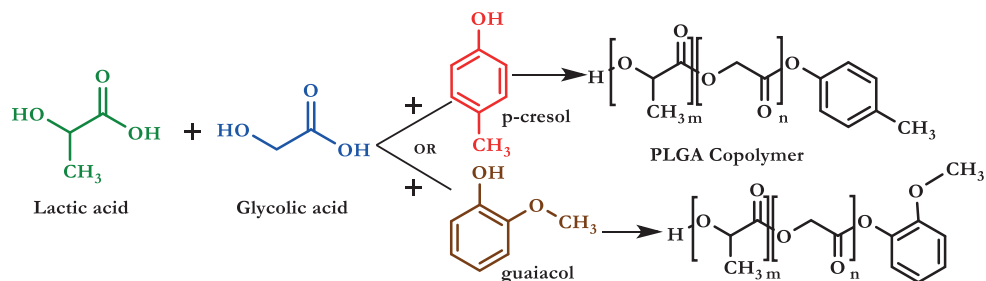
Scheme 4.1 General synthesis route of PLGA copolymers in the presence of p-cresol or guaiacol.

The monomers, solvent and catalyst were weighed in a three-necked round bottom flask with a mechanical stirrer (@ 105 rpm) and a nitrogen inlet and outlet. The esterification stage was carried out at 190 °C for about 9 hours under nitrogen atmosphere (30 mL·min^{-1}) at ambient pressure. Subsequently in the polycondensation stage the temperature was increased to 200 °C followed directly by a gradual reduction in pressure until reaching 1 mbar over 2 hours, with removal of the solvent. Also, experiments were performed with temperatures reaching as high as 210 °C in the polycondensation stage. Additional experiments were performed where during the esterification step the temperature was increased to 210 °C, followed by a decrease to 200 °C before reducing pressure. Different reaction times were also investigated (7.5-14 hours), however the polycondensation time under reduced pressure was always 2 hours. Additionally, the effect of the type of lactic acid (*L* or racemic) on the resulting product was investigated for both types of copolymers.

4.2.3 Solid state polymerization (SSP) of PLGA$_{10/90}$

SSP was carried out for PLGA$_{10/90}$ obtained from the polycondensation route described earlier (using p-cresol as reactive solvent). For this, a representative sample was ground and sieved to isolate the particles in the range between 60 and 120 µm. The separated fraction was then dried and crystallized at 115 °C for 4 hours at 2 mbar. Afterwards, SSP was performed at 2 mbar in a rotary evaporator at three different temperatures: 145, 155 and 165 °C. For each batch, 3 g of product was used. The reactions were carried out for up to 72 hours and the molecular weight distribution evolution was followed with GPC at different time intervals. The change in thermal transitions as result of the SSP reaction time was determined with DSC (dT/dt = 10 °C·min^{-1}).

4.2.4 Polyglycolic acid synthesis from polycondensation of GA

A similar method to the one described for PLGA copolymers was tested to synthesize PGA (**Scheme 4.2**). In this case the esterification temperature for the first stage was initially set at 190 °C and increased up to 210 °C within 8 hours. Until this time, the reaction mixture for most samples was soluble in DMSO-d$_6$, which allowed following the monomer conversion with ^{1}H NMR. Subsequently, the pressure was reduced from 400 to 1 mbar in about 1.5 hours and left at that pressure for about 0.5 hours. During this stage, the reaction temperature was increased to 220 °C and as the mixture became hazier and there were signs of solidification, the temperature was increased to 230 °C. A reference reaction without using solvent as well as one with a non-reactive solvent were also performed.
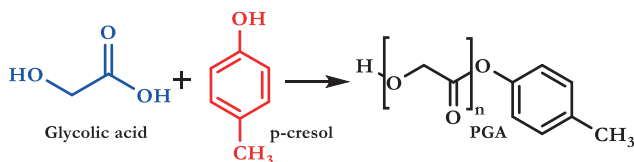
Scheme 4.2 General synthesis route of PGA homopolymers in the presence of p-cresol.

4.2.5 Measurements/Analytical techniques

4.2.5.1 ^{1}H NMR, DSC and TGA

The reaction progression for the polymers was followed using ^{1}H NMR spectroscopy on a Bruker AMX 400 (^{1}H, 400.13 MHz) with DMSO-d$_6$ as the solvent. The final products containing 100 and 90 mol% of GA were no longer soluble in this solvent. As they are only soluble in HFIP-d$_2$, only three samples were analyzed this way to obtain an understanding of the reaction mechanism. The molecular weight distribution was determined by Gel

Permeation Chromatography (GPC). The measurements were carried out in a Merck-Hitachi LaChrom HPLC system, equipped with two PL gel 5 μm MIXED-C (300×7.5 mm) columns using hexafluoroisopropanol as mobile phase and poly(methyl methacrylate) as calibration standards. The reported molecular weights were calculated with the Wyatt Astra 6.1 software package. The thermal transitions were determined using a differential scanning calorimeter DSC 3+ STAR^e system from Mettler Toledo. Approximatively 5 mg of each sample was introduced in a sealed aluminum pan. The PLGA copolymers were heated from room temperature to 215 °C (dT/dt = 10 °C·min^{-1}). The samples were maintained at that temperature for 2 minutes and subsequently cooled down to 25 °C at the same rate. Another heating scan was recorded under the same conditions. For PGA homopolymers, a similar method with two heating and cooling scans was applied from room temperature to 240 °C. The reported glass transition temperature T$_g$ and melting temperature T$_m$ were taken from the second scan. The thermal stability was determined using a TGA/DSC 3+ STARe system from Mettler Toledo. For this purpose, about 10 mg of copolymer was introduced in a sealed aluminum sample vessel. Subsequently, the samples were heated from room temperature to 400 °C (dT/dt = 10 °C·min^{-1}) under nitrogen flow (50 mL·min^{-1}).

4.2.5.2 Barrier property measurements for PLGA

The copolymers PLGA$_{10/90}$ and PLGA$_{20/80}$ prepared with the synthesis route proposed in this work were processed into films with compression molding using a thermal press (Carver AutoFour/3015-NE,H). The samples were first dried for 12 hours at 40 °C (5 mbar) and subsequently sandwiched between two PTFE films (0.14 mm thickness) and 2 aluminum plates (3 mm thickness each). Compression temperatures were set at 180 °C and 195 °C for PLGA$_{20/80}$ and PLGA$_{10/90}$ samples, respectively. In both cases the sandwich was held for 1 minute at 0.5 ton and subsequently at 1 and 3 tons for 30 seconds. The resulting films were quickly cooled down by putting the PTFE sandwich in contact with two cold aluminum plates. The film thickness was measured at 12 different points using an electronic micrometer and subsequently averaged. The oxygen and water permeability of the films (thickness 100-130 μm) were tested in a Totalperm (Permtech s.r.l) instrument. The measurement mechanism and principles have been described in previous work.[3] The system was calibrated with a standard PET film provided by Permtech (Italy) according to the ASTM F1927-14 (oxygen) and ASTM E96/E96M-15 (water) standard. Prior to measurement the films were conditioned for 20 hours and subsequently tested at 30 °C and 70% relative humidity for both cases.

4.2.5.3 Tensile properties of PLGA$_{10/90}$ and PLGA$_{20/80}$

For each copolymer a sample was dried in a vacuum oven (5 mbar) at 40 °C for 24 hours prior to treatment. Subsequently, they were injection molded with a Haake MiniJet II machine (Thermo Scientific) into tensile testing specimens according to the ISO 527-2,

sample type 5A. The injection parameters were defined as follows: injection temperature 195 °C for PLGA$_{10/90}$ and 180 °C for PLGA$_{20/80}$; injection pressure 900 bar and mold temperature 30 °C. Subsequently, the tensile properties were measured on an Instron universal tensile tester with a 1 kN load cell using an extensometer. The crosshead speed was 5mm·min^{-1}. For each type of copolymer, two specimens were tested at room temperature. The obtained mechanical properties from this test were the ultimate strength (σ_u), the elastic modulus (E) and elongation at break (ε).

4.3   Results and discussion

4.3.1   PLGA$_{10/90}$ and PLGA$_{20/80}$

Most phenols are readily available from fuel and biomass and their global annual production shows increasing growth.[10] Phenols can be esterified by the direct action of an organic acid.[11] They are known as good leaving groups during polymerization and some form azeotropes with water, which enhances its removal during esterification. The above together with the possibility to recycle and reuse them for further polymerizations, makes phenols interesting candidates as solvents for the direct polycondensation proposed in this work. The syntheses of PLGA 10/90 and 20/80 are typically performed in temperature ranges of 190-210 °C. Because the boiling point of the phenol-type solvent must be in the range of the reaction temperature, p-cresol (boiling point 202 °C) was selected.

Table 4.1 presents an overview of the reaction conditions together with the resulting molecular weight and molecular weight distribution and the thermal properties for all the synthesized PLGA copolymers. As expected, in the absence of solvent a very low M_n of around 10 kg·mol^{-1} was obtained in the regular polycondensation of both PLGA$_{10/90}$ and PLGA$_{20/80}$. By performing the polycondensation in the presence of 75 mol% p-cresol the M_n was more than doubled to 23.3 and 21.9 kg·mol^{-1} for PLGA$_{10/90}$ and PLGA$_{20/80}$, respectively. Further tuning to higher reaction temperature and lower catalyst concentration, led to an additional increase of the M_n to 30.8 kg·mol^{-1} for PLGA$_{10/90\_14}$ (PLGA$_{10/90}$ experiment 14). Overall the positive effect of p-cresol on the molecular weight is apparent, even with different catalysts and lower catalyst concentrations. The same was observed for PLGA$_{20/80}$ with M_n values between 17.1 and 27.2 kg·mol^{-1} when using p-cresol at varying concentrations. In **Table 4.1** the results of 32 experiments are presented, in which solvent, catalyst, amounts, temperatures and reaction times were varied in order to study the potential of this process.

Table 4.1 Overview of the different reaction conditions for PLGA$_{10/90}$ and PLGA$_{20/80}$ copolymers, resulting molecular weight distribution and thermal properties.

Sample	Solvent amount (mol%)	Catalyst	Catalyst amount (mol%)	T (°C)	t (h)	M_n (kg·mol^{-1})	M_w (kg·mol^{-1})	PDI	T_g (°C)	T_m (°C)
PLGA$_{10/90}$_1	0	BuSnO(OH)	0.1	190-200	11	9.4	22.7	2.4	36	185
PLGA$_{10/90}$_2	50	BuSnO(OH)	0.1	190-200	11	16.1	33.0	2.0	39	182
PLGA$_{10/90}$_3	75	BuSnO(OH)	0.1	190-200	11	23.3	46.9	2.0	40	186
PLGA$_{10/90}$_4	100	BuSnO(OH)	0.1	190-200	11	16.2	32.9	2.0	39	182
PLGA$_{10/90}$_5	75*	BuSnO(OH)	0.1	190-200	11	13.0	28.1	2.2	38	185
PLGA$_{10/90}$_6	75	none	0	190-200	11	3.7	12.7	3.4	n.d.	n.d.
PLGA$_{10/90}$_7	75	BuSnO(OH)	0.05	190-200	8	23.4	46.3	2.0	41	187
PLGA$_{10/90}$_8	75	BuSnO(OH)	0.05	190-205	8	21.0	45.3	2.2	41	183
PLGA$_{10/90}$_9	75	BuSnO(OH)	0.05	190-210	7.5	20.5	44.2	2.2	40	181
PLGA$_{10/90}$_10	75	BuSnO(OH)	0.02	190-200	10	17.2	34.5	2.0	39	181
PLGA$_{10/90}$_11	75	BuSnO(OH)	0.02	190-205	9	17.4	40.3	2.3	39	181
PLGA$_{10/90}$_12	75	BuSnO(OH)	0.02	190-210	8.5	21.5	43.7	2.0	40	180
PLGA$_{10/90}$_13	75	BuSnO(OH)	0.07	190-200	10	23.2	53.0	2.3	41	187
PLGA$_{10/90}$_14	75	BuSnO(OH)	0.05[a]	190-210; 200	7.5	30.8	62.8	2.0	41	185
PLGA$_{10/90}$_15[b]	75	BuSnO(OH)	0.05[a]	190-200	7.5	31.5	63.3	2.0	41	185
PLGA$_{10/90}$_16	75	Sn(Oct)$_2$	0.05 [a]	190-200	10	16.7	33.5	2.0	40	180

PLGA with 90 mol% of glycolic acid and 10 mol% of lactic acid in the feed

PLGA10/90_17	75	Ti(OBu)$_4$	0.05[a]	190-200	14	16.2	34.6	2.1	40	181
PLGA10/90_18	75	BuSnO(OH)	0.05[a]	190-200	10	25.2	53.5	2.1	41	186
PLGA10/90_19	75	Yb(OTf)$_3$	0.05[a]	190-200	10	6.3	12.3	2.0	38	185
PLGA10/90_20	75	pTSA+SnCl$_2$	0.05[a]	190-200	10	17.8	36.5	2.1	40	183
PLGA10/90_21	75	PTSA	0.05[a]	190-200	12	4.0	8.8	2.2	n.d.	172
PLGA10/90_22	75	SnCl$_2$	0.05[a]	190-200	14	19.3	38.7	2.0	40	182
PLGA10/90_23[c]	75	BuSnO(OH)	0.05	190-200	8	22.0	43.9	2.0	40	182
PLGA10/90_24[d]	75	BuSnO(OH)	0.05[a]	190-200	14	22.4	46.2	2.1	40	183
PLGA10/90_25[b,d]	75	BuSnO(OH)	0.05[a]	190-200	14	30.3	60.5	2.0	41	186
PLGA with 80 mol% of glycolic acid and 20 mol% of lactic acid in feed										
PLGA20/80_1	0	BuSnO(OH)	0.1	190-200	10	10.6	24.8	2.3	39	-
PLGA20/80_2	50	BuSnO(OH)	0.1	190-200	10	17.1	35.4	2.1	40	-
PLGA20/80_3	75	BuSnO(OH)	0.1	190-200	10	21.9	47.7	2.2	42	-
PLGA20/80_4	100	BuSnO(OH)	0.1	190-200	10	18.6	40.1	2.2	42	-
PLGA20/80_5	75	BuSnO(OH)	0.05	190-200	8	21.7	45.3	2.1	41	-
PLGA20/80_6[c]	75	BuSnO(OH)	0.05	190-200	8	20.2	41.0	2.0	41	-
PLGA20/80_7[d]	75	BuSnO(OH)	0.05[a]	190-200	12	27.2	54.8	2.0	42	-

[a] Catalyst added in two equal portions at the beginning of the reaction and before reducing pressure.
[b] Slow decompression from esterification stage.
[c] LD-lactic acid used as monomer instead of L lactic acid.
[d] 50 g of initial monomer load.
*1,4-dimethoxybenzene used as non-reactive solvent.
**For every reaction the second stage at reduced pressure was carried out in 2 hours.
n.d= not determined.

## 4.3.1.1   The role of p-cresol in the polycondensation

The effect of the solvent concentration on the molecular weight distribution was studied for copolymers with 90 and 80 mol% of glycolic acid in the feed (**Fig. 4.1**). For this purpose, the amount of p-cresol used was varied: 50, 75 and 100 mol% with respect to the monomer load. The reaction temperature, catalyst type and concentration were kept constant, as shown in **Table 4.1**. BuSnO(OH) was the first catalyst to be tested as it is known to exhibit very good catalytic activity for esterification and transesterification reactions.[12-14]

The results presented in **Fig. 4.1** show that for both PLGA 10/90 (M_n = 23.3 kg·mol^{-1}) and 20/80 (M_n = 21.7 kg·mol^{-1}) the highest molecular weights were obtained using 75 mol% p-cresol. This points to an optimum reactive solvent load close to 75%, which indicates that different factors play a role in facilitating the polycondensation reaction. In general the use of solvent reduces the viscosity of the reaction mixture, which is advantageous for heat and mass transfer. 1,4-dimethoxybenzene was therefore tested as a non-reactive solvent in the synthesis of PLGA 10/90 (PLGA$_{10/90\_5}$). This provided a small M_n improvement to 13 kg·mol^{-1} over the solvent free process (M_n = 9.4 kg·mol^{-1}), but not nearly as much as for the p-cresol. This shows that there is another effect in play in case of the phenolic solvent.
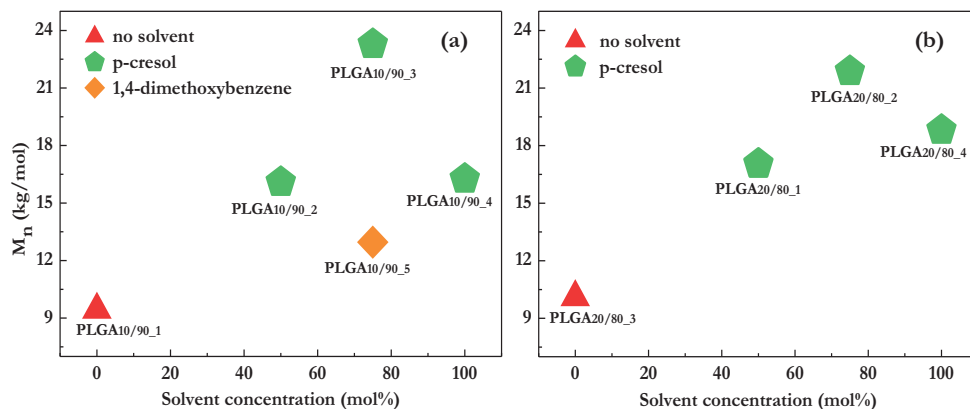
Fig. 4.1 Resulting M_n without solvent and with different solvent concentrations for PLGA copolymers with: **(a)** 90 mol% GA and **(b)** 80 mol% in the feed.

The peaks at 1.49 and 1.65 ppm in **Figure 4.2** correspond to the protons of the methyl group (CH$_3$) of LA for PLGA$_{10/90\_3}$ and PLGA$_{20/80\_3}$ in HFIP and DMSO, respectively. Similarly, methine resonances (CH$_3$) were assigned to the peaks at 5.23 and 5.37 ppm. Additionally, the protons of the methylene group (CH$_2$) of the glycolic acid repeating unit are observed at 4.91 and 4.94 ppm in HFIP and DMSO, respectively.
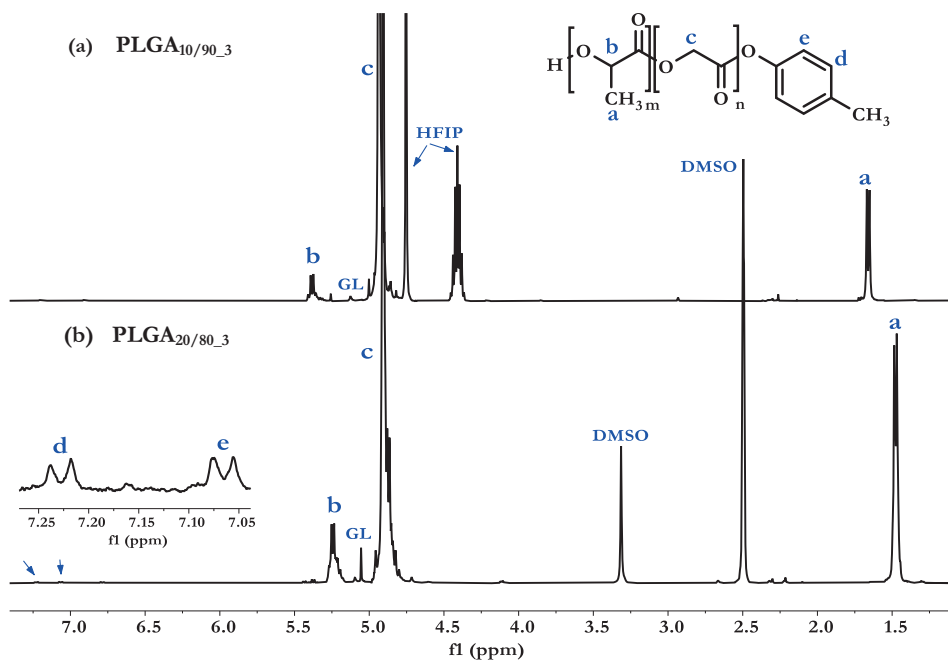
Fig. 4.2 ^{1}H-NMR of resulting product for **(a)** PLGA$_{10/90\_3}$ (in HFIP-d$_2$) and **(b)** PLGA$_{20/80\_3}$ (in DMSO-d$_6$).

Traces of glycolide, the cyclic dimer of glycolic acid and a known side product of PGA and PLGA polymerization, are observed at 5.12 (HFIP) and at 5.06 ppm (DMSO). The final comonomer ratio built in the copolymers can be calculated by integrating the CH$_2$ peak of GA and the CH or CH$_3$ peaks of the LA.[3] According to this method, the products presented in **Fig. 4.2** contain 11/91 and 18/82 of built in LA/GA, respectively. The higher reactivity for glycolic acid compared to lactic acid reported before for these types of copolymers, explains the systematic findings of slightly higher GA content in the copolymer compared to the feed ratio.

The small proton peaks at around 7.03 and 7.22 ppm (**Fig. 4.2**) can be assigned to the cresyl endgroups, as free p-cresol has these protons at around 6.65 and 6.95 ppm.[9] The endgroup concentration corresponds to 0.2 mol% in both cases. This confirms that the cresol reacts with the monomers, oligomers and/or polymers to form cresyl ester endgroups. Traces of free p-cresol (below 0.06 mol%) were sometimes observed when the reaction temperature did not exceed 200 °C. Complete solvent removal with the set up configuration used here, can become more challenging as the polymer viscosity increases and as stirring becomes more difficult when higher amounts of polymer are synthesized.
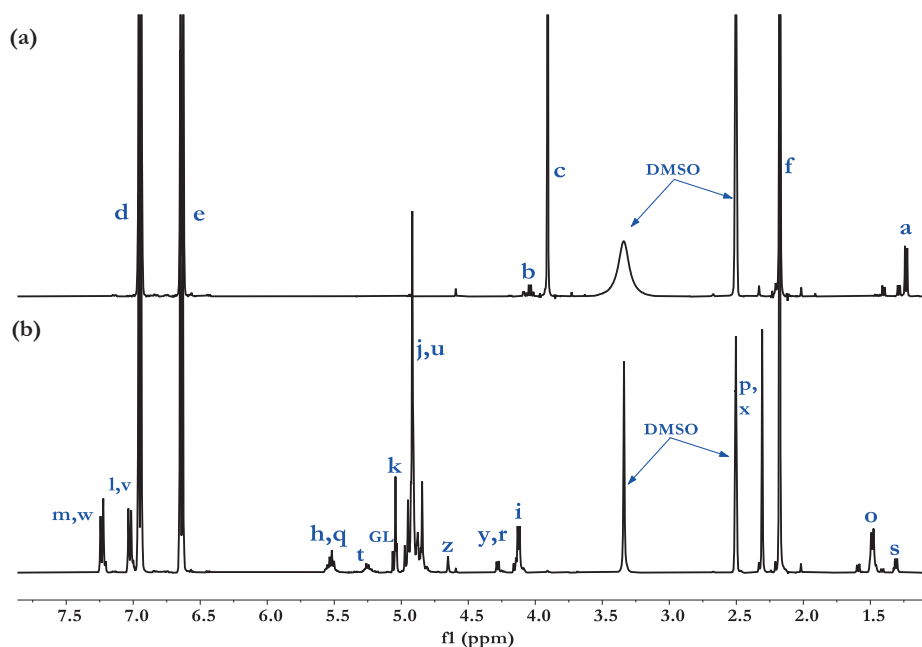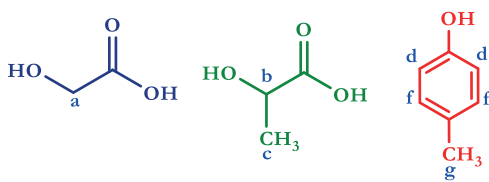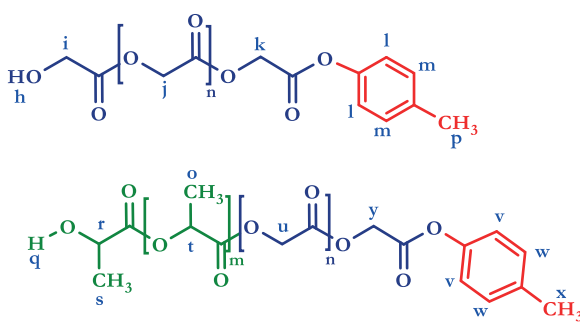
Fig. 4.3 ^{1}H NMR of **(a)** initial reaction mixture and **(b)** mixture at the end of the esterification stage for PLGA$_{10/90-3}$ in DMSO-d$_6$.

Due to the much higher quantity of GA in the reaction mixture, combined with its higher reactivity compared to LA, it is expected that mainly GA-GA oligomers will form initially and LA will be included over time. These oligomers continue reacting and form phenyl esters with p-cresol. **Fig. 4.3** shows two NMR spectra from the synthesis of PLGA$_{10/90}$: **(a)** the feed mixture and **(b)** the same reaction medium at the end of the esterification stage (after 9 hours at 190 °C). The peak assignments are presented in **Table 4.2**.

In **Fig. 4.3 (a)**, the peaks l, v and m, w at between 7.0-7.03 and 7.20-7.25 ppm correspond to the aromatic protons of cresyl esters, which confirms the formation of GA and/or LA cresyl esters endgroups observed in **Fig. 4.2**. Furthermore, the broad peak observed between 5.49 and 5.58 ppm (h, q) can be assigned to the terminal hydroxyl groups attached to GA and LA. The esterification was concluded once the ratio between the terminal phenyl ester peak (m, w) and the hydroxyl endgroup peak (h, q) was close to one. For experiments PLGA$_{10/90\_2, 3, 4}$ this occurred after about 9 hours of reaction. Additionally the peaks i and r, which are attributed to the CH$_2$ and CH attached to free OH groups, could also be used as an indication of the reaction progression. Also, at 4.64 ppm (z) a small peak attributed to the protons of the CH$_2$-COOH acid chain end of GA-GA oligomers is observed, which means a small amount of acid endgroups had not reacted with the cresol. This did not have a detrimental effect in the following polycondensation step.

Table 1. ^{1}H NMR chemical shifts in DMSO-d_6 of the initial reaction mixture and the phenyl esters formed during the first stage of the PLGA synthesis for sample PLGA$_{10/90\_26}$.

a) **Initial mixture**

Assignment	Chemical shift (ppm)	Assignment	Chemical shift (ppm)
a	1.21-1.25	d	6.93
b	4.02-4.06	e	6.65
c	3.90	f	2.17

b) **Reaction mixture after 7 hours**

h, q	5.49-5.58	k	5.04	p, x	2.30	t	5.20-5.29
i	4.11-4.14	l, v	7.0-7.03	y, r	4.26-4.29	o	1.47-1.50
j, u	4.87-4.94	m, w	2.30	s	1.28-1.32	GL	5.06

The reaction between LA and GA starts with oligomerization (**Scheme 4.3**) which is an equilibrium reaction with water as side product. In parallel, both acids can react with p-cresol forming cresyl ester endgroups which are more reactive compared to terminal carboxylic acids. At the end of the esterification stage (**Fig. 4.3 (b)**), the NMR spectra revealed only traces (<0.05 mol %) of unreacted glycolic or lactic acid. The following step consists of transesterification of the formed cresyl esters with exchange between the ester and terminal hydroxy groups. Since this reaction is reversible, p-cresol must be distilled out of the system to drive the equilibrium towards increasing molecular weight. As the polycondensation proceeds, the polymer with increasing viscosity remains in the reactor and the solvent is recovered separately. This step explains why the use of p-cresol is so effective compared to the basic melt polyesterification and the unreactive solvent addition: it effectively removes water from the mixture before the final polycondensation step. Since phenols are good leaving groups, ester endgroups of this type are much more reactive than

carboxylic acid endgroups and at the same time the free phenols are far less likely to react and break up the polymer chains to form new ester endgroups compared to free water. This is in line with our previous research on the polyesterification of secondary diols using phenolic solvents.[9]
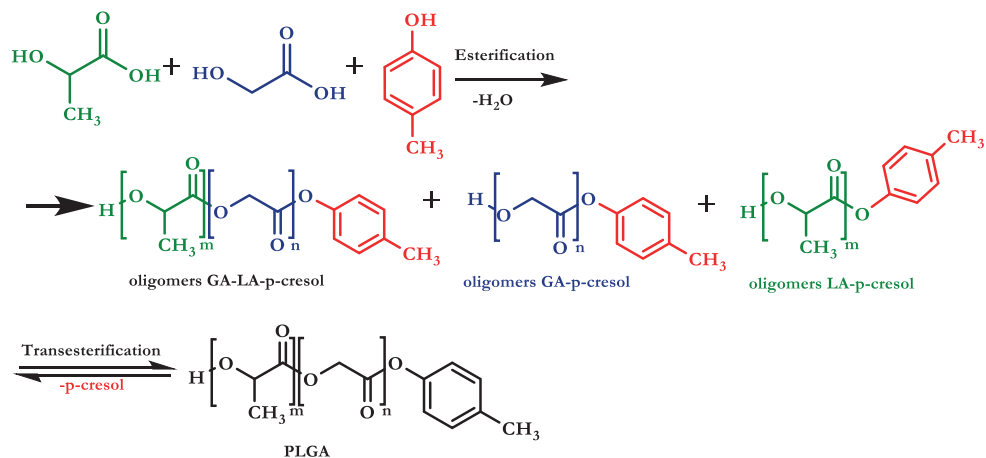
Scheme 4.3 Proposed synthesis route for PLGA copolymers rich in glycolic acid.

4.3.1.2 Thermal properties

It is well known that the T_g increase with increasing M_n until a plateau is reached at sufficiently high M_n.[15] The present research shows the same trends (**Fig. 4.4**). The lowest T_g values were measured for the copolymers with the lowest M_n, synthesized in the absence of solvent (T_g = 36 °C for PLGA$_{10/90}$ and T_g = 39 °C for PLGA$_{20/80}$) and the highest T_g values were measured for to those with the highest M_n (T_g = 41 °C for PLGA$_{10/90}$ and T_g = 42 °C for PLGA$_{20/80}$).

Copolymers with 80 mol% of GA (**Fig. 4.4 (b)**) in the feed present slightly higher T_g and a similar trend in terms of T_g increase with M_n. Nevertheless all the samples with this composition are amorphous while copolymers with about 90 mol% are semicrystalline according to the DSC thermograms (see **Fig. 4.17** and **4.18** in Appendix for DSC thermograms). These observations are in line with results previously reported for copolymers with similar compositions prepared via ROP.[3] Samples with 90 mol% of GA (**Fig. 4.4 (a)**), exhibit a melting transition between 182 and 187 °C and in most cases a recrystallization peak very close to the T_m. Compared to ROP copolymers (M_n of up to 36 kg·mol^{-1}) with similar composition reported previously[3], the T_m values from this work are lower, even at the highest M_n (M_n of up to 30 kg·mol^{-1}). Similarly, the degrees of crystallinity calculated from the second heating cycle (dT/dt = 10 °C·min^{-1}) are much lower with values below 2%. Interestingly, the reference copolymer for PLGA$_{10/90}$ (PLGA$_{10/90\_1}$), prepared without solvent, exhibited a T_m slightly higher than that of other PLGA copolymers synthesized in the presence of p-cresol, even though the molecular weight was much lower.
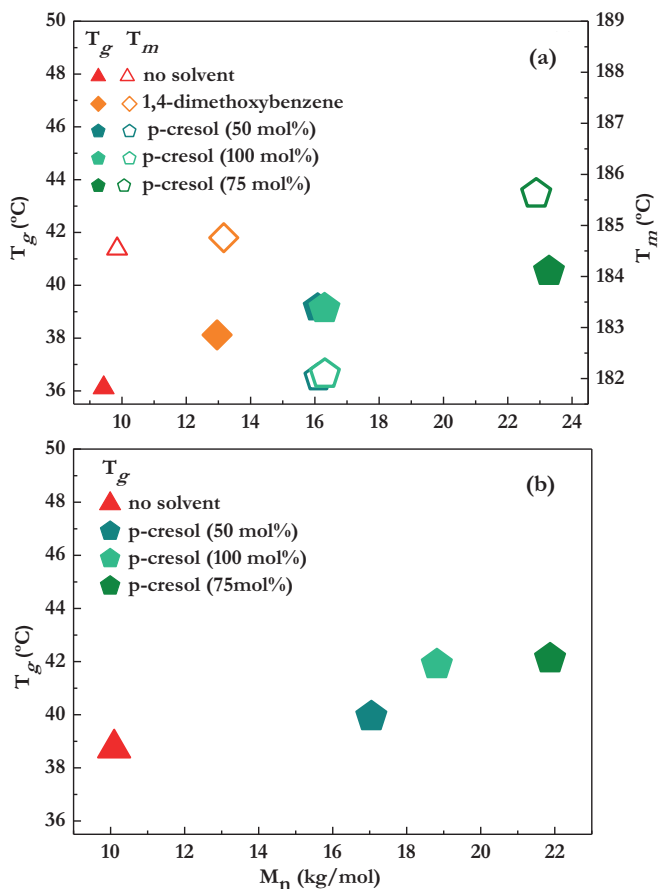
Fig. 4.4 T_g and T_m variation at different solvent concentrations for PLGA copolymers with **(a)** 90 mol% and **(b)** 80 mol% of GA in the feed.

For the samples prepared in the presence of p-cresol the T_m increased with increasing molecular weight. With the highest M_n values, the T_m approaches and even supersedes those attained without solvent (186 and 187 °C for PLGA$_{10/90\_3}$ and PLGA$_{10/90\_7}$). The melting behavior in semicrystalline polymers is mostly determined by the crystal morphology (perfection) and lamella thickness.[16,17] Both factors are affected by the molecular weight distribution and main chain structure (e.g. containing elements, bonds, terminal groups). The results obtained here suggest that increasing molecular weight reflects in higher T_m, which at the same time seems to be reduced by the presence of the cresyl ester endgroups. Possibly, these terminal groups are responsible for a disruption in the crystallization ability and at the same time a decrease of the energy required to mobilize polymer chains until the melt. Furthermore, lactide and glycolide can form in equilibrium with PGA, PLA and PLGA oligomers during a typical polycondensation reaction which can play a role in inhibiting nucleation.

4.3.1.3 Effect of catalyst and temperature on the molecular weight of PLGA$_{10/90}$

4.3.1.3.1 Catalyst type

BuSnO (OH) exhibited good performance as both esterification and transesterification catalyst for the polymerization of PLGA in the presence of p-cresol. However, the potential suitability of other catalysts had not yet been investigated. Based on their performance in previous studies[4,5,18], six other catalysts were tested: Yb(OTf)$_3$, pTSA, Sn(Oct)$_2$, SnCl$_2$, Ti(OBu)$_4$ and a mixture of pTSA/ SnCl$_2$ (50/50 mol%). All were added in two equal portions: one at the beginning of the reaction, and one shortly before starting the second stage at reduced pressure. This was done to avoid potential catalyst deactivation triggered by the presence of water in the reaction medium. The esterification stage was concluded when an equivalent amount of reactive terminal groups (phenyl esters and hydroxyl groups in the NMR spectra) was achieved. The conversion of glycolic and lactic acid in time, followed with ^{1}H NMR, is shown in **Fig. 4.5**.

Fig. 4.5 (a) Glycolic and **(b)** lactic acid conversion in time for different catalysts (0.05 mol%) at 190-200 °C with 75 mol% p-cresol.

Under the conditions tested $Yb(OTf)_3$ clearly showed the highest conversion rate for both acids (>93% after 4 hours for both GA and LA). This was followed by the mixture $SnCl_2$/p-TSA, p-TSA and BuSnO(OH), which showed a similar trend. The $Sn(Oct)_2$ gave a lower conversion after 4 hours, but provided a comparable conversion to the better performing catalysts after 8 hours. For both $Ti(OBu)_4$ and $SnCl_2$, the conversion of both acids was notably slower than for the other catalysts. Nevertheless, these different conversion rates only indicate the suitability of determined catalyst for the interaction between p-cresol and the acids. The catalyst must also exhibit good performance for the transesterification. Here, the final molecular weight distribution of each product is also used as an indication of the overall catalyst performance. The resulting molecular weights upon completion for PLGA products prepared with the different catalysts are shown in **Fig. 4.6**.
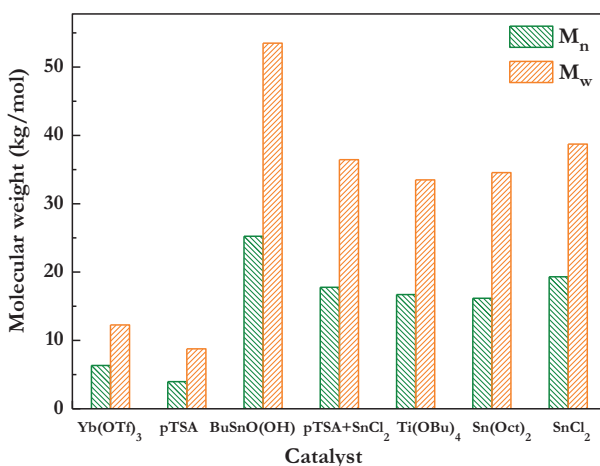
Fig. 4.6 Resulting molecular weights (GPC) with different types of catalysts for $PLGA_{10/90}$.

This shows that $Yb(OTf)_3$, the best performing esterification catalyst ($PLGA_{10/90-19}$), led to the worst transesterification performance, together with pTSA ($PLGA_{10/90-21}$), with the lowest M_n of 6.3 and 8.8 $kg \cdot mol^{-1}$ respectively. The highest M_n (25.2 $kg \cdot mol^{-1}$) was still attained when using BuSnO(OH) for sample $PLGA_{10/90\_18}$ and in fact, the addition in two times (start of the experiment and before applying vacuum) improved this result with respect to the experiments presented before. For the remaining cases, lower M_n values were obtained in the following order: p-TSA+$SnCl_2$ > $Sn(Oct)_2$ > Ti (OBu), with 17.8, 16.7 and 16.2 $kg \cdot mol^{-1}$ respectively. Nevertheless, as seen, the M_n differences for these last cases are not striking.

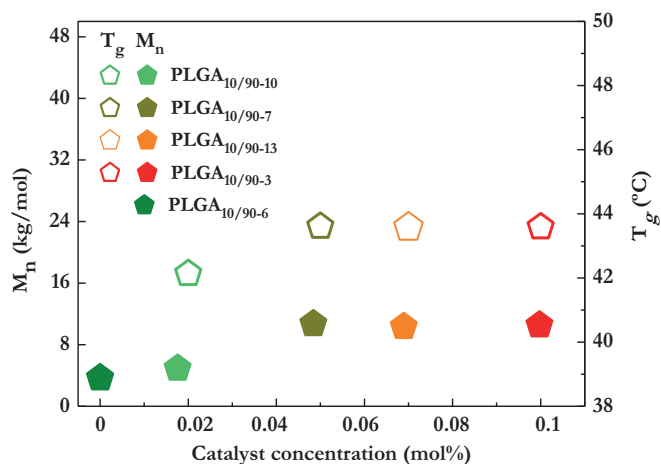## 4.3.1.3.2 Catalyst concentration

From the tested catalysts, BuSnO(OH) led to the highest M_n (25.2 $kg \cdot mol^{-1}$) so far. Since this is also a good catalyst for the formation of lactide and glycolide, it is desired to maintain

its concentration at the lowest possible levels, while assuring an adequate conversion rate. Consequently, the effect of BuSnO(OH) concentration on the resulting molecular weight distribution was studied. Therefore a set of experiments was carried out using 75 mol% of p-cresol at 190 to 200 °C. Concentrations between 0 and 0.1 mol% were tested and the product was analyzed with GPC and DSC.

In **Fig. 4.7** the resulting M_n and T_g are shown for some $PLGA_{10/90}$ samples prepared at similar conditions with variable BuSnO(OH) concentrations. The T_g change is directly linked to M_n increase. Up to 0.05 mol% the M_n increases with increasing catalyst concentration. At higher catalyst loadings the resulting M_n appears to remain constant, with conversions over 98% for both acids already after 6 hours. However, reaching a steady state where the amount of cresyl endgroups is equal to the amount of hydroxy endgroups took longer when using 0.1 mol% of catalyst compared to 0.05 mol%. It is likely that at some point the amount of available terminal acid groups has decreased such, that chain scission reactions could be triggered at higher catalyst concentrations. Interestingly, it was determined that the esterification reaction can be effectively catalyzed by the acid endgroups and even when no catalyst was present in this stage, most of the oligomers reacted with p-cresol after 9 hours at 190 °C. However, a catalyst is necessary to proceed with the transesterification. Without it and in the absence of reactive terminal acid groups, only a low M_n of 3.7 kg·mol^{-1} was achieved.

Fig. 4.7 Effect of catalyst concentration on M_n and T_g.

The thermal stability for some of the $PLGA_{10/90}$ copolymers prepared with different catalyst concentrations was measured (**Fig. 4.8, Table 4.3**). The decomposition proceeds in a single stage for all samples and about 5 % weight loss is already observed at 283-288 °C. The decomposition temperatures consistently decrease with increasing catalyst concentration: $T_{5\%} = 288$ °C, $T_{50\%} = 345$ °C and $T_{70\%} = 354$ °C at 0.02 mol% catalyst loading and $T_{5\%} = 283$ °C, $T_{50\%} = 332$ °C and $T_{70\%} = 340$ °C at 0.1 mol% catalyst loading. This is in line with

previous work, where residual catalyst was reported to enhance the thermal degradation of this type of polymer.[19]
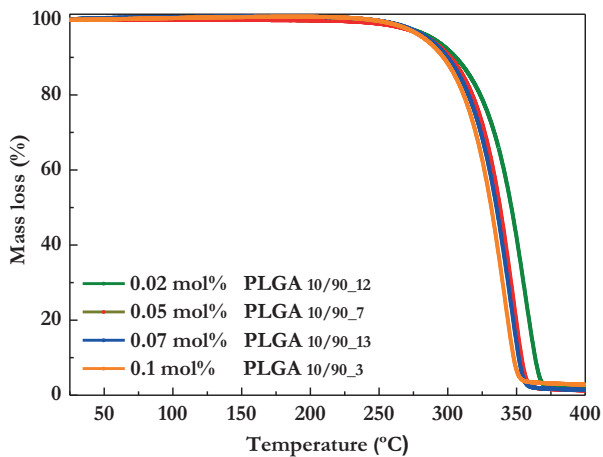
Fig. 4.8 TGA curves (non-isothermal conditions, $dT/dt = 10\ °C\cdot min^{-1}$) for $PLGA_{10/90}$ copolymers prepared with different catalyst concentration.

Table 4.3 Temperatures at which a mass loss of 5 wt.% ($T_{5\%}$), 50 wt.% ($T_{50\%}$) and 70 wt.% ($T_{70\%}$) was measured for PLGA copolymers with different catalyst concentrations.

Sample	BuSnO(OH) (mol%)	M_n (kg·mol⁻¹)	$T_{5\%}$ (°C)	$T_{50\%}$ (°C)	$T_{70\%}$ (°C)
$PLGA_{10/90\_12}$	0.02	21.5	288	345	354
$PLGA_{10/90\_7}$	0.05	23.4	286	338	346
$PLGA_{10/90\_13}$	0.07	23.2	286	335	343
$PLGA_{10/90\_3}$	0.1	23.3	283	332	340

4.3.1.3.3   Effect of reaction temperature

The effect of temperature program was researched, using two concentrations of BuSnO(OH), while the p-cresol content was kept constant at 75 mol%. When starting the reaction at 190 °C for 9 hours, followed by a temperature increase to 200 °C and subsequent pressure reduction to 1 mbar, 0.05 mol% BuSnO(OH) clearly resulted in a higher M_n of 23.4 kg·mol⁻¹ than the 17.2 kg·mol⁻¹ obtained with 0.02 mol% BuSnO(OH) (**Fig. 4.9**).

When the temperature was increased from 190 °C to either 205 °C or 210 °C within 3 hours the resulting molecular weights were comparable at both catalyst concentrations ($M_n \approx 20$ kg·mol⁻¹, $M_w > 40$ kg·mol⁻¹), with values between those obtained from the previous experiment. At the higher catalyst concentration (0.05 mol%), the increased temperature clearly has a negative effect on the molecular weight. A gel-like substance was recovered from the receiver, which was identified as a mixture of glycolide, lactide and 3-methylglycolide by ¹H NMR. At 0.02 mol% catalyst loading this was not observed.

This means that the combination of 0.05 mol% BuSnO(OH) and increased temperature is too severe, leading to decomposition of the polymer. The increased temperature profile does have a positive effect at lower catalyst concentration and total reaction time and could be further fine-tuned to optimize the molecular weight.

For this reason two additional experiments were performed (**Fig. 4.9**). In the first one, previously tested conditions were reproduced during esterification (75 mol % of p-cresol, T = 190 °C to 210 °C, and 0.05 mol% of BuSnO(OH) added in two portions). However, the polycondensation temperature was now reduced again to 200 °C upon applying vacuum, instead of increasing it as is common practice. The pressure was reduced as usual. The resulting product had a M_n of 30.8 kg·mol^{-1} (GPC), the highest molecular weight achieved so far. Here, efficient water removal was attained during the first stage of the reaction at increased temperature while less decomposition and side reactions occurred during polycondensation. In the second additional example (PLGA$_{10/90\_15}$), the esterification was carried out with gradual decompression. The esterification conditions of the first example were reproduced at ambient pressure. Once a conversion above 95% for both monomers was reached, the pressure was reduced to 450 mbar and then to 360 mbar leaving it for 1 hour each time (at 190 °C). Neither the monomers nor the solvent were distilled out and the reaction was monitored with ^{1}H NMR. By then, the system reached a conversion over 99% for both acids, with the majority bearing cresyl ester endgroups. Subsequently, the second portion of catalyst was added and the temperature was increased to 200 °C. Decompression until 1 mbar was carried out step-wise as usual. The resulting product with M_n= 31.5 kg·mol^{-1} showed a slightly higher molecular weight than the first example and overall the clearest color from all the products synthesized in this study. With the previous examples, it is shown that when using p-cresol, variable routes can be applied to achieve a satisfactory M_n.
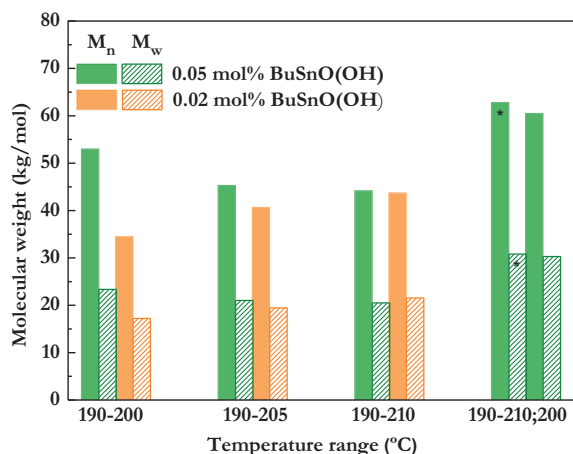

Fig. 4.9 The effect of reaction temperature on M_n for 0.02 and 0.05 mol % of BuSnO(OH). *Sample prepared at reduced pressure (PLGA$_{10/90\_15}$).

4.3.1.4   *L*-lactic acid vs. *LD*-lactic acid

Lactic acid is a chiral molecule that is most commonly produced in its *L*(+) form via an industrial fermentation process. PLA is typically produced from *L*(+)-lactic acid (in the form of lactide). Racemic (*LD*) lactic acid is commonly produced via petrochemical processes but it can also be derived from fermentation. Producing PLA from racemic lactic acid results in polymers with very different properties (crystallization kinetics, mechanical and barrier properties) than PLA from *L*(+)-lactic acid. A similar effect can be observed in PLGA copolymers, according to Gilding et al.[20] PLGA synthesized using *L*-lactide with between 25 and 70% of glycolide is amorphous. However, when using *DL*-lactide, this ratio extends to between 0 and 70% of glycolide.

When racemic LA was used in our study, instead of *L*-LA, for the synthesis of PLGA 10/90 and 20/80 this, as expected, did not appear to have a large effect on the polymer properties. No significant differences in M_n and T_g were observed (**Fig. 4.10**, **Table 4.4**). Copolymers with about 20 mol% of LA remain amorphous with a T_g of 41 °C, irrespective of using the *L* or *DL* form.
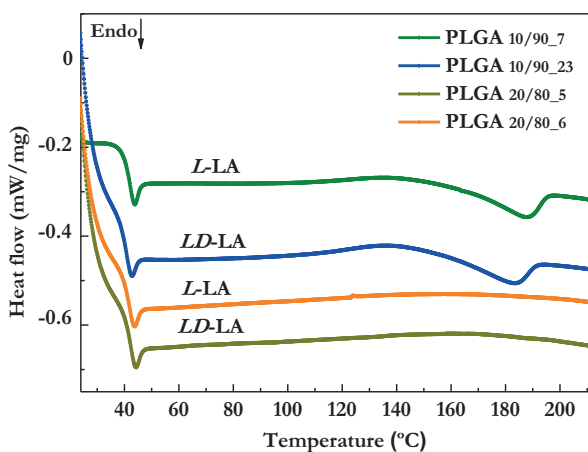
Fig. 4.10 DSC curves of PLGA$_{10/90}$ and PLGA$_{20/80}$ copolymers synthesized with *L* and racemic lactic acid.

For PLGA$_{10/90}$ copolymers the same trend is observed. Although for both *L*-LA and racemic LA a melting transition is observed, it appears to start at lower temperatures for the sample prepared with racemic LA (182 °C) than for *L*-LA (187 °C). In both cases, what looks like a broad recrystallization peak is observed close to the T_m. The thermal stability determined with TGA, was compared for the same group of PLGA copolymers displayed in **Fig. 4.10**. As can be observed in **Table 4.4**, all the samples showed single step decomposition with overall higher thermal stability for samples with higher GA content. Only minor differences according to the type of lactic acid are shown for the temperature dependent mass loss of PLGA$_{10/90}$ or PLGA$_{20/80}$.

Table 4.4 Mass loss of 5 wt.% ($T_{5\%}$), 50 wt.% ($T_{50\%}$) and 70 wt.% ($T_{70\%}$) of PLGA copolymers prepared from L or LD-lactic acid.

Sample	LA type	T_g (°C)	M_n (kg·mol⁻¹)	$T_{5\%}$ (°C)	$T_{50\%}$ (°C)	$T_{70\%}$ (°C)
PLGA₁₀/₉₀_₇	L	41	23.4	286	338	346
PLGA₁₀/₉₀_₂₃	LD	40	22.0	280	335	343
PLGA₂₀/₈₀_₅	L	41	21.7	276	333	343
PLGA₂₀/₈₀_₆	LD	41	20.2	281	333	343

4.3.1.5   Guaiacol as reactive solvent

In the previous paragraph it has been clearly shown that the presence of p-cresol has a positive effect on the target's polymer molecular weight. For this reason also another substituted phenol was tested. Guaiacol (2-methoxyphenol) was selected, as it allows similar synthesis temperatures to the ones used so far with p-cresol (T_b= 205 °C). It is a naturally occurring organic compound with a much broader application field than p-cresol. Some applications include synthetic flavors, manufacturing of pharmaceuticals, in stabilizers and antioxidants for plastics and rubbers, as local anesthetic, as an expectorant and as an antiseptic agent for the abdomen and intestines.[21] For the polycondensation of PLGA₁₀/₉₀, the general procedure was similar to the one described for the experiments with p-cresol, with some adjustments. Previously it was already observed that the esterification reaction between guaiacol and GA and/or LA works best above 200 °C. At lower temperature, the reactivity of this sterically hindered phenol is too low. Therefore a temperature profile starting at 190 °C and slowly increasing to 205 or 210 °C over 3 or 4 hours in the esterification step was applied. For PLGA₁₀/₉₀_₂₆ the reaction was kept at 205 °C for the polycondensation, while in the other experiments the temperature was decreased to 200 °C before applying vacuum (**Table 4.5**).

Table 4.5 Overview of the different reaction conditions for PLGA₁₀/₉₀ copolymers, resulting molecular weight distribution and thermal properties using 75 mol% guaiacol as reactive solvent.

Sample	Catalyst type	Catalyst amount (mol %)	T (°C)	t (h)	M_n (kg·mol⁻¹)	M_w (kg·mol⁻¹)	T_g (°C)	T_m (°C)
PLGA₁₀/₉₀_₂₆	BuSnO (OH)	0.05	190-205	12.0	21.5	44.2	40	187
PLGA₁₀/₉₀_₂₇	BuSnO (OH)	0.05	190-210; 200	10.5	28.6	58.4	40	185
PLGA₁₀/₉₀_₂₈	SnCl₂	0.05	190-210; 200	12.5	24.2	48.4	39	182
PLGA₁₀/₉₀_₂₉	SnOct₂	0.05	190-210; 200	10.5	22.5	49.2	40	181
PLGA₁₀/₉₀_₃₀	pTSA+ SnCl₂	0.05	190-210; 200	12.0	20.2	43.8	40	184

Similar to what was found for p-cresol (4.3.1.3), the highest molecular weight (M_n = 28.6 kg·mol^{-1}) was obtained with an esterification step going up to 210 °C, followed by a polycondensation under reduced pressure at 200 °C. Products with molecular weights comparable to those obtained with p-cresol can be obtained with guaiacol. Also, the T_g and T_m correspond to those found for the PLGA$_{10/90}$ products made in the presence of p-cresol. Still, the highest molecular weight increase so far was achieved with p-cresol after optimizing several reaction parameters ($M_n \approx$ 31 kg·mol^{-1}). Although similar reaction conditions are applied, longer reaction times are required with guaiacol, as it is less reactive than p-cresol regarding esterification, likely due to the steric hindrance of the hydroxy group by the methoxy group in the ortho position.

In **Fig. 4.11** the M_n of PLGA$_{10/90}$ products obtained from p-cresol and guaiacol under similar reaction conditions are compared. A similar trend in molecular weight distribution was observed for these phenols. The highest M_n is obtained when using BuSnO(OH) (M_n=28.6 kg·mol^{-1}), followed by SnCl$_2$ (M_n=24.2 kg·mol^{-1}), pTSA-SnCl$_2$(M_n=20.2 kg·mol^{-1}) and finally, SnOct$_2$ (M_n=22.5 kg·mol^{-1}). Higher esterification temperatures used with guaiacol (up to 210 °C) compared to p-cresol (up to 200 °C) overall resulted in greater M_n values using the same catalysts.
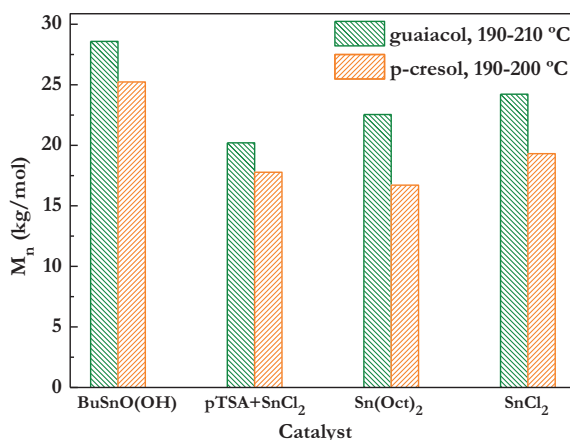
Fig. 4.11 Molecular weight (M_n) comparison between PLGA$_{10/90}$ samples prepared in the presence of guaiacol and p-cresol for different catalyst systems.

4.3.1.6   Solid state polymerization (SSP) of PLGA$_{10/90}$

SSP was applied to PLGA$_{10/90}$ at 145, 155, and 165 °C for up to 72 hours at 2 mbar. The molecular weight progression in time for a representative sample (PLGA$_{10/90}$_13) is shown in **Fig. 4.12** and the same trends were observed for other samples. The sample was crystallized beforehand at 115 °C to increase the sticking and agglomeration temperature.
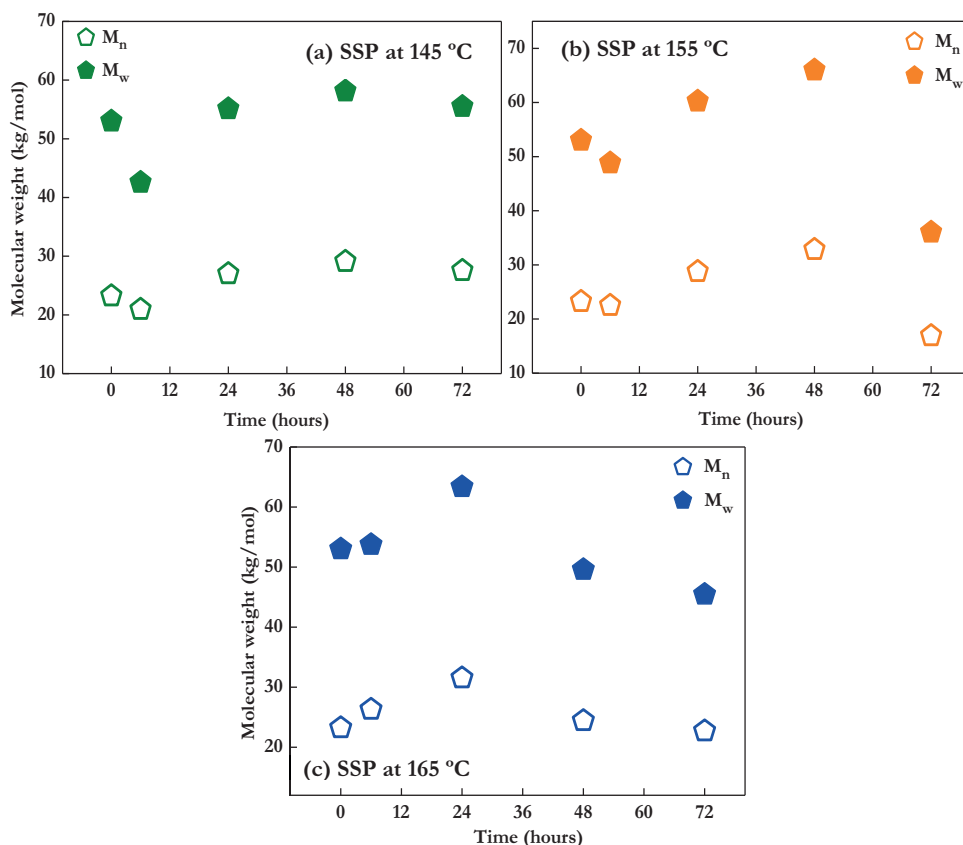
Fig. 4.12 Molecular weight as function of SSP time at **(a)** 145, **(b)** 155 and **(c)** 165 °C.

At 145 and 155 °C an initial molecular weight decrease was observed, followed by an increase exceeding the starting value. This decrease could have been caused by residual amounts of condensation products from the polymerization reaction reacting with the polymer, over time these were subsequently removed and the molecular weight increased. At 165 °C this drop in molecular weight was not observed, but given the increased reaction rate it is possible that such drop has taken place between the first two measuring points. At the same time the crystallization rate is expected to be faster at higher temperatures. This furthermore favors the rate of SSP, as the higher crystallinity after 6 hours in the case of 165 °C is expected to promote faster side-product removal, assuming a higher concentration of reactive endgroups in the amorphous phase.

Overall an optimum M_n was observed depending on each SSP temperature with the highest of all cases obtained at 155 °C after 48 hours (M_n=32.8 kg·mol^{-1}). Generally, a drop in molecular weight was registered from 72 hours at 145 and 155 °C and even sooner (48 hours) at 165 °C. With higher crystallinity (reached sooner at 165 °C) the mobility of the polymer chains is more limited, slowing down the reaction rate and hindering side-product diffusion.

In addition, the condensation product recovered at the latest stage of SSP was analyzed with NMR, revealing mainly glycolide and traces of lactide for all samples. This type of degradation reactions have been reported before for SSP of PLA at reduced pressure (via random chain scission or via chain end scission through a backbiting mechanism).[22,23]

The DSC heating curves (2nd run) of the samples taken at different SSP times and three reaction temperatures are presented in **Fig. 4.13**. Increasing SSP temperature and time led to higher degree of crystallinity (%X_c) irrespective of the molecular weight distribution. The %X_c, calculated from the normalized enthalpy of fusion of each heating curve was the highest for 165 °C after 72 hours with 35%. For 145 and 155 °C, %X_c of 28 and 29% were reached after the same time. Major changes in the glass transition temperature T_g were not detected with molecular weight variations and reorganization of the lamellae. In general, the T_g stayed between 39 and 41 °C. Although this part of the study provides initial observations on the SSP of PLGA copolymers, more experiments are required to tune other rate determining steps in the polymerization process (e.g. endgroup concentration and initial crystallinity) and achieve higher M_n and M_w increase.
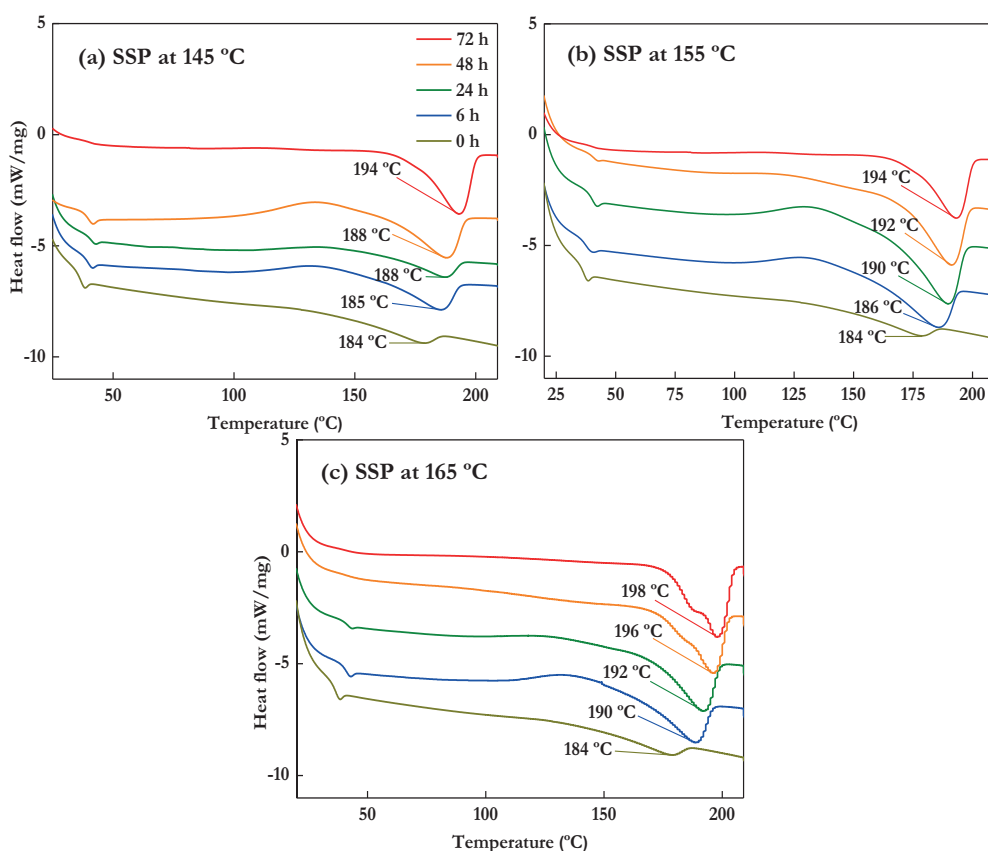

Fig. 4.13 DSC curves (10 °C·min⁻¹) for SSP products taken from t=0 up to t=72 hours at **(a)** 145, **(b)** 155 and **(c)** 165 °C.

4.3.1.7   Barrier properties

The oxygen (OP) and water permeability (WP) of PLGA$_{20/80}$ (M$_n$ = 27.2 kg·mol^{-1}) and PLGA$_{10/90}$ (M$_n$ = 30.0 kg·mol^{-1}) hot pressed films were measured. The same was done for PLLA and PET (RAMA). All films were prepared using the same method, which means no biaxial orientation was applied. The results are shown in **Fig. 4.14**.

Both PLGA copolymers show superior barrier performance for both oxygen and moisture compared to PLA and even PET. PLGA$_{20/80}$ exhibits a moisture permeability of 0.68 gr.mm.m^{-2}.day^{-1}.bar^{-1} and PLGA$_{10/90}$ has a moisture permeability of 0.31 gr.mm.m^{-2}.day^{-1}.bar^{-1}. These values are far superior compared to PLA (2.5 gr.mm.m^{-2}.day^{-1}.bar^{-1}) and modestly better than PET (0.83 gr.mm.m^{-2}.day^{-1}.bar^{-1}). For the oxygen permeability the numbers are even more impressive: for both PLGA copolymers the measured permeability is below 1 mm.cm^3.m^{-2}.day^{-1}.bar^{-1}, which is much better than both PLA (14.15 mm.cm^3.m^{-2}.day^{-1}.bar^{-1}) and PET (4.52 mm.cm^3.m^{-2}.day^{-1}.bar^{-1}).
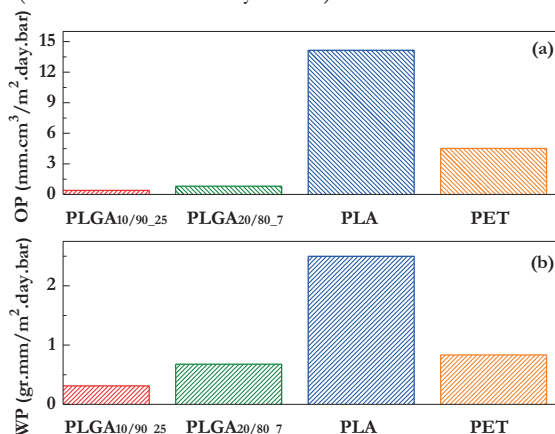
Fig. 4.14 Oxygen **(a)** and water **(b)** permeability for PLGA$_{10/90\_25}$ and PLGA$_{20/80\_7}$ measured at 30 ºC and 70% RH.

4.3.1.8   Tensile properties

For PLGA, the available information regarding mechanical properties is limited and studies on mechanical behavior have focused on lactide rich copolymers for biomedical applications. Although their degradability and biocompatibility makes them suitable candidates for the medical field, insufficient mechanical performance requires modification with other biocompatible materials.[24-28] In **Table 4.6** the average values for the ultimate strength (σ), elastic modulus (E) and elongation at break (ε) of PLGA$_{20/80}$ and PLGA$_{90/10}$ are given. For comparison the reported properties of PLA, PET and commercial PGA are also shown.

Table 4.6 Tensile properties of PLGA copolymers and other comparable polymers.

Material	Tensile strength σ (MPa)	Young's Modulus E (GPa)	Elongation at break ε (%)	M_w (kg·mol^{-1})	Ref.
PLGA$_{20/80\_7}$	42.7+-1.3	5.2+-654	5.7+-0.5	29.0[a]	this work
PLGA $_{10/90\_25}$	38.0+-3.1	6.1+-441	2.0+-0.2	35.1 [a]	this work
PLA	28	1.2	6.0	50	[29]
PET	50	1.7	4.0	30-80	[30]
PGA	83.3	n.r	3.7	n.r[b]	[31]
Kuredux[c]	109	7.0	2.1	n.r[b]	[32]

[a] After processing.
[b] n.r= not reported.
[c] PGA commercial resin produced by Kureha company.[32]

For both copolymers the tensile strength is lower than reported for PGA[31], although the tested samples here have M_w values lower than should be expected from industrial/commercial samples[32] or PGA prepared from ROP of glycolide[31], which are generally associated with high molecular weight. While PLGA$_{10/90}$ revealed a degree of crystallinity of 8.3 % in the DSC after processing the tensile specimens, the ones for PLGA$_{20/80}$ remained amorphous. The occurrence of more ordered crystalline regions can confer higher brittleness to the structure, with lower ability to absorb energy under stress and lower molecular diffusion, which promotes fast crack propagation. In fact, for both copolymers prepared within this study fracture occurred before observing plastic deformation. Still, σ is higher than PLA with higher M_w.

PGA is known to be very stiff with notably low elongation at break (2.1-3.7 %). Copolymerization with increasing amounts of lactic acid helps decrease the stiffness of the final material and increase, to some extent, the ability to undergo deformation (ductility). The elastic modulus is thus decreased from 7.0 GPa for PGA to 6.1 for PLGA$_{90/10}$ and 5.2 GPa for PLGA$_{20/80}$ (**Table 4.6**). The modulus *(E)* for both PLGAs is much higher than for PLA. Importantly, in both cases E is considerably higher than most commodity polymers (PP, HDPE, PP, PS, PVC)[33] and other degradable polyesters (PCL, PHB, PBS, PLA)[34]. In fact, the elastic modulus values for both of the tested PLGA copolymers are more closely related to those of some rigid engineering polymers and composites (e.g. PEEK, PAI, PC/PBT glass filled, POM mineral filled). Although higher elongation at break found for PLGA$_{20/80}$ compared to PLGA$_{10/90}$ and PGA suggests an increased ability of the copolymer to undergo deformation, both copolymers seem to deform in a brittle fashion as mentioned before, similarly to PGA and PLA. Even when PLA can exhibit variable mechanical properties for amorphous and semicrystalline polymers, the injection molding grade is in general known to exhibit elongation at break below 10% accompanied by brittle fracture.[35] Still, PLA is less rigid than pure PGA and slightly more flexible.

4.3.2 The role of p-cresol in the polycondensation of polyglycolic acid (PGA)

The synthesis method proposed earlier for PLGA was also tested for PGA. Although PGA is expected to dissolve in hexafluoroisopropanol (HFIP), none of the resulting products were readily soluble in this solvent for GPC analysis. Consequently, a treatment consisting of remelting the samples to posteriorly quench them in liquid nitrogen and then dissolve them in HFIP, while heating at 50 °C for about 12 hours, was required for all samples. Since the reaction mixture from the esterification stage for all the experiments is soluble in commonly used organic solvents (e.g. DMSO, CDlC$_3$), the progression could be followed with ^{1}H NMR.

Table 4.7 presents an overview of the reaction conditions, resulting molecular weight distributions and thermal properties for the prepared samples. At 0.1 mol% catalyst loading the use of 10 mol% of p-cresol in the reaction already caused a modest molecular weight improvement and when using 50 mol% the M_n is almost double compared to the case without solvent. When the solvent amount was increased to 75 mol% the resulting product (PGA$_5$) had a strong dark brown color and glycolide, accompanied by some PGA oligomers, was recovered as degradation product. By lowering the catalyst concentration to 0.05 mol% (PGA$_6$, PGA$_7$) while keeping other conditions constant, the molecular weight could still be improved with respect to no solvent and the side reactions observed before were reduced.

Table 4.7 Overview of reaction conditions, thermal transitions
(DSC, second heating scan at 10 ºC·min^{-1}), and molecular weight distribution (GPC) of PGA samples.

Sample	Solvent	Solvent amount (mol%)	Catalyst amount BuSnO (OH)	T_g (ºC)	T_m (ºC)	T_c (ºC)	ΔH_m (J·g^{-1})	X (%)	M_n (kg· mol^{-1})	M_w (kg· mol^{-1})
PGA$_1$	none	-	0.1	39	220	195	100.5	52	10.9	27.7
PGA$_2$	1,4-di methoxy benzene	10	0.1	41	220	191	79.9	42	11.2	26.4
PGA$_3$	p-cresol	10	0.1	42	219	194	98.6	52	14.2	29.0
PGA$_4$	p-cresol	50	0.1	41	220	196	96.9	51	16.7	33.4
PGA$_5$	p-cresol	75	0.1	40	221	184	97.1	51	n.d.	n.d.
PGA$_6$	p-cresol	50	0.05[a]	42	220	185	86.1	45	19.3	38.6
PGA$_7$	p-cresol	75	0.05[a]	41	220	183	100.1	52	24.2	49.0

[a] Catalyst added in two equal portions at the beginning of the reaction and before reducing pressure.
*All the reactions were carried out at 190-210 °C during the esterification stage and at 230 °C for the polycondensation. The reaction time was 10 hours in all cases.

The T_g (between 39 and 42 °C) and T_m (between 219 and 221 °C) for all samples remains similar regardless of the synthesis method and final molecular weight. These values correspond to previous reports in literature for the same type of polymer. Similarly, the crystallization of PGA does not appear to be strongly affected by the addition of solvent

during synthesis. The samples exhibited a degree of crystallinity between 42 and 52%. Before, it was shown that it fully crystallizes at standard cooling conditions (dT/dt = 10 °C·min^{-1}).[36]
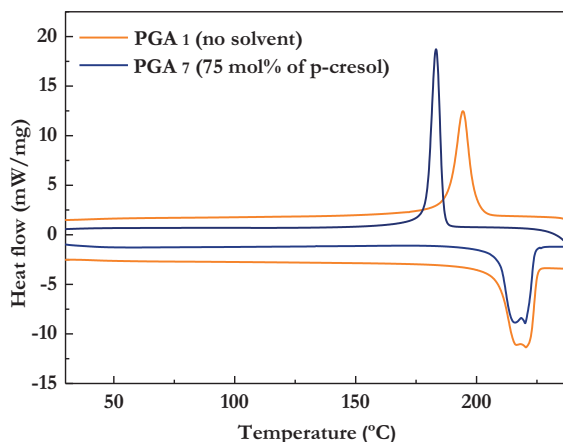
Fig. 4.16 DSC comparison of second heating scan from 20 to 235 °C and second cooling scan from the melt to room temperature (dT/dt = 10 °C·min^{-1}) for PGA$_1$ and PGA$_7$.

In **Fig. 4.16** the 2nd heating and cooling DSC scan of PGA prepared without solvent (PGA$_1$) is compared with PGA prepared with p-cresol (PGA$_7$). Although PGA$_1$ exhibited lower M$_n$ than PGA$_7$ with 11.0 vs 24.2 kg·mol^{-1} respectively, the T$_g$ (39 °C vs 41 °C), the T$_m$ (220 °C in both cases) and degree of crystallinity (52% in both cases) are comparable regardless of the synthesis conditions. The lower crystallization temperature observed for PGA$_7$ compared to PGA$_1$, could be due to small traces of residual p-cresol and/or decomposition products such as glycolide in the final product. They can act as plasticizers, delaying the crystallization rate. Still, the observed crystallization temperatures and ranges correspond to what has been reported previously for PGA.[37]

4.4   Applicability

P-Cresol and guaiacol have demonstrated to be beneficial to increase the molecular weight of PLGA and PGA via direct polycondensation. This synthesis route is not only more straightforward than the currently used ROP to produce the same type of materials, but also both solvents can be recycled and therefore reused for further polymerizations. Although emission of phenols and its derivatives into the environment have proven high toxicity, especially in aquatic ecosystems where they can remain for weeks[38], numerous studies have reported different types of phenol tolerant organisms (yeast, fungus and bacteria) that can contribute in their degradation in water and in soil.[39-41] Furthermore, phenols are already used in numerous applications including pesticides, dyes, coatings, and oil refining, among others. For guaiacol, besides its multiple uses in medicine and as flavoring agent, lower

hazard is associated in comparison to p-cresol. Although both are classified as sensitizing substances, high acute toxicity has been identified for p-cresol and the Environmental Protection Agency has categorized it as group C, possible human carcinogenic.

4.5   Conclusion

A new polycondensation route for the production of PGA homopolymer and PLGA copolymers directly from glycolic and *L*-lactic acid in the presence of p-cresol or guaiacol as reactive solvent was studied. The strategy was tested and validated for copolymers with an initial amount of 80 and 90 mol% of glycolic acid at a scale of up to 35 g. M_n values as high as 31.5 kg·mol^{-1} for $PLGA_{10/90}$ and 27.2 kg·mol^{-1} for $PLGA_{20/80}$ were attained using this method. This is an approximate threefold improvement compared to the values achieved in a typical direct polycondensation starting from GA and LA. Films prepared for barrier property assessment revealed a superior performance regarding water and oxygen permeability in comparison to PLA and PET. The polymerization method proposed here was also validated using racemic lactic acid, which led to results similar to *L*-lactic acid. Finally, SSP was demonstrated as a feasible alternative to further increase the molecular weight of PLGA copolymers produced in the presence of p-cresol. The polycondensation route presented in this work requires less time than other reported strategies to increase the molecular weight of similar type of polymers and it allows for solvent recycling for reuse.

4.6   Appendix

4.6.1 Thermal properties of PLGA copolymers synthesized with p-cresol
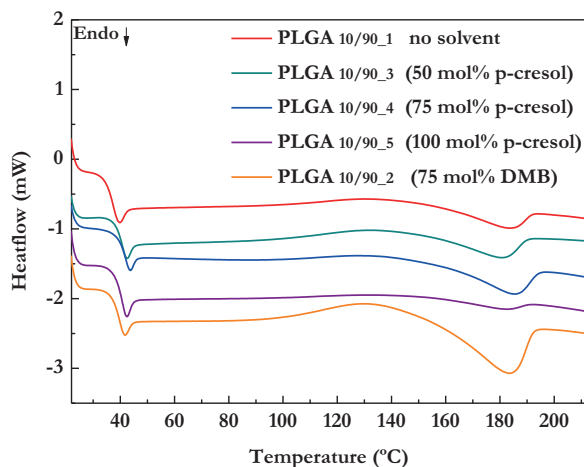

Fig. 4.17 DSC comparison of second heating scans (dT/dt = 10 C·min^{-1}) of $PLGA_{10/90}$ samples synthesized with variable amounts of solvent.
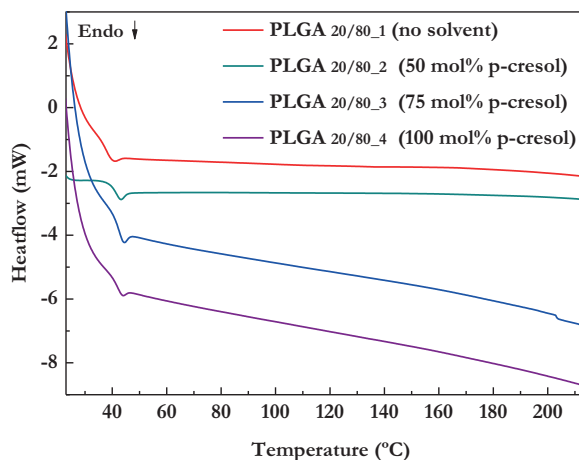
Fig. 4.18 DSC comparison of second heating scans ($dT/dt = 10$ C·min^{-1}) of PLGA$_{20/80}$ samples synthesized with variable amounts of solvent.

4.7 References

(1) Murcia Valderrama, M. A., van Putten, R.-J. & Gruter, G.-J. M. The potential of oxalic – and glycolic acid based polyesters (review). Towards CO$_2$ as a feedstock (Carbon Capture and Utilization – CCU). *Eur. Polym. J.* **2019**, *119*, 445-468. https://doi.org/10.1016/j.eurpolymj. 2019.07.036.

(2) Yamane, K.; Sato, H.; Ichikawa, Y.; Sunagawa, K.; Shigaki, Y. Development of an Industrial Production Technology for High-Molecular-Weight Polyglycolic Acid. *Polym. J.* **2014**, *46*, 769–775. https://doi.org/10.1038/pj.2014.69.

(3) Murcia Valderrama, M. A.; van Putten, R.-J.; Gruter, G.-J. M. PLGA Barrier Materials from CO$_2$. The influence of lactide comonomer on glycolic acid polyesters . *Appl. Polym. Mater.* **2020**, *2(7),* 2702-2718. https://doi.org/10.1021/acsapm.0c00315.

(4) Maharana, T.; Mohanty, B.; Negi, Y. S. Melt-solid polycondensation of lactic acid and its biodegradability. *Prog. Polym. Sci.* **2009**, *34*, 99–124. https://doi.org/10.1016/j.progpolymsci.2008. 10.001.

(5) Takahashi, K.; Taniguchi, I.; Miyamoto, M.; Kimura, Y. Melt/solid polycondensation of glycolic acid to obtain high-molecular- weight poly(glycolic acid). *Polymer.* **2000**, *41 (24)*, 8725–8728. https://doi.org/10.1016/S0032-3861(00)00282-2.

(6) Sanko, V.; Sahin, I.; Aydemir Sezer, U.; Sezer, S. A Versatile method for the synthesis of poly(glycolic acid): high solubility and tunable molecular weights. *Polym. J.* **2019,** *51 (7)*, 637–647. https://doi.org/10.1038/s41428-019-0182-7.

(7) Wang, Z.-Y.; Zhao, Y.-M.; Wang, F.; Wang, J. Syntheses of poly(lactic acid-co-glycolic acid) serial biodegradable polymer materials via direct melt polycondensation and their characterization. *J. Appl. Polym. Sci.* **2006**, *99 (1)*, 244–252. https://doi.org/10.1002/app.22468.

(8) Zhou, S.; Deng, X.; Li, X.; Jia, W.; Liu, L. Synthesis and characterization of biodegradable low molecular weight aliphatic polyesters and their use in protein-delivery systems. *J. Appl. Polym. Sci.* **2004**, *91 (3)*, 1848–1856. https://doi.org/10.1002/app.13385.

(9) Weinland, Daniel. Synthesis of rigid biobased polyesters: Overcoming the low reactivity of secondary diols in polyester synthesis. PhD thesis, University of Amsterdam, 2022.

(10) Pilato, L. *Phenolic Resins: A Century of Progress*; Springer Berlin Heidelberg, 2010. https://doi.org/10.1007/978-3-642-04714-5.

(11) Offenhauer, R. D. The direct esterification of phenols. journal of chemical education. division of chemical education. *J. Chem. Educ.* **1964**, *41(1)*, 39. https://doi.org/10.1021/ed041p39.

(12) Brito, Y. C.; Ferreira, D. A. C.; Fragoso, D. M. D. A.; Mendes, P. R.; Oliveira, C. M. J. D.; Meneghetti, M. R.; Meneghetti, S. M. P. Simultaneous conversion of triacylglycerides and fatty acids into fatty acid methyl esters using organometallic tin(iv) compounds as catalysts. *Appl. Catal. A Gen.* **2012**, 202–206. https://doi.org/10.1016/j.apcata.2012.07.040.

(13) de Mendonça, D. R.; da Silva, J. P. V.; de Almeida, R. M.; Wolf, C. R.; Meneghetti, M. R.; Meneghetti, S. M. P. Transesterification of soybean oil in the presence of diverse alcoholysis agents and Sn(IV) organometallic complexes as catalysts, employing two different types of reactors. *Appl. Catal. A Gen.* **2009**, 365 (1), 105–109. https://doi.org/10.1016/j.apcata.2009.06.002.

(14) Larkin, W.; Bossert, E. C.; Gibbon, Polyester compositions and organotin esterification catalysts therefor. EP0419254A2. March 27, 1989.

(15) Zhang, J.; Liang, Y.; Yan, J.; Lou, J. Study of the molecular weight dependence of glass transition temperature for amorphous poly(l-lactide) by molecular dynamics simulation. *Polymer.* **2007**, *48 (16)*, 4900–4905. https://doi.org/10.1016/J.POLYMER.2007.06.030.

(16) Weeks JJ. Melting temperature and change of lamellar thickness with time for bulk polyethylene. *J Res Natl Bur Stand A Phys Chem.* **1963**, *67A(5)*, 441-451. doi:10.6028/jres.067A.046.

(17) Bunn, C. W. The melting points of chain polymers. *J. Polym. Sci.* **1955**, *16 (82)*, 323–343. https://doi.org/10.1002/pol.1955.120168222.

(18) Masutani, K.; Kimura, Y. PLA synthesis. From the monomer to the polymer. *RSC Polym. Chem. Ser.* **2015**, *12*, 3–36. https://doi.org/10.1039/9781782624806-00001.

(19) Zeng, C.; Zhang, N. W.; Feng, S. Q.; Ren, J. Thermal stability of copolymer derived from L-lactic acid and poly(tetramethylene) glycol through direct polycondensation. *J. Therm. Anal. Calorim.* **2013**, *111 (1)*, 633–646. https://doi.org/10.1007/s10973-012-2542-9.

(20) Gilding, D. K.; Reed, A. M. Biodegradable polymers for use in surgery-polyglycolic/poly(actic acid) homo- and copolymers: 1. *Polymer.* **1979**, *20 (12)*, 1459–1464. https://doi.org/10.1016/0032-3861(79)90009-0.

(21) Feng, P.; Wang, H.; Lin, H.; Zheng, Y. Selective production of guaiacol from black liquor: effect of solvents. *Carbon Resour. Convers.* **2019**, *2 (1)*, 1–12. https://doi.org/10.1016/j.crcon.2018.07.005.

(22) Fukushima, K.; Kimura, Y. A novel synthetic approach to stereo-block poly(lactic acid). *Macromol. Symp.* **2005**, *224 (1)*, 133–144. https://doi.org/10.1002/MASY.200550612.

(23) Moon, S. Il; Kimura, Y. Melt polycondensation of L-lactic acid to poly(L-lactic acid) with Sn(II) catalysts combined with various metal alkoxides. *Polym. Int.* **2003**, *52 (2)*, 299–303. https://doi.org/10.1002/PI.960.

(24) Kobielarz, M.; Tomanik, M.; Mroczkowska, K.; Szustakiewicz, K.; Oryszczak, M.; Mazur, A.; Antończak, A.; Filipiak, J. Laser-modified PLGA for implants: in vitro degradation and mechanical properties. *Acta Bioeng. Biomech.* **2020**, *22 (1)*, 179–192. https://doi.org/10.37190/ABB-01532-2019-02.

(25) McKenna, E.; Klein, T. J.; Doran, M. R.; Futrega, K. Integration of an ultra-strong poly(lactic-co-glycolic acid) (PLGA) knitted mesh into a thermally induced phase separation (TIPS) PLGA porous structure to yield a thin biphasic scaffold suitable for dermal tissue engineering. *Biofabrication.* **2020**, *12 (1),* 015015. https://doi.org/10.1088/1758-5090/ab4053.

(26) Hong, D.; Song, B.; Kim, H.; Kwon, J.; Khang, G.; Lee, D. Biodegradable polyoxalate and copolyoxalate particles for drug-delivery applications. *Ther Deliv.* **2011**, *2(11)*, 1407–1417. https://doi.org/10.4155/tde.11.113.

(27) Buczynska, J.; Pamula, E.; Blazewicz, S. Mechanical properties of (poly(l-lactide-co-glycolide))-based fibers coated with hydroxyapatite layer. *J. Appl. Polym. Sci.* **2011**, *121 (6),* 3702–3709. https://doi.org/10.1002/app.34189.

(28) Ajalloueian, F.; Tavanai, H.; Hilborn, J.; Donzel-Gargand, O.; Leifer, K.; Wickham, A.; Arpanaei, A. Emulsion electrospinning as an approach to fabricate PLGA/chitosan nanofibers for biomedical applications. *Biomed Res. Int.* **2014**, 2014:475280. https://doi.org/10.1155/2014/475280.

(29) Engelberg, I.; Kohn, J. Physico-mechanical properties of degradable polymers used in medical applications: a comparative study. *Biomaterials.* **1991**, *12 (3)*, 292–304. https://doi.org/10.1016/ 0142-9612(91)90037-B.

(30) Langer, R. S.; Peppas, N. A. Present and future applications of biomaterials in controlled drug delivery systems. *Biomaterials.* **1981**, *2(4),* 201–214. https://doi.org/10.1016/0142-9612(81)90059-4.

(31) Chang, L. F.; Zhou, Y. G.; Ning, Y.; Zou, J. Toughening effect of physically blended polyethylene oxide on polyglycolic acid. *J. Polym. Environ.* **2020**, *28 (8)*, 2125–2136. https://doi.org/10.1007/ s10924-020-01752-5.

(32) Kureha Corporation. Kuredux-PGA-Technical Guidebook http://www.kuredux.com/pdf/Kuredux_technical_EN.pdf (accessed August 4, 2021).

(33) Delgado-Aguilar, M.; Puig, R.; Sazdovski, I.; Fullana-i-Palmer, P. Polylactic acid/polycaprolactone blends: on the path to circular economy, substituting single-use commodity plastic products. *Materials.* **2020**, *13 (11)*, 2655. https://doi.org/10.3390/ma13112655.

(34) Luzi, F.; Torre, L.; Kenny, J. M.; Puglia, D. Bio- and fossil-based polymeric blends and nanocomposites for packaging: structure-property relationship. *Materials,* **2019**, 12(3), 471. https://doi.org/10.3390/ma12030471.

(35) Sin, L. T.; Tueen, B. S. Mechanical properties of poly(lactic acid). in *Polylactic acid*; Elsevier, 2019, 167-202. https://doi.org/10.1016/b978-0-12-814472-5.00005-4.

(36) Yu, C.; Bao, J.; Xie, Q.; Shan, G.; Bao, Y.; Pan, P. Crystallization behavior and crystalline structural changes of poly(glycolic acid) investigated: via temperature-variable WAXD and FTIR analysis. *Cryst Eng Comm.* **2016**, *18 (40)*, 7894–7902. https://doi.org/10.1039/c6ce01623e.

(37) de la Cruz, L. I. S.; Rodríguez, F. J. M.; Velasco-Santos, C.; Martínez-Hernández, A.; Gutiérrez-Sánchez, M. Hydrolytic degradation and morphological characterization of electrospun poly(glycolic acid) [PGA] thin films of different molecular weights containing TiO_2 nanoparticles. *J. Polym. Res.* **2016**, *23 (6)*, 1–10. https://doi.org/10.1007/s10965-016-1002-9.

(38) Duan, W.; Meng, F.; Cui, H.; Lin, Y.; Wang, G.; Wu, J. *Ecotoxicol Environ Saf.* **2018**, *157*, 441-456. https://doi.org/10.1016/j.ecoenv.2018.03.089.

(39) Sachan, P.; Madan, S.; Hussain, A. Isolation and screening of phenol-degrading bacteria from pulp and paper mill effluent. *Appl. Water Sci.* **2019**, *9 (4)*, 3. https://doi.org/10.1007/s13201-019-0994-9.

(40) Bera, S.; Roy, A. S.; Mohanty, K. Biodegradation of phenol by a native mixed bacterial culture isolated from crude oil contaminated site. *Int. Biodeterior. Biodegrad.* **2017**, *121*, 107–113. https://doi.org/10.1016/j.ibiod.2017.04.002.

(41) Gu, Q.; Wu, Q.; Zhang, J.; Guo, W.; Wu, H.; Sun, M. Community analysis and recovery of phenol-degrading bacteria from drinking water biofilters. *Front. Microbiol.* **2016**, *7*, 495. https://doi.org/ 10.3389/fmicb.2016.00495.

CHAPTER 5

PLA synthesis via polycondensation using aromatic solvents

Abstract

Poly(lactic acid) (PLA) leads the current biobased polyester market and its demand is expected to continue increasing steadily. High molecular weight PLA is commercially synthesized via ring opening polymerization (ROP) of lactide, the cyclic dimer of lactic acid. Due to the intermediary steps involved in this process, the production is still relatively costly, which prompts the need to develop cost-effective and more straightforward strategies. Our group has previously researched the use of reactive phenolic solvents to improve the molecular weight of polyesters with high secondary diol content (isosorbide), as well as polyglycolic acid and poly(lactic-co-glycolic acid) (>80% glycolic acid content) via polycondensation reactions that generally would produce material of insufficient M_n (<11 kg·mol^{-1}). Consequently, the same route was evaluated for the synthesis of PLA via the polycondensation of L-lactic acid in the presence of phenol. Although M_w and M_n of up to 43.7 and 18.1 kg·mol^{-1} were reached adding 10 mol% of phenol and SnOct$_2$ as catalyst, a similar improvement with M_w and M_n of up to 44.1 and 20.5 kg·mol^{-1} was obtained with 25 mol% of a non-reactive solvent. Unexpectedly, higher amounts of phenol led to decreasing molecular weight and facilitated lactide formation. Racemization was observed, irrespective of the use of phenol, but the extent was lower when using SnOct$_2$ as catalyst instead of BuSnO(OH). Also, PLA prepared with phenol exhibited slightly faster thermal degradation than the one prepared without it. Even though the synthesis route with phenols is not as efficient for molecular weight improvement in PLA as has been reported for PLGA copolymers and other polyesters, it could be used alternatively for lactide production. Yet, it would require further optimization to determine its potential in comparison with the methods already used industrially.

5.1   Introduction

Poly(lactic acid) (PLA) currently leads the biobased polyester market. By 2020, it reached a global production capacity close to 335,000 tons[1], which represented 19% of the world's annual production volume of the group involving degradable and non-degradable bio-based plastics.[2] Although this corresponds to less than 1% of the total amount of plastic produced annually, PLA's demand is expected to continue rising steadily in the upcoming years as a result of new government policies encouraging the use of non-fossil derived polymers, combined with the increasing plastic demand and feedstock availability.

Lactic acid (2-hydroxypropanoic acid), the constituent unit of PLA, can be produced via fermentation or chemical synthesis.[3] At present, most of it is derived from bacterial fermentation of carbohydrates, using homolactic organisms (e.g. Lactobacillus).[4] Lactic acid exists as two enantiomers: L-and D-lactic acid. Therefore, PLA can be synthesized in three

general forms: poly (*L*-lactic acid) (PLLA), poly(*D*-lactic acid) (PDLA), and poly(*DL*-lactic acid) (PDLLA).[5]

Lactic acid can be directly converted into a polyester via a polycondensation reaction.[6] This is an equilibrium reaction where water generated as side product must be distilled out of the system to shift the equilibrium towards the product.[7] Water removal becomes challenging as the reaction progresses and the viscosity of the reaction mixture increases. This, in addition to the fact that esters from a secondary alcohol have shown to be more prone to the reverse reaction with water[8], leads to low molecular weights and consequently to polymers with poor mechanical properties.[9] Therefore, polycondensation of lactic acid is not a viable route for the industrial production of PLA.

Currently, commercial grade PLA is synthesized through ring opening polymerization (ROP) of lactide, the cyclic dimer of lactic acid.[10] Lactide is produced through the depolymerization of low molecular weight PLA.[11,12] In comparison to the direct polycondensation route, ROP offers the advantages of an easier control of molecular weight distribution and limitation of termination and transfer reactions (depending on the catalyst and reaction conditions).[13] Nevertheless, the intermediary steps involved in the overall process lead to a relatively costly production and hence a competitive disadvantage for PLA compared to fossil-based polymers. Considering this, it is highly desirable to develop strategies for producing commercial grade PLA through cheaper and more straightforward routes.

Polycondensation is still attractive as a simplified process starting directly from lactic acid. Hence, researchers have proposed strategies to use it for the production of high molecular weight PLA.[5,14-16] Although a M_n of up to 39 kg·mol^{-1} has been reported, the required reaction times are very long (24-50 hours) and multiple steps are often required. In previous research by our group[17,18] on polyesters with high secondary diol content (isosorbide), as well as polyglycolic acid and poly(lactic-co-glycolic acid) (>80% glycolic acid content)[17], reactive phenolic solvents were shown to strongly improve the molecular weights in polycondensation reactions that otherwise would not produce material of sufficient M_n. These findings were compared to those obtained after testing non reactive solvents and still the resulting molecular weights were consistently much higher when using reactive phenols.

Consequently, testing this same strategy for the synthesis of PLA, was a logical continuation of this research topic. This approach, using (substituted) phenols as reactive solvents, was applied to PLA synthesis to increase the molecular weight of PLA through direct polycondensation of *L*-lactic acid. Phenols are compounds in which a hydroxyl group is directly connected to the carbon atom of a benzene ring. As a consequence they are considered as excellent leaving groups in (poly)esterification reactions.[19] Regular phenol (C_6H_5OH) is the most obvious member of the phenol family.[20] It is widely used in the manufacture of products such as herbicides, fungicides, paint, insulation materials, adhesives, rubber, ink, dyes, explosives, perfumes, detergents, and it is a raw material for

producing aspirin.[21] Most of the phenol currently produced is synthesized through the catalytic alkylation of benzene using propylene followed by partial oxidation to phenol and acetone (the Hock Process).[22] However, alternative methods for producing benzene-free phenol are being explored.[23] Although the use of solvents has been reported for obtaining higher molecular weight PLA[24-26], with (substituted) phenols improved molecular weights can be obtained and their use in the direct polycondensation of lactic acid has not been reported yet. Notably, depending on the reaction conditions and type of catalyst, varying degrees of racemization have been observed during polycondensation of lactic acid in the presence of solvents.[25,26] The effect of phenol in the polycondensation of *L*-lactic acid was studied by varying the amount and comparing the results to cases with non- or less reactive (non-phenolic) solvent and a solvent-free synthesis. Additionally, temperature, solvent amount and catalyst-type were varied.

5.2   Experimental section

5.2.1   Materials

L-Lactic acid (L-LA) (90% solution in water), phenol (99%), 1,4-dimethoxybenzene and guaiacol (2-methoxyphenol, 99%) were purchased from ACROS Organics. Butyl stannoic acid (BuSnO(OH)) (97%), tin(II) 2-ethylhexanoate (Sn(Oct)$_2$), tin(II) chloride, p-toluenesulfonic acid (pTSA) and deuterated chloroform (DMSO-d$_6$) were obtained from Sigma Aldrich. All chemicals were used without additional purification.

5.2.2   Synthesis of PLA

The polymerization setup consisted of a 250 mL three necked glass reactor, fitted with a mechanical stirrer, a nitrogen inlet and a condenser. In a typical synthesis lactic acid solution, 0.1 mol% of BuSnO(OH) catalyst and the required amount of solvent (in mol% relative to the total monomer loading) were added to a reactor conditioned in an oil bath. The reaction mixture was heated at 190 °C and constantly stirred under a nitrogen flow at atmospheric pressure for up to 23 hours. Subsequently the temperature was increased to 200 °C and the pressure was gradually reduced (in intervals of 15 minutes) from 400 to 1 mbar. The reaction was maintained at 1 mbar for 30 minutes. The products were recovered and ground for analysis. Experiments in the absence of solvent and with 1,4-dimethoxy benzene were also assessed. Additional experiments were performed with other catalysts at variable reaction temperatures.

5.2.3   Analytical techniques

The reaction progression and structure of all samples was studied with ^{1}H NMR by recording their spectra in DMSO-d$_6$ using a Bruker AMX 400 (^{1}H, 400,13 MHz). The extent

of racemization in three of the PLA samples synthesized at different conditions was recorded with ^{13}C NMR in DMSO-d$_6$ in a Bruker Avance 500.

The molecular weight distribution was measured with a Merck-Hitachi LaChrom HPLC system, equipped with two PL gel 5 μm MIXED-C (300×7.5 mm) columns, using hexafluoroisopropanol as the mobile phase and poly(methyl methacrylate) (PMMA) calibration standards. The reported molecular weights were calculated with the software package Wyatt Astra 6.1.

The thermal transitions were measured with a DSC 3+ STARe (Mettler Toledo). Typically, about 5 mg of sample was weighed in a sealed 40μm aluminum crucible. All samples were heated from room temperature to 180 °C under nitrogen atmosphere (50 mL·min^{-1}) at 10 °C·min^{-1} and subsequently cooled down to 25 °C at the same rate. The same program was repeated a second time and the thermal transitions were taken from the resulting curve.

The thermal stability was determined using a TGA/DSC 3+ STARe system (Mettler Toledo). Approximately 6 mg of polymer was weighed in a sealed aluminum sample vessel (40μm). The samples were subsequently heated from room temperature to 450 °C (dT/dt = 10 °C·min^{-1}) under nitrogen atmosphere with a flow rate of 50 mL·min^{-1}.

5.3 Results and discussion

5.3.1 The role of phenol on the polycondensation of *L*-lactic acid

The effect of adding a reactive solvent on the polycondensation of *L*-LA was studied using variable amounts of phenol (**Scheme 5.1**). The choice of solvent was determined by the reaction temperatures, which are typically between 180 and 200 °C (oil temperature). Under these conditions, phenol remains in the reaction mixture during esterification and it can be removed efficiently under vacuum during polycondensation.
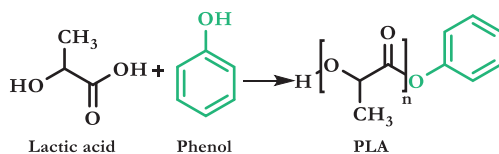
Scheme 5.1 General synthesis route of PLA in the presence of phenol.

Table 5.1 presents an overview of the reaction conditions, molecular weights and thermal transitions of the synthesized PLA samples. As expected, experiments without solvent typically result in low M_n (M_n = 10.6 kg·mol^{-1}).

Table 5.1 Overview of reaction conditions, resulting molecular weight distribution and thermal characterization of PLA samples. All the obtained PLA samples were amorphous.

Sample	Solvent type	Solvent amount (mol%)[a]	Catalyst	Catalyst amount (mol%)[a]	T (°C)	t (h)	M_n (kg·mol⁻¹)	M_w (kg·mol⁻¹)	T_g (°C)
PLA_0	none	0	BuSnO(OH)	0.1	190-200	23+2[b]	10.6	23.8	46
PLA_1	phenol	5					15.5	33.0	50
PLA_2	phenol	10					17.8	36.6	51
PLA_3	phenol	25					16.0	33.2	49
PLA_4	phenol	50					8.2	20.4	43
PLA_5	1,4-dimethoxy benzene	25					20.5	44.1	50
PLA_6	1,4-dimethoxy benzene						14.5	33.3	48
PLA_7	guaiacol	10					13.4	28.1	48
PLA_8	phenol		Sn(Oct)₂		200-180		12.2	27.8	45
PLA_9	phenol				200-190		15.1	30.5	48
PLA_10	phenol				190-200		16.5	40.5	48
PLA_11	phenol				200-180		16.6	39.6	48
PLA_12	phenol				200-190		18.2	43.7	48
PLA_13	phenol		SnCl₂		190-200		16.0	34.0	47
PLA_14	phenol				200-180		9.2	19.4	44
PLA_15	phenol				200-190		13.3	26.5	45
PLA_16	phenol	10	BuSnO(OH)	0.05	190-200	23+2[b]	17.2	35.8	50

[a] Relative to the total monomer load.

[b] 23 hours for esterification plus 2 hours at reduced pressure.

Fig. 5.1 a and **b** show the effect of different solvent concentrations on the molecular weight distribution of PLA samples prepared at the same reaction time and temperature. Initially, the phenol concentration was varied from 0 to 50 mol% relative to the initial *L*-lactic acid loading, using BuSnO(OH) as catalyst (0.1 mol%).
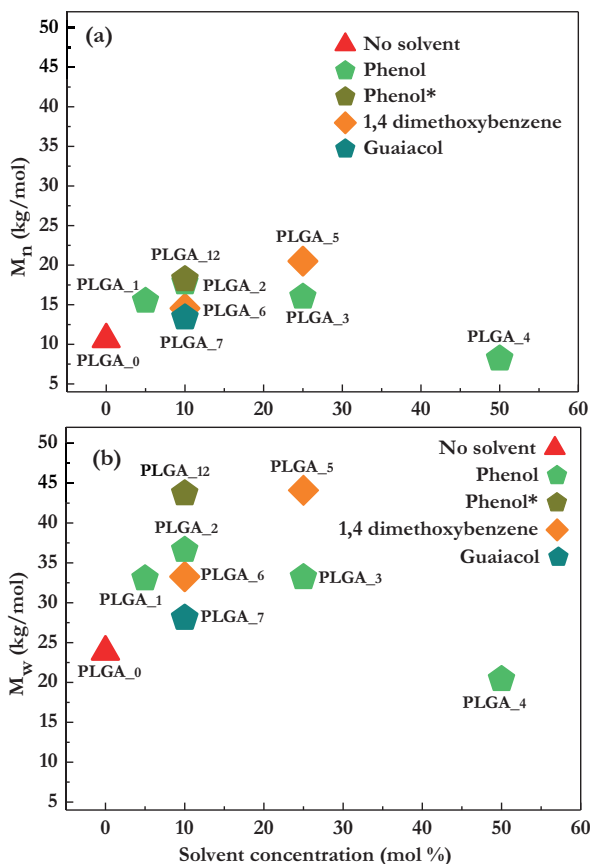
Fig. 5.1 Effect of solvent concentration on the **(a)** M_n and **(b)** M_w of PLA. For ***** $Sn(Oct)_2$ was used as catalyst instead of BuSnO(OH).

An optimum M_n of 17.8 kg·mol^{-1} was found with 10 mol% of phenol (PLA_2), which was similar to that obtained with $Sn(Oct)_2$ (PLA_10 M_n=16.5 kg·mol^{-1}) at equivalent conditions. Slightly higher molecular weight (PLA_12 M_n= 18.2 kg·mol^{-1}) could be achieved with $Sn(Oct)_2$ by increasing the esterification temperature. However, this catalyst led to broader molecular weight distributions (PDI up to 2.45) than with BuSnO(OH). This result is very different from those obtained with PLGA copolymers, researched previously using a similar strategy. There for PLGA copolymers with high glycolic acid/lactic acid ration, the optimum molecular weight was obtained with 75 mol% (relative to the total feed of acids) of phenolic solvent.

In this study, the use of non-reactive solvent showed molecular weight improvement when its amount was increased from 10 to 25 mol%. In fact, when using 25 mol% of 1,4-dimethoxy benzene, the molecular weight (PLA_5 M_n=20.5 and M_w=44.1 kg·mol^{-1}) was slightly higher than with phenol. This outcome was unexpected considering that in similar research with PLGA copolymers cited previously, the same non-reactive solvent (1,4-dimethoxybenzene) evaluated for the polycondensation, showed to be much less effective in improving the molecular weight than the substituted phenols.

Adding phenol helped reducing the viscosity of the reaction mixture compared to a typical polycondensation. As a consequence, better heat transfer was achieved throughout the polymerization and removal of water formed as condensation product was improved due to the formation of an azeotropic mixture with a boiling point of 99.8 °C. When phenol reacted with acid chain endgroups, phenyl ester terminated chains were produced, which were expected to be more reactive during polycondensation with secondary alcohol of lactic acid in comparison to carboxylic endgroups obtained in a typical polycondensation.

Fig. 5.2 shows two NMR spectra from the synthesis of sample PLA_2: **(a)** the reaction medium at the end of the esterification (after 23 hours at 190 °C) with 10 mol% of phenol and **(b)** the final product obtained after 25 hours of reaction. The peak assignments are presented in **Table 5.2.**
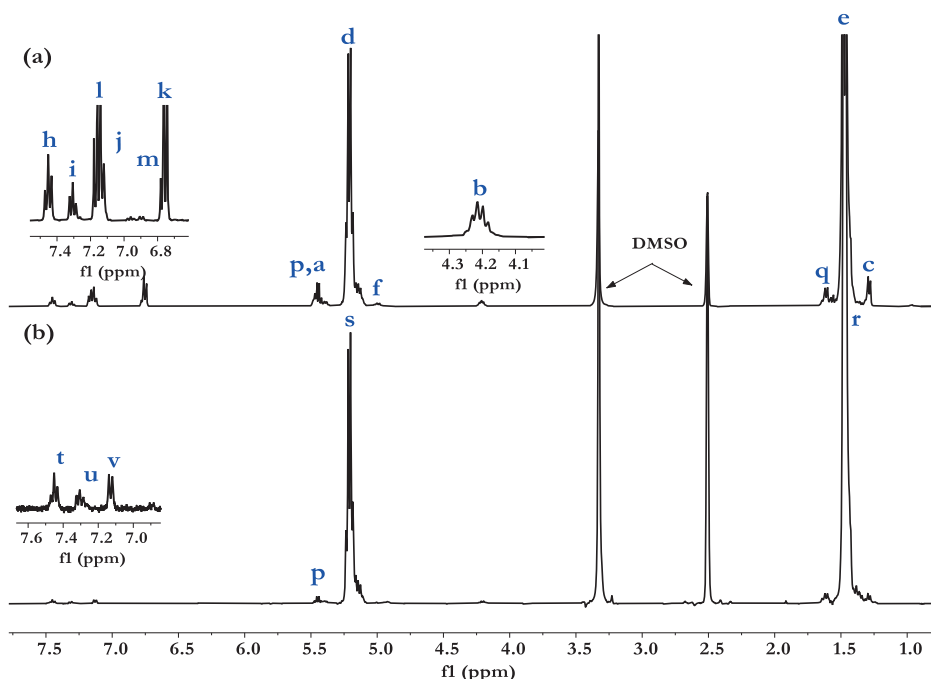
Fig. 5.2 ^{1}H NMR (DMSO-d$_6$) of **(a)** the reaction mixture after 23 hours (at the end of the esterification step) using 10 mol% of phenol and **(b)** the resulting PLA after 25 hours.

Table 5.2. ^{1}H NMR chemical shifts in DMSO-d_6 of **(a)** the reaction mixture after 23 hours of esterification with 10 mol% of phenol and **(b)** the resulting PLA product after polycondensation.

(a) Reaction mixture after 23 hours

Assignment	Chemical shift (ppm)	Assignment	Chemical shift (ppm)	Assignment	Chemical shift (ppm)
a	5.42	f	4.99	l	7.12-7.18
b	4.22	h	7.46	m	6.76
c	1.29	i	7.31	q	1.60
d	5.21	j	7.13	p	5.42-5.47
e	1.48	k	6.74		

(b) Polylactic acid

r	1.48	t	7.46	v	7.31
s	5.21	u	7.13	p	5.45

In **Fig. 5.2 (a)**, the two peaks at 7.46 (h) and 7.31 (i) ppm, corresponding to the CH ring protons from phenol bound to L-LA, indicate the formation of phenyl esters in the reaction medium. Peaks at 6.74 ppm (k), 6.76 ppm (m) and at 7.12-7.18 ppm (l), from the ring protons corresponding to the free phenol, show that unreacted solvent remains in the reaction mixture during the esterification step. The highest intensities around 5.21 (d) and 1.28 ppm (e), were assigned to the CH and CH$_3$ protons of the repeating units of oligomeric PLA. The CH attached to the terminal hydroxyl group (b), assigned to the resonance at 4.22 ppm, was used as reference to determine the ratio between hydroxyl and phenyl ester endgroups. After 23 hours reaction time this ratio was 1.5 while with 25 and 50 mol% of phenol a ratio of 1 was achieved after the same reaction time.

In **Fig. 5.2 b**, the NMR spectra of the resulting PLA shows the proton peaks of the CH and CH$_3$ repeating units at 1.48 (r) and 5.21 ppm (s) respectively. The small peaks visible between 7.13 and 7.46 ppm, corresponding to the terminal phenol ring protons, confirm the formation of phenyl terminated PLA. Additionally, the quartet observed between 5.42 and 5.47 ppm in **Fig. 5.2 (a)** and **(b)**, corresponds to the CH proton in the lactide ring. About 2 mol% of lactide was found in this PLA and, in fact, this side product was already observed for all the samples prepared with and without phenol before starting the stage at

reduced pressure. Also, when high amounts of phenol were added (e.g. 50 mol%), lactide crystals were also recovered in the receiver together with the phenol distilled out. Hence, the peaks observed in the ^{1}H NMR spectra do not necessarily reflect the actual amount of lactide produced during polycondensation. The presence of lactide is also reported after ring opening polymerization and is removed under vacuum in order to produce resin with a residual lactide content below 1%.[27]

During esterification L-LA can undergo oligomerization (by reacting with itself) and it can react in parallel with the phenol present in the reaction medium (**Scheme 5.2**). In the first case chains with OH and carboxylic acid endgroups are formed while the second leads to phenyl esters with OH and phenyl terminal groups. This interaction can continue until no more lactic acid is left in the mixture and all has been converted to phenyl esters. Lactide can also form here via the intramolecular transesterification of lactic acid dimers or by breaking down longer oligomers.[28] These reactions are in equilibrium. Additionally, lactide formation appeared to be further favored by increasing solvent concentration in the reaction medium. The above suggests that phenol terminated LA dimers possibly react faster to lactide than LA dimers lacking this phenol ester functionality. An additional important factor is that instead of water, phenols are released upon both polycondensation and lactide formation, which reduces the back reaction to lactic acid or a monoesters.

In the following step, the formed phenyl esters undergo transesterification with exchange between the ester and terminal hydroxy groups. To drive the equilibrium towards increasing molecular weight, phenol must be removed from the system.
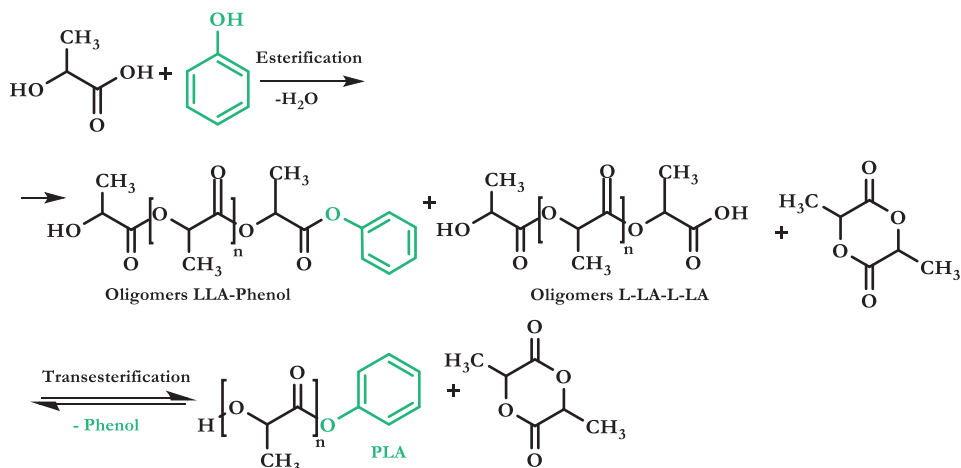
**Scheme 5.2** Proposed reaction path for the phenol assisted polymerization of PLA.

Based on the previously mentioned research with substituted phenols for the polycondensation of PLGA copolymers[17], it made sense that full conversion of *L*-LA to phenyl esters would be the ideal scenario to proceed with the transesterification. This was based on the initial assumption of higher reactivity of the phenyl ester endgroups compared

to terminal carboxyl groups found in a typical PLA polycondensation. Yet the results obtained here showed a different trend and imply that the transesterification is limited most likely due to the secondary OH group contained in the formed phenyl esters. In general, reactive hydroxyl and phenyl endgroups are still observed in the ^{1}H NMR spectra of the resulting PLA products. Hence, a higher amount of bound phenol during esterification does not necessarily mean higher molecular weight in the end product. This is especially relevant with increasing amounts of solvent in the reaction medium.

Typically, phenol was distilled out of the system as the transesterification proceeded with an exchange between the OH and phenyl terminal groups. With higher amounts of phenol (both bound to L-LA and free), its removal took longer, which increased the chance of backwards and/or decomposition reactions taking place. This appears to facilitate lactide formation. In sample PLA_2 with 10 mol% of phenol added, for example, around 2 mol% of lactide was found in the resulting product, while in PLA_4, with 50 mol% of phenol, 5 mol% of lactide was detected. This is only a rough indication of the actual amount of side product. Compared to 50 mol% phenol experiments, visually almost no lactide was accumulated in the distillation head or receiver when 10 mol% of phenol was added. In the former lactide was also found together with phenol in the receiver. In fact, it appears that at 200 °C, which is the temperature used for the transesterification, depolymerization to lactide is a more favored reaction than chain growth polycondensation. Even when the catalyst load was reduced from 0.1 to 0.05 mol%, lactide formation was shown without an improvement in molecular weight (M_n of 17.2 and 17.8 kg·mol^{-1} for PLA_2 and PLA_16 respectively). **Fig. 5.3** presents the influence of M_n on the T_g of the same group of PLA samples presented in **Fig. 5.1**. The samples exhibited T_g between 43 and 51 °C, with the highest T_g for the sample synthesized with 10 mol% of phenol and catalyzed by BuSnO(OH) (PLA_2).
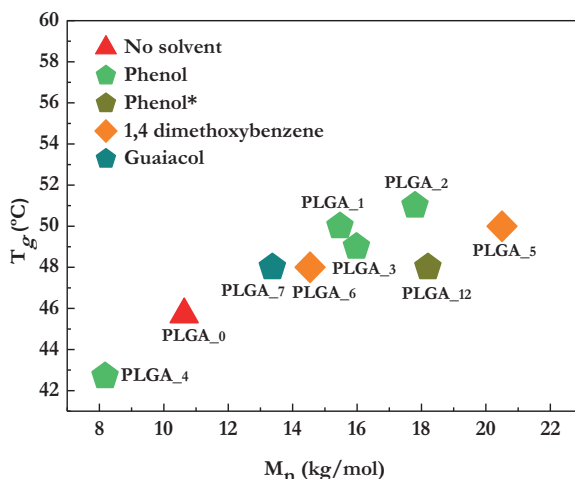
Fig. 5.3 M_n as function of T_g for PLA samples synthesized without or with different types of solvents. For ***** Sn(Oct)$_2$ was used as catalyst instead of BuSnO(OH).

In general, the T_g of the resulting samples was lower than that reported for commercial PLA (around 60 °C). Although the samples were prepared with L-LA, none of them exhibited semi-crystallinity in the second DSC scan (dT/dt = 10 °C·min⁻¹). Apart from insufficient molecular weight, the presence of lactide traces as side product can also hinder the slow crystallization already known for PLA. As it was described before, lactide was typically found in the resulting polymers. It can act as plasticizer and consequently reduce the T_g of PLA, which could explain the variations observed for samples with similar M_n (PLA_2,5,12). These variations can also be connected to the different polydispersity indexes in those cases.

The degree of racemization in PLA can also influence significantly its crystallization rate and thermal transitions together with other physical properties, such as density and mechanical behavior. Therefore, racemization of *L*-lactic acid in PLA was evaluated for two samples prepared with 10 mol% of phenol (PLA_2 and PLA_10), in comparison to PLA synthesized without solvent (PLA_0). The samples were prepared with either BuSnO(OH) or Sn(Oct)₂ as catalyst. **Fig. 5.3** presents the carbonyl region in the ¹³C NMR spectra of the evaluated samples. Although in all cases optically pure *L*-LA was used as starting monomer, the small signals between 169.3 and 169.6 ppm on the right side of the carbonyl group peak show disturbances in the stereoregularity of the resulting products. These signals correspond to sequences of isotactic and syndiotactic units and are consistent with the ones previously reported for the racemization of PLA.[29,30] Their integral ratio was used to determine the degree of racemization presented in **Table 5.3**.
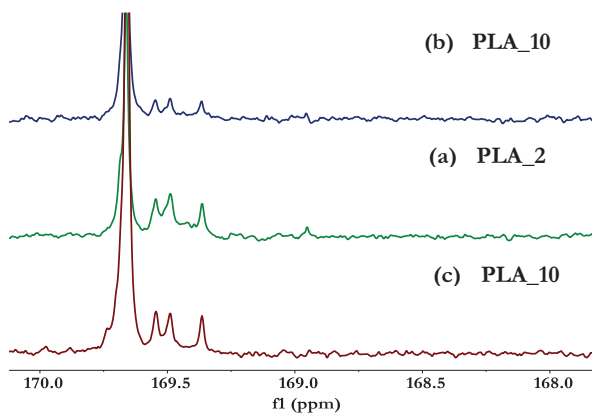
Fig. 5.3 Comparison of carbonyl region in ¹³C NMR of PLA samples prepared **(a, b)** with and **(c)** without phenol.

The stereoregularity of PLA can be disturbed not only by the type of monomer but also by reaction conditions, catalyst type and concentration, among other factors. Samples PLA_2 and PLA_10, prepared with 10 mol% of phenol and a resulting degree of racemization of 20 and 19% respectively, suggest that the addition of phenol for the synthesis has a negligible effect on racemization.

At equivalent reaction time, temperature and catalyst concentration, BuSnO(OH) induces more racemization than Sn(Oct)$_2$. Although the latter is known as a preferred catalyst to avoid racemization in PLA, the ester interchange reactions required for this exchange to occur, can still be favored by the reaction temperature used in this example and exposure to vacuum during polycondensation. Therefore, optimized reaction conditions are required to decrease this effect. Lactic acid can also undergo racemization in ROP with this same catalyst. It can be minimized and even suppressed with lower catalyst concentration, shorter reaction time (lower conversion), very high monomer purity.[31,32]

Table 5.3. Racemization degree of PLA samples prepared at different conditions.

| Sample	Solvent type	Solvent amount (mol%)*	Catalyst type	Catalyst amount (mol%)	Degree of racemization (%)
PLA_10	phenol	10	Sn(Oct)$_2$	0.1	13
PLA_2	phenol	10	BuSnO(OH)	0.1	20
PLA_0	-	-	BuSnO(OH)	0.1	19

*Relative to the total monomer load.

The results presented so far suggested that conducting the polycondensation of lactic acid in the presence of a small amount of phenol can help increase the resulting molecular weight to some extent. Contrary to previous research on PLGA, moderate amounts of a non-reactive solvent, like 1,4-dimethoxy benzene, led to a similar improvement. Overall, the balance between molecular weight increase and lactide formation must be controlled by carefully tuning the conditions, particularly considering that increasing phenol addition seems to benefit lactide production Yet, lactide in high yield can also be produced by esterification and subsequent thermal depolymerization of lactic acid at between 200 and 215 °C and reduced pressure, without the need of an additional solvent.[28] Therefore, this strategy does not offer an obvious advantage over existing ones. Hypotheses have been proposed on why this strategy was not as successful with lactic acid as it was with other polyesters studied previously, which require further investigation.

5.3.2 The effect of temperature on the polycondensation of PLA

With the purpose of favoring the chain growth reaction while trying to reduce the lactide formation, two more catalysts were evaluated together with BuSnO(OH) at variable temperatures. In all cases, the indicated initial temperature (between 190 and 210 °C) was maintained constant during esterification and it was subsequently increased or decreased before starting the step at reduced pressure. All the reactions were conducted with 10 mol% of phenol and 0.1 mol% of catalyst.

The comparison of the resulting molecular weight distribution of PLA prepared with three different catalysts at various temperatures is presented in **Fig. 5.4**. Sn(Oct)$_2$ showed the best performance over the entire range of tested temperatures.

Although the highest M_n of 18.2 kg·mol^{-1} reached with Sn(0ct)$_2$ was comparable with that obtained using BuSnO(OH) (17.8 kg·mol^{-1}), the M_w was overall higher with Sn(Oct)$_2$. Higher polydispersity was found with decreasing transesterification and polycondensation temperature. Sn(Oct)$_2$, known as a strong transesterification catalyst, is in fact not only used to efficiently promote depolymerization of oligomeric PLA into lactide but also for its ring opening. Here, it is thought that Sn(Oct)$_2$ was also involved in catalyzing the ring opening of some of the lactide already present in the reaction medium (formed in the esterification and formed later during transesterification). In this case, free phenol present in the mixture or any source of free OH group could initiate the ring opening of the six membered lactide ring. Furthermore, for BuSnO(OH), a transesterification temperature below 200 °C led to a slower polycondensation rate and a detrimental effect on the molecular weight. With SnCl$_2$, a well-known catalyst for PLA polycondensation, the highest M_n of 16.0 kg·mol^{-1} was obtained at 190-200 °C. The other temperature ranges were too low for transesterification and the resulting molecular weights were the lowest obtained in this set of experiments.
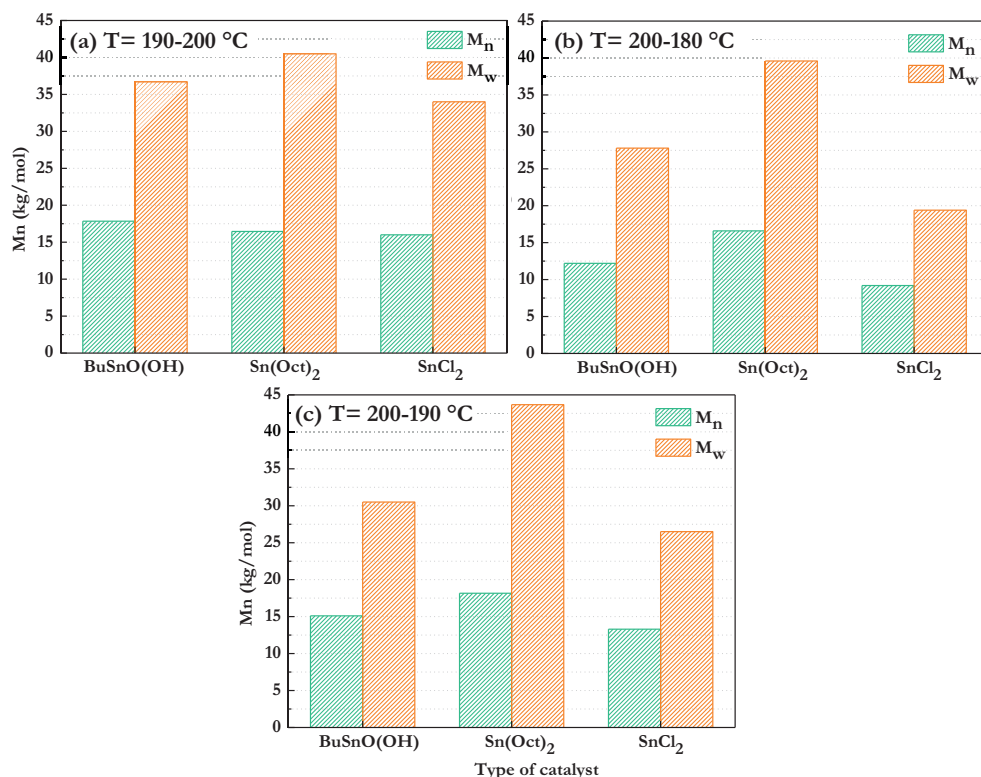
Fig. 5.4 Molecular weight distribution obtained for PLA synthesized with BuSnO(OH), Sn(Oct)$_2$ and SnCl$_2$ at variable temperature ranges: **(a)** 190-200 °C, **(b)** 200-180 °C and **(c)** 200-190 °C.

5.3.3 The effect of phenol on the thermal stability of PLA

To determine the impact on thermal degradation by the presence of phenyl ester endgroups in the resulting PLA, samples prepared at different reaction conditions were submitted to thermogravimetric analysis (TGA; **Table 5.4**). **Figure 5.5** shows the weight loss percentage as a function of temperature over time.
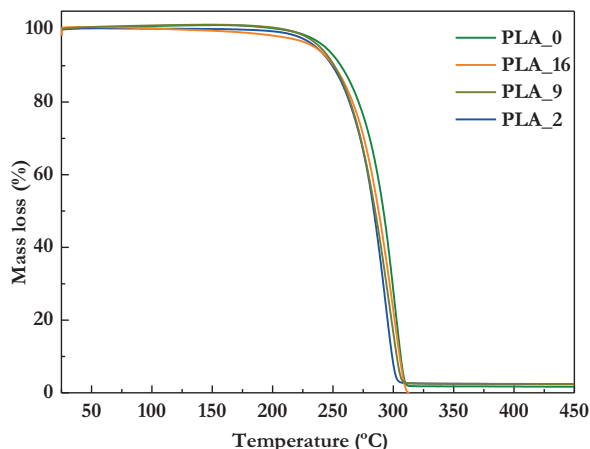
Fig. 5.5 Mass loss percentage as function of temperature for PLA samples (dT/dt = 10 °C·min^{-1}).

In general, none of the PLA samples exhibited weight loss below 234 °C. Notably, the PLA prepared without phenol exhibited slightly higher thermal stability than those with solvent even when the molecular weight was the lowest from the group. This suggests that with increasing temperature, phenyl endgroups are more prone to initiate transesterification reactions than hydroxyl endgroups. These reactions can lead to the formation of lactide and oligomers of lactic acid that can be evaporated at sufficiently high temperature causing sample weight loss. At the same time, these oligomers can react amongst each other and undergo insertion reactions resulting in molecular weight increase.

Table 5.4 Thermal decomposition of PLA samples prepared at different conditions.

Sample	Catalyst	Catalyst amount (mol%)	Phenol in feed (mol%)	M_n (kg·mol^{-1})	M_w (kg·mol^{-1})	$T_{5\%}$ (°C)	$T_{50\%}$ (°C)	$T_{70\%}$ (°C)
PLA_0	BuSnO(OH)	0.1	–	10.6	23.8	244	292	299
PLA_2	BuSnO(OH)	0.1	10	17.8	36.6	236	284	291
PLA_16	BuSnO(OH)	0.05	10	17.2	35.8	235	288	297
PLA_9	SnOct$_2$	0.1	10	18.2	43.7	239	285	294

5.4 Conclusion

In previous research by our group, phenolic solvents were shown to strongly improve the molecular weights in polycondensation reactions to produce polyglycolic acid and poly(lactic-co-glycolic acid) (>80% glycolic acid content) that otherwise would have too low M_n (<11 kg·mol^{-1}). The same approach, using phenol as reactive solvent, was applied in this research to increase the molecular weight of PLA synthesized through direct polycondensation of L-lactic acid. M_w and M_n of up to 43.7 and 18.1 kg·mol^{-1} were reached adding 10 mol% of phenol (relative to the acid in the feed) and SnOct$_2$ as catalyst. Higher amounts of phenol led to decreasing molecular weight and facilitated lactide formation. Unexpectedly, a similar outcome was obtained with M_w and M_n of up to 44.1 and 20.5 kg·mol^{-1}, when adding 25 mol% of 1,4-dimethoxy benzene, a non-reactive solvent. Racemization was observed, irrespective of the use of phenol. However, with SnOct$_2$ as catalyst, the extent was lower (13%) than with BuSnO(OH) (19_20%). PLA prepared with phenol, bearing phenyl endgroups, exhibited a slightly faster thermal degradation than PLA prepared via a typical polycondensation. Although the synthesis strategy with phenols is not as efficient for molecular weight improvement in PLA as has been reported for PLGA copolymers and other polyesters, it could be used alternatively for lactide production. Yet, it would require further optimization to determine its potential in comparison with the methods already used industrially.

5.5 References

(1)   Global Poly(Lactic acid) Market report 2021: market trends, production to 2030, main producers and production capacities. Research and Markets. https://www. researchandmarkets.com/reports /5459161/the-global-market-for-poly-lacticacid?utm_source=GNOM&utm_medium=Press Release&utm_code=kt96kn&utm_campaign=1617344+-+Global+Poly+(Lactic+Acid)+Market +Report+2021%3A+Market+Trends%2C+Production+to+2030%2C+Main+Producers+and+ Production+Capacities&utm_exec=chdo54prd (accessed December 9, 2021).

(2)   European bioplastics. Bioplastics market development update 2020. https://www.european-bioplastics.org/market (accessed December 14, 2021).

(3)   Lunelli, B. H.; Andrade, R. R.; Atala, D. I. P.; Maciel, M. R. W.; Filho, F. M.; Filho, R. M. I. Production of lactic acid from sucrose: strain selection, fermentation, and kinetic modeling. *Appl. Biochem. Biotechnol.* **2010**, *161 (1–8)*, 227-237. https://doi.org/10.1007/s12010-009-8828-0.

(4)   Singhvi, M.; Gokhale, D. Biomass to biodegradable polymer (PLA). *RSC Adv.* **2013**, *3*, 13558-13568. https://doi.org/10.1039/c3ra41592a.

(5)   Pivsa-Art, S.; Tong-Ngok, T.; Junngam, S.; Wongpajan, R.; Pivsa-Art, W. Synthesis of poly(d-lactic acid) using a 2-steps direct polycondensation process. *Energy Procedia.* **2013**, *34*, 604–609. https://doi.org/10.1016/j.egypro.2013.06.791.

(6)   Maharana, T.; Mohanty, B.; Negi, Y. S. Melt-solid polycondensation of lactic acid and its biodegradability. Prog. Polym. Sci. **2009**, *34(1)*, 99-124. https://doi.org/10.1016/ j.progpolymsci.2008.10.001.

(7) Ehsani, M.; Khodabakhshi, K.; Asgari, M. Lactide synthesis optimization: investigation of the temperature, catalyst and pressure effects. *E-Polymers.* **2014**, *14 (5)*, 353-361. https://doi.org/10.1515/EPOLY-2014-0055.

(8) Weinland, D. H.; van Putten, R.-J.; Gruter, G.-J. M. Evaluating the commercial application potential of polyesters with 1,4:3,6-dianhydrohexitols (isosorbide, isomannide and isoidide) by reviewing the synthetic challenges in step growth polymerization. *Eur. Polym. J.* **2022**, *164*, 110964. https://doi.org/10.1016/J.EURPOLYMJ.2021.110964.

(9) Masutani, K.; Kimura, Y. PLA synthesis. From the monomer to the polymer. *RSC Polym. Chem. Ser.* **2015**, 3-36. https://doi.org/10.1039/9781782624806-00001.

(10) De Vries, K. Preparation of polylactic acid and copolymers of lactic acids. US4797468A, January 10, 1989.

(11) Gruber, P. R; Hall, E. s; Kolstad, J. J; Iwen, M.L; Benson, R. D; Borchardt, R.L. et al. Continuous process for the manufacture of a purified lactide from esters of lactic acid. US5247059A, September 21, 1993.

(12) Sinclair, R. G; Markle, R. A; Smith, R.K. Lactide production from dehydration of aqueous lactic acid. US5274127A, December 28, 1993.

(13) Dechy-Cabaret, O.; Martin-Vaca, B.; Bourissou, D. Controlled ring-opening polymerization of lactide and glycolide. *Chem. Rev.* **2004**, *104 (12)*, 6147-6176. https://doi.org/10.1021/cr040002s.

(14) Chen, G. X.; Kim, H. S.; Kim, E. S.; Yoon, J. S. Synthesis of high-molecular-weight poly(l-lactic acid) through the direct condensation polymerization of l-lactic acid in bulk state. *Eur. Polym. J.* **2006**, *42 (2)*, 468-472. https://doi.org/10.1016/j.eurpolymj.2005.07.022.

(15) Kale, G.; Auras, R.; Singh, S. P. Comparison of the degradability of poly(lactide) packages in composting and ambient exposure conditions. *Packag. Technol. Sci.* **2007**, *20 (1)*, 49-70. https://doi.org/10.1002/pts.742.

(16) Gaudencio Baptista, C. M; Simoes Marques, D. A; Mendes Gil, M. H. Process for preparing high molecular weight poly(lactic acid) by melt polycondensation. WO2013184014A1, December 12, 2013.

(17) Murcia Valderrama, M. A. Stepping stones in CO_2 utilization: Synthesis and evaluation of oxalic- and glycolic acid (co)polyesters, PhD Thesis, University of Amsterdam, 2022.

(18) Weinland, Daniel. Synthesis of rigid biobased polyesters: Overcoming the low reactivity of secondary diols in polyester synthesis. PhD thesis, University of Amsterdam, 2022.

(19) Rodney, R. L.; Stagno, J. L.; Beckman, E. J.; Russell, A. J. Enzymatic synthesis of carbonate monomers and polycarbonates. *Biotechnol. Bioeng.* **1999**, *62 (3)*, 259-266. https://doi.org/10.1002/(SICI)1097-0290(19990205)62:3<259::AID-BIT2>3.0.CO;2-I.

(20) Pauling, L. *General Chemistry*; Dover Publications, Inc, 1988.

(21) Rappoport, Z. *The Chemistry of Phenols*. Part 2; John Wiley & Sons, 2003.

(22) Daowdat, B.; Hoeltzel, G.; Tannenbaum, R. *Direct Route to Phenol from Benzene.* Sr. Des. Reports 2017.

(23) Gibson, J. M.; Thomas, P. S.; Thomas, J. D.; Barker, J. L.; Chandran, S. S.; Harrup, M. K.; Draths, K. M.; Frost, J. W. Benzene-free synthesis of phenol. *Angew. Chem. Int. Ed. Engl.* **2001**, *40 (10)*, 1945-1948.

(24) Maryanty, Y.; Hadiantoro, S.; Widjajanti, K.; Putri, D. I. K.; Nikmah, l. Poly lactic acid (PLA) development using lactic acid product from rice straw fermentation with azeotropic polycondensation process. *IOP Conf. Ser. Mater. Sci. Eng.* **2021**, *1053 (1)*, 012043. https://doi.org/10.1088/1757-899X/1053/1/012043.

(25) Marques, D. A. S.; Jarmelo, S.; Baptista, C. M. S. G.; Gil, M. H. Poly(Lactic Acid) synthesis in solution polymerization. *Macromol. Symp.* **2010**, *296 (1)*, 63-71. https://doi.org/10.1002/MASY.201051010.

(26) Zhang, J.; Krishnamachari, P.; Lou, J.; Shahbazi, A. Synthesis of poly(L(+) lactic acid) by polycondensation method in solution. *Proc. 2007 Natl. Conf. Environ. Sci. Technol.* **2009**, 3-8. https://doi.org/10.1007/978-0-387-88483-7_1.

(27) De Vos, S.; Jansen, P.; Biochem, P. Industrial-Scale PLA Production from PURAC Lactides. https://www.researchgate.net/profile/Sicco_De_Vos/publication /228836284_IndustrialScale_PLA_Production_from_PURAC_Lactides/links/563efbb508ae8d65c 01460a0.pdf (accessed February 1, 2022).

(28) Groot, W.; Van Krieken, J.; Sliekersl, O.; De Vos, S. Production and purification of lactic acid and lactide. *Poly(Lactic Acid) Synth. Struct. Prop. Process. Appl.* **2010**, 1-18. https://doi.org/10.1002/9780470649848.CH1.

(29) Gao, Q.; Lan, P.; Shao, H.; Hu, X. Direct synthesis with melt polycondensation and microstructure analysis of poly(l-lactic acid-co-glycolic acid). *Polym. J.* **2002**, *34 (11)*, 786-793. https://doi.org/ 10.1295/polymj.34.786.

(30) Suganuma, K.; Matsuda, H.; Cheng, H. N.; Iwai, M.; Nonokawa, R.; Asakura, T. NMR analysis and tacticity determination of poly(lactic acid) in C5D5N. *Polym. Test.* **2014**, *38*, 35-39. https://doi.org/10.1016/J.POLYMERTESTING.2014.05.018.

(31) Du Sart, G. G.; Davidson, M. G.; Chuck, C. J. Method to manufacture PLA using a new polymerization catalyst . EP2799462A1, May 11, 2014.

(32) Dong, K. Y.; Kim, D.; Doo, S. L. Synthesis of lactide from oligomeric PLA: effects of temperature, pressure, and catalyst. *Macromol. Res.* **2006**, *14 (5)*, 510-516. https://doi.org/10.1007/bf03218717.

CHAPTER 6

Scale-up of PLGA polycondensation process assisted by aromatic solvents

Abstract

Previously, a strategy to enhance the molecular weight of poly(lactic-co-glycolic acid) (PLGA) copolymers produced via polycondensation using p-cresol and guaiacol was presented. With this route M_n and M_w as high as 31 and 63 kg·mol^{-1} were obtained up to 35 g scale for copolymers containing between 80 and 90 mol% of glycolic acid. In order to continue assessing the potential of this strategy, the present work focused on scaling it up to up to 1 kg scale in a 2 L autoclave. The results found so far showed new etherification side reactions with both p-cresol and guaiacol, which is thought to be the main cause for the lower molecular weights obtained compared to those achieved in small scale. Still, M_n of up to 17.4 kg·mol^{-1} was found when using guaiacol and the side reactions occurred at less extent. Even though significant optimization of this process is still required, initial insight into the g to kg scale-up of this route and its limitations is provided in this study.

6.1   Introduction

Poly(lactic-co-glycolic acid) (PLGA) is a well-known biobased and degradable copolymer applied largely in the medical field for applications such as sutures, implants and drug delivery systems.[1] PLGA copolymers rich in glycolic acid have shown very unique barrier properties and fast degradation.[2,3] Currently, PLGAs are industrially produced via ring opening polymerization of glycolide and lactide, the cyclic dimers of glycolic (GA) and lactic acid (LA), respectively. Since additional steps are required for this process, specifically in the production of high purity cyclic monomer, this polymerization strategy is more expensive than a direct polycondensation of the acids would be. However, the latter is not suitable for the preparation of high molecular weight copolymers. This is mainly because already at small scale the fast and efficient water removal required to drive the equilibrium between lactide/glycolide formation and the chain growth reaction towards increasing molecular weight is difficult and the backward reaction of (poly)ester with water is relatively fast.[4]

Lower cost strategies than those currently used for mass production of PLGA copolymers, specifically for those rich in glycolic acid, could help expand the use of these materials beyond high value applications and to other sectors where good barrier properties and degradability are desired features (unmet needs). Previously, a strategy for the polycondensation of GA and LA assisted by substituted phenols (p-cresol and guaiacol) was effectively performed up to 35 g scale with resulting M_n and M_w as high as 31 and 63 kg·mol^{-1}, respectively.[5] The process involved an initial esterification stage where GA and LA oligomers are formed and subsequently capped by phenyl esters. In the subsequent polycondensation stage these phenyl esters then undergo relatively fast transesterification and polycondensation with solvent removal from the system. This drives the reaction to high molecular weight, as substituted phenols are very good leaving groups, leading to fast transesterification and the backward reaction of phenols with (poly)ester is much slower than the backward reaction with water. Overall, this is a more straightforward strategy in comparison to the typical ring opening polymerization and it allows for solvent recovery and recycling. The present work focuses on upscaling this route for PLGA with high GA content from laboratory glassware (≤35 g) to up to 1 kg scale by studying variations in different operating parameters to maximize the resulting molecular weight.

6.2 Experimental section

6.2.1 Materials

All chemicals were used without further purification. Glycolic acid (99%), lactic acid solution (90% in water), guaiacol (99%) and p-cresol (99%) were purchased from Acros Organics. Butyl stannoic acid (BuSnO(OH)) (97%), 1,4-dimethoxybenzene and deuterated dimethyl sulfoxide (DMSO-d$_6$) were acquired from Sigma Aldrich.

6.2.2 Synthesis of PLGA$_{10/90}$ and PLGA$_{20/80}$ from polycondensation of GA and LA in a 2 L autoclave

A schematic representation of the reactor set-up and materials flow is presented in **Fig. 6.1**. In all cases the reactions were conducted in a 2 L autoclave (Büchi AG) consisting of a reactor vessel with a heating jacket, nitrogen inlet and outlet and a distillation system. Typically 90 or 80 mol% of glycolic acid and 10 or 20 mol% of lactic acid were loaded in the reactor together with the required amount of BuSnO(OH) catalyst and with the selected substituted phenol (p-cresol or guaiacol). Based on the studies at small scale, the first step of the reaction was carried out under nitrogen (flow up to 2 L/h) and atmospheric pressure with 75 mol% of p-cresol relative to the total monomer loading and 0.05 mol% of BuSnO(OH). The latter was added in two equal portions: at the beginning of the reaction and before starting the stage at reduced pressure (polycondensation).

Initially, the reaction was performed at 190 °C, followed by a gradual increase up to 210 °C (oil temperature) at 100 rpm during 10 hours. Subsequently, the temperature was lowered to 200 °C, after which the second portion of catalyst was added, followed by pressure reduction from 400 to 1 mbar within 3 hours. The system was maintained at 1 mbar for 3 hours while the temperature was increased to 210 °C. The reactor was then discharged, via a bottom drain into a water bath and the resulting PLGA was chipped, dried and analyzed.
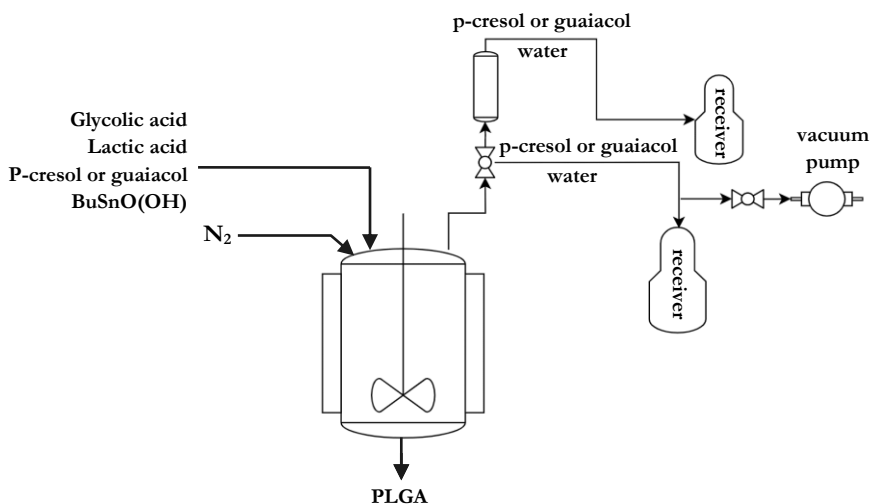
Fig. 6.1 Schematic of the reactor set-up and materials flow to produce PLGA in 2 L autoclave.

Unexpected ether formation side reactions were observed already in the first experiment. Therefore, a series of small scale tests was carried out to further explore possible strategies to suppress them and to understand what caused these. Some of these included the use of additives (monosodium phosphate (MSP) and tetraethylammonium hydroxide (TEAH)), variations in the reaction temperature, time, catalyst concentration (between 0.02 and 0.05 mol%), stirring speed (up to 130 rpm) and nitrogen flow (up to 4 L·h^{-1}) . Also, p-cresol was later replaced by guaiacol with adjustments to the process based on the small scale experiments using this solvent.

6.2.3 Analytical techniques

The reaction progression and final copolymer structures (when soluble) were determined using ^{1}H NMR spectroscopy on a Bruker AMX 400 (^{1}H, 400.13 MHz) with DMSO-d$_6$ as solvent. ^{13}C NMR analysis was also carried out to investigate the formed side products (Bruker Avance 500). The molecular weight distribution was determined by Gel Permeation Chromatography (GPC). The measurements were performed in a Merck-Hitachi LaChrom HPLC system, equipped with two PL gel 5 µm MIXED-C (300×7.5 mm) columns using hexafluoroisopropanol as mobile phase and poly(methyl methacrylate) (PMMA) as

calibration standards. The resulting molecular weights were calculated with the software package Wyatt Astra 6.1.

Differential scanning calorimeter DSC 3+ STAR^e was used to measure the thermal transitions using a system from Mettler Toledo. For this, between 5 and 6 mg of each sample were introduced in sealed aluminum pans (40 μm) and heated from room temperature to 215 °C (dT/dt = 10 °C·min^{-1}). The samples were maintained at that temperature for 2 minutes and subsequently cooled down to 25 °C at constant rate. A second heating scan was recorded at the same conditions. The reported glass transition temperature T_g and melting temperature T_m were taken from this scan. The thermal stability was determined with a TGA/DSC 3+ STARe system from Mettler Toledo. For this, about 6 mg of copolymer was introduced in a sealed aluminum sample vessel and then heated from room temperature up to 450 °C (dT/dt = 10 °C·min^{-1}) under nitrogen atmosphere with a flow rate of 50 mL·min^{-1}.

6.3   Results and discussion

PLGA copolymers with between 10 and 20 mol% of lactic acid were synthesized via a solvent assisted polycondensation according to the general reaction **Scheme 6.1**. Experiments were carried out initially with p-cresol and later with guaiacol at the conditions presented in **Table 6.1**. Additional small scale experiments were useful to gain more insight in the scaled up polymerization process.
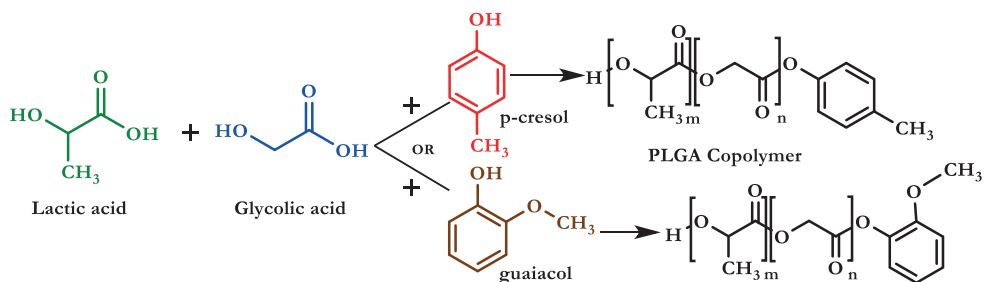
Scheme 6.1 Proposed synthesis strategy for polycondensation of PLGA copolymers from glycolic and lactic acid.

The resulting molecular weight distribution and thermal transitions for the experiments discussed in this chapter are presented in **Table 6.1**. In the autoclave, the polymerizations were done on a scale between 350 (PLGA_1 to PLGA_5) and 530 g (PLGA_6 and 7) while in small scale (PLGA_8 to 12) they were done in 20 g batches.

Table 6.1 Synthesis conditions and resulting molecular weight distribution and thermal transitions of PLGA copolymers.

Copolymers in 2L autoclave

Sample	Scale (g)	GA$_f$ (mol %)	LA$_f$ (mol %)	Solvent type	Solvent (mol%)	Catalyst (mol%) *	T (°C) and time (h) steps	GA$_p$ (mol %)	LA$_p$ (mol %)	M$_n$ (kg·mol⁻¹)	M$_w$ (kg·mol⁻¹)	T$_g$ (°C)	T$_m$ (°C)
PLGA_1	350	90	10	p-cresol	75	0.025 + 0.025	210°C 7h, 200°C 1h, 190°C 3h, 205°C 1h, 3h	94	6	12.4	23.6	37	187
PLGA_2		90	10			0.02 + 0.01	205°C 2h, 210°C 1h, 190°C 12h+3h, 180°C 1h, 170°C 1h	90	10	13.8	27.4	n.d.	183
PLGA_3ª + MSPᵇ		90	10			0.025 + 0.01	210°C 10h, 200°C 1h, 190°C 3h, 205°C 3h, 4h	n.s	n.s	10.8	21.9	36	184
PLGA_4		80	10			0.025	200°C 7.5 h, 4.5 h, 190°C 2h, 4h	86	14	13.0	26.0	37	–

Copolymers in 2L autoclave

Sample	Scale (g)	GA_f (mol%)	LA_f (mol%)	Solvent type	Solvent (mol%)	Catalyst (mol%) *	T (°C) and time (h)	GA_p (mol%)	LA_p (mol%)	M_n (kg mol⁻¹)	M_w (kg mol⁻¹)	T_g (°C)	T_m (°C)
PLGA_5	350	90	10	guaiacol	75	0.03 + 0.005	175°C 0.5h; 180°C 1h; 190°C 6h; 200°C 1h; 210°C 6h; 195°C 0.5h; 205°C 3.5h; 195°C 1h	92	8	17.4	34.9	36	187
PLGA_6 + MSP[b]	530	90	10		50	0.02ᶜ + 0.025	180°C 1h; 190°C 1h; 200°C 3h; 210°C 6.5h; 195°C 3.5h; 195°C 0.5h	92	8	14.0	28.1	37	183
PLGA_7		90	10			0.03ᶜ + 0.01	175°C 1h; 180°C 1h; 185°C 1h; 190°C 5h; 200°C 2h; 210°C 7h; 195°C 2.5h; 195°C 1h; 205°C 1h; 210°C 1h	93	7	16.0	32.1	37	187

Copolymers in glass reactor (20 g scale)

Sample	Scale (g)	GA_f (mol%)	LA_f (mol%)	Solvent type	Solvent (mol%)	Catalyst (mol%) *	T (°C) and time (h)	GA_p (mol%)	LA_p (mol%)	M_n (kg mol⁻¹)	M_w (kg mol⁻¹)	T_g (°C)	T_m (°C)

PLGA_8 + MSP[b]	20	80	20	p-cresol	0.025 + 0.01	190°C / 200°C **1h** / 210°C **1h** / **5h** / **3h**	81	19	18.0	37.09	42	-
PLGA_9	20	80	20	75	0.025 + 0.01	190°C / 200°C **1h** / 210°C **1h** / **5h** / **3h**	80	20	22.1	46.1	41	-
PLGA_ 10 + TEAH[b]	20	80	20		0.03 + 0.005	190°C / 205°C **1h** / 210°C **2h** / **4h** **195°C** / **3h**	82	18	15.5	31.9	41	-
PLGA_ 11 + MSP[b]	20	90	10	guaiacol	0.03 + 0.005	190°C / 200°C **3h** / 210°C **1h** / **7h** **195°C** / **3h**	n.s		23.4	48.1	41	186
PLGA_ 12	20	90	10	50	0.04[d]	190°C / 200°C **3h** / 210°C **1h** / **7h** **205°C** / **3h**	n.s		25.3	51.9	41	188

* In all cases BuSnO(OH) was used as catalyst and it was generally added in two portions: at the beginning of the reaction and before reducing the pressure.
GA$_f$ = glycolic acid in the feed; **LA$_f$** = lactic acid in the feed; **GA$_p$** = glycolic acid built in the polymer; **LA$_p$** = lactic acid built in the polymer.
[a] p-cresol was added after two hours of reaction; [b] 0.01 mol% relative to the total amount of acids in the feed; [c] The first portion of BuSnO(OH) was only added after three hours of reaction; [d] Catalyst only added before reducing pressure; **n.s** = not soluble in DMSO-d$_6$.

Linear scale-up of p-cresol and catalyst amount together with other reaction conditions did not lead to satisfactory molecular weight (PLGA_1). Although a small improvement was achieved (PLGA_2) by adjusting some process parameters such as reaction temperature, time and catalyst concentration, the resulting M_n and M_w (up to 13.8 and 27.4 kg·mol^{-1} respectively) were still much lower than those attained in small scale using the same strategy with p-cresol. Overall it was difficult to control the GA/LA ratio in the polymer. This was most likely due to reaction temperature changes and different extent of decomposition reactions depending on the experiment. Monomer evaporation due to high nitrogen flow and stirring speed is also seen as a contributing factor.

The autoclave experiments revealed the occurrence of side reactions that were not observed previously in small scale. In an attempt to reduce these ether formation side reactions, two additives were evaluated: monosodium phosphate (MSP) and tetraethylammonium hydroxide (TEAH). At small scale, two experiments at equivalent conditions revealed an M_n of 22.1 kg·mol^{-1} (PLGA_9) without MSP, while a lower value of 18.0 kg·mol^{-1} was found for the sample with MSP additive (PLGA_8). With an equivalent amount of TEAH added, the resulting M_n of 15.1 kg·mol^{-1} was even lower. Despite this outcome, MSP was tested in the autoclave (PLGA_3), hoping that the gain in molecular weight from the side reaction suppression could counteract for the negative effect observed in small scale. Unfortunately, this addition did not show any advantage for the molecular weight.

Although similar side reactions to those observed for p-cresol were identified when using guaiacol, they seem to occur to a lesser extent. Also, the addition of MSP (PLGA_11) seems to have a less negative impact on the resulting molecular weight with guaiacol than with p-cresol. Subsequently, the scale-up development proceeded with this solvent, now focusing on lowering the amount required for the polymerization while still trying to achieve the highest molecular weight possible. 75 mol% of guaiacol (relative to all other monomer) led to a better outcome than what was obtained with p-cresol at comparable reaction conditions, achieving a M_n and M_w of 17.4 and 34.9 kg·mol^{-1} respectively (PLGA_5). Later, a close M_n of 16 kg·mol^{-1} was obtained when lowering the guaiacol concentration to 50 mol% and adjusting the reaction parameters (PLGA_7). This suggested that although further fine tuning of the process conditions is still required, molecular weight improvements could still be made with a lower guaiacol amount.

6.3.1 Scale-up with p-cresol

All the experiments performed in the autoclave with p-cresol revealed the development of unexpected ether formation side products in the ^{1}H NMR spectra. Interestingly, most of these copolymers were soluble in DMSO-d_6 even though when prepared at small scale with comparable molecular weights to those obtained here, they would not dissolve.

Upon esterification of glycolic and lactic acid with p-cresol during the first stage of the reaction, a mixture of phenyl esters in solution with free solvent is expected. However, an additional signal detected at 4.33 ppm (in DMSO-d$_6$) was already visible at this point when the reaction was carried out at 190 °C and it remained visible even in the final product.
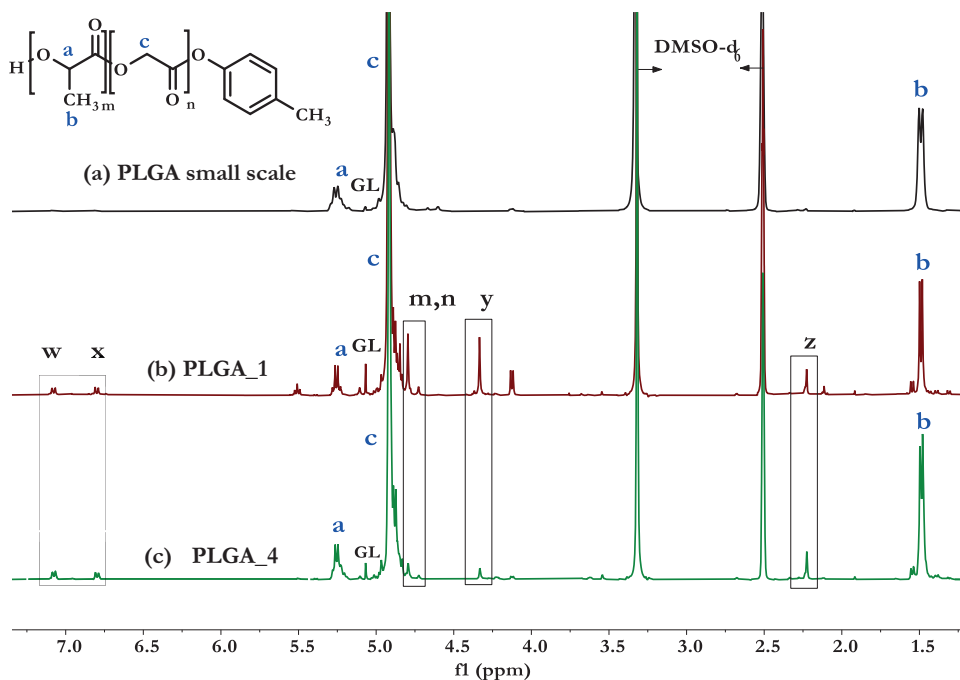

Fig. 6.2 ^{1}H NMR comparison of PLGA samples prepared with p-cresol in small scale and in the autoclave.

Fig. 6.2 (a) compares the ^{1}H NMR spectra of a PLGA sample synthesized in small scale (35g) with that of PLGA_1 and PLGA_4 (**Fig. 6.2 (b)** and **(c)**) prepared in the autoclave using the same molar concentration of p-cresol (75 mol%). In all cases the ^{1}H NMR signals corresponding to the protons of the PLGA repeating unit are observed. The peaks assigned to the CH (b) and CH$_3$ (a) protons of incorporated lactic acid can be found at 5.20-5.29 and 1.47-1.50 ppm, while the signal attributed to the CH$_2$ (c) protons of incorporated glycolic acid is observed between 4.87 and 4.94 ppm. In addition to these signals, PLGA_1 and PLGA_4 from the autoclave showed peaks that were not detected in the ^{1}H NMR spectra of the sample prepared at small scale. Notably, the singlet at 4.33 ppm (y), which for both cases had already been identified at the early stages of the reaction, and the two peaks with equivalent intensity at between 6.78 (x) and 7.07 ppm (w), correlated to the singlet at 2.22 ppm (z). Also, two new peaks only observed in the final product (and not after esterification) were identified at 4.73 (n) and 4.79 ppm (m). Heat and mass transfer differences were to be expected when scaling up from the glass reactor to the 2 L autoclave, not only due to the volume variations, but also due to the reactor and overall system design. Yet, the molecular

185

weight decrease in the autoclave compared to the glass reactor is so apparent that the identified side reactions are thought to be the main hindering factor.

In order to gain more insight about the mentioned side reactions, an experiment was carried out initially by adding only GA, LA and BuSnO(OH) in the reactor without any p-cresol as solvent (PLGA_3). A ^{1}H NMR sample taken after 3 hours of reaction at 190 °C revealed that the side product visible at 4.33 ppm (y) was already present in the reaction mixture by then. Therefore, it could not originate from the interaction of GA with p-cresol. Reducing the starting temperature to between 160 °C and 180 °C instead of 190 °C, helped decreasing the proportion of side product in esterification. Also, lowering the catalyst concentration, as in the case of PLGA_1 (0.05 mol%) compared to PLGA_4 (0.025 mol%), helped reduce the amount of generated side product, although this did not impact the final molecular weight significantly (M_n=12.4 vs 13.0 kg·mol^{-1} for PLGA_1 and PLGA_4). At first, it was assumed that such product (y) was derived from glycolic acid, given its much higher amount in the reaction mixture and its known higher reactivity compared to lactic acid. An additional experiment carried out later where GA was reacted with diglycolic acid DGA (the ether formed by two GA molecules), indicated that the unknown peak (y) matched best with oligomers of GA connected to diglycolic acid forming carboxylic acid terminated chains (**Fig. 6.3**). Etherification to DGA could have occurred during condensation of GA by the removal of a water molecule from the hydroxyl groups of two GA molecules. Consequently, DGA with both carboxylic acid end groups could react with free or oligomeric GA present in the reaction mixture via their terminal OH group. Although a similar interaction could be expected with free p-cresol at this point, it could not be evidenced in the ^{1}H NMR spectra.
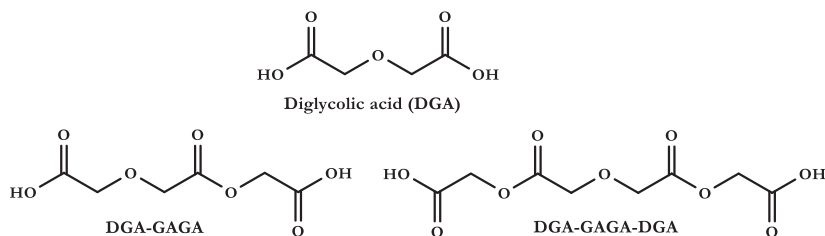
Fig. 6.3 Possible side products formed during esterification.

Generally, at the end of the esterification, two signals at 7.03 and 7.22 ppm corresponding to the cresyl endgroups could be identified and distinguished from those of free p-cresol at 6.65 and 6.95 ppm in the ^{1}H NMR spectra. In all the examples from **Fig. 6.2**, those peaks were also observed before the stage at reduced pressure but they were no longer visible in the final product. Instead, for the samples prepared in the autoclave, two symmetrical signals appeared at between 6.78 (x) and 7.07 (w) ppm, correlated to a singlet at 2.22 ppm (z). After evaluating different ^{1}H NMR spectra of PLGA samples prepared with phenol at small scale, it was found that peaks with similar chemical shifts were sometimes observed next to the two signals at 7.03 and 7.22 ppm when the reaction was carried out at up to 210 °C. However

they are in much lower proportion than in the autoclave experiments and no additional unidentified peaks to correlate to them were found. With this it was suggested that at reduced pressure, free p-cresol in the reaction mixture could undergo etherification to p-tolyl ether, predominantly with glycolic acid, in which case the peaks at 7.03 and 7.22 ppm would correspond to the CH protons of the phenol ring and the one at 2.22 ppm to the protons of the CH_3 attached to it. Because these integrals together with those of the peaks m, n and y were not always correlated in the same manner, it was assumed that more than one side product could have formed in the autoclave during polycondensation and their proportions varied according to the reaction conditions (e.g. p-tolyol ether of lactic acid).

Based on this and on ^{13}C NMR measurements carried out in parallel, it was proposed that the side products from the ^{1}H NMR spectra of the resulting PLGA samples (autoclave) corresponded to a mixture of either residual DGA bound to GA moieties or reacted with p-cresol and possibly free bis(p-tolyl) ether **(Fig. 6.4)**. p-Cresol connected to the DGA-GAGA already formed during esterification would act as chain stopper for the polycondensation hindering molecular weight growth. This would be the most detrimental side product for polymerization and as we expect, the one responsible for the molecular weight limitations found here. Free bis(p-tolyl) ether is not expected to impede molecular weight growth but given the high viscosity of the forming copolymer during polycondensation, it is possible that even at full vacuum, complete removal was not achieved (boiling point of 285 °C). Although dehydration of cresols to form ditolyl ethers has been reported before[6], a much higher reaction temperature of between 350 and 500 °C and the presence of tungsten oxide/alumina as catalyst were required. The mechanism that could have led to this formation is still unclear.
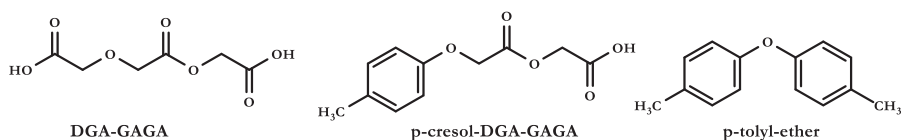
Figure 6.4 Proposed side products formed during polycondensation.

Monosodium phosphate (MSP) and tetraethylammonium hydroxide (TEAH) were used independently as additives with the aim of reducing the acidity of the reaction mixture and thereafter decreasing the likelihood of ether formation. However, both in small scale and in the autoclave they seemed to affect the molecular weight rather negatively without significant reduction of the formation of side products. Based on the cyclic diester glycolide, present in the final products, more thermal decomposition during polycondensation occurred in the autoclave compared to the small scale reactions. For PLGA_2 about 1.8 mol% of glycolide was found in the resulting polymer while for the other samples prepared in the autoclave it was around 0.6 mol%. Glycolide, lactide and 3-methylglycolide (the mixed GA+LA cyclic diester) were also found in the distilled solvent when analyzed with ^{1}H NMR.

DSC and TGA analyses were carried out to gain more insight in the side products observed in the autoclave and to determine how they affected the thermal transitions.

**Fig. 6.5** compares the second DSC heating curve (dT/dt = 10 °C·min^{-1}) of the samples prepared with p-cresol. PLGA_1, 2 and 3 (all with GA:LA 90:10) displayed a semi crystalline structure at the evaluated conditions while PLGA_4 (with GA:LA 80:20) showed an amorphous one. In general, the resulting T_g (between 36 and 37 °C) and T_m (between 183 and 187 °C) corresponded to what could be expected for this copolymer compositions and this range of molecular weight.[5] No additional endotherm transitions were recorded here. Additionally the broad recrystallization like peak right before the melting range had already been observed for this type of copolymers.[5]
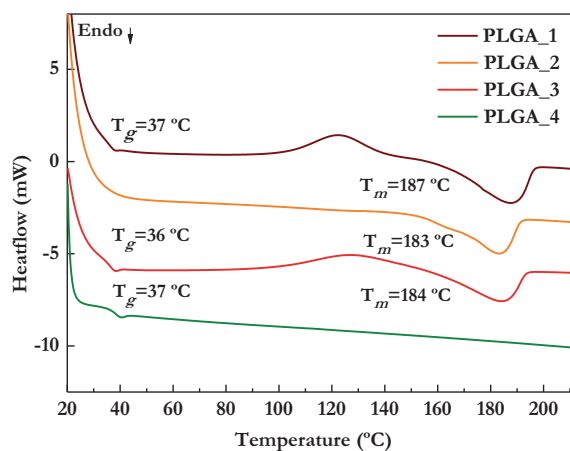
Fig. 6.5 Comparison of DSC curves (2nd heating scan dT/dt = 10 °C·min^{-1}) of samples prepared in the autoclave with p-cresol.

A TGA analysis carried out in parallel for the same samples allowed for the determination of the mass loss percentage as a function of temperature, presented in **Fig. 6.6** and **Table 6.2**. In all cases, the thermal decomposition occurred in a single stage with initially much higher mass loss for **PLGA_2**. This was attributed to a combination of possible factors. One is the degradation of glycolide, a side product, which from ^{1}H NMR, showed to be present in the highest amount for this sample (1.8 mol%). The other has to do with the degradation of ethylene glycol (about 6 mol%), another product visible in the final ^{1}H NMR, which was not seen in any of the samples taken in previous stages of the reaction. Ethylene glycol is the fluid used in the gas bubbler for the nitrogen outlet. This is suspected to have entered the reactor during the last stage of the polycondensation upon fast switching from reduced to ambient pressure for sampling. Evaporation of free p-cresol was discarded since residual solvent was not detected in the spectra.

With increasing temperature, at the point where 50 wt% and 70 wt% of mass loss had been registered, the trend became more comparable for all samples, except for PLGA_4 which had the lowest GA mol% (86 mol%) and it exhibited slightly lower thermal stability. For PLGA copolymers with similar compositions (87 and 91 mol% of GA) prepared via ROP, a 5% weight loss at 292 °C and a 70% at between 363 and 366 °C was previously reported.[2] Notably, this higher thermal stability is in agreement with a much higher molecular weight for the samples cited previously compared to those presented in **Fig. 6.6**. The former displayed M_n values between 33 and 36 kg·mol^{-1}, which is almost three times higher than those presented in **Table 6.2** and **Fig. 6.6**.
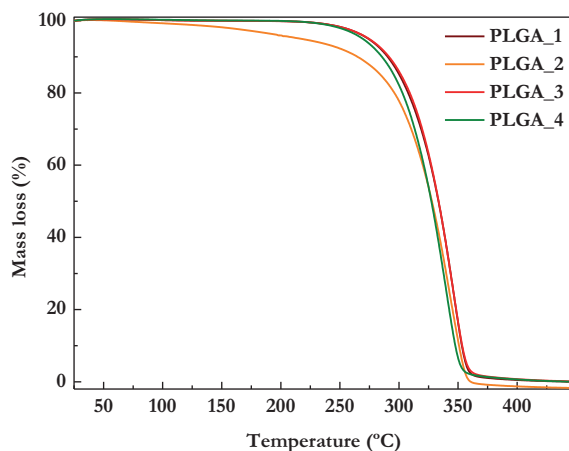
Fig. 6.6 Mass loss percentage as a function of temperature up to 450 °C (dT/dt = 10 °C·min^{-1}) of samples prepared in the autoclave with p-cresol.

Table 6.2. Mass loss of 5 wt.% ($T_{5\%}$), 50 wt.% ($T_{50\%}$) and 70 wt.% ($T_{70\%}$) of PLGA copolymers prepared with p-cresol in the autoclave.

Sample name	GA (polymer)	LA (polymer)	M_n (kg·mol^{-1})	$T_{5\%}$ (°C)	$T_{50\%}$ (°C)	$T_{70\%}$ (°C)
PLGA_1	94	6	12.4	277	337	346
PLGA_2	90	10	13.8	221	331	346
PLGA_3	nd	nd	10.8	278	337	347
PLGA_4	86	14	13.0	272	331	341

6.3.2 Scale-up with guaiacol

Since variation of other process parameters did not lead to significant molecular weight improvement, p-cresol was replaced by guaiacol, another substituted phenol evaluated previously for the same synthesis strategy in small scale with satisfactory results. Guaiacol is a naturally occurring organic compound with a much broader application field than p-cresol (in medicine and as flavoring agent) and lower associated hazard, which is advantageous

when considering the scaling up of this process.[7] Based on the observations gathered from the experiments with p-cresol, the catalyst concentration and initial reaction temperature was reduced with respect to the one applied in small scale with guaiacol. **Fig. 6.7** displays the ^{1}H NMR spectra of PLGA_5, with a resulting built in ratio of 91 mol% GA and 9 mol% LA, synthesized with 75 mol% of guaiacol versus total monomers. The same signals corresponding to the PLGA repeating unit defined before are observed here. In addition, the peaks which were also identified in the experiments with p-cresol and were attributed to side ether products, were also detected. Importantly, these products appear in much lower proportion than in the case of p-cresol. Guaiacol, being sterically hindered, displays a lower reactivity than p-cresol, which is evident not only from the higher reaction temperature and longer times required for the polymerization but also from the fact that side reactions appear to occur less when using this solvent.
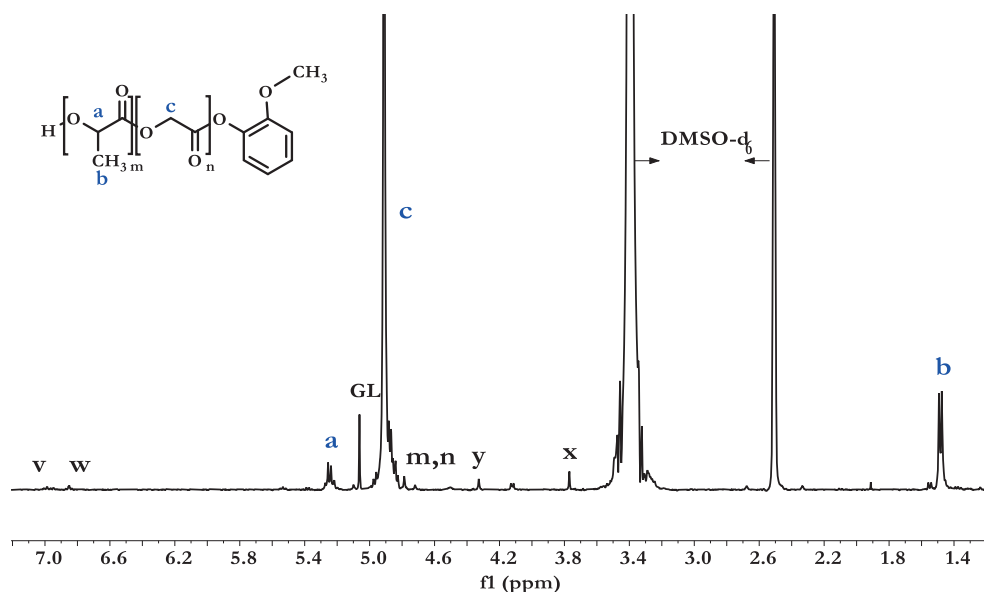
Fig. 6.7 ^{1}H NMR spectra of PLGA_5 prepared with guaiacol in the autoclave.

Following PLGA_5, two more polymerizations were performed reducing the amount of guaiacol from 75 to 50 mol% and adding MSP in one case to suppress the etherification reactions. Although in both PLGA_6 and 7 the side products remain at very low levels, the resulting molecular weight was in fact reduced in comparison to PLGA_5 (M_n=17.4 kg·mol^{-1}), especially when adding MPS (M_n=14.0 kg·mol^{-1}). Yet, without MPS addition (PLGA_7), and adjustments in the reaction conditions, an M_n of 16 kg·mol^{-1} was achieved still using 50 mol% of guaiacol.

The thermal transitions recorded from the second heating scan of this set of samples presented in **Fig. 6.8**, revealed comparable T_g and T_m to those obtained for the copolymers synthesized with p-cresol. Besides the same exotherm-like signal before the melting range, also recorded previously for this type of sample, no additional transitions were observed.
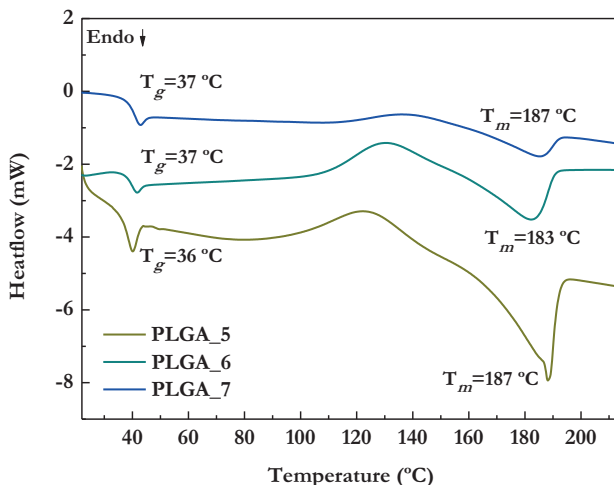
Fig. 6.8 Comparison of DSC curves (2nd heating scan $dT/dt = 10\ °C\cdot min^{-1}$) of $PLGA_{10/90}$ samples prepared in the autoclave with guaiacol.

6.4   Future considerations

The results presented here provide initial insight into the scale-up of a direct polycondensation process of GA and LA assisted by substituted phenols. When transferring from small scale to 1 kg, transport phenomena differences, reactor design and resulting newly found side reactions seemed the more influential factors on the molecular weight of the polymers. Although different process parameters were adjusted to deal with this changes, further fine-tuning and even retesting in an alternative polymerization set up are still needed to assure the production of a high enough molecular weight copolymer, which is necessary for subsequent processing and application assessment. Considering other key factors such as safety and economic aspects, this optimization is specially relevant to reduce the amount of required solvent while still assuring a material with satisfactory properties.

6.5   Conclusions

A strategy for the direct polycondensation of PLGA copolymers (with above 80 mol% of GA) assisted by substituted phenols (p-cresol and guaiacol) was effectively evaluated up to 35 g scale in a previous chapter. The present research focused on transferring this route to up to 1 kg scale and on studying variations in different operating parameters to enhance the resulting molecular weight.

Linear scale-up of p-cresol (75 mol%) and catalyst amount together with other reaction conditions led to lower molecular weight (M_n 13.8 kg·mol^{-1}, M_w 27.4 kg·mol^{-1}) than that obtained at a small scale (M_n 30.8 kg·mol^{-1}, M_w 62.8 kg·mol^{-1}). This was attributed to etherification side reactions, the products of which were visible in ^{1}H NMR. Adjustments in process variables and inclusion of two different additives to suppress these reactions did not have a significant impact on the resulting molecular weight. However, when guaiacol was tested at similar conditions, a higher M_n of 17.4 kg·mol^{-1} and M_w of 34.9 kg·mol^{-1} were obtained and side reactions were significantly reduced. Decreasing the guaiacol concentration from 75 to 50 mol% had a negative effect on the molecular weight. Even though the molecular weights of PLGA from the initial experiments at 500 g scale results do not approach those obtained in glassware, it is believed that a different reactor design along with further optimization of the process, could improve this outcome. Although additional work needs to be carried out in order to assure a high enough molecular weight copolymer for subsequent processing and application assessment, this research provides initial insight into the g to kg scale-up and its limitations.

6.6   References

(1)   Murcia Valderrama, M. A.; van Putten, R.-J.; Gruter, G.-J. M. The potential of oxalic – and glycolic acid based polyesters (review). Towards CO_2 as a feedstock (Carbon Capture and Utilization – CCU). *Eur. Polym. J.* **2019**, *119*, 445-468. https://doi.org/10.1016/j.eurpolymj.2019.07.036.

(2)   Murcia Valderrama, M. A.; van Putten, R.-J.; Gruter, G.-J. M. PLGA barrier materials from CO_2 . The influence of lactide co-monomer on glycolic acid polyesters . *ACS Appl. Polym. Mater.* **2020**. 2 (7), 2706-2718. https://doi.org/10.1021/acsapm.0c00315.

(3)   Wang, Y.; Valderrama, M. A. M.; Putten, R.-J. van; Davey, C. J. E.; Tietema, A.; Parsons, J. R.; Wang, B.; Gruter, G.-J. M. Biodegradation and non-enzymatic hydrolysis of poly(lactic-co-glycolic acid) (PLGA12/88 and PLGA6/94). *Polym.* **2022**, *14 (1)*, 15. https://doi.org/10.3390/POLYM14010015.

(4)   Gao, Q.; Lan, P.; Shao, H.; Hu, X. Direct synthesis with melt polycondensation and microstructure analysis of poly(l-lactic acid-co-glycolic acid). *Polym. J.* **2002**, *34 (11)*, 786-793. https://doi.org/10.1295/polymj.34.786.

(5)   Murcia Valderrama, M. A. Stepping Stones in CO_2 Utilization: Synthesis and evaluation of oxalic- and glycolic acid (co)polyesters, PhD thesis, University of Amsterdam, 2022.

(6)   Richmond, J. R.; Beach, H.; Tahir, S. F. Diaryl ethers by dehydration of phenols. US5144094A, September 1, 1992.

(7)   Feng, P.; Wang, H.; Lin, H.; Zheng, Y. Selective production of guaiacol from black liquor: effect of solvents. *Carbon Resour. Convers.* **2019**, *2 (1)*, 1-12. https://doi.org/10.1016/j.crcon.2018.07.005

Summary

Plastic materials have become indispensable in everyday life because of their versatility, high durability, lightness and low cost. As a consequence their demand continues to increase steadily, accompanied by an increasing requirement of fossil resources, both for energy and building blocks, as about 99 % of the current feedstock for polymers is fossil-based. Unfortunately, this trend is accompanied by higher emissions by the industry and leakage during production, transport and through consumer usage and disposal. This mismanaged plastic waste causes unprecedented harm to ecosystems. The aforementioned issues prompt the need to rethink the entire plastic value chain. While for energy many options are available to decouple from fossil feedstocks, for plastic materials the only alternative carbon sources are biomass, existing plastics (via recycling) and in the long-term CO_2. The fact that CO_2 is naturally abundant, nontoxic, inexpensive, a non-oxidant and renewable, makes it a promising feedstock. Finally, the use of CO_2 as feedstock can lead to negative emissions required to reach "net zero" in the second half of this century. The research presented in this thesis is part of the OCEAN (EU Horizon 2020 Spire program) project in which a new route to produce polymers using CO_2 as circular feedstock is developed. CO_2 can be electrochemically reduced to formic acid derivatives that can be subsequently converted into useful monomers such as oxalic acid and glycolic acid. We focused on investigating synthesis routes to produce polyesters based on those monomers and on studying their properties and assessing potential applications.

Polyesters are one of the most promising families of polymers based on renewable resources, due to their tunable performance combined with their potential towards reuse, closed-loop recycle and biodegradability. In **Chapter 1** the future potential of glycolic acid and lactic acid as polyester building blocks is evaluated. This involves a literature and patent review of representative synthesis methods, general properties, general degradation mechanisms, and recent applications for polyesters derived from these two monomers. This shows that opportunities for these materials to contribute to a circular economy in the biomedical, agricultural and packaging field are certainly promising, especially considering that technologies for the transformation of CO_2 into their building blocks is continuously progressing. The process being developed by Avantium, which aims for monomer production costs that at scale could compete with fossil counterparts (€1-2/kg) is a relevant example. Still, extremely efficient monomer and polymer production routes need to be established to be able to start using these materials in large-scale applications (e.g. for degradable drinking straws, degradable barrier films, degradable seed/fertilizer coatings, etc.).

In **Chapter 2**, the structure−property relationships of a series of poly(lactide-co-glycolide) (PLGA) copolymers rich in glycolic acid, which are for the most part unexplored, are discussed together with their suitability as barrier materials. For this, copolymers with between 50 and 91 mol% glycolic acid were synthesized via ring opening polymerization (ROP) of lactide and glycolide, the cyclic dimers of glycolic acid and lactic acid, respectively. In general, increasing density, thermal stability and better barrier to oxygen and water vapor are observed with increasing glycolic acid content. In fact, at room temperature and a relative humidity below 70%, these PLGA copolymers outperform non-oriented polyethylene terephthalate PET, a widely used packaging material. A crystallization study under non-isothermal conditions revealed that copolymerization reduces the crystallization rate for PLGA copolymers almost 10 times compared to PLA and PGA homopolymers at 10 °C·min⁻¹ cooling rate. The combination of remarkable barrier performance, recyclability, degradability and possibility of future production from CO_2, make these polyesters interesting in areas such as films for packaging.

So far, little has been reported on materials combining both oxalic acid and glycolic acid building blocks. The aim of **Chapter 3**, is to evaluate if and how the remarkable barrier performance of polyglycolic acid (PGA) could be combined with the high thermal stability and fast hydrolysis of the polyoxalate poly(1,4-cyclohexanedimethanol oxalate) (PCHDMOX). For this we used different feed ratios of either PGA, glycolide (GL), PLA and lactide (LAC) with PCHDMOX (50/50 and 30/70 wt%). As a comparison PLA was also assessed. Overall, copolyesters from PCHDMOX and glycolic acid/ glycolide showed lower T_g, higher thermal stability, better barrier to oxygen and water vapor and a faster hydrolysis rate than those prepared with lactic acid/lactide. For both of the former compositions the barrier performance was superior to that of non-oriented PET at the same conditions. All the samples hydrolyzed at a faster rate than the respective homopolymers they were made from, with those derived from glycolic acid (30 wt%) and PCHDMOX exhibiting a degree of hydrolysis of up to 86% after 215 days. These results initially suggest that copolymers from α-hydroxy acids and oxalates have potential for application in coatings for controlled release, single-use packaging not suitable for recycle or even for the medical field.

High molecular weight PGA and PLGA copolymers are currently commercially produced via ROP of glycolide and lactide, which is still a costly process. Given their interesting properties and the ongoing demand for more sustainable polymers, cheaper production routes are required. This is why in **Chapter 4** we studied a new polycondensation route for the production of these materials directly from glycolic and L-lactic acid in the presence of p-cresol or guaiacol as reactive solvent at a scale between 20 and 35 g. This route was evaluated for copolymers with an initial amount of 80, 90 and 100 mol% of glycolic acid, for which M_n values of up to 27.2, 31.5 and 24.2 kg·mol⁻¹, respectively, were achieved. For the copolymers, this represents an approximate three fold improvement compared to M_n

values achieved in a typical direct polycondensation starting from GA and LA. Furthermore, the route presented in this work requires less time than other reported strategies to increase the molecular weight of similar type of polymers and it allows for solvent recycling for reuse. Based on these results, we evaluated the same synthesis strategy for the production of PLA via polycondensation of lactic acid in **Chapter 5,** this time using phenol as the reactive solvent. Unexpectedly, this showed a different trend than the one observed previously with PLGA and PGA. Here, the molecular weight could be improved using up to 10 mol% of phenol but with higher amounts a detrimental effect was observed and lactide formation was facilitated. Surprisingly, a similar improvement in molecular weight could be achieved with a non-reactive solvent, which was contrary to the results obtained for PLGA, PGA and other polyesters synthesized within our research group using the same strategy. Although this route could be used alternatively for lactide production, it would require further optimization to determine its potential in comparison with the methods already used industrially.

Finally, we aimed to upscale the synthesis route presented in **Chapter 4** from laboratory glassware ($\leq$35 g) to up to 1 kg scale. **Chapter 6** presents the results found so far, in which lower molecular weights than those achieved in small scale are obtained with both p-cresol and guaiacol. This was mainly attributed to new etherification side reactions evidenced in ^{1}H NMR. Although higher M_n values of up to 17.4 kg·mol^{-1} were obtained with guaiacol and side reactions were significantly reduced, further optimization of the process is still required. Still, this research provides initial insight into the g to kg scale-up and its limitations.

Samenvatting

Plastic is onmisbaar geworden in het dagelijks leven vanwege de veelzijdigheid, lange levensduur, lage kosten en het lage gewicht. Daardoor stijgt de vraag naar plastic gestaag en daarmee ook de behoefte aan fossiele grondstoffen voor zowel energieopwekking als voor bouwstenen voor kunststof materialen. Ongeveer 99% van de huidige grondstoffen voor polymeren komt namelijk uit fossiele bronnen. Deze trend zorgt voor een hogere industriële CO_2-uitstoot en het weglekken van plastic in het milieu tijdens de productie en logistiek, maar ook wanneer consumenten plastic gebruiken en weggooien. Dit plastic afval veroorzaakt grote schade aan ecosystemen. De bovengenoemde problemen benadrukken de noodzaak om de hele plastic waardeketen te heroverwegen. Voor energieopwekking zijn er naast fossiele grondstoffen veel duurzame alternatieven. Echter, voor kunststoffen zijn de enige alternatieve koolstofbronnen biomassa, bestaande kunststoffen (via recycling) en op termijn CO_2. Koolstofdioxide is een veelbelovende grondstof, want het is van nature in overvloed aanwezig, niet giftig en goedkoop. Daarnaast is CO_2 is hernieuwbaar en geen oxidator. Bovendien leidt het gebruik van CO_2 als grondstof tot negatieve emissies waardoor de benodigde "net zero" in de tweede helft van deze eeuw haalbaar is. Het onderzoek in dit proefschrift maakt deel uit van het OCEAN-project (EU Horizon 2020 Spire-programma) waarin een nieuwe route wordt ontwikkeld om polymeren te produceren uit CO_2 als circulaire grondstof. CO_2 kan elektrochemisch worden gereduceerd tot mierenzuur derivaten welke vervolgens kunnen worden omgezet in bruikbare monomeren zoals oxaalzuur en glycolzuur. We richtten ons op het onderzoeken van syntheseroutes om polyesters op basis van die monomeren te produceren en op het bestuderen van hun eigenschappen en op het vinden van mogelijke toepassingen.

Polyesters zijn één van de meest veelbelovende polymerenfamilies vanuit het duurzaamheidsperspectief vanwege de beschikbare duurzame monomeren (veelal met alcohol- en carbonzuurgroepen) in combinatie met controleerbare/aanpasbare materiaaleigenschappen, in het bijzonder in relatie tot hergebruik-, recyclings- en biologische afbreekbaarheidspotentie. In **Hoofdstuk 1** wordt het toekomstige potentieel van glycolzuur en melkzuur als polyesterbouwstenen geëvalueerd. Dit omvat een overzicht van representatieve synthesemethoden, algemene eigenschappen, afbraakmechanismen en recente toepassingen voor polyesters afgeleid van deze twee monomeren. Dit toont de veelbelovendheid aan van deze materialen om bij te dragen aan een circulaire economie in de biomedische, landbouw- en verpakkingssector. Vooral gezien het feit dat technologieën voor de omzetting van CO_2 naar de monomeren steeds verder vorderen. Het door Avantium ontwikkelde proces dat streeft naar productiekosten voor monomeren die op grote schaal kunnen concurreren met fossiele tegenhangers (€ 1-2/kg) is een relevant voorbeeld. Toch moeten er uiterst efficiënte productieroutes voor monomeren en polymeren worden ontwikkeld om deze materialen in grootschalige toepassingen te kunnen

gebruiken (voor bijvoorbeeld afbreekbare rietjes, afbreekbare barrièrefilms, afbreekbare zaad-/mestcoatings, enzovoorts).

In **Hoofdstuk 2** wordt de relatie tussen structuur en eigenschappen besproken van een reeks poly(lactide-co-glycolide) (PLGA)-copolymeren rijk aan glycolzuur, die voor het grootste deel nog niet eerder onderzocht zijn, samen met hun geschiktheid als barrièremateriaal. Hiervoor werden copolymeren tussen 50 en 91 mol% glycolzuur gesynthetiseerd via ring opening polymerisatie (ROP) van respectievelijk lactide en glycolide, de cyclische dimeren van respectievelijk glycolzuur en melkzuur. In het algemeen wordt een toenemende dichtheid en thermische stabiliteit waargenomen, evenals een betere barrière tegen zuurstof en waterdamp bij een toenemend glycolzuurgehalte. Bij kamertemperatuur en een relatieve vochtigheid van minder dan 70% presteren deze PLGA-copolymeren zelfs beter dan niet-georiënteerd polyethyleentereftalaat (PET, een veelgebruikt verpakkingsmateriaal). Een kristallisatiestudie onder niet-isotherme omstandigheden onthulde dat copolymerisatie de kristallisatiesnelheid voor PLGA-copolymeren bijna 10 keer verlaagt in vergelijking met PLA- en PGA-homopolymeren bij een afkoelsnelheid van 10 °C·min^{-1}. De combinatie van opmerkelijke barrièreprestaties, recyclebaarheid, afbreekbaarheid en de mogelijkheid van toekomstige productie uit CO_2 maakt deze polyesters interessant voor bijvoorbeeld verpakkingsfolies.

Tot nu toe is er weinig gerapporteerd over materialen die zowel oxaalzuur- als glycolzuurbouwstenen combineren. Het doel van **Hoofdstuk 3** is om te evalueren of en hoe de opmerkelijke barrièreprestaties van polyglycolzuur (PGA) gecombineerd kunnen worden met de hoge thermische stabiliteit en snelle hydrolyse van het polyoxalaat poly(1,4-cyclohexaandimethanol oxalaat) (PCHDMOX). Hiervoor gebruikten we verschillende verhoudingen van PGA, glycolide (GL), PLA of lactide (LAC) met PCHDMOX (50/50 en 30/70 gewichtsverhouding). Ter vergelijking werd ook PLA onderzocht. Over het algemeen vertoonden copolyesters van PCHDMOX en glycolzuur/glycolide een lagere T_g, hogere thermische stabiliteit, betere barrière tegen zuurstof en waterdamp en snellere hydrolysesnelheid dan die bereid met melkzuur/lactide. Voor beide samenstellingen was de barrièreprestatie onder dezelfde omstandigheden superieur aan die van niet-georiënteerd PET. Alle monsters hydrolyseerden sneller dan de homopolymeren waarvan ze waren gemaakt, waarbij die afgeleid van glycolzuur (30 gew.%) en PCHDMOX een hydrolysegraad tot 86% vertoonden na 215 dagen. Deze resultaten suggereren aanvankelijk dat copolymeren van α-hydroxyzuren en oxalaten potentieel hebben voor toepassing in coatings voor gecontroleerde afgifte, verpakkingen voor eenmalig gebruik die niet geschikt zijn voor recycling of zelfs in de medische sector.

PGA- en PLGA-copolymeren met een hoog molecuulgewicht worden momenteel commercieel geproduceerd via ROP van glycolide en lactide, wat nog steeds een kostbaar proces is. Gezien hun interessante eigenschappen en de aanhoudende vraag naar

duurzamere polymeren, zijn goedkopere productieroutes nodig. Om die reden hebben we in **Hoofdstuk 4** een nieuwe polycondensatieroute bestudeerd voor de productie van deze materialen direct uit glycolzuur en L-melkzuur in aanwezigheid van p-cresol of guaiacol als reactief oplosmiddel op een schaal tussen 20 en 35 gram. Deze route werd geëvalueerd voor copolymeren met een initieel gehalte van 80, 90 en 100 mol% glycolzuur, waarvoor M_n-waarden tot respectievelijk 27,2, 31,5 en 24,2 kg·mol-1 werden verkregen. Voor de copolymeren betekent dit een ongeveer drievoudige verbetering vergeleken met M_n-waarden die worden verkregen bij een typische directe polycondensatie uitgaande van GA en LA. Bovendien vereist de route die in dit werk wordt gepresenteerd minder tijd dan andere gerapporteerde strategieën om het moleculgewicht van vergelijkbare typen polymeren te verhogen en maakt het de recycling van de gebruikte oplosmiddelen voor hergebruik mogelijk. Op basis van deze resultaten hebben we dezelfde synthesestrategie geëvalueerd voor de productie van PLA via polycondensatie van melkzuur in **Hoofdstuk 5**, dit keer met fenol als reactief oplosmiddel. Dit liet onverwacht een andere trend zien dan eerder waargenomen bij PLGA en PGA. Hier kon het moleculgewicht worden verbeterd met tot 10 mol% fenol, maar bij grotere hoeveelheden werd een nadelig effect waargenomen en werd lactide vorming vergemakkelijkt. Verrassend genoeg kon een vergelijkbare verbetering in moleculgewicht worden bereikt met een niet-reactief oplosmiddel, wat in tegenspraak was met de resultaten die werden verkregen voor PLGA, PGA en andere polyesters die binnen onze onderzoeksgroep zijn gesynthetiseerd met dezelfde strategie. Hoewel deze route als alternatief kan worden gebruikt voor de productie van lactide, zou deze verder moeten worden geoptimaliseerd om het potentieel ervan te bepalen in vergelijking met de reeds industrieel gebruikte methoden.

Ten slotte wilden we de in **Hoofdstuk 4** gepresenteerde syntheseroute opschalen van laboratoriumglaswerk (≤35 g) naar een schaal van maximaal 1 kg. **Hoofdstuk 6** presenteert de resultaten die tot nu toe zijn gevonden, waarbij met zowel p-cresol als guaiacol lagere moleculgewichten dan op kleine schaal werden bereikt. Dit werd voornamelijk toegeschreven aan veretheringsreacties die werden aangetoond met ^{1}H NMR. Hoewel hogere M_n-waarden tot 17,4 kg·mol-1 werden verkregen met guaiacol en nevenreacties aanzienlijk werden verminderd, is verdere optimalisatie van het proces nog steeds vereist. Toch geeft dit onderzoek een eerste inzicht in de opschaling van gram- naar kilogramschaal en de beperkingen hiervan.

Acknowledgements

The research presented here, is the result of generous contributions from many people without whose time, trust, patience, encouragement and love this would not have been possible. To them, I would like to express my sincere gratitude.

To my promotor Pr. Gert-Jan Gruter: thank you very much for giving me the opportunity to come to the Netherlands and becoming part of this project where I could experience academic research in cooperation with industry. Since the beginning, you have guided and supported our group in making mindful decisions driven by the common vision of bringing better materials to the world. You have not only provided me with the resources and freedom to work towards becoming an independent researcher, but you also encouraged me to develop additional soft skills that have been crucial for defining and shaping future steps for my career. I will always be grateful for the tremendously positive impact that you have brought to my life for more than 4 years now.

To my co-promotor and daily supervisor Robert-Jan van Putten: thank you very much for your patience and generosity in the process of teaching me to write scientific texts. Your trust over the years to work independently was fundamental to help build up my confidence as researcher. It was very challenging at the beginning but you constantly made sure I knew my work was valued and this was essential to remain motivated even when facing failure. I would also like to thank you for always making time for discussions, for guiding me with structuring new ideas and for your always honest and effective feedback. Thank you also to all the members of the PhD committee for agreeing on being part of this experience and for taking the time to review our research.

Thank you Parana members for creating a working space where I continuously felt happy and proud to be part of. Bing, I am grateful for your guidance and willingness to share knowledge and experience. Especially thank you for teaching me how to operate the autoclave and for staying to help me out on those sometimes, very long days. Daniel, I am extremely grateful for your generosity. You never hesitated to make time for discussions on new ideas, NMR results and doubts about organic chemistry. Thank you for your always positive attitude in the lab. Bruno, thank you for triggering us to be more critical and mindful about the repercussions of our research beyond the laboratory. Thank you also for your kindness and willingness to help me out regardless of the situation. Kevin, thank you for teaching me tips and hacks about the set-ups, for your timely advises on experiments and for your thoughtfulness towards everybody in our team. Also, thank you for the very meaningful 3D-printed presents. Yue, thank you for your always sweet and kind attitude towards me, for teaching about China and for the always entertaining conversations when you were in the lab. Thank you specially for your valuable contributions to this project and for the learnings about biodegradation that I acquired through them. Marian, I am very grateful for your arrival in our group and for the positive energy you brought along. You

have been flexible and open with your schedule to help all of us out. I wish you lots of fun and success in the continuation of your project. Eric, thank you guiding me since the beginning with all the administrative matters and for the happy times shared during the OCEAN meetings. To all the former members of our group: Deepti, Sevil, Ewa, Narciza, Alexander, Dio, Lei, Stefan, Sanae and Anmol, thank you for contributing to the great memories from these past years.

Thank you to Truc Ngo-Ha and Pauline Lusink from the University of Amsterdam for assisting me with all the visa procedures to live in the Netherlands. Thank you Marcel Bartels, Steffanie Igel and Renate Hippert from the HIMS Institute for your help with different administrative matters. Thank you Andreas Ehlers and Ed Zuidinga for teaching me how to use the NMR equipment and for assuring that we had liquid nitrogen for our experiments.

I am also very grateful with the many inspiring people from Avantium that contributed in various ways to the development of this project. Volta team: Julia, Arnaud, Brian, Mariana, Bart, Bert, Stanislav, Annelie, you made working at the Science Park much more enjoyable. Thank you for your kind and positive attitude towards me, for the international lunches and the beloved sweet fridays. Arnaud, thank you for your support with OCEAN and for introducing me to Wie is de mol! I enjoyed our conversations around it. Julia, thank you for the uplifting sweets and homemade treats, which you often shared with all of us.

A special acknowledgement goes to Avantium Renewable Polymers for allowing me to carry out analysis in their facilities, which were essential for the development of this project. Suzanne, Danny and Angela, thank you for efficiently carrying out the GPC measurements for this thesis. Ahmad, than you for the support when I was carrying out the tensile tests. Sullivan, thank you for teaching me how to make compression molded films and for having such a positive attitude to help me out every time I was there. Julia, thank you for helping me with the density measurements. Hindawe, thank you for your guidance on SSP.

To my family: Mami, Jo, thank you for your unconditional support, for your wise advises and for your always comforting calls and texts, which make the distance feel less significant. To my Timo: you have been here every day of this journey. Thank you for advising me in difficult situations, celebrating together the little accomplishments, encouraging me to always do my best and constantly reminding me the importance of balance. Mami, Jo, Timo, I love you and I thank you sincerely for living this experience with me.

Finally, I would like to thank the OCEAN consortium and the European Union for funding this project. Experiencing the interaction between industrial and academic partners from different countries has been very enrichening and it made a tremendous impact in my communication skills.

Publications

This thesis is based on the following publications:

M.A. Murcia Valderrama, R.-J. van Putten, G.-J.M. Gruter, The potential of oxalic - and glycolic acid based polyesters (review). Towards CO_2 as a feedstock (Carbon Capture and Utilization - CCU), *Eur. Polym. J.* **2019**, *119*, 445-468. doi: 10.1016/j.eurpolymj.2019.07.

M.A. Murcia Valderrama, R.-J. van Putten, G.-J.M. Gruter, PLGA Barrier Materials from CO_2. The influence of Lactide Comonomer on Glycolic Acid Polyesters, *ACS Appl. Polym. Mater.* **2020***, 2 (7)*, 2706-2718. doi: 10.1021/acsapm.

Wang, Y.; Valderrama, M. A. M.; Putten, R.-J. van; Davey, C. J. E.; Tietema, A.; Parsons, J. R.; Wang, B.; Gruter, G.-J. M. Biodegradation and non-enzymatic hydrolysis of poly(lactic-co-glycolic acid) (PLGA12/88 and PLGA6/94). Polym. **2022**, 14, 15. https://doi.org/10.3390/ POLYM14010015.